RELIABILITY ASSESSMENT OF A PRESTRESSED CONCRETE MEMBER

by
W.W. BRAND

Thesis presented in partial fulfilment
of the requirements for the degree
Master in Engineering (Civil) at
the University of Stellenbosch

Study Leader
Prof. J.V. Retief

STELLENBOSCH DECEMBER 2001

DECLARATION

I, the undersigned, hereby declare that the work contained in this thesis is my own original work and has not previously in its entirety or in part been submitted at any university to obtain a degree.

SYNOPSIS

First-order second-moment structural reliability methods are used to assess the reliability of a prestressed concrete beam. This beam was designed for imposed office floor loads and partitions following the limit states design method as provided for by the applicable South African structural codes, *viz* SABS 0100-1:1992 and SABS 0160:1989.

The reliability is examined at two limit states. At the ultimate limit state of flexure the ultimate moment of resistance must exceed the applied external moment at the critical section, while at the serviceability limit state of deflection the deflection must satisfy the code-specified deflection criteria. Realistic theoretical models are selected to express the flexural strength and deflection of the prestressed concrete member, while appropriate probabilistic models are gathered from the literature for loading, resistance and modelling uncertainties.

The calculated reliability index at the ultimate limit state of flexure (3.10) is lower than expected in view of the fact that this represents a non-critical limit state in the case of a Class 2 prestressed concrete member. This condition can be explained with reference to the relatively high uncertainty associated with the modelling error for flexural strength. The calculated reliability index at the serviceability limit state of deflection (1.67) compares well with acceptable practice.

The study further focuses on the sensitivity of the reliability at the two limit states of interest to uncertainty in the various design parameters. The ultimate limit state of flexure is dominated by the uncertainty associated with the modelling error for flexural strength, while the contribution to the overall uncertainty of the ultimate strength and area of the prestressing steel and the effective depth is less significant. In comparison the reliability at the serviceability limit state of deflection is not dominated by the uncertainty associated with a single basic variable. Instead, the uncertainty associated with the modelling error, creep factor and prestress loss factor are all significant. It was also demonstrated that the variability in beam stiffness is not a major source of uncertainty in the case of a Class 2 prestressed concrete member.

It is recommended that the present code provisions for ultimate strength and deflection should be reviewed to formulate theoretical models with reduced systematic and random errors. The effect of the uncertainty associated with the creep and prestressed loss factors should also be adressed by adjustment of the partial material factor for concrete at the serviceability limit state of deflection. Furthermore, research must be directed towards formulating an objective failure criterion for deflection. The uncertainty in the deflection limit must therefore be quantified with a probability distribution.

SAMEVATTING

Eerste-orde tweede-moment struktuur betroubaarheid metodes word ingespan om die betroubaarheid van 'n voorspanbeton balk te bereken. Hierdie balk is ontwerp vir opgelegte kantoor vloerbelasting en partisies volgens die grenstoestand ontwerp metode soos beskryf in die toepaslike Suid-Afrikaanse boukodes, naamlik SABS 0100-1:1992 en SABS 0160:1989.

Die betroubaarheid word ondersoek by twee grenstoestande. By die swiglimiet van buiging moet die weerstandsmoment die eksterne aangewende moment oorskrei by die kritieke balksnit, terwyl die defleksie die kriteria soos voorgeskryf deur die kode moet bevredig by die dienslimiet van defleksie. Realistiese teoretiese modelle word gebruik om die buigsterkte en defleksie van die voorspanbeton balk te bereken. Verder is geskikte waarskynlikheid modelle uit die literatuur versamel om die belasting, weerstand en model onsekerhede te karakteriseer.

Die betroubaarheid indeks soos bereken vir die swiglimiet van buiging (3.10) is laer as wat verwag sou word in die lig van die feit dat hierdie nie 'n kritieke grenstoestand verteenwoordig in die geval van 'n Klas 2 voorspan element nie. Dit kan verklaar word met verwysing na die relatiewe groot onsekerheid wat geassosieer word met die modellering fout vir buigsterkte. Die berekende betroubaarheid indeks vir die dienslimiet van defleksie (1.67) vergelyk goed met aanvaarde praktyk.

Die studie fokus verder op die sensitiwiteit van die betroubaarheid by die twee grenstoestande onder beskouing ten opsigte van die onsekerheid in die verskillende ontwerp parameters. By die swiglimiet van buiging word die onsekerheid oorheers deur die bydrae van die modelering fout vir buigsterkte. Die bydraes tot die totale onsekerheid deur die swigsterkte en area van die voorspanstaal sowel as die effektiewe diepte is minder belangrik. By die dienslimiet van defleksie word die betroubaarheid nie oorheers deur die onsekerheid van 'n enkele basiese veranderlike nie. In stede hiervan is die onsekerheid van die modellerings fout, kruipfaktor en voorspan verliesfaktor almal noemenswaardig. Daar word verder aangetoon dat die veranderlikheid in balkstyfheid nie 'n belangrike bron van onsekerheid in die geval van 'n Klas 2 voorspan element is nie.

Daar word aanbeveel dat die bestaande voorskrifte in die kode vir buigsterkte en defleksie aangespreek moet word deur teoretiese modelle met klein modelonsekerhede te formuleer. Die uitwerking van die onsekerheid van die kruip- en voorspan verliesfaktore kan aangespreek word deur 'n aanpassing te maak in die parsiële materiaalfaktor vir beton in die geval van die dienslimiet van defleksie. Navorsing moet verder daarop gemik wees om 'n objektiewe falingskriterium vir defleksie te formuleer. Die onsekerheid van die toelaatbare defleksie moet dus gekwatifiseer word deur 'n waarskynlikheidsverdeling.

to my parents, for giving
me the opportunity
and
to my wife, for giving
me encouragement

ACKNOWLEDGEMENTS

The author would like to express his appreciation to the following persons and organisations who made this thesis possible:

Prof J.V. Retief from the Department of Civil Engineering at the University of Stellenbosch who acted as study leader, for his academic guidance and unceasing patience.

Mr G.P. Maritz from the Department of Civil Engineering at the University of Stellenbosch who acted as assistant examiner.

Mr W.A. van Metzinger from the Bellville office of BKS (Pty) Ltd who acted as external examiner.

Maryke, my wife, for her support and personal sacrifice.

COURSE CURRICULUM

Code	Subject	Credits
DS02	Probability, Reliability and Decision-analysis	4
SB02	Prestressed Concrete Design	4
SB04	Design of Steel Structures	4
SM03	Structural Dynamics	4
SM05	Continuum Mechanics	4
SM08	Finite Element Methods in Structural Mechanics	4
GG02	Foundation Design and Construction	4
SB01	Structural Materials	4
GG01	Applied Geotechnical Engineering	4
GK02	Project Economy and Financing	4
IW01	Linear Algebra	2
TW01	Vectors, Tensors and Index notation	2
	Total:	44

TABLE OF CONTENTS

APPENDIX B DETAILED CALCULATIONS

LIST OF ILLUSTRATIONS

page

Figures

Tables

LIST OF SYMBOLS

The following notation is used to differentiate among the nominal/characteristic value, design value or mean value of a *random variable X*.

X_n	nominal or characteristic value of X
X_d	design value of X
$\bar{X}$	mean value of X

However, the subscript n has been ommitted in those cases where the context define the nominal/characteristic value of a particular quantity. Where possible, a capital letter is used for a random variable, while the same letter in lowercase represents its possible realizations. A letter in bold typeface represents a vector of variables.

Reliability Based Design

a_i	constant
A_i	applied structural load
A_I	influence area
A_T	tributary area
b_i	constant
B_i	statistical or load modelling variable
c_i	influence coefficient for load effects
$[C_{X'}]$	covariance matrix of the reduced variables
$[C_Y]$	covariance matrix of uncorrelated transformed variables
CDF	cumulative distribution function
CFS	central factor of safety
D	total dead load
D_1	beam self-weight
D_2	superimposed dead load
EUDL	equivalent uniformly distributed load
$EX_{I,L}$	Type I Extreme Value distribution (largest values)
f_k	characteristic material strength
$f_X(x)$	probability density function (PDF) of X
$F_X(x)$	cumulative distribution function (CDF) of X
FOSM	first-order second-moment reliability methods
$g(\boldsymbol{X})$	performance function of vector $\boldsymbol{X}$
G	permanent load effect
I_n	diagonal unit matrix
L_0	unreduced imposed office floor load
L_1	reduced imposed office floor load

L_2	partition load
L_{sus}	sustained office floor load
L_{var}	variable office floor load
L	total live load
LN	Log-Normal distribution
m_Y	median of Y
N	Normal distribution
n	sample size
p_F	true probability of structural failure
$p_{F,G}$	probability of structural failure due to gross errors
$p_{F,N}$	notional probability of structural failure
p_{ij}	point-estimates
p_S	probability of survival
PDF	probability density function
PEM	point estimate method of finding moments
Q	combined load effect (or demand)
$Q(t)$	combined load effect process
Q_i	dominant time-varying load effect
$Q_i(t)$	load effect process
Q_j	additional time-varying load effect
R	structural resistance (or capacity)
R_M	member response predicted by theoretical model
R_T	true *in-situ* member response
SLS	serviceability limit state
$s_{T/M}$	sample standard deviation of test to theoretical response ratio
t	time variable
t^*	arbitrary point in time
T	specified design life
$[T]$	orthogonal transformation matrix
u_0	parameter (mode) of $EX_{I,L}$ distribution
ULS	ultimate limit state
V_X	coefficient of variation (c.o.v.) of X
$\hat{V}$	estimate of V_X
V_{spec}	see § 4.5
V_{test}	see § 4.5
$V_{T/M}$	c.o.v. of ratio of test to theoretical response
V_ε	random error
V_i	eigenvector of the covariance matrix $[C_{X'}]$
$\hat{x}$	estimate of μ_X
x_l	lower limit on range of X
x_u	upper limit on range of X
x_i^*	coordinate of the most probable failure point

X_i'	reduced basic variable in standard normal space
Y	functionally dependent random variable
$\boldsymbol{Y}$	vector of uncorrelated transformed variables
α_0	parameter (dispersion) of $EX_{I,L}$ distribution
α_i	direction cosine
β_N	notional reliability index
β_T	target reliability index
γ_1	coefficient of skewness
γ_c	importance factor
γ_{fD}	partial dead load factor
γ_{fi}	partial load factor
γ_{fL}	partial live load factor
γ_m	partial material factor
γ_{mc}	partial material factor for concrete
γ_{ms}	partial material factor for steel
ε	modelling error
ε_M	modelling error for flexural strength
ε_δ	modelling error for deflection
ε_i	modelling error for instantaneous deflection
ε_t	modelling error for ratio of 33 day to instantaneous deflection
ε_∞	modelling error for ratio of long-term to instantaneous deflection
$\varepsilon_{\delta t}$	modelling error for 33 day deflection
$\varepsilon_{\delta\infty}$	modelling error for long-term deflection
$\bar{\varepsilon}$	systematic error
λ_i	eigenvalue of the covariance matrix $[C_{X'}]$
μ_X	mean value of X
μ_X^N	mean value of *equivalent* Normal distribution
σ_X	standard deviation of X
σ_X^N	standard deviation of *equivalent* Normal distribution
$\hat{\sigma}_X$	estimate of σ_X
$\sigma_{T/M}$	true standard deviation of test to theoretical response ratio
$\sigma_{X,Y}$	covariance of X and Y
$\rho_{X,Y}$	correlation coefficient of X and Y
$[\rho_X]$	correlation matrix of the correlated original variables
ϕ	standardised Normal PDF
ϕ_l	partial resistance factor
Φ	standardised Normal CDF
χ^2	Chi-square distribution
ψ_i	load combination factor
ψ_L	live load combination factor (sustained live load ratio)
ω_i	contribution of X_i to uncertainty in limit state function

Prestressed Concrete Design

A	area of gross concrete section
A_{trans}	area of uncracked transformed section
A_p	cross-sectional area of prestressing steel
b	width of flange of PC beam section
b_w	width of web of PC beam section
c_1	concrete strength reduction factor
c_2	long-term concrete cube strength factor
c_3	long-term concrete modulus factor
C	compressive force acting in concrete compression zone
$C_{c\infty}$	long-term specific creep
CGC	centre of gravity of concrete section
CGS	centre of gravity of prestressing steel
d	effective depth to prestressing steel
e	eccentricity of prestressing force
e_1	eccentricity at midspan section
e_2	eccentricity at support sections
E_c	modulus of elasticity of 28 day concrete
E_{ci}	modulus of elasticity of concrete at transfer
$E_{c\infty}$	long-term modulus of elasticity of concrete
$E_{c\ eff}$	effective modulus of elasticity of concrete
E_p	modulus of elasticity of prestressing steel
E_{p2}	stiffness of prestressing steel, as defined in § B.4.1
$E_{p\ eff}$	effective modulus of elasticity of prestressing steel
$f_{bot,i}$	concrete stress in extreme bottom fibre at transfer
$f_{bot,\infty}$	concrete stress in extreme bottom fibre under maximum service loads
f_c	sustained concrete stress
f_c'	concrete cylinder strength at 28 days
f_{ci}	concrete cube strength at transfer
f_{cmax}	maximum compression in concrete at transfer
f_{co}	*in situ* concrete flexural strength
f_{cperm}	concrete stress at centroid of steel, due to P_i and M_{perm}
f_{cu}	concrete cube strength at 28 days
$f_{c\infty}$	long-term concrete cube strength
f_p	stress in prestressing steel
f_{pe}	effective long-term prestress
f_{pi}	initial prestress just after transfer
f_{po}	prestress due to jacking force
f_{pt}	effective 33 day prestress
f_{pu}	ultimate strength of prestressing steel
f_{py}	yield strength of prestressing steel, as defined in § 3.3.2

f_{pI}	proof stress of prestressing steel, as defined in § A.1.3
f_r	modulus of rupture of concrete
$f_{top,i}$	concrete stress in extreme top fibre at transfer
$f_{top,\infty}$	concrete stress in extreme top fibre under maximum service loads
Δf_{pT}	total long-term loss of prestress
$\Delta f_{pT}'$	total 33 day loss of prestress
Δf_{pE}	loss of prestress due to elastic deformation
Δf_{pC}	loss of prestress due to long-term creep of concrete
$\Delta f_{pC}'$	loss of prestress due to 33 day creep of concrete
Δf_{pS}	loss of prestress due to long-term shrinkage of concrete
$\Delta f_{pS}'$	loss of prestress due to 33 day shrinkage of concrete
Δf_{pR}	loss of prestress due to long-term relaxation of steel
$\Delta f_{pR}'$	loss of prestress due to 33 day relaxation of steel
h	overall depth of PC beam section
h_{agg}	maximum size of coarse aggregate
h_{f1}	min flange depth
h_{f2}	max flange depth
H	ambient relative humidity (%)
I	second moment of area of gross uncracked section
I_{trans}	second moment of area of uncracked transformed section
k	factor related to volume/surface ratio of beam
k_E	factor related to elastic loss of prestress
K	deflection coefficient i.r.o. externally applied loads
K_1	deflection coefficient for midspan section, i.r.o. prestressing force
K_2	deflection coefficient for support sections, i.r.o. prestressing force
L_e	span of PC member
M	total applied external midspan moment
M_{cr}	cracking moment at midspan
M_D	applied dead load moment at midspan
M_{D1}	applied midspan moment due to self-weight
M_{D2}	applied superimposed dead load moment at midspan
M_L	applied live load moment at midspan
M_{max}	applied midspan moment due to maximum service loads
M_{min}	applied midspan moment at transfer of prestress (due to self-weight)
M_{perm}	applied midspan moment due to permanent loads
M_P	bending moment due to maximum prestressing force at transfer
$M_{\eta P}$	bending moment due to effective long-term prestressing force
M_u	ultimate moment of resistance at midspan
M_T	true *in-situ* ultimate moment of resistance at midspan
M_{var}	applied midspan moment due to variable component of live load
n	modular ratio
n_i	modular ratio for instantaneous deflection

n_t modular ratio for 33 day deflection
n_∞ modular ratio for long-term deflection
P_o jacking force
P_i initial prestressing force just after transfer
P_{1i} initial prestressing force just after transfer, at midspan section
P_{2i} initial prestressing force just after transfer, at support sections
P_∞ effective long-term prestressing force
r_t 33 day relaxation loss of prestressing steel
r_∞ long-term relaxation loss of prestressing steel
t age of concrete after casting (days)
t_i age of concrete at initial loading
T_p tensile force acting in prestressing steel
u_1 exposed perimeter of PC beam section
w uniformly distributed load at ULS
w_{min} uniformly distributed load at transfer of prestress
w_{max} uniformly distributed load due to maximum service loads
w_{perm} uniformly distributed load due to permanent loads
w_{var} uniformly distributed load due to variable component of live load
x depth to the neutral axis OR distance along span
y_{top} distance of extreme top fibre from section centroid
y_{bot} distance of extreme bottom fibre from section centroid
$y_{bot\ trans}$ distance of extreme bottom fibre from transformed section centroid
z internal lever arm
Z_{top} section modulus with respect to extreme top fibre
Z_{bot} section modulus with respect to extreme bottom fibre

α_1 concrete rectangular stress-block factor
β_1 concrete rectangular stress-block factor
δ midspan deflection affecting partitions and finishes
δ_a allowable deflection at midspan
δ_i midspan deflection at transfer of prestress
δ_p instantaneous elastic deflection due to prestressing force
δ_{pi} instantaneous elastic deflection at transfer due to P_i
δ_{pt} instantaneous elastic plus 33 day creep deflection due to prestressing force
$\delta_{p\infty}$ instantaneous elastic plus long-term creep deflection due to prestressing force
δ_t midspan deflection before construction of partitions and application of finishes
δ_{var} instantaneous elastic deflection due to variable load
δ_w instantaneous elastic deflection due to externally applied loads
δ_{wi} instantaneous elastic deflection at transfer due to M_{min}
δ_{wt} instantaneous elastic plus 33 day creep deflection due to M_{min}
$\delta_{w\infty}$ instantaneous elastic plus long-term creep deflection due to permanent loads
δ_∞ total long-term midspan deflection under service loads

δ_M deflection predicted by theoretical model
δ_T true *in-situ* deflection
ε_c instantaneous elastic concrete strain
ε_{cc} long-term creep strain
ε_{ce} see § 3.4.2
ε_{cp} see § 3.4.2
ε_{cs} long-term shrinkage strain
ε_{cu} ultimate concrete strain in extreme compression fibre
ε_p strain in prestressing steel
ε_{pe} see § 3.4.2
ε_{pu} ultimate strain in prestressing strand (at fracture)
ε_{py} yield strain of prestressing steel, as defined in § A.1.3
ε_{p1} proof strain, as defined in § A.1.3
ζ_i initial loss factor
η_t 33 day loss factor
η_{1t} 33 day loss factor at midspan section
η_{2t} 33 day loss factor at support sections
η_∞ long-term loss factor
$\eta_{1\infty}$ long-term loss factor at midspan section
$\eta_{2\infty}$ long-term loss factor at support sections
ρ_b balanced steel ratio
σ_{ci} permissible concrete compressive stress at transfer
$\sigma_{c\infty}$ permissible concrete compressive stress under maximum service loads
σ_{ti} permissible concrete tensile stress at transfer
$\sigma_{t\infty}$ permissible concrete tensile stress under maximum service loads
ϕ_{1i} elastic curvature at transfer at midspan section due to prestressing force
ϕ_{2i} elastic curvature at transfer at support sections due to prestressing force
ϕ_{1t} total 33 day curvature at midspan section due to prestressing force
ϕ_{2t} total 33 day curvature at support sections due to prestressing force
$\phi_{1\infty}$ total long-term curvature at midspan section due to prestressing force
$\phi_{2\infty}$ total long-term curvature at support sections due to prestressing force
ϕ_{ct} 33 day creep factor
$\phi_{c\infty}$ long-term creep factor
ϕ_{p1} elastic curvature at midspan section due to prestressing force
ϕ_{p2} elastic curvature at support sections due to prestressing force
$\phi_{p\infty}$ instantaneous elastic plus long-term creep curvature due to prestressing force
ϕ_w elastic curvature at midspan section due to externally applied loads

CHAPTER 1

INTRODUCTION

This introductory chapter serves to provide a background to the chosen field of study in terms of the literature that was consulted. This review is not exhaustive, however, and perspectives gained from literature are referenced throughout the text. The chapter closes by defining the objectives and scope of this thesis.

1.1 STRUCTURAL RELIABILITY

The main objective of structural design is to ensure, at an acceptable level of probability, that a structure or structural member will not become unfit for its intended purpose at any time during its specified design life. Structural reliability may therefore be defined as the probability that the capacity of the structure will be adequate to accommodate the lifetime maximum demand. By reliability in this context will be understood not just reliability against extreme events such as structural collapse, but against the violation of any engineering requirement which the structure is expected to satisfy.

Structural reliability theory is concerned with the rational treatment of uncertainties in structural engineering design. In the presence of uncertainty, absolute reliability is an unattainable goal. However, reliability theory and limit states design provide a formal framework for developing criteria for design which ensure that the probability of unfavourable performance is acceptably small.

The conceptual framework for structural reliability and limit states design is provided by the classical reliability theory described by Freudenthal, Garrelt and Shinozuka (Ref. 1-1) and by Ang and Cornell (Ref. 1-2). The load effect and resistance terms are modelled as random variables and the statistical information necessary to describe their probability laws is assumed to be known. A structure is considered to have failed when the resistance R is less than the load effect Q. The probability of structural failure p_F, which is the complement of the probability of survival p_S, can therefore be stated as follows.

$$p_F = 1 - p_S = P[R \leq Q] \tag{1-1}$$

The concepts of reliability theory is being increasingly applied in structural engineering not only to assess the probability of failure of a structure but also to determine rational values for partial safety factors prescribed by the various building codes. More consistent reliability can be achieved for different design situations because the different uncertainties related to the various strengths and load effects are considered explicitly and independently. Furthermore,

the desired reliability level can be chosen to reflect the consequences of failure, such as loss of life and financial loss.

1.2 NOTIONAL PROBABILITY OF FAILURE

It is necessary to distinguish among the many types of uncertainty that affect the loading and response of structures in order to understand how they contribute to the probability of structural failure. The two major categories of uncertainty which cause failure are variations within accepted practice and departures from accepted practice (Ref. 1-3). The types of uncertainty associated with the first category include the following.

- *Physical uncertainty*: This represents the inherent random nature of physical quantities, such as loads, material properties and dimensions. These quantities are modelled as random variables of which the first two moments are used in reliability analyses.

- *Statistical uncertainty*: This is the uncertainty that remains when using limited data to suggest the distribution and parameters of a random variable. This uncertainty arises solely as a result of lack of information and should be included within the distribution of the random variable itself.

- *Modelling uncertainty*: This is caused by the use of a simplified prediction model to represent the physical phenomenon of interest. This type of uncertainty can conveniently be expressed in terms of the distribution of a modelling variable, which is defined as the ratio between the actual and predicted response.

Physical uncertainty is essentially a state of nature and cannot be controlled or reduced, while statistical and modelling uncertainty may be reduced through the acquisition of additional data and the use of more accurate models.

The second category of uncertainty deals with gross human error, as distinct from random and systematic errors, and abnormal events such as fires, collisions or severe corrosion. The underlying causes of gross human error include the following (Ref. 1-4, Chp 36, § 3.2.4).

- A conceptual misunderstanding of structural function on the part of the designer.
- The use of incorrect assumptions as the basis for design.
- Gross computational errors.
- A breakdown in communication (design specifications, drawings, site instructions).
- Undetected flaws in materials and serious omissions or errors in the workmanship.

All the possible uncertainties that exist cannot be accurately accounted for in reliability analysis. Reliability analysis considering only a subset of uncertainties will result in a

probability estimate termed the *notional probability of failure*. In view of the above the true probability of structural failure p_F can be represented by two components (Ref. 1-5).

$$p_F = p_{F,N} + p_{F,G} \tag{1-2}$$

where $p_{F,N}$ = notional probability of failure due to variations within accepted practice
$p_{F,G}$ = probability of failure due to departures from accepted practice

Gross human error will remain the most serious threat to the safety of structures and p_F is typically one order of magnitude greater than $p_{F,N}$. However, the notional probability of failure deals only with those uncertainties that can rationally be controlled by partial safety factors and hence neglects the effects of gross human error. The effects of gross human error should be controlled through quality assurance procedures. $p_{F,N}$ may be used as a surrogate for p_F in a comparative sense if it is assumed that the effects of gross human error affects each of the alternatives in a manner roughly proportional to $p_{F,N}$ (Ref. 1-6). In this case, the notional probability of failure cannot be interpreted as a relative frequency of failure, but rather as a subjective degree of belief.

Reliability analyses will therefore predict values of the notional probability of failure. These probabilities can then be compared with target values which may be obtained either on purely empirical grounds or from acceptable levels of reliability that is reflected in existing codes of practice.

1.3 HIERARCHY OF RELIABILITY MEASURES

It was noted in § 1.1 that reliability theory is concerned with the rational treatment of uncertainties in structural engineering design in order to ensure that the probability of unfavourable performance is acceptably small. As is often reported in the literature (e.g. Refs. 1-6 and 1-7), the concepts of reliability may be considered at different levels of sophistication to achieve this objective. The three levels of reliability assessment are briefly discussed below, in the order of being increasingly deterministic.

1.3.1 Level 3 Reliability Methods

Making use of a full probabilistic description of the joint occurrence of the various quantities which effect the loading and response of a structure, procedures at this level attempt to estimate the notional probability of failure $p_{F,N}$ from Eq. 1-3. This expression follows from the theorem of total probability.

$$p_{F,N} = \int_{-\infty}^{+\infty} F_R(q) f_Q(q)\, dq \tag{1-3}$$

where F_R = CDF of the resistance R
f_Q = PDF of the load effect Q

A general scarcity of data and numerical complexity usually make the evaluation of Eq. 1-3 difficult, and as a result it is normally evaluated with the aid of numerical integration and simulation methods, such as the Monte Carlo method. Because of their sophistication and the computational effort required, level 3 reliability methods are normally only used in the case of unique structures and for some research applications.

1.3.2 Level 2 Reliability Methods

The difficulties associated with Level 3 reliability methods have motivated the development of First-Order Second-Moment (FOSM) methods, so called because of the way they characterise uncertainty in the basic variables and the linearizations performed during the reliability analysis. Basic variables are a set of quantities that govern the response of a structure. They are basic in the sense that they are the most fundamental quantities normally used by designers in structural calculations.

Level 2 reliability methods also deal with the notional probability of failure $p_{F,N}$ but are an approximation of Level 3 methods. In principle, only the first two probability moments are used to summarise the behaviour of each basic random variable. With these methods, $p_{F,N}$ is directly related to the notional reliability index β_N as follows,

$$p_{F,N} = \Phi(-\beta_N) \tag{1-4}$$

where Φ = standardised Normal CDF

As the reliability index varies linearly, the corresponding notional probability of failure varies inversely by orders of magnitude. Level 2 reliability methods are employed for the purposes of this study and are dealt with in more detail in § 2.2.

Level 2 methods provide a tool for exercising judgement on the safety of non-routine designs, for which structural design codes of practice are either not available or not wholly acceptable. Furthermore, these methods are ideally suited to the derivation of rational values for partial safety factors in code development procedures. The purpose of these procedures is to derive safety factors such that the average notional reliability β_N reflected in existing codes remain approximately unchanged in future codes, while the scatter with respect to this average is reduced.

Once the reliability of a structure has been assessed by the use of either Level 3 or Level 2 methods, it must be compared with a target reliability. It is interesting to note that, after

extensive mathematical manipulations, the test for adequacy of the reliability index generally rests on comparing computed values with recommended values.

1.3.3 Level 1 Reliability Methods

Normal routine designs which are carried out according to specified structural code requirements are classified as Level 1 reliability methods. The design resistance and the design load effect are calculated in a *deterministic* manner by the application of partial safety factors to the nominal or characteristic values specified by structural codes for the basic variables.

At this level the aim is not to explicitly achieve a certain target reliability. Instead, an appropriate degree of structural reliability is provided by the fact that the partial safety factors are derived by applying Level 2 reliability methods. Design codes of practice are therefore essentially instruments used for the provision of adequate structural reliability. The discussion on Level 1 reliability methods is continued in § 1.4 in terms of the limit states design method.

The identification of target reliabilities is a complex task. According to the Canadian guidelines for the development of limit states codes (Ref. 1-8), the choice of a level of reliability should take the following factors into account.

- The possible consequences of failure in terms of the risk to human life or injury.
- The number of human lives at risk.
- Economic losses.
- The degree of social inconvenience resulting from failure.
- The cost and effort required to reduce the risk of failure.

However, in practice it is not possible to quantify these items on a statistical basis alone. Neither is it possible to arrive at a target level of reliability from fundamental considerations. Instead, a calibration procedure is used to establish currently acceptable levels of reliability in terms of existing codes of practice and these principles are then used by code committees to make subjective decisions that take the above into account (Ref. 1-9).

1.4 LIMIT STATES DESIGN

The South African design code of practice for the structural use of concrete SABS 0100-1:1992 (Ref. 1-10) and the loading code SABS 0160:1989 (Ref. 1-11) are based on the so called *limit states design* method. Any condition at which a structure or structural member may become unfit for its intended purpose constitutes a *limit state*. The objective of the design procedure is then to recognize the various limit states and to proportion the structure such that an acceptable probability exists that these limit states will not be reached at any time

during the specified design life. In this context structural reliability may be seen as the probability of not exceeding a certain limit state.

For most structures the various limit states can be placed in one of the following two categories.

- *Ultimate limit states* (ULS), which are concerned with the maximum load-carrying capacity of a structure. These limit states should have a very low probability of exceedence since they may lead to loss of life and major financial losses.

- *Serviceability limit states* (SLS), which are concerned with the durability and/or functional use of the structure. The probability of exceedence should reflect the consequences of unserviceability and is generally higher than in the case of the ULS.

For a satisfactory design, the design resistance R_d must exceed the design load effect Q_d at the ULS, while at the SLS the specified design criteria must be satisfied. It is important to note that serviceability limit states are most often judged on subjective criteria based on human reactions and not on a failure criterion, as is the case for ultimate limit states (Ref. 1-12). However, a general criterion for assessing the adequacy of a structure or structural member at a particular limit state may be stated as follows.

$$R_d \geq Q_d \tag{1-5}$$

A margin of safety is introduced by the application of partial material and resistance factors to the characteristic strength and partial load and load combination factors to the nominal load effect. This safety margin is conceived to be proportional to the uncertainty that is present and to the desired level of safety. Appropriate values for the partial safety factors are specified by the South African structural codes with reference to the particular limit state that is being considered, the type of loading and the material being used. All the relevant limit states should be considered during the design process, but as a general rule the design is carried out on the basis of the expected critical limit state while the remaining limit states are examined to check that they are not reached.

In practice the general criterion of Eq. 1-5 may be expressed in numerous ways. However, only those formulations recommended by SABS 0100-1:1992 (Ref. 1-10) and SABS 0160:1989 (Ref. 1-11) regarding the design resistance and design load effect are discussed in § 1.4.1 and § 1.4.2, respectively. It should be noted here that material strengths are normally specified in terms of their characteristic values, which are defined as the strength below which not more than 5% of test results may be expected to fall. Material strengths are therefore based on statistical evidence. In contrast, the various loads acting on a structure are specified in terms of their nominal values. These may be defined as principal representative values, which are fixed on a non-statistical basis such as acquired experience. The statistical

information required to establish characteristic values for loads are generally not available at present (Ref. 1-12).

1.4.1 Design Resistance

The nominal resistance at any particular limit state is often calculated from an expression based on the principles of structural mechanics. However, to determine the design resistance R_d, the nominal resistance is scaled down by partial safety factors in accordance with the general formulation given in Eq. 1-6 (Refs. 1-12 and 1-13). This approach represents a combination of earlier British practice in which all uncertainty was included in the partial material factors and United States practice in which all uncertainty was included in the resistance factor.

$$R_d = \phi_l R \left[\frac{f_k}{\gamma_m} \right] \tag{1-6}$$

where $R(\,)$ = function defining the resistance of the structure at a particular limit state
f_k = characteristic material strength
γ_m = partial material factor
ϕ_l = partial resistance factor

The partial material factor γ_m is intended to account for the uncertainty in predicting the different material strengths (i.e. physical and statistical uncertainty). On the other hand, the partial resistance factor ϕ_l allows for the uncertainty in predicting the in-situ resistance of the structure at the different limit states (i.e. modelling uncertainty) and enable a clear distinction to be made between ductile and brittle modes of failure.

It is conceivable that the use of a resistance factor should allow for a consistent set of partial material factors to be used for the various materials, irrespective of the limit state. However, ϕ_l usually takes on a value of unity, while γ_m is dependent on the limit state that is being considered.

1.4.2 Design Load Effect

The design value of the load effect Q_d is specified by SABS 0160:1989 (Ref. 1-11) in terms of nominal load effects, load factors and load combination factors. This standard formulation, restated in Eq. 1-7, represents a Turkstra-type combination of the various components of loading on the structure or structural member and can be used to consider load cases at either the ULS or the SLS. Each load case must be considered in turn and the most severe is then adopted for design purposes. Load combinations are discussed in greater detail in § 4.3.2.

$$Q_d = \gamma_{fG} G_n + \gamma_{fi} Q_{ni} + \sum_{\substack{j=1 \\ j \neq i}}^{n} \psi_j \gamma_{fj} Q_{nj} \qquad (1\text{-}7)$$

where G = permanent load effect
Q_i = dominant time-varying load effect
Q_j = additional time-varying load effect
γ_f = partial load factor
ψ_j = load combination factor

This formulation reflects a combination of the permanent load effect, the time-varying load effect that is considered dominant for the load case under consideration and the combined effect of other additional time-varying loads. At the ULS the product of the partial load factors γ_f and the nominal load effects may be considered to reflect the lifetime maximum values of these load effects, while the lifetime maximum values of the additional time-varying load effects are reduced to their arbitrary point-in-time values by the load combination factors ψ_j. These arbitrary point-in-time values are intended to represent the sustained or usual values of the additional time-varying load effects which are likely to occur simultaneously with the lifetime maximum value of the dominant time-varying load effect (Ref. 1-13).

At the discretion of the designer, the design load effect given by Eq. 1-7 may be adjusted to allow for the consequences of failure by multiplying by an importance factor γ_c with a value ranging between 0.9 and 1.2. For the normal range of structures a value of 1.0 should be adopted representing serious consequences of failure. A structure might therefore be designed to take higher loads, but this is to reduce the probability of failure, not because higher loads are actually expected (Ref. 1-14).

For analysis at certain serviceability limit states it is desirable to separate that component of the total load effect which may be considered as being of a permanent nature from the instantaneous component (e.g. for evaluation of the long-term behaviour of the materials of construction). For this purpose Eq. 1-7 may be rewritten as follows (Ref. 1-12).

$$Q_d = \left[\gamma_{fG} G_n + \sum_{j=1}^{n} \psi_j \gamma_{fj} Q_{nj} \right] + \left(1 - \psi_i\right) \gamma_{fi} Q_{ni} \qquad (1\text{-}8)$$

The first term of Eq. 1-8 includes the lifetime maximum value of the permanent load effect as well as the sum of the arbitrary point-in-time values of *all* the time-varying load effects and is used to evaluate long-term material behaviour. The second term represents the instantaneous or variable component of the dominant time-varying load effect and may be used to evaluate instantaneous elastic behaviour.

Ideally, the load factors γ_f are intended to take into account the variability of the load effects (i.e. physical and statistical uncertainty), and the inaccuracies in the transformation of the load into load effect (i.e. modelling uncertainty). On the other hand, the load combination factors ψ_j account for the reduced probability of two or more lifetime maximum time-varying load effects occurring at the same instant in time.

1.4.3 South African Structural Codes

Even though the limit states design method has been extensively researched and discussed over the last few decades (Ref. 1-14), most limit states codes nevertheless are evolutionary in nature. Changes are introduced or major revisions are made at intervals of 3 to 10 years to allow for new types of structural form, the effects of improved understanding of structural behaviour, the effects of changes in quality control procedures, or a better understanding and modelling of loads (Ref. 1-7).

It is an accepted principle of code theory that new codes should be calibrated on the basis of existing standards, which are proven by past experience, so as to effectively obtain the same level of reliability. This principle was adopted in drafting the South African structural codes on which this study is based (Refs. 1-15 and 1-16). In particular, for ductile, gradual modes of failure at the ULS, partial material factors were chosen such that, on average, a target value of 3.0 would be obtained for the notional reliability index β_N.

In recent years a worldwide trend was to remove partial load factors from individual material codes and to replace them with a set of statistically defined partial load factors in the loading code. This is highly desirable as in principle, the materials of construction cannot have any bearing on the (live) loads which a structure must be designed to resist. It follows then that it should be possible to prescribe the partial load factors independently from the materials of construction (Ref. 1-15). That is, the partial load factors should be material-independent and the partial material factors should be load-independent. Once again, this approach applies to SABS 0100-1:1992 (Ref. 1-10) and SABS 0160:1989 (Ref. 1-11).

The limit states formulation for design resistance (i.e. the left-hand side of Eq. 1-5) may be expressed in several ways. However, the final choice of the formulation must balance theoretical appeal, computational ease, accuracy and user acceptance (Ref. 1-17). The expression recommended by SABS 0160:1989 (see Eq. 1-6) enables the following sources of uncertainty to be represented consistently (Ref. 1-13).

- Through using partial material factors γ_m, strength variations in each of the different materials contributing to the resistance are taken into account.

- Varying degrees of uncertainty in modelling different limit states are provided for by using different values of the partial resistance factor ϕ_l.

- A larger margin of safety in the case of brittle collapse mechanisms in which there is no warning of failure, compared to ductile mechanisms, can be provided by adjusting the value of ϕ_l.

SABS 0160:1989 (Ref. 1-11) therefore advocates the use of a consistent set of partial material factors, irrespective of the limit state being considered, together with a set of partial resistance factors to take account of the uncertainty associated with different limit states. This more comprehensive approach has, as yet, not been implemented in SABS 0100-1:1992 (Ref. 1-10) in that different partial material factors are specified for various categories of limit states. As this code is currently being reviewed it is time, in the writer's opinion, for this inconsistency to be addressed by the selection of a set of partial resistance factors for the various limit states.

1.5 OBJECTIVES AND SCOPE

Research has been carried out on numerous different aspects related to structural reliability, the reports of which represent a considerable body of knowledge. It was therefore necessary at the outset to clearly define the objectives and scope of this study and to be aware of how this work might complement the mass of existing knowledge. These objectives are set out in the following sections, together with an overview of essential literature that were consulted. For the purposes of this thesis a sound knowledge of several other subjects were also required, such as the formulation of limit states codes, probability theory and prestressed concrete design.

1.5.1 Research Objectives

This study was carried out with the following specific aims in mind.

- To gain an insight into the background to the limit states formulation of SABS 0160:1989 and SABS 0100-1:1992. In particular, to obtain an understanding of the implications of this formulation on the various limit states of a prestressed concrete member and to study the behaviour of the structure in meeting these code requirements.

- For prestressed concrete design, to estimate the level of reliability implied by the limit states design method (i.e. the partial safety factors and design criteria) as specified by the South African structural codes on which this study is based. This should be done for a Class 2 prestressed concrete member at the ULS of flexure and the SLS of deflection. Taking due cognisance of the nominal load ratio (see § 3.1), the calculated values of the notional reliability index β_N must be evaluated in terms of target values as reported in the literature.

- To examine the relative contributions to the overall uncertainty at the two limit states of interest of those fundamental quantities normally used by designers in structural calculations. Subsequently, to identify those basic variables which contribute in a significant manner to the uncertainty at a particular limit state. This will indicate those areas where caution should be taken during the design process as well as the need for improved specification by the code.

- To evaluate the effect of the gain in concrete strength beyond 28 days on the reliability of a prestressed concrete member at the limit states of interest. This will indicate the advantage, if any, of taking cognisance of increased concrete strength during the design process.

- To demonstrate a practical approach to reliability analysis using the FOSM reliability method when the limit state equation of interest is expressed as a function of many basic variables.

1.5.2 Summary of Procedure

The particulars of achieving these objectives are contained in the body of this thesis, while detailed calculations are presented in the appendices. The following is an abbreviated description of the procedure that was followed.

- Design a simply supported pretensioned concrete T-beam in accordance with SABS 0100-1:1992 (Refs. 1-10) and SABS 0160:1989 (Ref. 1-11). For a Class 2 prestressed concrete member the SLS of cracking, as stated in terms of the permissible concrete stress criteria, represents the critical limit state.

- Select theoretical models to express the structural response of the member at the ULS of flexure and the SLS of deflection in terms of the basic variables. In general, the mathematical models used for the reliability analyses may be more comprehensive than normal design procedures. These models should be realistic rather than conservative code-based approximations.

- From available literature, select appropriate probabilistic models (i.e. realistic estimates of the mean and standard deviation, as well as the distribution type) for all the basic random variables. The basic random variables of interest include those associated with the loading, resistance and modelling uncertainty of the prestressed concrete member.

- From basic theory, select appropriate probabilistic procedures for analysis of the moments of the basic random variables in order to reduce the limit state equations to

a manageable form, where necessary. Also select a FOSM reliability algorithm for practical reliability analysis.

- Using the above information, calculate the notional reliability index β_N at the two limit states of interest. In terms of the direction cosines, examine the sensitivity of the reliability of the design to uncertainty in the various design parameters.

- Interpret the results of the analyses, with specific emphasis on the level of reliability that was achieved, on identification of those basic variables which contribute in a significant manner to the overall uncertainty at a particular limit state, and on the effect of the gain in concrete strength on the reliability of a prestressed concrete member.

- Reflect on the implications of the results of the present study on existing code provisions in SABS 0100-1:1992 (Ref. 1-10).

1.5.3 Scope of Research

To obtain a realistic estimate of the level of reliability of prestressed concrete members, as embodied in the structural codes on which this study is based, it is necessary to analyze a large number of structural elements over the practical range of material properties, dimensions and nominal load ratios. However, this study does not centre on the actual implied level of reliability, but rather on the sensitivity of the reliability of a design to uncertainty in the various design parameters. For the purposes of this study, it is therefore considered sufficient to determine the reliability of a single pretensioned concrete T-beam. Furthermore, since the focus of this study falls on the reliability aspects associated with the response of the prestressed concrete member, the only load combination that is treated is that which involves dead and imposed floor loads in office buildings. This load combination was chosen since it governs design situations in many practical instances.

At the ULS a simply supported prestressed concrete beam can be visualized as a series (weakest link) system in which failure would occur if the midspan section failed in flexure, if one of the two end sections failed in shear, or if one of several sections failed in bond. The probability of failure of the system would be greater than any of the individual probabilities of failure. If, however, the probability of failure in shear was intentionally set lower than that in flexure, the overall probability of failure would be close to that of a flexural failure.

No work of substance has been reported in the literature dealing with the system reliability of prestressed concrete members. Reliability analyses are usually performed on the assumption that a given member is subject to only one failure mode at a time. This is clearly a simplification and it is desirable to investigate the system reliability. However, it will be of little value if the system reliability is declared to be at a certain level without specifying

the target reliability to which it should be compared. Since acceptable levels of reliability applicable to the ULS differs from those applicable to the SLS, it follows that it is necessary to evaluate the system reliability separately for each category. Since, for the purposes of this study, only one limit state is considered in each category, the evaluation of system reliability clearly falls outside the scope of this study.

As a pilot study, based only on the prestressed concrete member of this thesis, partial resistance factors applicable to the ULS of flexure and the SLS of deflection may be derived. This would represent a calibration of SABS 0100-1:1992 as the calculated values of the notional reliability index β_N will be regarded as target values and would be an attempt to address the inconsistency noted at the end of § 1.4.3. This exercise, however, falls outside the scope of the current study, but may be undertaken as a sequel to this work.

1.5.4 Literature Review

The research for this thesis commenced with a comprehensive literature study, the aims of which may be summarised as follows.

- To gain an insight into the background to the limit states formulation of South African structural codes.

- To study the basic theory related to structural reliability and other probabilistic procedures in order to analyze the statistical properties of the basic random variables and to perform FOSM reliability analyses.

- To study the basic theory related to prestressed concrete design in order to select theoretical prediction equations to express the structural response of the pretensioned concrete T-beam at the two limit states of interest in terms of the basic variables.

- To obtain statistical descriptions of all the basic random variables related to the two limit states of interest, as required for Level 2 reliability analysis.

- To obtain an overview of the research that has been carried out related specifically to the reliability of prestressed concrete beams and to be aware of how the present study might complement the body of existing knowledge.

Perspectives gained from literature are referenced throughout the text of this thesis. The following presents only a brief overview of the essential sources that were consulted.

The formulation of limit states requirements for South African structural codes was spearheaded by a Working Group established by the South African Institution of Civil Engineers. This transition came about in the late 1980's and is documented in papers by

Kemp *et al*, Milford and others (see Refs. 1-5, 1-9, 1-12, 1-13 and 1-15). Target reliability levels, as applicable to the structural codes on which this study is based, are also reported in these references. Guidelines on the calibration of limit states codes may be obtained from Refs. 1-8, 1-16, 1-18 and 1-19, where Ref. 1-16 is applicable to SABS material codes.

Recently the South African concrete community has initiated an investigation into the possible adoption of Eurocode 2 for reinforced and prestressed concrete (Ref. 1-20). This has opened the question of whether Eurocodes can be used with the load factors and load combinations specified in the South African loading code, which is essentially in line with North American practice. As codes of practice should be regularly reviewed to ensure that they continually meet the needs of industry and society, and reflect appropriate developments in research and engineering practice, a new Working Group has now been established to review SABS 0160:1989. Recognising that most of the development for this code was undertaken in the mid-1980's, this review is most welcome.

The conceptual framework for structural reliability and limit states design is provided by the classical reliability theory described by Freudenthal, Garrelt and Shinozuka (Ref. 1-1) and by Ang and Cornell (Ref. 1-2). It is a subject which has grown to such an extent over the last three decades that a variaty of standard texts on this topic now exist. For the purposes of this thesis texts by Melchers, Thoft-Christensen and Baker, and Ang and Tang served as references on Level 2 reliability methods (Refs. 1-6, 1-7 and 1-21), while a text by Benjamin and Cornell (Ref. 1-22) provided a background on probability theory.

Course notes compiled by Marshall and Robberts (Ref. 1-23) and a text by Collins and Mitchell (Ref. 1-24) on prestressed concrete theory provided sufficient background for the selection of appropriate prediction equations to express the structural response of the member at the two limit states of interest in terms of the basic variables.

Fundamental research regarding the statistical variability of concrete strength in tension or compression, the yield strength of reinforcement and the dimensions of cross-sections are reported in Refs. 1-25 through 1-27. Much of this research was carried out by Mirza and MacGregor. However, the statistical properties quoted in this thesis were often collected from literature that is an interpretation of these results (e.g. Refs. 1-17, 1-28 and 1-29). The report prepared by Ellingwood *et al* (Ref. 1-30) for the National Bureau of Standards in the United States represents a synthesis of time-invariant statistical properties of basic variables as reported in numerous previous studies.

Judging on the limited amount of available literature specifically related to the reliability of prestressed concrete members, it is apparent that reinforced concrete has received more attention in this regard (e.g. Refs. 1-31 and 1-32). However, Refs. 1-28, 1-29 and 1-33 through 1-35 represent examples of reports on the FOSM reliability analysis of prestressed

concrete members at the ULS as well as the SLS. Perspectives gained from some of these references are discussed below.

Mirza and MacGregor (Ref. 5-31) observed that, due to the small c.o.v. of the ultimate strength of prestressing steel relative to that of the yield strength of reinforcement (0.025 *vs.* 0.093), the c.o.v. of the ultimate moment of resistance of prestressed concrete members is considerably smaller than that of reinforced concrete members (0.050 *vs.* 0.080). The c.o.v. of plant-produced, pretensioned concrete members is also lower than that for post-tensioned, cast-in-place members due to the better quality control for such members (0.045 *vs.* 0.050).

As the reinforcement ratio increases and approaches the balanced steel ratio ρ_b, a compression failure occuring in a memeber designed to fail in tension becomes more likely, beyond which the limit state function is no longer valid. Israel, Ellingwood and Corotis (Ref. 5-32) found that the possibility of compression failures was still significant at nominal reinforcement ratios well below $0.75\rho_b$. Consideration should be given to reducing the maximum reinforcement ratio permitted to $0.65\rho_b$.

Al-Harthy and Frangopol (Ref. 1-33) investigated the reliability of prestressed concrete beams designed according to the provisions of ACI 318 (1989). Using FOSM methods, the reliability levels of 73 single span PC beams commonly used in the construction industry for offices and retail buildings were estimated with respect to several limit states. These included permissible compressive and tensile stresses at both the initial and final stages, flexural cracking and ultimate flexural strength. The beams were designed for two levels of live load, namely 2.4 kPa and 4.8 kPa, and for spans ranging from 7.3 to 30.5 m. The least possible amount of prestressing strands was selected to satisfy permissible stresses at the most critical sections along the span at the initial and final stages. Reliability with respect to the ULS of flexure was generally high, ranging from 2.8 to 5.5 and was found to be more consistent than reliabilities with respect to other limit states. Its variation with span length and live load level was not significant. It was found that positive correlation among certain variables resulted in slightly smaller reliability for the ULS of flexure than for the case of independence. It was therefore considered to have an insignificant effect on reliability at the ULS of flexure. In conclusion it was considered that reliability levels implied by the use of ACI 318 (1989) for PC beams were non-uniform over various live load ratios, span lengths, and limit states.

Since most precast concrete beams in practice are under-reinforced, a variation in concrete cube strength should have little effect on the probability of failure. This was confirmed by Chandrasekar and Dayaratnam (Ref. 1-34) who found that the reliability index tends to increase only marginally as the specified concrete strength increases.

Naaman and Siriaksorn (Ref. 5-29) investigated the reliability of partially prestressed concrete beams at six serviceability limit states, including immediate and long-term deflection. They evaluated 64 different beam designs representative of current practice in the precast

prestressed concrete industry in the United States. They found that for each SLS the reliability spans a relatively wide range of values reflecting uncertainties in the basic variables and theoretical models, and that SLS are on the average more critical than ULS. They also found that the reliability of rectangular beams is much lower than that for T-beams. Thus, the probability of unserviceability of rectangular beams, or one-way slabs, is in general greater than that of T-beams. For T-beams and for rectangular beams, the reliability at the long-term deflection limit state decreases substantially as the partial prestressing ratio decreases, while it appears that, when the span length increases, the reliability decreases at the immediate live load deflection and long-term deflection limit states.

1.6 SUMMARY

An introduction to the chosen field of study has been provided in this chapter. The reliability of a prestressed concrete member is to be determined, where structural reliability has been defined, in general terms, as the probability that the capacity of a structure will not be exceeded by the lifetime maximum demand. FOSM methods, which represent Level 2 reliability methods in the hierarchy of reliability measures, will be employed for the analyses. It was stressed that, since only a subset of all the uncertainties that exist are considered, these analyses will yield notional values of the reliability index. The prestressed concrete member should be designed following the limit states design method as provided for by the applicable South African structural codes. The limit states of interest are flexural strength at the ULS and deflection at the SLS.

The basic theory required for FOSM reliability analysis are briefly dealt with in Chapter 2. This is followed in Chapter 3 by a description of the prestressed concrete member on which this study is based, namely a simply supported pretensioned concrete T-beam. The structural response of the member at the two limit states of interest are also considered in that chapter. Before the reliability analyses are actually undertaken in Chapter 5, all the information regarding the statistical properties of the relevant basic random variables are discussed and analyzed in Chapter 4. The study is concluded in Chapter 6 with an interpretation of the results of the analyses, in accordance with the research objectives.

It is hoped that this research will contribute to the future revision of South African structural codes as well as provide insight into the effect of deterministic assumptions during design on the reliability of prestressed concrete members.

1.7 REFERENCES

1-1 Freudenthal, A.M., Garrelt, J.M. and Shinozuka, M., *The analysis of structural safety*, J Struct Div, Proc ASCE, Vol.92, No.ST1, Feb 1966, pp.267-325.

1-2 Ang, A.H-S. and Cornell, C.A., *Reliability bases of structural safety and design*, J Struct Div, Proc ASCE, Vol.100, No.ST9, Sept 1974, pp.1755-1769.

1-3 Nowak, A.S. and Carr, R.I., *Sensitivity analysis for structural errors*, J Struct Engrg, ASCE, Vol.111, No.8, Aug 1985, pp.1734-1746.

1-4 Kong, F.K., Evans, R.H., Cohen, E. and Roll, F., *Handbook of Structural Concrete*, Pitman Books Limited, London, 1983.

1-5 Milford, R.V., *Risk and structural design*, Civ Eng S Afr, Vol.30, No.12, Dec 1988, pp.569-575.

1-6 Melchers, R.E., *Structural Reliability: Analysis and Prediction*, Ellis Horwood Series in Civil Engineering, Ellis Horwood Ltd., Chichester, 1987.

1-7 Thoft-Christensen, P. and Baker, M.J., *Structural Reliability Theory and its Applications*, Springer-Verlag, Berlin, 1982.

1-8 Canadian Standards Association, *Guidelines for the development of limit states design*, CSA Special Publication S408-1981, Ontario, Dec 1981.

1-9 Milford, R.V., *Target safety and SABS 0160 load factors*, Civ Eng S Afr, Vol.30, No.10, Oct 1988, pp.475-481.

1-10 SABS 0100:1992, *Code of Practice, The Structural Use of Concrete, Part 1: Design*, SA Bureau of Standards, Pretoria, 1992.

1-11 SABS 0160:1989 (as amended 1990), *Code of Practice, The General Procedures and Loadings to be Adopted in the Design of Buildings*, SA Bureau of Standards, Pretoria, 1990.

1-12 Kemp, A.R., Milford, R.V. and Laurie, J.A.P., *Proposals for a comprehensive limit states formulation for South African structural codes*, Civ Eng S Afr, Vol.29, No.9, Sept 1987, pp.351-360.

1-13 Kemp, A.R., *Innovations and implications of new limit states formulation for South African structural codes*, Design of Portal Frames Course, Appendix 2, SA Institution of Steel Construction, 1990.

1-14 Goldstein, A.E., *Changes in SABS 0100: Some Effects on Reinforced Concrete Design*, Concrete Beton, J CSSA, No.62, Feb 1992, pp. 6-10.

1-15 Milford, R.V., *Development of Load Factors for inclusion in SABS 0160 (The General Procedures and Loadings to be Adopted in the Design of Buildings)*, Internal Report 85/11, Structural and Geotechnical Engineering Division, National Building Research Institute, CSIR, Pretoria, Oct 1985.

1-16 Milford, R.V., *A Guide for Calibrating SABS Material Codes*, Internal Report 86/16, Structural and Geotechnical Engineering Division, National Building Research Institute, CSIR, Pretoria, Oct 1986.

1-17 Mirza, S.A. and MacGregor, J.G., *Probabilistic Study of Strength of Reinforced Concrete Members*, Can J Civ Eng, Vol.9, 1982, pp. 431-448.

1-18 Standards Association of Australia, *Guidelines for Conversion to Limit State Codes*, Committee BD/6 - Loading of Structures, Canberra, Jan 1985.

1-19 Nowak, A.S. and Lind, N.C., *Practical Code Calibration Procedures*, Can J Civ Eng, Vol.6, 1979, pp. 112-119.

1-20 Kemp, A.R., *Comparisons of International Loading Codes and Options for South Africa*, Proceedings of the S.A. National Conference on Loading, SAICE, Midrand, South Africa, Sept 1998.

1-21 Ang, A.H-S. and Tang, W.H., *Probability Concepts in Engineering Planning and Design, Vol. 2: Decision, Risk, and Reliability*, John Wiley and Sons, New York, 1984.

1-22 Benjamin, J.R. and Cornell, C.A., *Probability, Statistics, and Decision for Civil Engineers*, McGraw-Hill, New York, 1970.

1-23 Marshall, V. and Robberts, J.M., *Prestressed Concrete: Design and Practice*, Concrete Society of Southern Africa, Halfway House, Oct 1995.

1-24 Collins, M.P. and Mitchell, D., *Prestressed Concrete Basics*, Canadian Prestressed Concrete Institute, Ottawa, 1987.

1-25 Mirza, S.A., Hatzinikolas, M. and MacGregor, J.G., *Statistical Description of the Strength of Concrete*, J Struct Div, Proc ASCE, Vol.105, No.ST6, 1979, pp.1021-1037.

1-26 Mirza, S.A. and MacGregor, J.G., *Variability of Mechanical Properties of Reinforcing Bars*, J Struct Div, Proc ASCE, Vol.105, No.ST5, 1979, pp.921-937.

1-27 Mirza, S.A. and MacGregor, J.G., *Variations in the Dimensions of Reinforced Concrete Members*, J Struct Div, Proc ASCE, Vol.105, No.ST4, 1979, pp.751-766.

1-28 Mirza, S.A., Kikuchi, D.K. and MacGregor, J.G., *Flexural Strength Reduction Factor for Bonded Prestressed Concrete Beams*, ACI J, Vol.77, Jul/Aug 1980, pp. 237-246.

1-29 Naaman, A.E. and Siriaksorn, A., *Reliability of Partially Prestressed Beams at Serviceability Limit States*, PCI J, Vol.27, No.6, Nov/Dec 1982, pp. 66-85.

1-30 Ellingwood, B., Galambos, T.V., MacGregor, J.G. and Cornell, C.A., *Development of a Probability Based Load Criterion for American National Standard A58*, NBS Special Publication 577, National Bureau of Standards, Washington, 1980.

1-31 Mirza, S.A. and MacGregor, J.G., *Probabilistic Study of Strength of Reinforced Concrete Members*, Can J Civ Eng, Vol.9, 1982, pp. 431-448.

1-32 Israel, M., Ellingwood, B. and Corotis, R., *Reliability-Based Code Formulations for Reinforced Concrete Buildings*, J Struct Engrg, ASCE, Vol.113, No.10, Oct 1987, pp. 2235-2252.

1-33 Al-Harthy, A.S. and Frangopol, D.M., *Reliability Assessment of Prestressed Concrete Beams*, J Struct Engrg, ASCE, Vol.120, No.1, Jan 1994, pp. 180-199.

1-34 Chandrasekar, P. and Dayaratnam, P., *Analysis of Probability of Failure of Prestressed Concrete Beams*, Build Sci, Vol.10, 1975, pp. 161-167.

1-35 Floris, C., *Reliability of a Prestressed Concrete Beam: A Comparison between the Methods of Third and Second Level*, Reliab Engrg and Syst Saf, Vol.23, 1988, pp. 1-22.

CHAPTER 2

STRUCTURAL RELIABILITY THEORY

Engineering decisions must be made in the presence of uncertainty arising from imperfect modelling and the inherent randomness in many design parameters. While resistance and loading parameters are non-deterministic, they nevertheless exhibit statistical regularity. This suggests that probability theory should furnish the framework for setting limits of acceptable structural performance. Probability theory and structural reliability methods provide a formal framework to select partial safety factors which will ensure that the probability of unfavourable performance is acceptably small. This affords the possibility for more uniform performance in structures and a reduction in cost where a design appears to be excessively conservative.

Reliability theory has developed rapidly over the last few decades and FOSM methods in particular have received the attention of several researchers and design code institutions. This chapter provides a concise overview of the basic theory.

2.1 BASIC RELIABILITY THEORY

Structural reliability is defined as the probability that the capacity of a structure will be adequate to withstand the lifetime maximum demand. In the initial application of this concept to structural reliability problems the limit state was considered to contain just two basic variables, the resistance R and the load effect Q, dimensionally consistent with R (Ref. 2-1). In order to explicitly represent the significance of uncertainty, both these variables must be modeled as random variables. The failure event is then $R - Q \leq 0$ and the probability of failure p_F is given by Eq. 2-1, on the condition that R and Q are statistically independent. Failure is defined in a generic sense relative to any limit state and does not necessarily imply collapse or other catastrophic events.

$$p_F = P[R - Q \leq 0] = \int_{-\infty}^{+\infty} F_R(q)\, f_Q(q)\, dq \tag{2-1}$$

where F_R = CDF of the resistance R
f_Q = PDF of the load effect Q

Eq. 2-1 is the convolution integral with respect to q and gives the probability of failure p_F as the product of the probabilities of two independent events, namely $F_R(q)$ and $f_Q(q)dq$, summed over all possible joint occurrences (Ref. 2-2). As illustrated in Fig. 2-1, the overlapping of

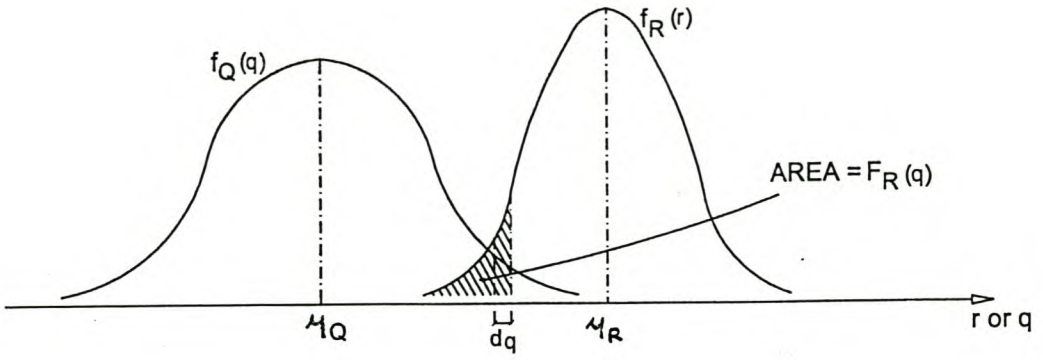

Figure 2-1: Overlapping of resistance and load effect curves.

the curves $f_R(r)$ and $f_Q(q)$ represents a qualitative measure of the probability of failure p_F. The overlap region depends both on the relative positions and the degree of dispersions of $f_R(r)$ and $f_Q(q)$. It follows, therefore, that any measure of reliability ought to be a function of the mean values and standard deviations of the basic variables.

In general, closed-form solutions do not exist for the integral of Eq. 2-1 (Ref. 2-3). There are, however, a number of special cases. For example, if R and Q are independent normally distributed variables, then in terms of the standardised Normal CDF Φ it follows that

$$p_F = \Phi\left[-\frac{\mu_R - \mu_Q}{\sqrt{\sigma_R^2 + \sigma_Q^2}}\right] = 1 - \Phi(\beta) \tag{2-2}$$

$$\beta = \frac{\mu_R - \mu_Q}{\sqrt{\sigma_R^2 + \sigma_Q^2}} \tag{2-3}$$

The expression in Eq. 2-3 is called the *reliability index* and is a useful comparative measure of reliability which can serve to evaluate various design alternatives. It may be observed that the reliability index is defined as the ratio of the mean to the standard deviation of the function R - Q. Eq. 2-4 below states that, if the basic variables are independent and normally distributed, then a direct relationship exists between β and p_F.

$$p_F = 1 - \Phi(\beta) \quad \Leftrightarrow \quad \beta = \Phi^{-1}(1 - p_F) \tag{2-4}$$

Reliability at a particular limit state may involve multiple basic variables. Only in the simplest of cases can the reliability be expressed in terms of only two random variables R and Q. Indeed, the capacity of a structure and the lifetime maximum demand may be functions of several other variables and may not be statistically independent. In particular, the resistance may be a function of material properties and dimensions, while the load effect may be a function of applied loads, densities and dimensions. For such cases the capacity vs. demand problem of Eq. 2-1 must be generalized. For this purpose a mathematical model is first derived, from principles of mechanics and experimental data, which relates material and geometrical properties to structural element behaviour. This model is termed the *performance function* and expresses each limit state in terms of a set of n basic variables X_i which affect structural performance (Ref. 2-4). Suppose this relationship is given by

$$g(\boldsymbol{X}) = g\left(X_1, X_2, \ldots\ldots, X_n\right) \tag{2-5}$$

The *limit state function* is defined by setting $g(\boldsymbol{X}) = 0$ and places a limit on structural performance. Geometrically, the limit state function is an n-dimensional surface, commonly referred to as the failure surface (Ref. 2-4). This surface divides all possible combinations of the basic variables X_i which cause failure from all possible combinations which do not. It follows therefore, for any ultimate or serviceability limit state, that

$g(\boldsymbol{X}) < 0$: the failure region
$g(\boldsymbol{X}) = 0$: the limit state
$g(\boldsymbol{X}) > 0$: the safe region

Hence, if the joint PDF for the vector of basic variables $\boldsymbol{X}$ is known, then the probability of failure can be expressed by Eq. 2-6. This is simply the volume integral of $f_{\boldsymbol{X}}(\boldsymbol{x})$ over the failure region and is illustrated in Fig. 2-2 for the two variable case (Ref. 2-4).

$$p_F = \int_{g(\boldsymbol{X}) < 0} f_{\boldsymbol{X}}(\boldsymbol{x})\, d\boldsymbol{x} \tag{2-6}$$

where $\boldsymbol{X} = \left(X_1, X_2, \ldots\ldots, X_n\right)$

$f_{\boldsymbol{X}}(\boldsymbol{x}) = f_{X_1, X_2, \ldots\ldots, X_n}\left(x_1, x_2, \ldots\ldots, x_n\right)$

It is tacitly assumed that all uncertainties in design are contained in the joint PDF $f_{\boldsymbol{X}}(\boldsymbol{x})$ and Eq. 2-6 therefore provides a basis for quantitatively measuring structural reliability. However, the evaluation of Eq. 2-4 is generally a formidable task. Firstly, due to a general scarcity of data in structural reliability analyses, there is almost never sufficient data to define the joint PDF. Moreover, the limit state function may be highly non-linear in the basic variables. Secondly, the required multi-dimensional integration may be impractical to perform and the

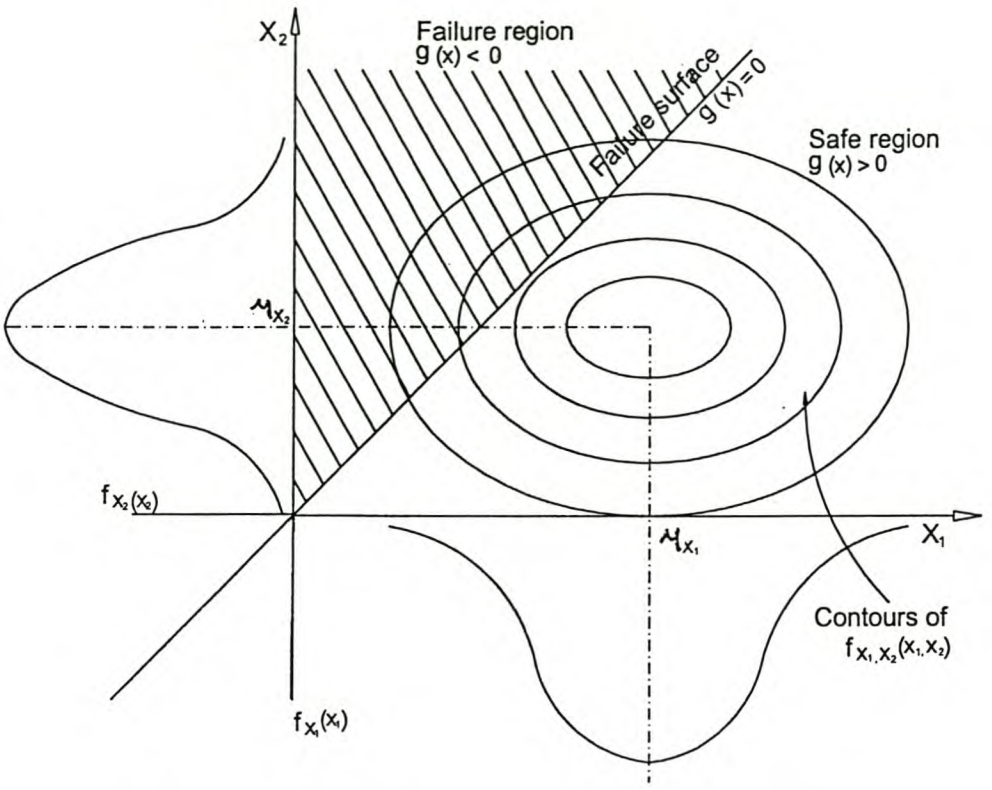

Figure 2-2: Definition of the probability of failure.

analyst must then resort to numerical methods. For practical purposes, alternative methods for evaluating p_F is necessary. These practical methods are dealt with in § 2.2.

Alternatively, Monte Carlo techniques may be used to mathematically simulate the variability in the performance of a family of similar structures. Research efforts reported in the literature often simulate the probability distributions of the strengths of representative members and then calculate their first and second moments. These can be used directly when the limit state function is formulated as a linear combination of resistance and load effect variables. This is a convenient approach when the objective is to derive partial resistance factors.

2.2 SECOND MOMENT FORMULATION

In most cases available data is sufficient only to evaluate the first and second order moments of the basic variables. This has motivated the development of First-Order Second-Moment (FOSM) methods, which represent Level 2 reliability methods in the hierarchy of reliability measures (see § 1.3.2). With the second-moment approach, the reliability may be measured entirely with a function of the first and second order moments, namely with the reliability index β. This can be clearly demonstrated for a linear performance function of independent normally distributed variables, as expressed by Eq. 2-7. Due to the properties of the Normal distribution, $g(X)$ is also normally distributed and the (nominal) reliability index β can be defined as the ratio of the mean to the standard deviation of $g(X)$.

$$g(\boldsymbol{X}) = a_0 + \sum_{i=1}^{n} a_i X_i \tag{2-7}$$

$$\beta = \frac{a_0 + \sum_{i=1}^{n} a_i \mu_{X_i}}{\sqrt{\sum_{i=1}^{n} \left(a_i \sigma_{X_i}\right)^2}} \tag{2-8}$$

In general, however, the performance function is non-linear in X_i and will therefore not be normally distributed. For Eq. 2-4 to be valid, $g(\boldsymbol{X})$ must be linearized by expanding it as a Taylor-series, retaining only the first-order terms (see § 4.2.2). The reliability analysis is then performed with respect to this linearized version. It can be shown that to ensure invariance of p_F with respect to the exact mathematical formulation of the limit state, $g(\boldsymbol{X})$ must be linearized about some point on the failure surface. For this purpose it is appropriate to transform the basic variables X_i into standard normal space (Ref. 2-5). This transformation is given by Eq. 2-9 where the *reduced* variables X_i' has zero mean and unit variance and are therefore symmetrically distributed about the origin.

$$X_i' = \frac{X_i - \mu_{X_i}}{\sigma_{X_i}} \quad , \qquad i = 1, 2, \ldots\ldots, n \tag{2-9}$$

In FOSM methods it is assumed that the failure surface can sensibly be approximated by a tangent hyperplane at the point on the failure surface closest to the origin (Ref. 2-4). This is illustrated in Fig. 2-3 in the reduced variable space. Depending on whether the actual non-linear failure surface is convex or concave towards the origin, this approximation will be conservative or unconservative. As the surface moves relative to the origin, the failure region $g(\boldsymbol{X}) < 0$ increases or decreases accordingly. The position of the failure surface can be represented by the *minimum distance* from the origin in the reduced variable space to $g(\boldsymbol{X}) = 0$ and this may therefore serve as a measure of reliability, as indicated by Eq. 2-10.

$$\beta = \min_{g(\boldsymbol{X}) = 0} \left[\sum_{i=1}^{n} X_i'^2 \right]^{\frac{1}{2}} \tag{2-10}$$

The point on the failure surface corresponding to this minimum distance is called the *most probable failure point* $\boldsymbol{x}'^*$. This set of values will fall in the upper range of the probability distributions for basic variables associated with the load effect Q and in the lower range for basic variables associated with the resistance R. The failure point is determined from Eqs. 2-11 through 2-13, searching for the direction cosines α_i which minimize β. Since the failure point is not known *a priori*, an iterative method must be used, such as that proposed by

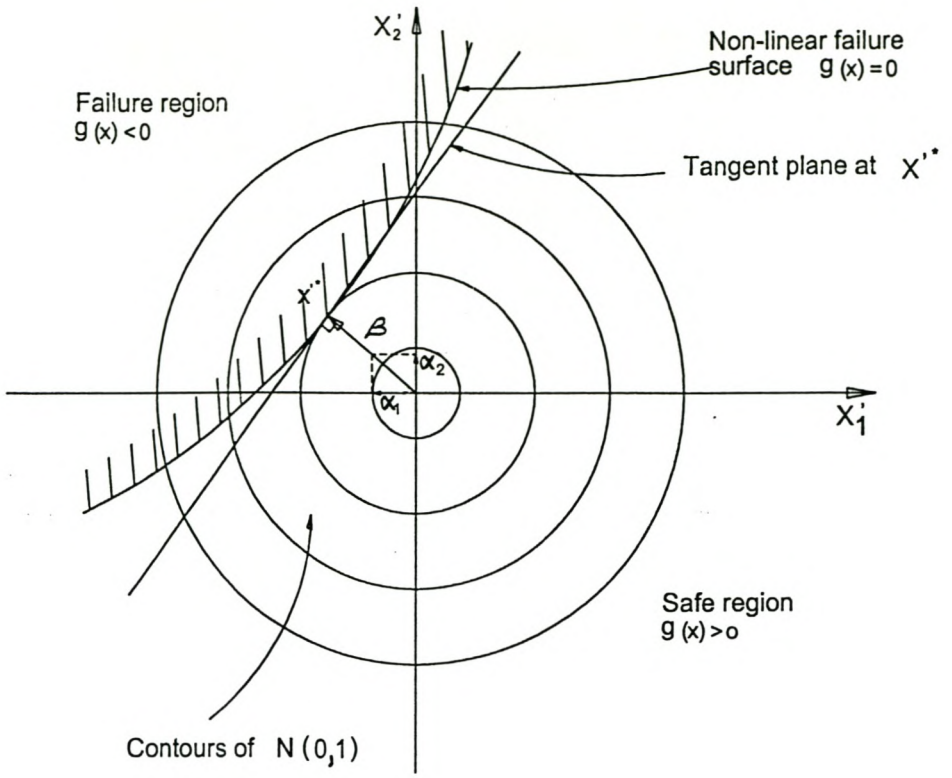

Figure 2-3: Tangent plane to the failure surface.

Rackwitz and Fiessler (Ref. 2-6). The derivatives in Eq. 2-12 are evaluated at x'^* and the solution of Eq. 2-13 then yields β.

$$x_i'^* = -\alpha_i \beta \quad , \qquad i = 1, 2, \ldots\ldots, n \tag{2-11}$$

$$\alpha_i = \frac{\left[\dfrac{\partial g}{\partial X_i'}\right]_*}{\sqrt{\displaystyle\sum_{i=1}^{n}\left[\dfrac{\partial g}{\partial X_i'}\right]_*^2}} \tag{2-12}$$

$$g(x_1^*, x_2^*, \ldots\ldots, x_n^*) = 0 \tag{2-13}$$

where $x_i^* = \mu_{X_i} + \sigma_{X_i} x_i'^* = \mu_{X_i} - \sigma_{X_i} \alpha_i \beta$

The above procedure is equivalent to expanding $g(X)$ as a Taylor-series about $x'^{\star}$, which lies on the failure surface. This is known as Hasofer and Lind's reliability index (Ref. 2-7) and is given by Eq. 2-14.

$$\beta = \frac{-\sum_{i=1}^{n} x_i'^{\star} \left[\frac{\partial g}{\partial X_i'}\right]_{\star}}{\sqrt{\sum_{i=1}^{n} \left[\frac{\partial g}{\partial X_i'}\right]_{\star}^{2}}} \qquad (2\text{-}14)$$

The relative magnitude of the direction cosines along the axes X_i' may be used to indicate those basic variables which contribute significantly to the uncertainty at a particular limit state (see Fig. 2-3). This is an indication of the sensitivity of the reliability to the uncertainty in the various basic variables. For design purposes, partial load and resistance factors γ_i corresponding to a predetermined design criterion may be derived. The most general criterion is to specify a partial safety factor on the nominal value $x_{i,n}$ of each basic variable. For a target reliability β_T, this is tantamount to equating $\gamma_i x_{i,n}$ to the most probable failure point. The relationship between Level 1 and Level 2 reliability methods is therefore established by Eq. 2-15a.

$$\gamma_i = \frac{x_i^{\star}}{x_{i,n}} \qquad (2\text{-}15a)$$

With the aid of Eq. 2-9 and 2-11, it follows that

$$\gamma_i = \left[\frac{\mu_{X_i}}{x_{i,n}}\right]\left(1 - \alpha_i \beta_T V_{X_i}\right) \qquad (2\text{-}15b)$$

where $\frac{\mu_{X_i}}{x_{i,n}}$ = the mean value ratio

V_X = coefficient of variation

For routine designs, however, the design criterion should be in a simple format familiar to designers. Such a format is found in the South African building codes on which this study is based and was expressed in Eq. 1-5 through 1-7.

2.3 EXTENDED FOSM MEDHODS

The FOSM procedure outlined in the previous section is based on the premise that the basic variables X_i are normally distributed and mutually independent. However, many structural problems involve basic variables which are clearly non-normal and which may be correlated. It seems appropriate that this information be incorporated in the analysis in a way that does not require the multidimensional integration of Eq. 2-6 (Ref. 2-1). This can be achieved by transforming the non-normal variables into equivalent normal variables. Furthermore, where the basic variables are correlated, a suitable transformation can be made to eliminate such dependence. Following these transformations, the solution proceeds exactly as previously described in Eq. 2-11 through 2-13.

For a non-normal basic variable, an equivalent normal distribution may be obtained such that the cumulative probability as well as the probability density ordinate of the *equivalent normal* distribution are equal to those of the corresponding *non-normal* distribution at the appropriate point on the failure surface $\boldsymbol{x}^*$ (Ref 2-4). The justification for this lies in the fact that if the normalization takes place at the point where failure is most likely to occur, then the estimate of the probability of failure p_F is likely to be a close approximation of the true probability of failure. Eqs. 2-16a and 2-16b can thus be derived, where the superscript N denotes the first order moments corresponding to the equivalent normal distribution.

$$\sigma_{X_i}^N = \frac{\phi\left\{\Phi^{-1}[F_{X_i}(x_i^*)]\right\}}{f_{X_i}(x_i^*)} \tag{2-16a}$$

$$\mu_{X_i}^N = x_i^* - \sigma_{X_i}^N \Phi^{-1}[F_{X_i}(x_i^*)] \tag{2-16b}$$

where $\mu_{X_i}^N$, $\sigma_{X_i}^N$ = mean and std dev of equivalent Normal distribution

$F_{X_i}(x_i^*)$, $f_{X_i}(x_i^*)$ = orginal CDF and PDF of X_i evaluated at x_i^*

$\Phi(-)$, $\phi(-)$ = CDF and PDF of the standardized Normal distribution

For basic variables that are correlated, the original variables may be transformed to a set of uncorrelated variables (Ref. 2-3). The ability to calculate failure probabilities in accordance with Eqs. 2-11 through 2-13 is thereby retained. The required transformation is necessarily dependent on the covariance matrix of the reduced variables $[C_{X'}]$. It can further be shown that $[C_{X'}]$ is equal to the corresponding correlation matrix of the original variables X_i, as indicated by Eq. 2-17.

$$[C_{X'}] = [\rho_X] = \begin{bmatrix} 1.0 & \rho_{12} & \cdots\cdots & \rho_{1n} \\ \rho_{21} & 1.0 & \cdots\cdots & \rho_{2n} \\ \vdots & \vdots & \cdots\cdots & \vdots \\ \rho_{n1} & \rho_{n2} & \cdots\cdots & 1.0 \end{bmatrix} \tag{2-17}$$

where ρ_{ij} = correlation coefficient between pairs of variables X_i and X_j

Clearly no correlation will exist between any pair of random variables if this matrix is a diagonal matrix. The objective, therefore, is to construct a new set of random variables $\boldsymbol{Y}$, where Y_i are linear functions of X_i, so that the corresponding covariance matrix $[C_Y]$ is a diagonal matrix. According to well-known theorems in linear algebra such a set of uncorrelated variables can be obtained from $\boldsymbol{X}'$ through the orthogonal transformation given by Eq. 2-18 (Ref. 2-4). This transformation represents a rotation of the coordinates from $\boldsymbol{X}'$ to $\boldsymbol{Y}$, where the origin of the $\boldsymbol{Y}$ axes remains the same as that of the $\boldsymbol{X}'$ axes. Again, Hasofer and Lind's reliability index β is defined as the minimum distance from the origin to the failure surface in the $\boldsymbol{Y}$ coordinate system.

$$\boldsymbol{Y} = [T]^{\mathrm{T}} \boldsymbol{X}' \tag{2-18}$$

where $\boldsymbol{Y} = \{ Y_1 , Y_2 , \ldots\ldots , Y_n \}^{\mathrm{T}}$

$\boldsymbol{X}' = \{ X_1' , X_2' , \ldots\ldots , X_n' \}^{\mathrm{T}}$

$[T]$ = transformation matrix (superscript T denotes transpose)

The transformation matrix $[T]$ is composed of the eigenvectors of the covariance matrix $[C_{X'}]$ (see Eq. 2-19), where the eigenvectors $\boldsymbol{V}_i$ are obtained as solutions to Eq. 2-20. It may be emphasized that since the covariance matrix is real and symmetric, the eigenvectors are mutually orthogonal and thus $[T]$ is an orthogonal matrix.

$$[T] = \left[\boldsymbol{V}_1 , \boldsymbol{V}_2 , \ldots\ldots , \boldsymbol{V}_n \right] \tag{2-19}$$

$$\left[C_{X'} - \lambda_i I_n \right] \boldsymbol{V}_i = 0 \tag{2-20}$$

It can subsequently be shown that the eigenvalues of $[C_{X'}]$ are also the variances of the transformed variables $\boldsymbol{Y}$ so that the corresponding covariance matrix is a diagonal matrix.

$$[C_Y] = [T]^T [C_{X'}] [T] = \begin{bmatrix} \lambda_1 & 0 & \cdots & 0 \\ 0 & \lambda_2 & \cdots & 0 \\ \vdots & \vdots & \cdots & \vdots \\ 0 & 0 & \cdots & \lambda_n \end{bmatrix} \tag{2-21}$$

Eq. 2-22 below gives the relationships among the original variables X_i and the transformed variables Y_i and follows from Eqs. 2-18 and 2-9.

$$\boldsymbol{X} = [\sigma_X] [T] \boldsymbol{Y} + \mu_X \tag{2-22}$$

where $$[\sigma_X] = \begin{bmatrix} \sigma_{X_1} & 0 & \cdots & 0 \\ 0 & \sigma_{X_2} & \cdots & 0 \\ \vdots & \vdots & \cdots & \vdots \\ 0 & 0 & \cdots & \sigma_{X_n} \end{bmatrix}$$

and $$\mu_X = \{ \mu_{X_1}, \mu_{X_2}, \ldots\ldots, \mu_{X_n} \}^T$$

These expressions can now be used to write the performance function in terms of the set of uncorrelated transformed variables (see Eq. 2-23). Again, if the distributions of the original variables are non-normal, the corresponding probability of failure may be evaluated using equivalent normal distributions.

$$g(\boldsymbol{X}) = g\left(Y_1, Y_2, \ldots\ldots, Y_n\right) \tag{2-23}$$

2.4 EFFECT OF CORRELATION

The correlation coefficient is frequently used to make deductions about the joint behaviour of two random variables X and Y. If the coefficient is near unity in absolute value, strong dependence is assumed verified; if the coefficient is low, it is concluded that one variable has little or no effect on the other. The correlation coefficient is defined by the covariance of X and Y, normalized by the product of their standard deviations.

$$\rho_{X,Y} = \frac{COV[X,Y]}{\sigma_X \sigma_Y} \tag{2-24}$$

where $-1.0 \leq \rho_{X,Y} \leq 1.0$

In reliability analysis the trend is often towards accounting for complex interrelationships among the components in the resistance and load effect terms of the performance function, while generally disregarding the dependency between the two (Ref. 2-8). This can have a profound effect and is easily illustrated for the linear performance function given below.

$$M = R - Q$$

If the basic variables R and Q are assumed to be normally distributed and with correlation coefficient $\rho_{R,Q}$, then, analogous to Eq. 2-3, the reliability index is given by Eq. 2-25. It is evident that β will take on a maximum value when $\rho_{R,Q} = +1$, and a minimum value when $\rho_{R,Q} = -1$.

$$\beta = \frac{\mu_R - \mu_Q}{\sqrt{\sigma_R^2 + \sigma_Q^2 - 2\rho_{R,Q}\sigma_R\sigma_Q}} \tag{2-25}$$

Setting $V_R = V_Q = V$ and $\frac{\mu_R}{\mu_Q} = \text{CFS}$, where CFS is the central factor of safety, leads to

$$\beta = \frac{\text{CFS} - 1}{V\sqrt{\text{CFS}^2 + 1 - 2\rho\,\text{CFS}}}$$

With $V = 40\%$ and CFS $= 2$ in the above expression, the following results are obtained.

$\rho = 0$: $\beta = 1.12$ and $p_F = 0.131$

$\rho = +1$: $\beta = 2.5$ and $p_F = 0.006$

As an approximation, weak correlation ($\rho < 0.2$) can usually be ignored and the variables treated as independent, whereas strong correlation ($\rho > 0.8$) can usually be treated as fully dependent, with one of the two correlated variables replaced by the other.

2.5 SUMMARY

This chapter dealt with the evaluation of the probability of failure and it was shown that, for a linear limit state function of independent normally distributed variables, the probability of failure can be obtained directly from the reliability index β. For a non-linear limit state function β can still be defined, but only with respect to a tangent hyperplane to approximate the actual non-linear failure surface. In each case β is defined as the minimum distance from the failure surface to the origin in standardized normal space. The corresponding point on the failure surface is called the most probable failure point and must be found by an iteration

routine. This is the essence of the FOSM method through which the complications associated with a full probabilistic presentation of the probability of failure can be avoided.

When more than second-moment information is available for some or all of the basic variables, the FOSM method may still be used, provided that each basic variable is first transformed into an equivalent normal random variable. Similarly, when the basic variables are correlated, an orthogonal transformation must be made to eliminate such dependence. It was shown that correlation among basic variables should not be neglected as it may have a profound effect on the probability of failure.

2.6 REFERENCES

2-1 Ellingwood, B., Galambos, T.V., MacGregor, J.G. and Cornell, C.A., *Development of a Probability Based Load Criterion for American National Standard A58*, NBS Special Publication 577, National Bureau of Standards, Washington, 1980.

2-2 Melchers, R.E., *Structural Reliability: Analysis and Prediction*, Ellis Horwood Series in Civil Engineering, Ellis Horwood Ltd., Chichester, 1987.

2-3 Thoft-Christensen, P. and Baker, M.J., *Structural Reliability Theory and its Applications*, Springer-Verlag, Berlin, 1982.

2-4 Ang, A.H-S. and Tang, W.H., *Probability Concepts in Engineering Planning and Design, Vol. 2: Decision, Risk, and Reliability*, John Wiley and Sons, New York, 1984.

2-5 Melchers, R.E., *Reliability Calculation for Structures*, Civ Engrg Trans, Institution of Engineers, Australia, Vol.CE27, No.1, Feb 1985, pp. 124-129.

2-6 Rackwitz, R. and Fiessler, B., *Structural Reliability under Combined Random Load Sequences*, Computers and Struct, Vol.9, No.5, November 1978, pp. 489-494.

2-7 Hasofer, A.M. and Lind, N.C., *An Exact and Invariant First-Order Reliability Format*, J Engrg Mech Div, Proc ASCE, Vol.100, No.M1, Feb 1974, pp. 111-121.

2-8 Harr, M.E., *Reliability-Based Design in Civil Engineering*, McGraw-Hill, Johannesburg, 1987.

CHAPTER 3

PRESTRESSED CONCRETE DESIGN

The purpose of this chapter is to give an overview of the design aspects relevant to the prestressed concrete member on which the reliability analyses of this study are based. This is done in the context of the prestressed concrete theory that was required to carry out the design. The chapter commences with a motivation for the choice of this particular type of member, then highlights certain aspects of the design philosophy and the relevant material properties, and close with a description of the two limit states of interest, i.e. flexural strength at the ultimate limit state (ULS) and deflections at the serviceability limit state (SLS).

3.1 CHOICE OF MEMBER

The objectives of this thesis required the design of a prestressed concrete member. The choice of the member had to be such that the theoretical models applicable to the limit states of interest would be relatively simple. This would reduce the number of approximations required to enable simple analytical treatment during the subsequent reliability analyses.

A simply supported pretensioned concrete T-beam was chosen as a basis for the reliability analyses. Pretensioning implies a construction method whereby the tendons are bonded to the surrounding concrete. For this study, this had the advantage that friction and anchorage seating losses did not have to be considered during the calculation of prestress losses. Furthermore, the beam was designed as a Class 2 member for which tensile stresses are allowed within certain limits, but with no visible cracking. This had the distinct advantage that the beam was predicted not to have reached its cracking moment under service load conditions. As a result deflection calculations could be based on the assumption of linear elastic behaviour and attention could be focused on the reliability aspects of that limit state and not on the structural response.

The design was carried out strictly in accordance with the provisions of the South African design code of practice for the structural use of concrete SABS 0100-1:1992 (Ref. 3-1), while the design loads were obtained from the loading code SABS 0160:1989 (Ref.3-2). The limit states design method, as briefly set out in § 1.4, was therefore followed and the detailed design calculations are presented in Appendix A of this thesis. The beam section and cable profile as designed are shown in Figure 3-1. The gross section properties of the uncracked beam section are also listed in this figure.

Environmental loads were not considered for the purposes of this study; only gravity loads (i.e. dead and live loads) were included in the design. In addition to its self-weight, the beam

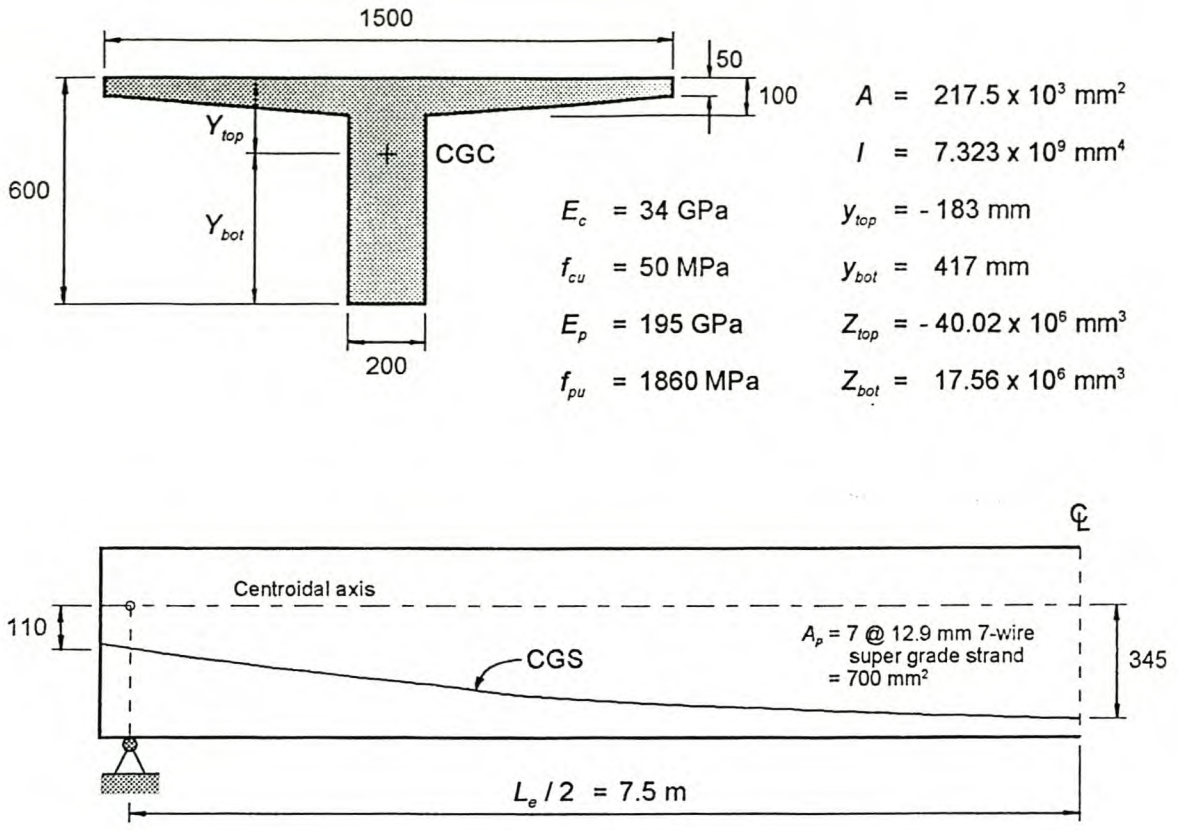

Figure 3-1: Beam section and cable profile.

was designed to support a superimposed dead load of 1.2 kPa, representing finishes, as well as an imposed live load of 3.4 kPa, consisting of office floor loads and partitions. The beam is intended for use in a typical office building over a span of 15 m. The decision about the occupancy type was based on the fact that the statistical analysis of load surveys as reported in the literature deals almost exclusively with imposed floor loads in office buildings (see § 4.3.4). Since the random variation of live load relative to that of dead load has a significant effect on structural reliability, reliability analyses are usually performed as a function of the nominal live to nominal dead load ratio. The analyses of this study are based on a nominal load ratio of 0.70 and the calculated reliability should be seen in this context.

It is assumed that the beam would be prefabricated on site in a precasting yard and that the process would be subject to good control of quality, as intended by SABS 0100-2:1980. Economic considerations dictate that transfer of prestress should occur only a few days after casting of the concrete and this usually requires a period of accelerated curing to ensure a sufficient gain in strength before the time of transfer.

The following assumptions were made regarding the loading history. Transfer of prestress occurs at 3 days after stressing of the tendons and casting of the concrete and only the self-weight of the member and the prestressing force act at this time. The superimposed dead load as well as the sustained component of the total live load (see § 4.3.4) are applied at one

month after the time of transfer (i.e. at 33 days), while the variable component of the live load may act at any time beyond this.

3.2 DESIGN PHILOSOPHY AND PROCEDURE

The normal procedure in limit states design is to design on the basis of the expected critical limit state and then to examine the remaining limit states to check that they are not reached. Generally, the design of Class 1 and Class 2 members is governed by the SLS of cracking (Ref. 3-3). The criteria which limit crack width are stated by SABS 0100-1:1992 (Ref. 3-1) in terms of permissible concrete flexural tensile stresses which may not be exceeded at service load levels. The code also specifies permissible concrete flexural compressive stresses. Therefore, the design of Class 1 and Class 2 members commences with flexural design at the SLS. Note that the magnitude of the permissible concrete stresses imposed by the design code of practice (see § A.2.1) makes it possible to assume a linear elastic uncracked section for purposes of analysis; stresses may therefore be calculated on the basis of standard engineering beam theory (see Eqs. 3-1).

The procedure for flexural design at the SLS, as recommended by Marshall and Robberts (Ref. 3-3), was followed for preliminary design of the prestressed concrete beam (see § A.2) and an overview is presented in the rest of this section. After completion of this preliminary design the beam was analyzed at the ULS of flexure and at the SLS of deflection. The ultimate moment of resistance is checked against the applied external moment at midspan in § A.3, while the deflection is compared with allowable values in § A.4. The appropriate partial load and material factors are also given in these sections. The fact that flexural design at the SLS served as the point of departure for the design of the beam led to a higher than required margin of safety at the (non-critical) limit state of flexure. It was noted in § 1.4 and is again emphasized here that the design criterium at the ULS differs from that at the SLS. At the ULS the design resistance must exceed the design load effect, while at the SLS the deflection must satisfy some arbitrarily chosen design criteria (with a historical background and based on experience). Remaining limit states which were not considered for the purposes of this study but which in practice should be checked that they are not reached are, shear strength at the ULS, bond stress at the ULS, and crack widths at the SLS.

The sign convention followed in the design is defined by the rules listed on the next page. Any deviation from these rules will be self-evident.

- Stress and force are both taken as positive when tensile and negative when compressive.
- A positive bending moment corresponds to a concave deflected shape of the beam while a negative bending moment corresponds to a convex deflected shape.

- Both the eccentricity of the prestressing force and the distance to a particular fibre are always measured from the centroid of the concrete section and are taken positive when below the centroidal axis.

The design process for Class 1 and Class 2 prestressed concrete members differs from that used for reinforced concrete members because a number of critical stages during the design life of the structure, all related to the presence of the prestressing force, can be identified. Of these the following two stages are generally the most important.

- *At transfer of prestress:* Directly after transfer the prestressing force will be acting at its maximum value P_i because the long-term losses have not yet taken place, while the applied external load effect will be acting at its minimum value M_{min} because only the self-weight of the member will be present at this stage. Also, at this stage the concrete has a relatively low strength f_{ci}.

- *Under maximum service loads:* In the presence of the maximum long-term service loads the applied external load effect will be acting at its maximum value M_{max} together with the effective long-term prestressing force P_∞, which represents a minimum value because all the long-term losses would have taken place at this stage. The concrete has reached its long-term strength $f_{c\infty}$ at this stage (see § 3.3.1).

It is important to note that the magnitude of the prestressing force used for stress calculations must reflect the reduction of prestress appropriate to the age of the prestressed concrete member at the stage under consideration. This can conveniently be done in terms of the initial loss factor ζ_i and the long-term loss factor η_∞. The former is defined as the ratio of the initial prestress just after transfer f_{pi} to the ultimate strength of the prestressing steel f_{pu} , and the latter as the ratio of the effective long-term prestress f_{pe} to the initial prestress f_{pi} just after transfer.

Apart from the limitation on the magnitude of the jacking stress (i.e. 75 % of the characteristic ultimate strength), the subsequent loss of prestress can be divided into *instantaneous losses* which take place at the time of transfer, and *long-term losses* which gradually develop with time and are attributed to the time-dependent behaviour of the materials (see § 3.3). For a pretensioned concrete member the instantaneous loss is caused by elastic deformation of the concrete, while the long-term losses are caused by relaxation of the tendons and by creep and shrinkage of the concrete. The initial loss factor ζ_i makes provision for the limitation on the jacking stress as well as for the instantaneous loss, whereas the long-term loss factor η_∞ provides only for the long-term losses.

Any method used for estimating the long-term loss of prestress should account for the complex interaction which exists among the various loss components. This can either be done directly by using a time-step procedure, where the total time under consideration is divided

into successive time steps, or indirectly, by using separate lump sum estimates of the individual loss components which make provision for the interaction among the various components. The latter approach is recommended by SABS 0100-1:1992 (Ref. 3-1) and was followed for the design of the prestressed concrete member.

The objective of flexural design at the SLS of a prestressed concrete member is to select a least weight concrete section, together with the magnitude and eccentricity of the minimum required prestressing force, to satisfy the permissible concrete stresses at all sections along the span, at transfer and under maximum service loads. This may be achieved by using the critical stages described above as the point of departure and by expressing the concrete stress criteria in terms of the following four stress inequality equations.

At transfer of prestress:

$$f_{top,i} = \frac{P_i}{A} + \frac{P_i e}{Z_{top}} + \frac{M_{min}}{Z_{top}} \leq \sigma_{ti} \tag{3-1a}$$

$$f_{bot,i} = \frac{P_i}{A} + \frac{P_i e}{Z_{bot}} + \frac{M_{min}}{Z_{bot}} \geq \sigma_{ci} \tag{3-1b}$$

Under maximum service loads:

$$f_{top,\infty} = \frac{\eta_\infty P_i}{A} + \frac{\eta_\infty P_i e}{Z_{top}} + \frac{M_{max}}{Z_{top}} \geq \sigma_{c\infty} \tag{3-1c}$$

$$f_{bot,\infty} = \frac{\eta_\infty P_i}{A} + \frac{\eta_\infty P_i e}{Z_{bot}} + \frac{M_{max}}{Z_{bot}} \leq \sigma_{t\infty} \tag{3-1d}$$

where $f_{top,i}$, $f_{bot,i}$ = stress in the extreme top and bottom fibres, respectively, at transfer

$f_{top,\infty}$, $f_{bot,\infty}$ = stress in the extreme top and bottom fibres, respectively, under maximum service loads

σ_{ti} , σ_{ci} = permissible tensile and compressive stresses, respectively, at transfer

$\sigma_{t\infty}$, $\sigma_{c\infty}$ = permissible tensile and compressive stresses, respectively, under maximum service loads

Z_{top}, Z_{bot} = section modulus, with respect to the extreme top and bottom fibre, respectively

The design process basically involves a manipulation of the four stress inequality equations and the following steps are required (Ref. 3-3).

- Estimate the minimum required section properties in terms of the section moduli Z_{top} and Z_{bot} , and select a satisfactory concrete section.

- Construct the Magnel diagram (which represents a geometric interpretation of the four inequality equations) and select values from the feasibility domain for the initial prestressing force P_i and the eccentricity e of the prestressing force at the midspan section.

- Determine the permissible *cable zone*, and place the cable so that it falls within this zone to ensure that nowhere along the span will the permissible concrete stresses be exceeded.

- All the calculations required for the previous steps require that a value for η_∞ be assumed initially, because the prestress losses can only be evaluated after completing the third step. In this step, the prestress losses are calculated at each section of interest.

- Once the prestress losses have been calculated, the concrete stresses must be checked at a representative number of sections along the span to ensure that none of the permissible values are exceeded. The prestress losses calculated in the previous step must be used in these calculations.

The above steps were carried out in § A.2 and led to the beam section shown in Figure 3-1. The materials of construction were assumed to be high quality concrete with a characteristic cube strength of 50 MPa and 12.9 mm diameter 7-wire super grade strand (see § A.1.3). The prestressing force is provided by seven strands with a total nominal area of 700 mm^2 and stressed initially to 75 % of their characteristic ultimate strength. The initial prestressing force at midspan was predicted to reduce in time to the long-term effective prestressing force as follows.

$$\zeta_i = \frac{f_{pi}}{f_{pu}} = 0.706$$

$$\therefore \quad P_i = -\zeta_i f_{pu} A_p = -919.8 \text{ kN}$$

$$\eta_\infty = \frac{f_{pe}}{f_{pi}} = 0.839$$

$$\therefore \quad P_\infty = -\eta_\infty f_{pi} A_p = -771.6 \text{ kN}$$

Though not practical in the case of pretensioned concrete, a parabolic cable profile was selected for the purposes of this study. This significantly simplifies the theoretical model for deflection (see, for instance, Ref. 3-3, Table 8-1) and can be closely approximated with a harped profile. With two draping points at, say, $0.4L$ and $0.6L$ along the span, the profile will fall within the permissible cable zone (see § A.2.5). The concrete stress criteria imposed

by the code was shown to be satisfied at all sections along the span. The distribution of bending moment due to the prestressing force and the applied external loads at transfer and under maximum service loads is shown in Figure 3-2.

It should be noted that it is theoretically more correct to base the calculation of concrete stresses on the transformed section properties, which take account of the presence of the prestressing steel. Furthermore, a distinction should be made between the transformed section properties used for calculating stresses induced at transfer and those for calculating stresses induced by the maximum service loads. In both cases the transformed section properties should reflect the effects of creep of the concrete and relaxation of the prestressing steel at that stage. This is done by using an effective modulus of elasticity for both the concrete and prestressing steel when assessing the modular ratio used in the calculation of the transformed section properties.

However, stress calculations are usually carried out using the properties of the gross concrete section only. This approach greatly simplifies the calculations, under normal circumstances provides a close approximation, and for bonded construction will always be conservative. For these reasons the properties of the gross concrete section were used for the purposes of this study.

3.3 MATERIAL PROPERTIES

The materials of construction were assumed to be high quality concrete and 7-wire super grade strand. The relevant mechanical properties of these materials are briefly outlined in the sections below, while their variability is discussed in § 4.4. The statistical properties quoted in that paragraph were collected from available literature and are subject to the following assumptions (Ref. 3-4).

- The concrete properties and dimensions correspond to good quality construction, as applicable to precast, pretensioned concrete beams.

- The prestressing steel is assumed to be drawn from a population representing all sources of reinforcement, rather than a specific mill or area.

- The material strengths are representative of lower loading rates than those generally used during material tests.

- Long-term strength changes of the concrete and steel due to increasing maturity of the concrete and possible future corrosion of the reinforcement is ignored. This aspect is however further investigated in § 3.3.1.

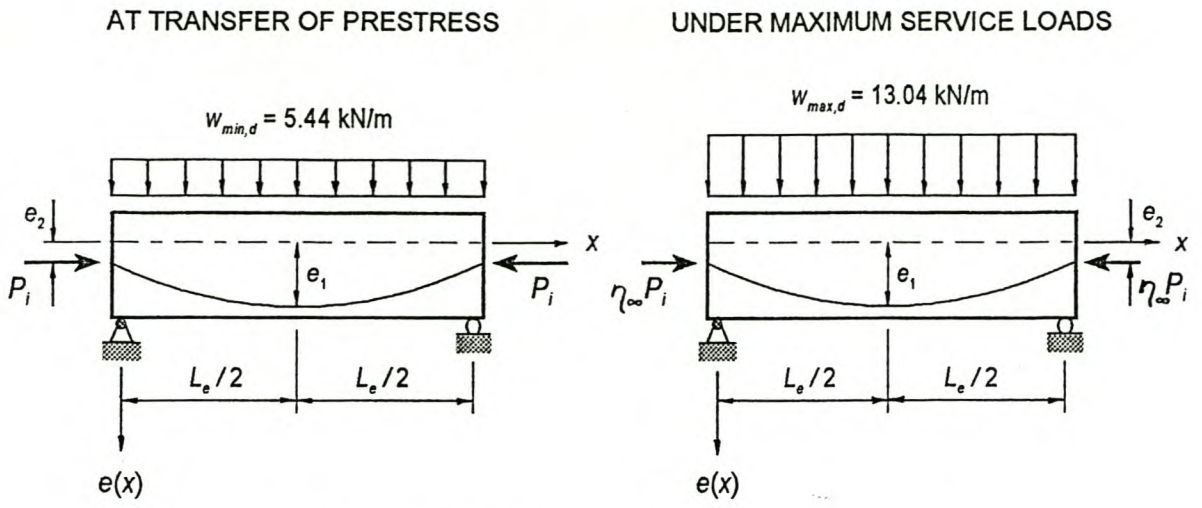

$$e(x) = 4 / L_e^2 \, (e_2 - e_1) \, x^2 + 4 / L_e \, (e_1 - e_2) \, x + e_2$$

(a) Loads acting on prestressed concrete member

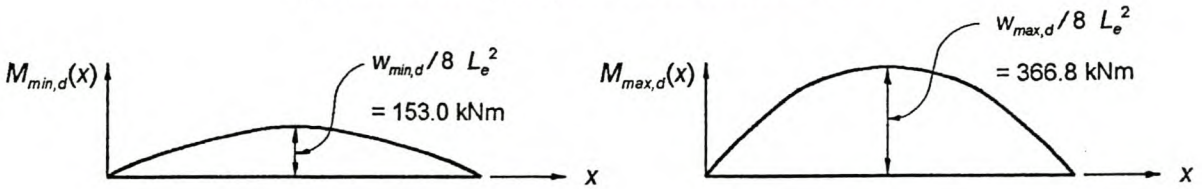

$$M_{min,d}(x) = w_{min,d} / 2 \; x \, (L_e - x)$$

$$M_{max,d}(x) = w_{max,d} / 2 \; x \, (L_e - x)$$

(b) BM due to min. and max. applied external design loads

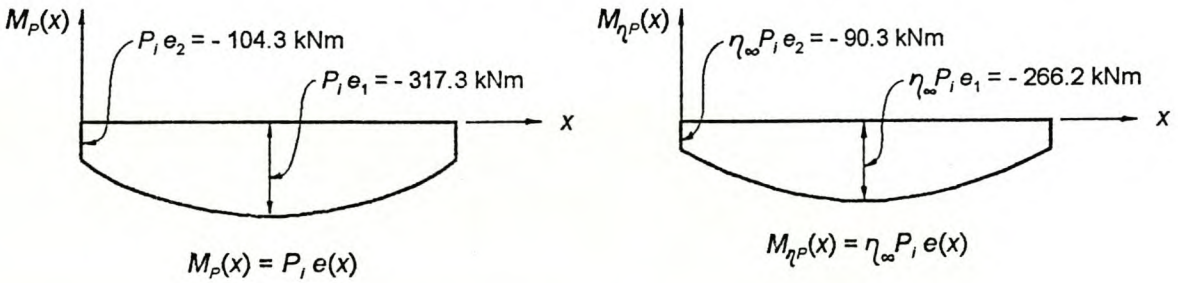

$$M_P(x) = P_i \, e(x)$$

$$M_{\eta P}(x) = \eta_\infty P_i \, e(x)$$

(c) BM due to max. and effective long-term prestressing force

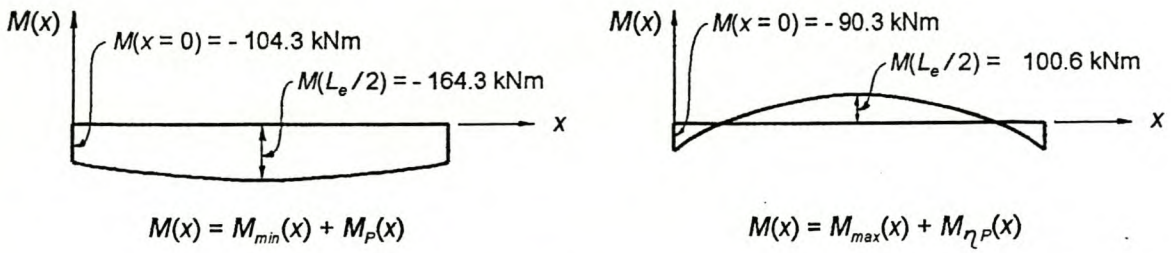

$$M(x) = M_{min}(x) + M_P(x)$$

$$M(x) = M_{max}(x) + M_{\eta P}(x)$$

(d) Combined BM at transfer and under max. service loads

Figure 3-2: Distribution of bending moment.

3.3.1 Concrete

The compressive strength of concrete is easy to determine and many other mechanical properties required for the design of prestressed concrete members can be expressed in terms of this property. The compressive strength can be obtained from standard testing procedures and gives reasonably consistent results. It is therefore used extensively for quality control purposes. It should be noted that the measured results depend on the test method and that they can only be regarded as an index of strength for applications in structural design.

The design of the prestressed concrete member was based on the assumption that normal density concrete with a characteristic cube strength of 50 MPa at 28 days is specified and that the concrete would reach a strength of 32.5 MPa at transfer of prestress to accommodate the high flexural and bond stresses at that time, i.e.

$$f_{cu} = 50.0 \text{ MPa} \qquad \text{and} \qquad f_{ci} = 32.5 \text{ MPa}$$

Because of micro-cracking which occurs at the aggregate-paste interfaces, concrete in uniaxial compression exhibits a non-linear stress-strain behaviour over the entire loading spectrum (Ref 3-3). It is important to note, however, that the stress-strain relationship of concrete acting in *flexure* differs from that of concrete acting in direct compression. The most notable research in this regard was carried out by Hognestad *et al* (Ref. 3-5). The South African design code of practice SABS 0100-1:1992 (Ref. 3-1) recommends the use of a parabolic-rectangular stress-strain relationship for concrete acting in flexure, where the *in situ* flexural strength f_{co} is obtained by applying a concrete strength reduction factor c_1 of which the nominal value is 0.67.

$$f_{co} = c_1 f_{cu} \tag{3-2}$$

The concrete strength reduction factor takes account of the following considerations:

- the differences between cube strengths (i.e. direct compression) and experimentally obtained flexural strengths for eccentrically loaded beam specimens,
- the difference between laboratory control and quality control on site, and
- the fact that the *in situ* loading rate is lower than that during material tests.

Provided that it is properly cured, the compressive strength of concrete increases with time due to continued hydration. Conservative estimates of this gain in strength ranges between 20 % and 40 %. On the other hand, the compressive strength can be reduced by as much as 20 % if the load is applied over several months (Ref. 3-6). This reduction in strength caused by long-term loading is usually ignored in design because the unconservative consequence of this assumption is more than offset by the usual design practice according to which a design

is based on the 28 day strength, which ignores the significant time-dependent strength increase which occurs after 28 days (Ref. 3-3).

However, it is an objective of this thesis to evaluate the effect of the gain in strength beyond 28 days on the reliability of a prestressed concrete member at the limit states of interest (the effect of strain-hardening of the prestressing steel at the ULS on the level of reliability might be considered in a similar manner). The South African design code of practice SABS 0100-1:1992 recognizes the long-term gain in concrete strengths (see Ref. 3-1, Table 28), and in particular requires that concrete with a characteristic cube strength of 50 MPa at 28 days should reach a long-term cube strength value of 58 MPa. This implies a nominal value of 1.16 for c_2 , the long-term concrete cube strength factor.

$$f_{c\infty} = c_2 f_{cu} \tag{3-3}$$

The stress-strain response of concrete in uniaxial tension is nearly linear up to cracking, which occurs at relatively low stresses. Various standard testing procedures are available from which the tensile strength may indirectly be measured, but these results should only be viewed as an index of the real tensile strength and can only be used as comparative measures. The tensile strength of concrete is usually expressed as a function of the compressive strength and SABS 0100-1:1992 (Ref. 3-1) gives the following expression for the modulus of rupture.

$$f_r = 0.65\sqrt{f_{cu}} \tag{3-4}$$

The initial portion of the ascending branch of the stress-strain relationship of concrete may be seen to be approximately linear. Concrete can therefore be approximated as a linear elastic material at service load levels, because the magnitude of the induced stresses generally fall within this quasi-linear range. For a given aggregate type, the modulus of elasticity of concrete increases with an increase in compressive strength. Since this is often the only property of the concrete available at the design stage, the modulus of elasticity is usually correlated with the compressive strength. Nominal values of the secant modulus of elasticity at 28 days and at the time of transfer were obtained from SABS 0100-1:1992 (Ref. 3-1) as functions of the concrete cube strengths at these times, as follows.

$$E_c = 34.0 \text{ GPa} \qquad \text{and} \qquad E_{ci} = 28.8 \text{ GPa}$$

As the concrete gains strength beyond 28 days the modulus of elasticity also increases. As a function of the long-term cube strength, a value of 37.4 GPa was obtained from Fulton's Concrete Technology (Ref. 3-7, Fig. 7-17) for the long-term secant modulus of elasticity. This gives a nominal value of 1.10 for c_3 , the long-term concrete modulus factor.

$$E_{c\infty} = c_3 E_c \tag{3-5}$$

When concrete is subjected to a sustained stress, the resulting strain can be divided into three components, i.e. the instantaneous elastic strain, shrinkage strain and creep strain. Shrinkage strain may be defined as that part of the time-dependent strain which, in the absence of temperature variations, is independent of stress, while creep strain is that component which is dependent on the applied stress. Creep and shrinkage of concrete can be ascribed to the movement of moisture within the crystalline structure of the cement paste and loss of moisture to the surrounding environment by evaporation.

When the sustained stress falls within the service load range, then, based on linear creep theory, the conventional creep factor ϕ_c is defined as the ratio of the creep strain ε_{cc} to the instantaneous elastic strain ε_c (see Eq. 3-6). The creep factor can be established experimentally from standard prism tests, or, for design purposes may be calculated from Eq. 3-7 at any age after casting of the concrete (Ref. 3-6).

$$\phi_c = \frac{\varepsilon_{cc}}{\varepsilon_c} \tag{3-6}$$

$$\phi_c(t) = 3.5\,k \left[1.58 - \frac{H}{120}\right] t_i^{-0.118} \frac{(t - t_i)^{0.6}}{10 + (t - t_i)^{0.6}} \tag{3-7}$$

where t = age of concrete after casting (days)
t_i = 3 days, the age of concrete at initial loading
k = factor related to volume/surface ratio of beam
H = ambient relative humidity (%)

For the purposes of this study, the long-term creep factor $\phi_{c\infty}$ and the creep factor ϕ_{ct} at the time of construction of partitions and application of finishes (see § 3.1) were calculated from Eq. 3-7, based on the assumption of an ambient relative humidity of 60 % (valid for most inland areas).

$$\phi_{c\infty} = 3.04 \quad \text{and} \quad \phi_{ct} = 1.23$$

3.3.2 Reinforcement

For reasons of simplicity the reinforcement of the prestressed concrete member consists of prestressing steel only. In practice, however, non-prestressed reinforcement (e.g. hot-rolled high yield steel) is usually required as shear reinforcement, as supplementary reinforcement for crack control and to satisfy strength requirements in the case of partially prestressed concrete. The material used for prestressing is high tensile strength steel which exhibits a larger tensile strength than hot-rolled high yield steel, but is less ductile. The mechanical properties of prestressing steel can be determined from tests on axially loaded specimens,

since the reinforcement in prestressed concrete members is usually subjected to an almost uniaxial state of stress.

It was assumed for the purposes of design that 12.9 mm diameter 7-wire super grade (low relaxation) strand is specified for which the characteristic ultimate strength f_{pu} is 1860 MPa. The South African design code of practice SABS 0100-1:1992 (Ref. 3-1) recommends that the actual stress-strain behaviour of the prestressing steel is approximated with a tri-linear curve, which ignores the effects of strain-hardening. The stress-strain response of prestressing steel does not show a definite yield plateau, but the code defines the yield strength f_{py} as the characteristic ultimate strength divided by the partial material factor for steel. Furthermore, the code does not specify a value for the maximum strain at fracture ε_{pu}, but this may be taken between 5% and 6.5%. The modulus of elasticity of the prestressing steel E_p is independent of strength, but vary slightly depending on the type of steel. SABS 0100-1:1992 (Ref. 3-1) suggests a nominal value of 195 GPa for 7-wire strand.

Relaxation of the prestressing steel may be defined as the time-dependent loss of tensioning force required for maintaining a constant strain in a highly stressed steel tendon. The potential relaxation loss can be reduced by strain-tempering, which involves heat treatment under tension. This process does not only remove the significant residual stresses which arises during the manufacturing process, but also yields low relaxation steel. A large part of the relaxation loss occurs within a relatively short time period after application of the load and proceeds with time, but at a decreasing rate.

3.4 FLEXURAL STRENGTH AT ULS

By making use of equilibrium requirements and the basic assumptions listed in § 3.4.1 below, the model required to predict the flexural strength of the prestressed concrete member at the ULS is derived in § 3.4.2. The design resistance is calculated based on the characteristic concrete strength at 28 days as well as on the long-term concrete strength and these are then compared with the design load effect, as required by the limit states design method. It should be noted that interest lies only in the maximum moment that the section can resist when the concrete fails in compression, i.e. the ultimate moment of resistance, and not in the complete moment-curvature response over the full range of loading.

3.4.1 Basic Assumptions

The flexural analysis of the prestressed concrete beam section is based on the following basic assumptions (Ref. 3-1).

- The design resistance is calculated by scaling down the characteristic material strengths with the following partial material factors, for the concrete and prestressing steel respectively.

$\gamma_{mc} = 1.50$ and $\gamma_{ms} = 1.15$

- The strain distribution in the concrete is derived from the assumption that plane sections before bending remain plane after bending (i.e. the Bernoulli/Navier hypothesis). This implies that a linear relationship exists between the strain in a fibre and its distance from the neutral axis and that the strain is uniform over the width of the section.

- Since the actual stress-strain relationship for concrete acting in flexure is usually difficult to determine and to deal with computationally, the stress distribution in the compression zone of the member at ultimate is represented by an equivalent rectangular stress-block (see Fig. 3-3). Stress-block factors α_1 and β_1 are used such that the magnitude and line of action of the resultant compressive force are the same as that for the actual stress-strain relationship. The following values are used for rectangular sections.

$$\alpha_1 = \frac{c_1}{\gamma_{mc}} = \frac{0.67}{1.50} = 0.45 \quad \text{and} \quad \beta_1 = 0.9$$

- Failure of the section is defined in terms of a limiting strain ε_{cu} being reached in the concrete at the extreme compression fibre when the concrete fails in compression (see § 3.4.4). This ultimate strain is a function of the concrete strength, decreasing with an increase in strength. However, a constant value of - 0.0035 is recommended for ε_{cu} , irrespective of the concrete strength (see Fig. 3-3).

- The tensile strength of the concrete is neglected because its influence on the ultimate moment of resistance is small. At sections containing flexural cracks no tensile stresses exist in the concrete adjacent to the cracks, while between the cracks tensile stresses are introduced into the concrete by the bonded prestressing steel. However, flexural failure of a member will typically occur at a section containing a crack where the influence of the remaining concrete in tension is small.

- For design purposes the stress-strain relationship for the prestressing steel is approximated with a tri-linear curve, which ignores the effect of strain-hardening.

- Since the prestressing steel is bonded to the surrounding concrete, the change in strain in the steel is assumed to be equal to the calculated change in strain in the concrete at the level of the steel.

3.4.2 Design Resistance

An expression can be derived for the design value $M_{u,d}$ of the ultimate moment of resistance of the prestressed concrete member by considering equilibrium of forces and moments at the critical section (Refs. 3-3 and 3-8). These requirements are expressed by Eqs. 3-8 and 3-9, respectively (see Fig. 3-3). The critical section is located at midspan in the case of a symmetrically loaded simply supported beam.

$$T_p = C \tag{3-8}$$

$$M_{u,d} = T_p z \tag{3-9}$$

The tensile force T_p acting in the prestressing steel at ultimate is calculated from Eq. 3-10, while the compressive force C acting in the compression zone of a rectangular section at ultimate is obtained from Eq. 3-11, where the volume of the equivalent rectangular stress prism is evaluated. The lever arm z between the two forces T_p and C is given by Eq. 3-12.

$$T_p = f_p A_p \tag{3-10}$$

$$C = \alpha_1 f_{cu} b \beta_1 x \tag{3-11}$$

$$z = d - \beta_1 \frac{x}{2} \tag{3-12}$$

where f_p = stress in prestressing steel
A_p = cross-sectional area of prestressing steel
f_{cu} = characteristic concrete cube strength at 28 days (for simplicity, the absolute value is taken here)
b = width of flange of beam section
x = depth to the neutral axis
d = effective depth to prestressing steel

All quantities can be directly calculated if the depth to the neutral axis x at ultimate is known. If an assumption is made about the range within which the strain in the prestressing steel ε_p lies at the ultimate condition, the stress in the prestressing steel at ultimate f_p corresponding to this value of ε_p can be determined from the stress-strain relationship for the steel. This then allows the depth to the neutral axis x to be solved from Eq. 3-8. The assumption must, however, be checked using the calculated value of x. The ultimate strain in the prestressing steel consists of the following components (see § A.3.2).

$$\varepsilon_p = \varepsilon_{cp} - \varepsilon_{ce} + \varepsilon_{pe} \tag{3-13}$$

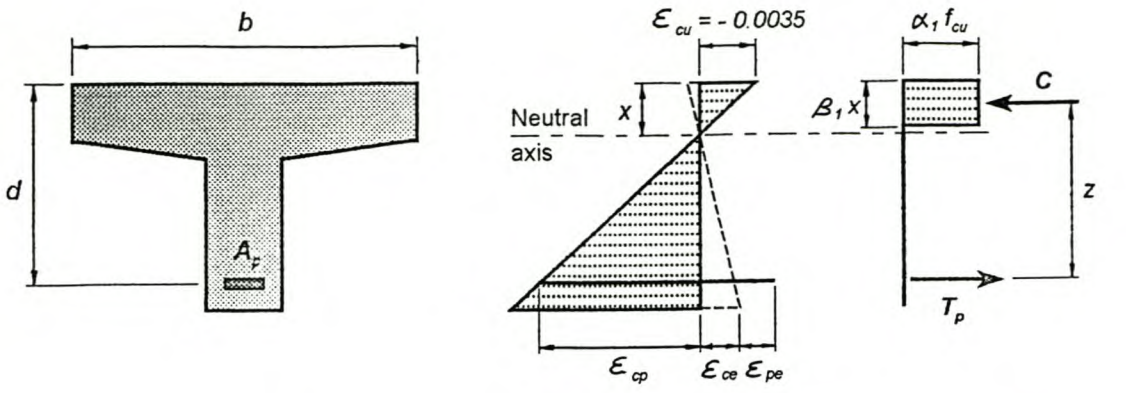

(a) beam section

(b) concrete and steel strain at ultimate

(c) stress at ultimate

Figure 3-3: Assumed strain and stress distribution at ULS.

where ε_{pe} = the tensile strain induced in the prestressing steel by the effective long-term prestress f_{pe} , which includes all losses

ε_{ce} = compressive strain in the concrete at the level of the prestressing steel, induced by f_{pe} acting alone on the elastic uncracked section

ε_{cp} = the change in the strain in the prestressing steel caused by the application of the external moment and is equal to the strain in the concrete at the level of the prestressing steel

For an underreinforced section (see § 3.4.4), which represents most beam sections encountered in practice, the assumption can safely be made that the strain in the prestressing steel ε_p has exceeded the yield strain ε_{py} at the ultimate condition. In this case, from the stress-strain relationship for the steel, f_p may be set equal to f_{py} and the depth to the neutral axis can then be solved from Eq. 3-8 as follows.

$$x = \frac{f_{py} A_p}{\alpha_1 f_{cu} b \beta_1} \tag{3-14}$$

When this result, together with Eqs. 3-10 and 3-12, is substituted into Eq. 3-9, a closed-form solution for the ultimate moment of resistance is obtained, as expressed by Eq. 3-15a. Note that this expression conforms to the general formulation of design resistance (with $\phi_l = 1.0$) as specified by SABS 0160:1989 (Ref. 3-2) and stated in Eq. 1-6.

$$M_{u,d} = f_{py} A_p \left[d - \frac{f_{py} A_p}{2 \alpha_1 f_{cu} b} \right] \qquad (3\text{-}15a)$$

where $f_{py} = \frac{f_{pu}}{\gamma_{ms}}$ and $\alpha_1 = \frac{c_1}{\gamma_{mc}}$

In § A.3.2 the depth to the neutral axis was calculated from Eq. 3-14 as 37.26 mm, based on the initial assumption that the prestressing steel has yielded (i.e. $\varepsilon_p > \varepsilon_{py} = 0.0133$). This value of x indicated that the compression zone falls entirely within the flange. The value of ε_p corresponding to this value of x was subsequently calculated from Eq. 3-13 as 0.05222, which confirmed the assumption. Finally, the design value of the ultimate moment of resistance was calculated from Eq. 3-15a.

$$M_{u,d} = 578.6 \text{ kNm}$$

A minor modification to Eq. 3-15a results in Eq. 3-15b below, where cognisance is taken of the long-term gain in concrete strength.

$$M_{u,d} = f_{py} A_p \left[d - \frac{f_{py} A_p}{2 \alpha_1 f_{c\infty} b} \right] \qquad (3\text{-}15b)$$

where $f_{c\infty} = c_2 f_{cu}$

This expression was used in § B.1.1 to calculate the long-term ultimate moment of resistance. It is well known from experience that the ultimate moment capacity is relatively insensitive to variations in the concrete strength (compared to, for example, the depth to the reinforcement). This is confirmed in § 5.2.3. Only a marginal increase above the previous value is therefore to be expected.

$$M_{u,d} = 581.3 \text{ kNm}$$

3.4.3 Design Load Effect

In terms of the general criterion of the limit states design method stated by Eq. 1-5, the design value $M_{u,d}$ of the ultimate moment of resistance must exceed the design value M_d of the applied external moment at the critical section at the ULS of flexure. In accordance with Eq. 1-7, the design load effect at midspan is given by Eq. 3-16, where nominal values of the applied dead and live load moments ($M_{D,n}$ and $M_{L,n}$, respectively) are obtained with the aid of the nominal loadings specified by SABS 0160:1989 (Ref. 3-2).

$$M_d = \gamma_c\left(\gamma_{fD} M_{D,n} + \gamma_{fL} M_{L,n}\right) = 473.3 \text{ kNm} \qquad (3\text{-}16)$$

where $\gamma_{fD} = 1.2$, $\gamma_{fL} = 1.6$ and $\gamma_c = 1.0$

The design resistance therefore exceeds the design load effect as required, albeit by a considerable margin (approximately 22 %). This is a consequence of the fact that the ULS of flexure represents a non-critical limit state for the prestressed concrete member of this study, as pointed out in § 3.2.

At the ULS, the product of the partial dead and live load factors (γ_{fD} and γ_{fL}, respectively) with their respective nominal dead and live load effects reflect the lifetime maximum values of these load effects, as was indicated in § 1.4.2. Furthermore, since the prestressed concrete member is subjected to only one time-varying load, i.e. the live load, Eq. 3-16 represents the only load combination that needs to be considered at the ULS of flexure (see § 4.3.2).

3.4.4 Mode of Failure in Flexure

The mode in which a given prestressed concrete beam section with bonded tendons fails in flexure depends on the amount of steel provided, and three possible types can be identified (Ref. 3-3), as follows.

- *Very lightly reinforced sections*: This represents an extremely brittle type of failure in which the prestressing steel fractures immediately after the concrete has cracked (at failure: $\varepsilon_p = \varepsilon_{pu}$). This failure mode is highly undesirable and such sections are not frequently encountered in practice.

- *Underreinforced (moderately) sections*: Failure is induced by crushing of the concrete compression zone (when $\varepsilon_{cu} = -0.0035$) after the prestressing steel has yielded and undergone a large non-linear elongation (at failure: $\varepsilon_{py} < \varepsilon_p < \varepsilon_{pu}$). Becuase of its ductility, this type of failure is highly desirable and it is conventional design practice to proportion flexural members as underreinforced sections.

- *Overreinforced sections*: In this case failure is induced by crushing of the concrete (when $\varepsilon_{cu} = -0.0035$) prior to yielding of the prestressing steel and takes place suddenly once the ultimate moment capacity has been reached (at failure: $\varepsilon_p < \varepsilon_{py}$). This failure mode is undesirable due to its brittle nature.

The prestressed concrete member which forms the basis of this thesis can be classified as an underreinforced section. The design calculations in § A.3.3 indicate that the ultimate moment of resistance is preceded by the cracking moment and that the prestressing steel has undergone a large non-linear elongation at the time when the concrete fails in compression. Also, the prestressing steel ratio is equal to 0.09 % and is smaller than the balanced steel

ratio of 0.26 %. The balanced steel ratio marks the transition from an underreinforced section to an overreinforced section.

3.5 DEFLECTIONS AT SLS

Normally, a prestressed concrete beam is designed on the basis of flexure, either at the SLS or at the ULS, after which compliance with other serviceability criteria is ensured. Deflection is frequently the most important SLS and need to be checked explicitly. A theoretical model is presented in § 3.5.1 for calculation of deflection of a prestressed concrete beam, uncracked in flexure. Based on the nominal modulus of elasticity of the concrete at 28 days as well as on its long-term value, design values δ_d of the deflection at the critical section are calculated for the prestressed concrete member of this study and these are then compared in § 3.5.2 to the allowable value δ_a, as specified by SABS 0100-1:1992 (Ref. 3-1).

The approach to be followed for the calculation of deflection depends on whether the member is uncracked or cracked under maximum service loads (Ref. 3-3). The prestressed concrete member of this study was designed as a Class 2 member and, as shown below, the design calculations in § A.3.3 indicate that the cracking moment M_{cr} exceeds the applied moment M_{max} due to the maximum service loads. The cracking moment is usually taken as the externally applied moment which, by elastic theory, induces a tensile strain in the extreme fibre equal to the modulus of rupture. It may be used to indicate the end of uncracked section behaviour and the onset of cracked section behaviour.

$$M_{cr} = 409.3 \text{ kNm} > 366.8 \text{ kNm} = M_{\max}$$

Before cracking, deflection of a prestressed concrete member may be calculated on the basis of the gross uncracked section. In addition, calculations can be based on the assumption of linear elastic behaviour of the materials and the total deflection may therefore be obtained by superposition of the various increments of deflection (see § 3.5.1). However, if the member is cracked in flexure, its flexural stiffness is reduced, and the calculation of deflection becomes more complicated. In this case, the second moment of area of the gross concrete section must be replaced by an effective second moment of area, which accounts for the extent of cracking and the effect of tension-stiffening over the span of the beam. Furthermore, even though the material properties are assumed to be linear elastic, the moment-curvature relationship, as influenced by the flexural stiffness, is non-linear and the principle of superposition therefore does not apply.

The long-term deflection of a cracked prestressed concrete member cannot be expressed by a single analytical function. The deflection model representing the response of such a member therefore requires that the reliability analysis be performed numerically. However, these difficulties are avoided by the selection of a Class 2 member as basis of this study. In practice, however, the deflection of prestressed concrete members are often governed by their

cracked section properties. Nevertheless, the main objective of this thesis can still be achieved at the SLS of deflection, in that the reliability analysis will indicate the important areas of uncertainty pertinent to the design of a Class 2 prestressed concrete member.

The deflection of a prestressed concrete member must be investigated at various stages during the design life of the structure. For the prestressed concrete member of this study, deflection at the SLS was controlled by that part which is associated with damage to partitions and finishes (see § A.4). For the purposes of the reliability analyses to be undertaken in Chapter 5, interest therefore only lies in that component of the total deflection which takes place after the construction of partitions and the application of finishes, as expressed by Eq. 3-17.

$$\delta_d = \delta_\infty - \delta_t \tag{3-17}$$

where δ_d = deflection affecting partitions and finishes
δ_∞ = total long-term deflection under service loads
δ_t = deflection before construction of partitions and application of finishes

For design purposes, it was assumed that the construction of partitions and the application of finishes occur at one month after transfer of prestress. In other words, the superimposed dead load as well as the sustained component of the total live load (see § 4.3.4) are applied at one month after the time of transfer (i.e. at 33 days), while the variable component of the live load may act at any time beyond this.

3.5.1 Uncracked Response

The total deflection of an uncracked prestressed concrete member may be obtained by superposition of the various increments of deflection. The expressions defining these increments are briefly reviewed below, after which the complete model for calculation of the design value δ_d of the deflection component affecting partitions and finishes (see Eq. 3-17), as appropriate to the prestressed concrete member of this study, is presented. This value represents deflection at the critical section, which is located at midspan in the case of a symmetrically loaded simply supported beam.

In a prestressed concrete flexural member, the deflection consists of instantaneous elastic increments due to the externally applied loads and the prestressing force, and long-term increments due to creep under the combined action of the prestressing force and all permanent loads, as defined later in this section (Ref. 3-8). The long-term creep deflection, which is usually of the same magnitude or larger than the instantaneous elastic deflection, primarily arises from the time-dependent action of creep and shrinkage of the concrete and relaxation of the steel. Long-term shrinkage deflection is a further increment of deflection and is caused by the restraining effect of reinforcement which is not symmetrically placed with respect to the centroid of the concrete, as is usually the case in beams. This increment of deflection is

usually small compared to the creep component, but is highly variable. However, in order not to further complicate the reliability analyses, this increment of deflection will be disregarded for the purposes of this thesis.

Expressions for the deflection of an uncracked prestressed concrete beam can be derived from Eq. 3-18 below (Ref. 3-3). The right-hand side of this differential equation represents the curvature of a linear elastic section and must be integrated twice with respect to x to obtain the deflection. Note that the deflection and the eccentricity are both measured from the centroidal axis of the concrete section and are taken positive downward.

$$\frac{d^2\delta(x)}{dx^2} = -\frac{M(x)}{E_c I} \tag{3-18}$$

where δ = deflection at any section x
M = bending moment at any section x
E_c = modulus of elasticity of concrete
I = second moment of area of gross uncracked section

Using Eq. 3-18, it can be shown that the instantaneous elastic increment of deflection δ_w at the critical section due to the externally applied loads can be expressed in the following general form (Refs. 3-1 and 3-3).

$$\delta_w = K\phi_w L_e^2 = K\left[\frac{M}{E_c I}\right]L_e^2 \tag{3-19}$$

where K = deflection coefficient, depending on the type of load and boundary conditions of the beam
ϕ_w = curvature due to applied external moment at the critical section
M = applied external moment at the critical section

Similarly, the instantaneous elastic deflection δ_p at the critical section caused by the prestressing force may be derived from Eq. 3-18 and expressed in the following general form (Ref. 3-3), where the curvatures at the midspan and support sections are considered.

$$\delta_p = \left(K_1\phi_{p1} + K_2\phi_{p2}\right)L_e^2 = \left[K_1\frac{\eta_1 P_{1i} e_1}{E_c I} + K_2\frac{\eta_2 P_{2i} e_2}{E_c I}\right]L_e^2 \tag{3-20}$$

where K_1 , K_2 = deflection coefficients at the midspan and support sections respectively, depending on the cable profile and boundary conditions of the beam
ϕ_{p1} , ϕ_{p2} = curvature due to prestressing force, at the midspan and support sections

e_1 , e_2 = eccentricity at midspan and support sections, respectively
P_{1i} , P_{2i} = initial prestressing force at midspan and support sections, respectively
η_1 , η_2 = loss factor at the time under consideration, at midspan and support sections, respectively

It should be noted that for a pretensioned concrete beam, uncracked in flexure, it is theoretically more correct to use the second moment of area of the *uncracked transformed section*. However, this is seldom done in practice and deflection calculations are usually carried out using the second moment of area of the *gross uncracked section*. This approach significantly simplifies the calculations and under normal circumstances provides a sufficiently close approximation. For the purposes of this study deflection calculations were therefore based on the second moment of area of the gross uncracked section.

The time-dependent properties of the concrete and the prestressing steel give rise to the long-term component of deflection, which develops over time under the action of the prestressing force and all permanent loads. Before the long-term creep deflection induced by a sustained state of stress can be quantified, an effective or reduced modulus of elasticity $E_{c\,eff}$ must be defined for the concrete. This is done in Eq. 3-21 below, by adding the long-term creep strain to the instantaneous elastic strain and by using the definition of the creep factor (see Eq. 3-6).

$$E_{c\,eff} = \frac{f_c}{\varepsilon_c + \varepsilon_{cc}} = \frac{E_c}{1 + \phi_{c\infty}} \tag{3-21}$$

where f_c = sustained concrete stress
ε_c = instantaneous elastic strain
ε_{cc} = long-term creep strain
$\phi_{c\infty}$ = long-term creep factor

An expression can subsequently be obtained for the instantaneous elastic plus long-term creep deflection, caused by the permanent loads, by using an expression similar to Eq. 3-19, the only difference being that the usual modulus of elasticity E_c is replaced by the effective modulus $E_{c\,eff}$. By substituting Eq. 3-21 for $E_{c\,eff}$ and by making use of Eq. 3-19, the long-term deflection $\delta_{w\infty}$ at the critical section due to the permanent loads is found as a multiple of the instantaneous elastic deflection δ_w (Ref. 3-9).

$$\delta_{w\infty} = K\left[\frac{M}{E_{c\,eff}I}\right]L_e^2 = K\left[\frac{M}{E_cI}\right]L_e^2\left(1 + \phi_{c\infty}\right) = \delta_w\left(1 + \phi_{c\infty}\right) \tag{3-22}$$

Similarly, the instantaneous elastic plus long-term creep deflection under the action of the prestressing force must be evaluated. For this purpose the curvatures at the midspan and support sections are calculated with the aid of Eq. 3-23 below (Refs. 3-3 and 3-10). The first

term in this equation represents the instantaneous elastic curvature due to the effective prestressing force, including all losses, at the section under consideration. The long-term change in curvature which results from the time-dependent loss of prestress is accounted for by the long-term loss factor η_∞.

The second term in Eq. 3-23 represents the long-term curvature due to creep of the concrete under the action of the prestressing force at the section under consideration, where it is assumed that the creep curvature is proportional to the instantaneous elastic curvature. Note that the average value of the prestressing force is used to account for the fact that the magnitude of the prestressing force, under which the creep is taking place, gradually reduces from P_i to $\eta_\infty P_i$ over the life of the member.

$$\phi_{p\infty} = \frac{\eta_\infty P_i e}{E_c I} + \frac{P_i e}{E_c I}\left[\frac{1+\eta_\infty}{2}\right]\phi_{c\infty} \qquad (3\text{-}23)$$

$$= \frac{P_i e}{E_c I}\left[\eta_\infty + \left[\frac{1+\eta_\infty}{2}\right]\phi_{c\infty}\right]$$

where $\phi_{p\infty}$ = instantaneous elastic plus long-term creep curvature due to prestressing force
η_∞ = long-term loss factor at the section under consideration
P_i = initial prestressing force at the section under consideration
e = eccentricity at the section under consideration

The long-term deflection $\delta_{p\infty}$ at the critical section due to the prestressing force can subsequently be obtained by calculating the associated long-term curvatures at the midspan and support sections, using Eq. 3-23, and by substituting these results into an expression analogous to Eq. 3-20.

Before the complete theoretical model for calculation of the design value δ_d of deflection at the SLS (see Eq. 3-17) can be presented, the design values of the material strengths and the appropriate load effects must first be defined in terms of their partial material and load factors. The following values are specified by SABS 0100-1:1992 (Ref. 3-1) for the partial material factors of the concrete and prestressing steel, respectively.

$$\gamma_{mc} = 1.0 \quad \text{and} \quad \gamma_{ms} = 1.0$$

Therefore, the values to be used for the material properties relevant to the assessment of deflection, namely the modulus of elasticity and the creep factor of the concrete and the relaxation of the prestressing steel, are those associated with the characteristic strength of the materials.

The only externally applied loads which result in long-term creep deflection are those which may be considered as being of long duration (Ref. 3-1). As was emphasized in § 1.4.2, it is therefore necessary to separate the permanent component of the total external load effect from the instantaneous or variable component. The various load effect terms relevant to the SLS of deflection, as appropriate to the prestressed concrete member of this study, may thus be defined as follows.

- M_{perm} represents the applied external bending moment due to the permanent loads, and is responsible for long-term creep in addition to instantaneous elastic deflection. For the purposes of this study these loads include the self-weight of the member, the superimposed dead load and the sustained component (taken as 30%) of the total live load. The total live load consists of imposed floor loads, as well as an additional load due to partitions.

- M_{var} reflects the applied external bending moment due to the variable load, causing only instantaneous elastic deflection. This load represents the balance of the total live load and is considered as being of a transient nature.

- M_{min} represents the applied external bending moment due to only the self-weight of the member. The deflection resulting from this load effect includes an instantaneous elastic increment, as well as the creep increment occurring before the age at which the superimposed dead load and the sustained component of the total live load are assumed to be applied.

Calculation of the design value δ_d of deflection at the SLS, as defined by Eq. 3-17, requires that the design value at midspan of the external load effect contributing to the total long-term deflection δ_∞ as well as that which contributes to the deflection which occurs before the construction of partitions and the application of finishes δ_t , be determined. In accordance with Eq. 1-8, these load effects are given by Eqs. 3-24a and 3-24b, respectively, where the design values are obtained with the aid of the partial dead and live load factors, γ_{fD} and γ_{fL}, and the live load combination factor ψ_L, as specified by SABS 0160:1989 (Ref. 3-2). The values to be used for the partial load factors should be selected bearing in mind whether a particular load effect induces a relieving or compounding effect (with regard to Eq. 3-17, the permanent load effect M_{perm} induces a compounding effect).

$$\begin{aligned} M_d &= M_{perm,d} + M_{var,d} \\ &= \gamma_c \left[\left(\gamma_{fD} M_{D,n} + \psi_L \gamma_{fL} M_{L,n} \right) + \left(1 - \psi_L \right) \gamma_{fL} M_{L,n} \right] \\ &= 266.9 \text{ kNm} + 100.1 \text{ kNm} \end{aligned} \qquad (3\text{-}24a)$$

where $\gamma_{fD} = 1.1$, $\gamma_{fL} = 1.0$, $\psi_L = 0.3$ and $\gamma_c = 1.0$

$$M_{min,d} = \gamma_c\left(\gamma_{fD} M_{D_1,n}\right)$$
$$= 153.0 \text{ kNm} \qquad (3\text{-}24b)$$

where $\gamma_{fD} = 1.0$ and $\gamma_c = 1.0$

Since the prestressed concrete member is subjected to only one time-varying load, i.e. the live load, Eqs. 3-24 represents the only load combination that needs to be considered for reliability analysis at the SLS of deflection (see § 4.3.2).

In terms of the theory presented above (Eqs. 3-19 through 3-24), the complete theoretical model for calculation of the design value of deflection δ_d , as appropriate to the prestressed concrete member of this study, can now be constructed. As noted before, interest lies only in that component affecting partitions and finishes and δ_d is therefore obtained as the difference between the long-term deflection under service loads and the deflection at 33 days, before the construction of partitions and application of finishes (see Eq. 3-17). The deflection model based on the 28 day modulus of elasticity of the concrete is followed by a model based on the long-term value.

For the purposes of this study, the prestressing force was assumed to act at a constant magnitude over the entire span of the beam, equal to the value at the midspan section. This approach simplifies the calculations and provides a sufficiently close approximation, since most curvature occurs at the midspan section in the case of a simply supported beam. This is also evident when the values to be used for the deflection coefficients K_1 and K_2 are compared (see Eqs. 3-25a and 3-26a below).

Deflection under Long-term Service Loads

In the long-term, the prestressing force will be acting at its minimum value, while the externally applied load will be acting at its maximum value. The total long-term deflection at midspan δ_∞ under these loads consists of the following increments.

$$\delta_\infty = \delta_{p\infty} + \delta_{w\infty} + \delta_{var} \qquad (3\text{-}25)$$

where $\delta_{p\infty}$ = instantaneous elastic plus long-term creep deflection due to prestressing force
$\delta_{w\infty}$ = instantaneous elastic plus long-term creep deflection due to permanent load
δ_{var} = instantaneous elastic deflection due to variable load

An expression for the first term in Eq. 3-25 is given by Eq. 3-25a below. This expression follows from Eqs. 3-20 and 3-23, with the values of K_1 and K_2 taken as 5/48 and 1/48, respectively, as appropriate to a simply supported beam with a parabolic cable profile. The

initial prestressing force P_i and the long-term loss factor η_∞ assume their values at the midspan section and is taken constant over the span of the beam.

$$\delta_{p\infty} = \frac{P_i}{48 E_c I}(5e_1 + e_2)L_e^2 \left[\eta_\infty + \frac{(1 + \eta_\infty)}{2}\phi_{c\infty} \right] \qquad (3\text{-}25a)$$

In Eq. 3-25a the magnitude of the prestressing force reflects the loss of prestress appropriate to the age of the prestressed concrete member at the stage under consideration. This is achieved through the use of the long-term loss factor η_∞ which may be defined as follows.

$$\eta_\infty = \frac{f_{pe}}{f_{pi}} = \frac{f_{po} + \Delta f_{pT}}{f_{po} + \Delta f_{pE}}$$

where f_{pe} = effective long-term prestress
f_{pi} = initial prestress just after transfer
f_{po} = prestress due to jacking force
Δf_{pT} = total long-term loss off prestress
Δf_{pE} = loss of prestress due to elastic deformation

An expression for the second term in Eq. 3-25 is given by Eq. 3-25b below. This expression follows from Eq. 3-22, with the value of K taken as 5/48, as appropriate to a simply supported beam subjected to an uniformly distributed loading.

$$\delta_{w\infty} = \frac{5}{48}\left[\frac{M_{perm,d}}{E_c I} \right] L_e^2 (1 + \phi_{c\infty}) \qquad (3\text{-}25b)$$

An expression for the last term in Eq. 3-25 is given by Eq. 3-25c below. This expression follows from Eq. 3-19, with the value of K taken as 5/48, as appropriate to a simply supported beam subjected to an uniformly distributed loading.

$$\delta_{var} = \frac{5}{48}\left[\frac{M_{var,d}}{E_c I} \right] L_e^2 \qquad (3\text{-}25c)$$

Using Eqs. 3-25, the design value of the total long-term deflection at midspan could therefore be calculated in § A.4.3 and § A.4.4. As is evident below, a major advantage of prestressed concrete over reinforced concrete is that deflection can be controlled.

$$\delta_\infty = \delta_{p\infty} + \delta_{w\infty} + \delta_{var}$$

$$= - 115.48 + 101.50 + 9.42$$

$$= - 4.56 \text{ mm}$$

Before Construction of Partitions and Application of Finishes

At 33 days, before construction of partitions and application of finishes, the prestressing force will be acting at an intermediate magnitude, lying between its maximum value just after transfer and its minimum value in the long-term, while the externally applied load will be acting at its minimum value. The total deflection at midspan δ_t under these loads consists of the following increments.

$$\delta_t = \delta_{pt} + \delta_{wt} \tag{3-26}$$

where δ_{pt} = instantaneous elastic plus 33 day creep deflection due to prestressing force
δ_{wt} = instantaneous elastic plus 33 day creep deflection due to self-weight

An expression for the first term in Eq. 3-26 is given by Eq. 3-26a below and, as before, this expression follows from Eqs. 3-20 and 3-23. However, in this case the 33 day loss factor η_t and the 33 day creep factor ϕ_{ct} reflect the time at which the conctruction of partitions and application of finishes are assumed to occur.

$$\delta_{pt} = \frac{P_i}{48 E_c I}\left(5e_1 + e_2\right)L_e^2\left[\eta_t + \frac{\left(1 + \eta_t\right)}{2}\phi_{ct}\right] \tag{3-26a}$$

In Eq. 3-26a, η_t reflects only that portion of the time-dependent loss of prestress which occurs before 33 days and may be defined as follows.

$$\eta_t = \frac{f_{pt}}{f_{pi}} = \frac{f_{po} + \Delta f_{pT}'}{f_{po} + \Delta f_{pE}}$$

where f_{pt} = effective 33 day prestress
$\Delta f_{pT}'$ = total 33 day loss of prestress

An expression for the second term in Eq. 3-26 is given by Eq. 3-26b below and, as before, this expression follows from Eq. 3-22.

$$\delta_{wt} = \frac{5}{48}\left[\frac{M_{min,d}}{E_c I}\right] L_e^2 (1 + \phi_{ct}) \qquad (3\text{-}26b)$$

Using Eqs. 3-26, the design value of the total deflection at midspan, before construction of partitions and application of finishes, was calculated in § A.4.4 as follows.

$$\begin{aligned}\delta_t &= \delta_{pt} + \delta_{wt} \\ &= -66.72 + 32.12 \\ &= -34.60 \text{ mm}\end{aligned}$$

Deflection affecting Partitions and Finishes

The deflection model based on the 28 day modulus of elasticity of the concrete is concluded with calculation of the design value of that component of deflection which affects partitions and finishes δ_d , as defined by Eq. 3-17.

$$\begin{aligned}\delta_d &= \delta_\infty - \delta_t \\ &= -4.56 - (-34.60) \\ &= 30.0 \text{ mm}\end{aligned}$$

With Long-term Concrete Strength

Since the modulus of elasticity of the concrete continually increases with age, the value to be used for the calculation of deflections should correspond to the age of the concrete at the time under consideration. When E_c is replaced with $E_{c\infty}$ in Eqs. 3-25, a deflection model is obtained where cognisance is taken of the long-term gain in concrete strength. This model was used in § B.1.2 to calculate the design value of deflection δ_d in a manner similar to the above procedure.

$$\begin{aligned}\delta_d &= \delta_\infty - \delta_t \\ &= -4.15 - (-34.60) \\ &= 30.5 \text{ mm}\end{aligned}$$

This value is essentially the same as that previously obtained and is a result of the way in which the model has been constructed. The value of δ_t is based on E_c and therefore remains

unchanged, while δ_∞ decreases slightly, in an absolute sense, resulting in an increase in δ_d. This effect will be more pronounced when a greater value of $E_{c\infty}$ is used and δ_d will be altered to an appreciable extent in an unconservative manner. For this reason the effect of the gain in concrete strength on reliability at the limit state of deflection will not be considered any further for the purposes of this thesis.

3.5.2 Design Criteria

The serviceability limit state of deflection may be regarded as a problem of capacity versus demand, in the sense of the general criterion of the limit states design method, as stated by Eq. 1-5. For a satisfactory design, the design value of deflection at the critical section δ_d must satisfy δ_a , the allowable deflection.

It was noted in § 1.4 that serviceability limit states are most often judged on subjective criteria based on human perceptions and not on an objective failure criterion, as is the case for the ultimate limit states. In general it is difficult to define appropriate design criteria for serviceability limit states, as these are much more dependent on the consequences of exceeding the limit state. Different serviceability requirements are best judged using different subjective design criteria and the selection of a single acceptable criterion is therefore difficult, if not impossible.

Nevertheless, conformance with allowable deflection criteria is often viewed as assurance of satisfactory service performance throughout the life of a structure. Based on the record of satisfactory performance of most structures, it is believed that the relatively simple act of limiting the deflections to certain traditional values somehow protects the structure against a set of very complicated serviceability demands (Ref. 3-11). These include local damage to nonstructural elements (such as ceilings, partitions, walls or windows), impairment of the normal functions of furniture or equipment and noticeable deflection causing distress to occupants. Deflection control therefore becomes one of the basic serviceability requirements in limit states design procedures.

Although high accuracy cannot generally be expected from the calculations of deflections, this precision is often not required because allowable deflections are difficult to define. The point at which unserviceability occurs depends on the nature of the building and the perceptions of the building occupants. In addition, deflection calculations are normally based on an idealized structure, whilst the influence of mitigating features such as beam end-restraints and cladding are difficult to quantify. Design codes of practice therefore often specify traditional deflection limits (the origin of which cannot be clearly documented), whilst allowing the designer to exercise his judgement.

In view of the above, the deflection criteria specified by SABS 0100-1:1992 (Ref. 3-1) and SABS 0160:1989 (Ref. 3-2) should only be regarded as reasonable limits. The following

design criterium is selected for the purposes of this thesis and is taken as a deterministic value of the allowable deflection.

$$\delta_a = \frac{L}{500} = 30.0 \text{ mm}$$

The deflection limit applicable to the deflection that takes place after the construction of partitions and the application of finishes is therefore just satisfied. This limitation is intended to inhibit damage to nonstructural elements, and may, or may not prevent or control the occurrence of other states of unserviceability.

3.6 SUMMARY

Theoretical models for prediction of the structural response of a simply supported pretensioned concrete T-beam, at the ULS of flexure and the SLS of deflection, were presented in this chapter. These models will be used in the reliability analyses undertaken in Chapter 5, where the analyses are based on a nominal live to dead load ratio of 0.7.

The design of the member was carried out in accordance with the limit states design method, as required by the South African structural codes on which this study is based. The design of a Class 2 prestressed concrete member commences with flexural design at the SLS and, as a result, the design resistance at the ULS of flexure exceeds the design load effect by approximately 22 %. The mode of failure at this limit state may be classified as that of an underreinforced section.

At the SLS of deflection interest lies in that component of deflection which affect partitions and finishes. In this case, the design criterium which has been selected is just satisfied. The response considered is that of an uncracked section and the conclusions to be drawn from the subsequent reliability analysis would therefore apply to such a member.

The mechanical properties of the materials of construction, including the gain in concrete strength beyond 28 days, were briefly reviewed. This will form a basis for the discussion of the variability of the basic variables associated with resistance, as well as for evaluation of the effect of increased concrete strength on reliability at the ULS of flexure.

3.7 REFERENCES

3-1 SABS 0100:1992, *Code of Practice, The Structural Use of Concrete, Part 1: Design*, SA Bureau of Standards, Pretoria, 1992.

3-2 SABS 0160:1989 (as amended 1990), *Code of Practice, The General Procedures and Loadings to be Adopted in the Design of Buildings*, SA Bureau of Standards, Pretoria, 1990.

3-3 Marshall, V. and Robberts, J.M., *Prestressed Concrete: Design and Practice*, Concrete Society of Southern Africa, Halfway House, Oct 1995.

3-4 Mirza, S.A. and MacGregor, J.G., *Probabilistic Study of Strength of Reinforced Concrete Members*, Can J Civ Eng, Vol.9, 1982, pp. 431-448.

3-5 Hognestad, E., Hanson, N.W. and McHenry, D., *Concrete Stress Distribution in Ultimate Strength Design*, ACI J, Vol.12, 1955, pp. 52-58.

3-6 Collins, M.P. and Mitchell, D., *Prestressed Concrete Basics*, Canadian Prestressed Concrete Institute, Ottawa, 1987.

3-7 Portland Cement Instiute, *Fulton's Concrete Technology, 6th ed.*, Addis, B.J. (ed), Midrand, South Africa, 1986.

3-8 Kong, F.K., Evans, R.H., Cohen, E. and Roll, F., *Handbook of Structural Concrete*, Pitman Books Limited, London, 1983.

3-9 Scholz, H. and Pretorius, P.C., *Alternative Creep Deflection Model for Prestressed Sections*, Concrete Beton, Journal of the Concrete Society of Southern Africa, No.67, Feb 1993, pp. 13,16-19.

3-10 Kong, F.K. and Evans, R.H., *Reinforced and Prestressed Concrete, 3rd ed.*, Van Nostrand Reinhold, U.K., 1987.

3-11 Galambos, T.V. and Ellingwood, B., *Serviceability Limit States: Deflection*, J Struct Engrg, ASCE, Vol.112, No.1, Jan 1986, pp. 67-84.

CHAPTER 4

STATISTICAL PROPERTIES OF BASIC VARIABLES

It was stated in Chapter 2 that the evaluation of structural reliability requires information on the variability of the basic variables, which for practical purposes is limited to the first two moments of the random variables. The statistical properties of the basic variables for the two limit states of interest were collected from available literature and in some instances were obtained by analysis. The discussion of these properties is the topic of this chapter, but it is preceded by certain concepts that were required for the analyses.

4.1 MODELLING OF UNCERTAINTY

It was noted in § 1.2 that Level 2 reliability analysis is concerned with only a subset of all the uncertainties that exist in structural engineering design. The following discussion attempts to indicate how the three types of uncertainty which constitute this subset are included in the reliability analysis.

When a basic variable is modelled as a random variable it does not assume a discreet value any longer, but its behaviour is governed by a probabilistic model. The selection of a probabilistic model for a particular basic random variable can be divided into two parts: the choice of a suitable probability distribution to characterize the *physical uncertainty* and the choice of suitable values for the parameters of this distribution.

If sufficient sample data of a basic random variable is in hand, various methods are available by which a suitable probability distribution may be selected. The simplest of these is to base the choice on a comparison between the shape of the histogram of the data and the shape of the mathematical distribution. When there is good agreement, the probability density function can be interpreted as the limiting case of the histogram as the sample size tends to infinity and the class interval is reduced.

However, unless the experimental data is obtained from an effectively homogeneous source, and unless the sample size is sufficiently large, formal attempts to fit standard forms of probability distributions to the data are hardly worthwhile. In structural reliability analysis such data is often not available for some basic random variables. Therefore, in these cases it is preferable to base the choice of a distribution on physical or subjective reasoning about the nature of the probabilistic mechanism generating the randomness in order to justify extrapolation beyond available data. Furthermore, the emphasis is on the use of two-parameter distributions because, with few exceptions, the quantity of data necessary to

estimate higher order statistics with any confidence does not exist in the structural reliability context.

When sufficient sample data is available various techniques exist whereby the parameters of a probability distribution can be estimated, such as the method of moments or the method of maximum likelihood. However, sample-derived parameter values are no more than estimates of the true values. Therefore, when only limited data is available *statistical uncertainty* remains, which constitutes the uncertainty associated with the estimation of the parameters and the uncertainty associated with the selection of a probability distribution. Instead of just ignoring this uncertainty, it may be included in the moments of the distribution of a basic random variable X as follows (Refs. 4-1 and 4-2).

$$\mu_X = \bar{B}\,\hat{x} \tag{4-1}$$

$$V_X = \left(V_B^2 + \hat{V}_X^2\right)^{\frac{1}{2}} \tag{4-2}$$

where μ_X = true mean of X
V_X = true c.o.v. of X
$\hat{x}$ = estimate of μ_X
$\hat{V}$ = estimate of V_X
$\bar{B}$ = bias factor
V_B = random error

It was noted in § 1.2 that *modelling uncertainty* may conveniently be expressed in terms of the distribution of a modelling variable. This random variable can be treated in a manner similar to the above, and it is considered separately in § 4.3.1 with respect to the load effect model and in § 4.5 with respect to the theoretical models of structural response.

FOSM reliability analysis requires information on the moments (i.e. the mean and standard deviation) of each basic random variable, rather than their entire distributions. These moments are discussed and analyzed in detail for the loading and resistance basic variables in § 4.3 and § 4.4 respectively. The moments were collected from available literature and in particular from Elligwood *et al* (Ref. 4-1), which represents a synthesis of time-independent statistical properties of basic variables as reported in numerous previous studies. Though it is often implied in the literature that was consulted, it is stated here that for the purposes of this thesis it is assumed that the moments already make provision for statistical uncertainty and that they therefore represent true moments of the distributions.

The mean values of basic random variables are often normalized with respect to their characteristic or nominal values (as defined in § 1.4) and are reported as such in the literature, together with their coefficients of variation. This is done for convenience and

makes the statistics applicable to a wide range of design situations. The moments for a particular basic random variable can then easily be calculated as follows.

$$\bar{X} = \left(\bar{X}/X_n\right) X_n \tag{4-3}$$

$$\sigma_X = V_X \bar{X} \tag{4-4}$$

where $\bar{X}/X_n$ = the mean value ratio

In general, the mean value ratio is greater than unity when it applies to basic random variables associated with resistance and smaller than unity when associated with loading variables (see Figure 2-1).

FOSM reliability analysis is not concerned with absolute accuracy. It may therefore be mentioned here that, for the purposes of this thesis, it was considered to be of greater importance that the moments of a particular variable displaying a definite probabilistic behaviour be in fact reflected in the analysis, rather than the exact numerical values thereof. Furthermore, when knowledge of the source of materials of construction is unavailable or limited to regional averages, it is appropriate that conservative estimates of the c.o.v. be made. Such a situation applies, for example, to structural code calibration procedures.

4.2 ANALYSIS OF MOMENTS

A limit state equation which is expressed in terms of its fundamental basic random variables can become very complicated and should be reduced to a manageable form before any reliability analysis is attempted. This may be accomplished by grouping certain functionally related random variables together and to determine moments for a single random variable which represents them. The various methods required for the purposes of this study to estimate these moments are set out in § 4.2.1 through 4.2.4. However, the formal definitions for the first and second moments of a random variable are first restated (Ref. 4-3).

The complete behaviour of a random variable X is described by its probability density function $f_X(x)$, but as noted before, FOSM reliability analysis is concerned with only the first two moments. These are the first moment about the origin (the mean μ_X), which characterizes the central tendency of a random variable, and the second central moment (the variance σ_X^2), which is a measure of the dispersion about the mean. These definitions are stated in common probabilistic symbolism in Eqs. 4-5 and 4-6 below.

$$\mu_X = E[X] = \int_{-\infty}^{\infty} x f_X(x)\, dx \tag{4-5}$$

$$\sigma_X^2 = VAR[X] = \int_{-\infty}^{\infty} (x - \mu_X)^2 f_X(x)\, dx \tag{4-6}$$

The coefficient of variation (c.o.v.) V_X is defined as the ratio between the standard deviation and the mean of a random variable, where the standard deviation σ_X is the positive square root of the variance. This dimensionless ratio facilitates comparisons among a number of random variables with different units.

$$V_X = \frac{\sigma_X}{\mu_X} \tag{4-7}$$

The covariance $\sigma_{Xi,Xj}$ of two random variables is a measure of the tendency of the random variables to vary together and is defined in Eq. 4-8 in terms of the correlation coefficient $\rho_{Xi,Xj}$. The implications of the values that the correlation coefficient may take on were discussed in § 2.4.

$$\sigma_{X_i,X_j} = COV[X_i, X_j] = \rho_{X_i,X_j}\, \sigma_{X_i}\, \sigma_{X_j} \tag{4-8}$$

where $-1.0 \leq \rho_{X_i,X_j} \leq 1.0$

The identities quoted in Eqs. 4-9 and 4-10 below follow from an expansion of the definition of expectation and often prove to be useful.

$$VAR[X] = E[X^2] - E^2[X] \tag{4-9}$$

$$COV[X_i, X_j] = E[X_i X_j] - E[X_i]E[X_j] \tag{4-10}$$

4.2.1 Moments of Simple Functions

The properties of expectation can be used to derive the moments of simple functions of random variables. These useful results were used in the analyses whenever possible and a number of cases are outlined below. Further guidance was obtained from Refs. 4-3 and 4-4.

Moments of a Linear Function

It is often required to find the moments of a random variable Y which is a *linear* function of a number of jointly distributed random variables X_i (see Eq. 4-11). In this case the mean and variance of Y can be computed from Eqs. 4-12 and 4-13 respectively.

$$Y = a_o + \sum_{i=1}^{n} a_i X_i \tag{4-11}$$

$$\mu_Y = a_o + \sum_{i=1}^{n} a_i \mu_{X_i} \tag{4-12}$$

$$\sigma_Y^2 = \sum_{i=1}^{n} a_i^2 \sigma_{X_i}^2 + 2 \sum_{i=1}^{n} \sum_{j=i+1}^{n} a_i a_j \rho_{X_i,X_j} \sigma_{X_i} \sigma_{X_j} \tag{4-13}$$

Two random variables Y_1 and Y_2 which are functions of corresponding random variables X_i will be correlated even though the original variables may be uncorrelated. For the two linear functions of Eq. 4-14 their covariance may then be calculated from Eq. 4-15 below.

$$Y_1 = a_0 + \sum_{i=1}^{n} a_i X_i \qquad \text{and} \qquad Y_2 = b_0 + \sum_{i=1}^{n} b_i X_i \tag{4-14}$$

$$\sigma_{Y_1,Y_2} = \sum_{i=1}^{n} a_i b_i \sigma_{X_i}^2 + 2 \sum_{i=1}^{n} \sum_{j=i+1}^{n} a_i b_j \rho_{X_i,X_j} \sigma_{X_i} \sigma_{X_j} \tag{4-15}$$

Both Eq. 4-13 and 4-15 reduce to only their first term when the original random variables are uncorrelated.

Moments of a Product

A random variable Y which is the product of two random variables (see Eq. 4-16) also lends itself to simple analytical treatment. In this case the mean and variance can be computed from Eqs. 4-17 and 4-18 respectively.

$$Y = X_1 X_2 \tag{4-16}$$

$$\mu_Y = \mu_{X_1} \mu_{X_2} + \rho_{X_1,X_2} \sigma_{X_1} \sigma_{X_2} \tag{4-17}$$

$$\sigma_Y^2 = \left[\left(\mu_{X_1} \sigma_{X_2} \right)^2 + \left(\mu_{X_2} \sigma_{X_1} \right)^2 + \left(\sigma_{X_1} \sigma_{X_2} \right)^2 \right] \left(1 + \rho_{X_1,X_2}^2 \right) \tag{4-18}$$

Eq. 4-19 below is often used for the special case when the random variables X_1 and X_2 are uncorrelated. This expression is of considerable practical importance and the last term is typically negligible.

$$V_Y^2 = V_{X_1}^2 + V_{X_2}^2 + V_{X_1}^2 V_{X_2}^2 \tag{4-19}$$

Furthermore, the moments of the product of any number of mutually *uncorrelated* variables (see Eq. 4-20) can be found with Eqs. 4-21 through 4-23.

$$Y = \prod_{i=1}^{n} X_i \tag{4-20}$$

$$\mu_Y = \prod_{i=1}^{n} \mu_{X_i} \tag{4-21}$$

$$\sigma_Y^2 \simeq \sum_{i=1}^{n} \left[\prod_{\substack{j=1 \\ j \neq i}}^{n} \mu_{X_j}^2 \right] \sigma_{X_i}^2 \tag{4-22}$$

$$V_Y^2 \simeq \sum_{i=1}^{n} V_{X_i}^2 \tag{4-23}$$

Division of Random Variables

For the random variable Y of Eq. 4-24, *first-order* approximations to the moments (see § 4.2.2) are as stated in Eqs. 4-25 and 4-26. These expressions are valid for random variables with reasonably small c.o.v.

$$Y = \frac{X_1}{X_2} \tag{4-24}$$

$$\mu_Y \simeq \frac{\mu_{X_1}}{\mu_{X_2}} \tag{4-25}$$

$$V_Y^2 \simeq V_{X_1}^2 - 2\rho_{X_1,X_2} V_{X_1} V_{X_2} + V_{X_2}^2 \tag{4-26}$$

4.2.2 Taylor-Series Approximations

The moments of functions of increasing complexity were derived with the aid of the approximate expressions listed below (Ref. 4-3). These expressions follow from a multidimensional Taylor-series expansion of the functionally dependent random variable Y about the means of the independent random variables X_i (see Eqs. 4-27). The justification for

this approach lies in the observation that if V_{Xi} is small, then X_i is very likely to lie close to μ_{Xi}.

$$Y = g(\boldsymbol{X}) = g(X_1, X_2, \ldots\ldots, X_n) \quad \text{with} \quad \boldsymbol{\mu_X} = (\mu_{X_1}, \mu_{X_2}, \ldots\ldots, \mu_{X_n}) \tag{4-27}$$

The *second-order* approximation to the mean of Y is given by Eq. 4-28, where the contribution of the last two terms are negligible when the c.o.v. of the original random variables X_i and the nonlinearity in the function are small.

$$\mu_Y \simeq g(\boldsymbol{\mu_X}) + \frac{1}{2}\sum_{i=1}^{n}\left[\frac{\partial^2 g(\boldsymbol{X})}{\partial X_i^2}\right]_{\boldsymbol{\mu_X}} \sigma_{X_i}^2 + \sum_{i=1}^{n}\sum_{j=i+1}^{n}\left[\frac{\partial^2 g(\boldsymbol{X})}{\partial X_i \partial X_j}\right]_{\boldsymbol{\mu_X}} \rho_{X_i,X_j}\sigma_{X_i}\sigma_{X_j} \tag{4-28}$$

The *first-order* approximation to the variance of Y can be obtained from Eq. 4-29,

$$\sigma_Y^2 \simeq \sum_{i=1}^{n}\left[\frac{\partial g(\boldsymbol{X})}{\partial X_i}\right]_{\boldsymbol{\mu_X}}^2 \sigma_{X_i}^2 + 2\sum_{i=1}^{n}\sum_{j=i+1}^{n}\left[\frac{\partial g(\boldsymbol{X})}{\partial X_i}\right]_{\boldsymbol{\mu_X}}\left[\frac{\partial g(\boldsymbol{X})}{\partial X_j}\right]_{\boldsymbol{\mu_X}} \rho_{X_i,X_j}\sigma_{X_i}\sigma_{X_j} \tag{4-29}$$

while the *first-order* approximation to the covariance between two functions $Y_1 = g_1(\boldsymbol{X})$ and $Y_2 = g_2(\boldsymbol{X})$ of corresponding random variables X_i can be obtained from Eq. 4-30.

$$\sigma_{Y_1,Y_2} \simeq \frac{1}{2}\sum_{i=1}^{n}\left[\frac{\partial g_1(\boldsymbol{X})}{\partial X_i}\right]_{\boldsymbol{\mu_X}}\left[\frac{\partial g_2(\boldsymbol{X})}{\partial X_i}\right]_{\boldsymbol{\mu_X}} \sigma_{X_i}^2 + \sum_{i=1}^{n}\sum_{j=i+1}^{n}\left[\frac{\partial g_1(\boldsymbol{X})}{\partial X_i}\right]_{\boldsymbol{\mu_X}}\left[\frac{\partial g_2(\boldsymbol{X})}{\partial X_j}\right]_{\boldsymbol{\mu_X}} \rho_{X_i,X_j}\sigma_{X_i}\sigma_{X_j} \tag{4-30}$$

When the functionally independent random variables are uncorrelated Eqs. 4-28 through 4-30 are all simplified in that their last terms fall away.

The first term of Eq. 4-29 may be interpreted as meaning that each of the n random variables X_i contributes to the dispersion of Y in a manner proportional to its own variance and proportional to a factor which is related to the sensitivity of Y to changes in X_i (Ref. 4-3). In order to reduce any limit state equation to a manageable form before attempting a reliability analysis, certain independent variables may be assumed to be deterministic rather than stochastic. The effect of this action is to neglect contributions to the variance of Y and it is a justified approximation if either the variance or the "sensitivity" factor of a particular

variable is small enough so that their product is negligible compared to the contribution of other variables in the limit state in question.

4.2.3 The Point Estimate Method

The Point Estimate Method can be used to obtain the moments of a nonlinear function of any amount of random variables (Ref. 4-5). This approach may be preferable when,

- it is difficult to obtain the partial derivatives of the function, as required by the Taylor-series approximations of the moments, or
- when the Taylor-series approach becomes cumbersome due to many independent random variables, or
- when the function is given implicitly in the form of charts or graphs.

Following this approach, each of the continuous functionally independent random variables X_i is replaced with a discrete random variable, and their continuous joint distribution $f_X(x)$ is approximated by a finite number of equivalent *point-estimates*. For the particular case of a function of two random variables, i.e. $Y = g(X_1,X_2)$, the set of possible realizations of the discrete random variables are,

$$\begin{aligned} x_{1+} &= \mu_{X_1} + \sigma_{X_1} \qquad & x_{2+} &= \mu_{X_2} + \sigma_{X_2} \\ x_{1-} &= \mu_{X_1} - \sigma_{X_1} \qquad & x_{2-} &= \mu_{X_2} - \sigma_{X_2} \end{aligned} \tag{4-31}$$

while the point-estimates associated with these values are,

$$p_{++} = p_{--} = \frac{1}{2^2}\left(1 + \rho_{X_1,X_2}\right) \quad \text{and} \quad p_{+-} = p_{-+} = \frac{1}{2^2}\left(1 - \rho_{X_1,X_2}\right). \tag{4-32}$$

Once the associated values of the functionally dependent random variable Y have been determined (Eq. 4-33), the the first two moments of the function can be computed from Eqs. 4-34 through 4-36.

$$y_{\pm\pm} = g\left(x_{1\pm}, x_{2\pm}\right) \tag{4-33}$$

$$\mu_Y = E[Y] = \sum_{all\ y} p_{ij} y_{ij} = p_{++}\, y_{++} + p_{+-}\, y_{+-} + p_{-+}\, y_{-+} + p_{--}\, y_{--} \tag{4-34}$$

$$E[Y^2] = \sum_{all\ y} p_{ij}\left(y_{ij}\right)^2 = p_{++}\left(y_{++}\right)^2 + p_{+-}\left(y_{+-}\right)^2 + p_{-+}\left(y_{-+}\right)^2 + p_{--}\left(y_{--}\right)^2 \tag{4-35}$$

$$\sigma_Y^2 = VAR[Y] = E[Y^2] - E^2[Y] \tag{4-36}$$

Whereas symmetrical distributions have tacitly been assumed for the functionally independent random variables, the coefficient of skewness γ_1 may be calculated for the distribution $f_Y(y)$ to establish whether this assumption still holds for the dependent random variable Y. The coefficient is positive for distributions skewed to the right (i.e. with longer tails to the right) and negative for those skewed to the left.

$$\gamma_1 = \frac{\sum_{all\ y} (y_{ij} - \mu_Y)^3 p_{ij}}{\sigma_Y^3} \tag{4-37}$$

In general, for a function of n independent random variables X_i, the coefficient on the right-hand side of Eqs. 4-32 is $(\frac{1}{2})^n$, and 2^n values of Y are obtained from Eq. 4-33. The information required for the analysis comprises the moments of each independent random variable as well as $n(n - 1)/2$ correlation coefficients $\rho_{Xi,Xj}$, when available. The Point Estimate Method lends itself to computer programming and is a conceptually simple method used for the analysis of moments.

4.2.4 Range of Values Known

Based on past experience, the variability of a basic random variable X can often only be expressed in terms of a lower limit x_l and an upper limit x_u. Given the range of possible values, the first two moments can be evaluated by prescribing a suitable probability distribution within this range.

If, for example, it is judged that there is a bias toward the lower values within the specified range, then a skewed distribution such as the lower triangular distribution would be appropriate. In this case, the mean and c.o.v. are given by the following expressions.

$$\mu_X = \frac{1}{3}(2x_l + x_u) \tag{4-38}$$

$$V_X = \frac{1}{\sqrt{2}} \left[\frac{x_u - x_l}{x_u + 2x_l} \right] \tag{4-39}$$

The statistics of other common distributions that may be prescribed are summarized by Ang and Tang (see Ref. 4-2, Table 6-3).

4.3 LOADING VARIABLES

Loading is usually the most uncertain factor in structural reliability analysis. Efforts spent on loading data collection and on load modelling may be more productive than refinement of the reliability estimation techniques (Ref. 4-4). It is essential, therefore, to review the statistical

properties of the relevant dead and live loads (see § A.1.2), even though this study centres on the reliability aspects associated with the response of the prestressed concrete member.

Nominal values for the dead and live loads to be supported by the prestressed concrete member were obtained from the South African loading code SABS 0160:1989 (Ref. 4-6). However, for the purposes of reliability analysis they must be regarded as uncertain quantities and are therefore treated as random variables. The moments of the basic random variables associated with these loads are considered in § 4.3.3 and § 4.3.4, respectively, and are summarized in Table 4-1, while detailed calculations are presented in Appendix B. However, the implications of the load effect model on the statistical properties and of the load combination model on the limit state equations are first investigated.

4.3.1 Load Effect Model

Load effects, or actions, are internal forces such as bending moment and shear, and are the result of loads acting on a structural member. It is important to note that the reliability analyses undertaken in Chapter 5 use these load *effects* as the basic variables in the limit state equations, and not the applied structural loads themselves. It is convenient from a conceptual point of view to gain some insight into how the actual spatial and time-varying loads (which are obtained from long-term load records, when available) are modelled to arrive at the statistical properties of the load effects.

Firstly, appropriate probabilistic load models are used to transform the actual spatial and time varying loads into statically equivalent uniformly distributed loads (EUDL), such that the EUDL produce the same particular load effects as the actual loads (Ref. 4-4). These are then specified by structural loading codes and can be used for design purposes. Secondly, during the design process, the specified loads are transformed into load effects, where a particular load effect Q_i is assumed to be related as follows to the corresponding applied structural load (Refs. 4-1 and 4-8).

$$Q_i = c_i B_i A_i \qquad i = 1, \ldots\ldots, n \tag{4-40}$$

where c_i = influence coefficient, converting load into load effect
B_i = load modelling variable
A_i = applied structural load
n = number of load effects

If it is assumed that the transformation from load into load effect is linear and that the above parameters are statistically independent, then the mean and c.o.v. of the load effect are given by Eqs. 4-41 and 4-42 below.

$$\bar{Q}_i = \bar{c}_i \bar{B}_i \bar{A}_i \tag{4-41}$$

$$V_{Q_i} = \left(V_{c_i}^2 + V_{B_i}^2 + V_{A_i}^2 \right)^{\frac{1}{2}} \tag{4-42}$$

The various factors which contribute to the overall uncertainty V_{Qi} in the load effect on a structural member can, with reference to Eq. 4-42, be delineated as follows.

- V_{Ai} reflects the inherent physical variability in the applied structural load. As stated in § 4.1, it is assumed that statistical uncertainty is also incorporated here.

- V_{Bi} reflects uncertainties arising from the load model which transform the actual spatial and time varying-load into an EUDL, which can be used for design purposes. When this model is unbiased the load modelling variable has a mean of unity.

- V_{ci} represents uncertainties that arise from the analysis which transforms the EUDL into a load effect (e.g. two-dimensional idealizations of three-dimensional members, fixity at supports, continuity).

It is again emphasized here that the moments of the load *effects* are used in the reliability analyses to follow. These moments thus already include all the previously mentioned uncertainties. Furthermore, it should be noted that the only load effects considered for the two limit sates of interest are that of bending moment.

4.3.2 Load Combinations

Unlike resistance variables, most of which change very little during the life of a structure, structural loads are typically time-varying quantities. The main exception of course is the load effect caused by the self-weight of permanent structural and non-structural components. If a structure is subjected to only one time-varying load in addition to the dead load, its reliability may be determined simply by considering the sum of the dead load effect and the maximum effect produced by the time-varying load during the life of the structure. It should be noted that with time-varying loads interest lies in the likely value of the greatest load during the lifetime of the structure. Success or failure may depend on the ability of the structure to function under maximum load, and not simply typical values.

It is frequently the case, however, that more than one time-varying load will be acting on a structure at any given time. Then, the maximum effect resulting from the combination of these loads must be considered in the ensuing reliability analysis. Conceptually, these load combinations should be dealt with by applying the theory of stochastic (random) processes, which account for the stochastic nature and correlation of the loads in time and space (Ref. 4-1 and 4-7).

Loads acting on structures can generally be classified into the following load process models. Permanent loads, such as dead loads, maintain a constant magnitude with relatively small and

slow random variation. Other loads can be either sustained loads changing at discrete times but of relatively constant magnitude during the time intervals, or transient loads changing continually with time. An example of the former is the sustained portion of imposed floor loading, while wind loading represents a transient load.

Reliability analysis at the ultimate limit states requires that the maximum total load during the service life of a structure be characterized. When more than one time-varying load is acting, it is extremely unlikely that each load will reach its lifetime maximum value at the same moment. Consequently, a structural member may be designed for a magnitude of load which is less than the sum of the lifetime peak loads. For practical reliability analyses, it is necessary to work with random variable representations of the load effects rather than random process representations.

A usefull procedure for combining time-varying load effect processes is Turkstra's rule. This rule says, in effect, that the maximum of a combination of time-varying load effects will occur when one of these load effects acts at its lifetime maximum while the others assume their arbitrary point-in-time values. Furthermore, it assumes that the probability of two or more time-varying loads effects attaining their lifetime maximum values at the same time is negligible. As noted in § 1.4.2 the arbitrary point-in-time values are intended to represent the sustained or usual values of the additional time-varying load effects. Eq. 4-43 below indicates a combination of load effect processes (i.e. random functions of time), but also includes the permanent load effect, which may be represented by a single random variable. Turkstra's rule for this combination is subsequently given by Eq. 4-44.

$$Q(t) = G + Q_1(t) + Q_2(t) + \ldots\ldots\ldots + Q_n(t) \qquad t \in T \tag{4-43}$$

$$\max Q(t) = G + \max_i \left[\max_T Q_i(t) + \sum_{\substack{j=1 \\ j \neq i}}^{n} Q_j(t^*) \right] \tag{4-44}$$

where $Q(t)$ = combined load effect process
G = permanent load effect
$Q_i(t)$ = load effect process
t = time variable
t^* = arbitrary point in time
T = specified design life

The similarity between Eq. 4-44 and Eq. 1-7 in § 1.4.2 should not escape the reader's attention. The standard formulation for load combinations specified by the South African loading code SABS 0160:1989 (Ref. 4-6) is essentially an application of Turkstra's rule. This rule is frequently adopted as a model for combining time-varying load effects not only

because of its simplicity, but also because it has been shown to be a good approximation in many practical cases and because it is consistent with the observation that failures frequently occur as a consequence of one time-varying load attaining an extreme value.

When there are n time-varying load effects in the limit state equation, then in general it is necessary to consider n distinct load combinations in computing the associated reliability. However, for the prestressed concrete member of this study the application of Eq. 4-44 is extremely simple and there is only one load combination to consider for the reliability analysis of each of the two limit states of interest (see Eqs. 4-45 and 4-46 below). Since the member is subjected to only one time-varying load, i.e. the live load, in addition to the dead load, its reliability at the ULS of flexure may be determined simply by considering the sum M of the dead load effect and the maximum effect produced by the live load during the life of the member.

$$M = M_D + M_L \tag{4-45}$$

For reliability analysis at the SLS of deflections the sustained component of the live load effect must, however, be seperated from the variable component. This is done in accordance with Eq. 1-8 of § 1.4.2, where ψ_L is the live load combination factor.

$$M = \left(M_D + \psi_L M_L\right) + \left(1 - \psi_L\right) M_L \tag{4-46}$$

Accordingly, the moments and probability distributions of the random variables in the above two equations are required for the reliability calculations.

4.3.3 Dead Loads

Dead loads are of a permanent nature, since their variation in magnitude with time is negligible in relation to their mean value. The dead load is therefore assumed to remain constant throughout the life of the structure, even though its actual value may be uncertain. For the purposes of this study the dead load D includes the self-weight of the prestressed concrete member D_1 as well as a superimposed dead load D_2 which results from all finishes and materials of construction which are to be supported permanently by the structure.

$$D = D_1 + D_2 \tag{4-47}$$

It is generally accepted (Ref. 4-1 and 4-8) that the total dead load *effect* can be modelled as a random variable in accordance with Eqs. 4-41 and 4-42, with the following values for the mean and c.o.v.

$$\bar{D} = 1.05\, D_n \qquad \text{and} \qquad V_D = 0.10$$

The assumption that the mean dead load effect is greater than the nominal (estimated) value, arises from the belief that the weights of many finishes and non-structural items tend to be omitted during the assessment of dead loads, i.e. a systematic error on the part of the designers (Ref. 4-8). Furthermore, the random variation of D appears to be mainly due to the variability of the superimposed dead load, rather than due to that of the load-bearing materials themselves (Ref. 4-1).

The distribution function for the dead load effect is generally assumed to be either Normal or Log-Normal. The argument in support of the former is based on the fact that the total dead load is generally the sum of the self-weights of many individual structural elements and other parts. This suggests that the central limit theorem applies. Also, the variability of the total dead load is less than that of the individual items, as measured by the c.o.v (Ref. 4-4). On the other hand, the self-weights of the individual parts are the products of material densities and dimensions, all of which may be assumed to be statistically independent and normally distributed. In addition, the transformation of load into load effect in Eq. 4-40 involves the product of statistically independent random variables. Consequently, the Log-Normal distribution may also be appropriate (Ref. 4-8).

Compared to the Normal distribution, the most salient characteristic of the Log-Normal is its skewed shape. However, for a small c.o.v. the shape of the distribution of a Log-Normally distributed random variable Y is approximately Normal (Ref. 4-3). This is exemplified by the ratio of the mean μ_Y to the median m_Y, which depends only on the c.o.v. of Y. For the dead load effect this ratio was found to be almost unity (see § B.2.1) and the Normal distribution is therefore adopted.

The reliability analysis at the limit state of deflection (see § 5.3) requires that the dead load be seperated into its two components (see Eq. 4-47) and that the moments of the load effect due to each are determined. Moments reported in the literature are usually relevant only to the load effect due to the total dead load and the required moments therefore had to be estimated, based on previous observations in this section. However, in § B.2.2 they were chosen such that, when combined, they are comparable to the moments of total dead load effect.

$$\bar{D}_1 = 1.0 D_{1,n} \qquad \text{and} \qquad V_{D_1} = 0.107$$

$$\bar{D}_2 = 1.2 D_{2,n} \qquad \text{and} \qquad V_{D_2} = 0.230$$

4.3.4 Live Loads

The total live load L on the prestressed concrete member consists of imposed floor loads L_1 as well as an additional load due to partitions L_2 (see Eq. 4-48). Nominal values of these loads are specified in SABS 0160:1989 (Ref. 4-6) for a 50-year reference period. The concept

of live load reduction (see Eq. 4-49) applies to the imposed floor loads, where a reduction in load per unit area is allowed as the area being considered is increased.

$$L = L_1 + L_2 \tag{4-48}$$

$$L_{1,n} = L_{0,n}\left[0.3 + \frac{3.1}{\sqrt{A_T}}\right] \text{[kPa]} \tag{4-49}$$

where $L_{0,n}$ = nominal unreduced imposed floor load (2.5 kPa)
A_T = tributary area

The imposed floor load L_1 may conveniently be separated into two components, namely a sustained load L_{sus} and a variable load L_{var} (Ref. 4-1, 4-4 and 4-8). The sustained part of the imposed floor load is most likely to act on the structure at any point in time and is equivalent to the arbitrary point-in-time load value referred to in § 1.4.2. This load include office furniture and normal personnel loads, and it is assumed to act continually with time and to remain relatively constant within a particular occupancy. The variable part of the imposed floor load stems from extraordinary events such as the infrequent gathering of large groups of people or the stacking of furniture during renovation activities. These extraordinary loads are of a transient nature and may be modelled as Poisson events.

The statistical properties of the sustained part of the imposed floor load may be obtained directly from data derived from load surveys. As noted before, appropriate probabilistic load models are used to transform the actual spatial and time-varying loads into a statically EUDL. The results of these analyses, as reported in the literature, deal primarily with imposed floor loads in office buildings with little or no information covering retail establishments, hospitals, schools or industrial premises (Ref. 4-8).

While the mean value of L_{sus} for office occupancies appears to be independent of the tributary area, its c.o.v. decreases as the area being considered increases. This is a consequence of the load averaging which occurs over large areas (Refs. 4-1 and 4-8). The values below are used for the purposes of this study, where the c.o.v. is a function of the plan area of the prestressed concrete member. The c.o.v includes allowances for the uncertainties related to the load model and the analysis (see Eq. 4-42) and thus represents the variability of the load effect. This load effect appears to be best fitted by a Gamma distribution.

$$\bar{L}_{sus} = 0.575 \text{ kPa} \qquad \text{and} \qquad V_{L_{sus}} = 0.68$$

While load surveys describe the imposed loads acting on a structure at any point in time, they are insufficient to describe the lifetime maximum imposed floor load L_1 which may be expected to act during the life of a structure. This is because extraordinary load events are

usually not reflected in load survey data and must be estimated seperately. However, using Monte Carlo simulation the distributions of the sustained and variable loads can be combined to yield the statistics of the lifetime maximum imposed load effect (Ref. 4-1).

$$\bar{L}_1 = \bar{L}_0 \left[0.25 + \frac{4.6}{\sqrt{A_I}} \right] [\text{kPa}] \qquad \text{and} \qquad V_{L_1} = 0.25$$

where $\bar{L}_0$ = mean unreduced imposed floor load (2.4 kPa)

A_I = 2 A_T , for beams (influence area, defined as that area over which the influence function for load effect is significantly different from zero)

The c.o.v. given here represents the total variability of the lifetime maximum imposed load effect and is obtained by augmenting the data-based variability with modelling and analysis uncertainties, as discussed previously. In this case the dependence of the c.o.v. on the tributary area is weak and may be ignored (Ref. 4-1). This load effect is assumed to be fitted by a Type I Extreme Value distribution of largest values. This may be interpreted physically as the distribution that would be obtained if the lifetime maximum imposed load effects were measured in a set of many nominally identical structures.

The reliability analyses to be undertaken in Chapter 5 require the statistical properties of the load effect due to the total live load L, rather than the properties of the load effect due to L_1 only (see Eqs. 4-45 and 4-46). The following moments of the total live load effect were calculated in § B.2.3, where it was assumed that the mean value ratio obtained for L_1 also applies to L_2.

$$\bar{L} = 0.941\, L_n \qquad \text{and} \qquad V_L = 0.25 \qquad \text{at the ULS}$$

Structural reliability depends on the time of exposure to the loading environment and loading criteria at the ULS are based on a 50-year reference period. However, it does not seem reasonable to base serviceability criteria on such a severe requirement. Instead, loading criteria for deflections might be founded on the premise that the deflection limit should not be exceeded more than once, on the average, during one tenancy (Ref. 4-9). The average period between tenant changes in office buildings is eight years. The mean value ratio given below represents the proportion of the (code-specified) lifetime maximum live load expected to act during this shorter period. Note that a smaller mean value leads to a higher value for the c.o.v.

$$\bar{L} = 0.650\, L_n \qquad \text{and} \qquad V_L = 0.32 \qquad \text{at the SLS}$$

It is an objective of this thesis to examine the relative contributions to the overall uncertainty at the two limit states of interest of those fundamental quantities normally used by designers in structural calculations. The live load combination factor ψ_L, which aims at reducing the lifetime maximum live load effect to its sustained value (in accordance with Eq. 1-8, § 1.4.2) is such a quantity, and as such, it should be modelled as a random variable. The moments of this basic variable are therefore required (see Eq. 4-46), rather than those of the load effect due to L_{sus}.

Ambiguity exist in respect of the value specified for ψ_L by the South African loading code SABS 0160:1989 (Ref. 4-6) and a nominal value of either 0.3 or 0.5 may be adopted for design purposes (compare clause 4.4.2, Table 2 and clause 5.4.1.1, respectively). Accordingly, the live load combination factor is often ignored in design practice and the total live load, comprising both the sustained and variable components, is conservatively used to evaluate long-term material behaviour at the SLS of deflection.

A rough estimate of the live load combination factor can be obtained from the ratio of the sustained load to the lifetime maximum live load (Ref. 4-8). As such, ψ_L may also be termed the sustained live load ratio, as defined in Eq. 4-50. The moments stated below were derived in § B.2.4, where a value of 0.3 was used for the expected correlation between L_{sus} and L (a value of either zero or 1.0 would be inappropriate for office occupancies). Furthermore, the variation of ψ_L is assumed to follow a Normal distribution, where this assumption is for convenience and not based on physical grounds.

$$\psi_L = \frac{L_{sus}}{L} \tag{4-50}$$

$$\bar{\psi}_L = 0.870\,\psi_{L,n} \qquad \text{and} \qquad V_{\psi_L} = 0.659$$

It is of some interest to note that the c.o.v. of the sustained load effect is significantly greater than that of the lifetime maximum live load effect (0.68 compared to 0.32). This is explained by the fact that the former increases as the tributary area being considered decreases (which is relatively small in the case of the prestressed concrete member), while the dependence of the latter on the tributary area is insignificant. Even though the random variation of the sustained load effect is reflected in the c.o.v. of the sustained live load ratio for the purposes of this study, it is expected to have a meaningful effect on the calculated reliability at the limit state of deflection. The lack of a clearly specified value by the loading code should be viewed in this light.

Table 4-1: Statistical properties of loading variables.

X	X_n [kPa]	$\bar{X}/X_n$	V_X *	Distribution	Ref.
Dead Load					
D	4.83	1.05	0.100	N	4-1
D_1	3.63	1.00	0.107	N	§ B.2.2
D_2	1.20	1.20	0.230	N	§ B.2.2
Live Load for ULS of Flexure					
L	3.39	0.941	0.250	$EX_{I,L}$	§ B.2.3
Live Load for SLS of Deflection					
L	3.39	0.650	0.320	$EX_{I,L}$	4-9
ψ_L	0.3	0.870	0.659	N	§ B.2.4

* V_X represents variability of load effect, save for dimensionless ψ_L.

4.4 RESISTANCE VARIABLES

The *in-situ* response of a prestressed concrete member may vary from the theoretical or calculated response due to variations in the material properties and the dimensions of the member as well as variations inherent in the models used to predict the structural response. The moments of the basic random variables associated with the material properties and dimensions are discussed in the following sections and are subject to the assumptions set out at the beginning of § 3.3. These properties are summarized in Table 4-2, while detailed calculations are presented in Appendix B. Variations inherent in the theoretical models are treated in § 4.5.

It was noted in § 4.1 that when sufficient sample data is unavailable, it is preferable to base the choice of a distribution with which to model a random variable on an understanding of the underlying mechanism giving rise to the distribution. For the purposes of this study the example of many researchers is followed (e.g. Refs. 4-1 and 4-10) in that the Normal distribution has been adopted for all the basic variables associated with resistance. The justification for this lies in the fact that there are many sources of physical variability, each difficult to isolate and observe independently, which contribute in an additive manner to the overall random variation of many natural phenomena. As a result histograms approximating the Normal distribution are frequently observed in nature.

The Normal distribution arises naturally as a limiting distribution when the random variable of interest is the sum of a number of independent identically distributed component variables, *viz* the *central limit theorem*. This theorem also applies even when the component variables are not independent or identically distributed, as long as no one variable dominates and as long as the interdependence among variables is small (Ref. 4-3). The rate at which the sum tends to normality depends in practice on the presence of any dominant non-normal components. The Normal distribution always predicts a small but finite probability of occurence of negative values. Yet it may still be usefull in practice to assume that some variable, which is physically limited to positive values, is normally distributed if the range of validity of the model is appreciated.

The characteristic value of a resistance variable has been defined in § 1.4 as the value below which not more than 5 % of sample values may be expected to fall. In terms of the standardized Normal distribution this definition can now be expressed as follows.

$$P\left(f \leq f_k\right) = \Phi\left[\frac{f_k - \mu_f}{\sigma_f}\right] = 0.05 \qquad (4\text{-}51)$$

$$\therefore \quad f_k = \mu_f - 1.645\,\sigma_f$$

where f_k = characteristic value of resistance variable f
Φ = standardized cumulative Normal distribution function

However, this definition does not always prove to be accurate when used with the moments obtained from available literature. This is an indication of the inability of design codes of practice to accurately specify characteristic values for resistance variables.

4.4.1 Concrete

Although the statistical distribution of concrete compressive strength has been of interest for a long time it has a much smaller influence on structural behaviour than the reinforcement properties (Ref. 4-4). This is due entirely to the conventional design philosophy of attempting to achieve ductility in a structural member (see § 3.4.4). The following statistical properties are of interest for the purposes of this study.

Cube Strength at 28 Days

The standard deviation of the strength of concrete produced by a given contractor is often regarded to be a constant for all mean strengths and to be a measure of the quality control practised in his work. The c.o.v. therefore decreases as the mean strength increases. A standard deviation of 5 MPa is specified by SABS 0100-2:1980 (Ref. 4-11) for good quality

of construction. This dispersion about the mean would apply to precast, pretensioned concrete beams and was used in § B.3.1 to derive the first two moments of the concrete cube strength at 28 days. The physical uncertainty was augmented with statistical uncertainty to obtain the following mean and c.o.v.

$$\bar{f}_{cu} = 1.165\, f_{cu,n} \qquad \text{and} \qquad V_{f_{cu}} = 0.10$$

Comparable variability is reported in Ref. 4-10 for cylinder strength f_c' at 28 days where control is excellent. For good quality concrete a Normal distribution has been suggested for f_{cu} by many authors (e.g. Ref. 4-10), whereas a Log-Normal distribution appears to be more appropriate where control is poor.

In-situ Flexural Strength

The flexural strength of *in-situ* concrete was defined in Eq. 3-2, where the concrete strength reduction factor c_1 may be regarded as a material modelling variable to model the stress-strain relationship of concrete behaving in flexure. This factor is intended to take the considerations listed in § 3.3.1 into account. The first and second moments of the *in situ* flexural strength f_{co} were acquired from Refs. 4-12 and 4-13, respectively. In particular a c.o.v. of 0.135 is suggested. These moments correspond to good quality of construction and is based on a 1-h loading to failure, which represents a lower loading rate than those generally used during material tests.

However, reliability analysis requires the statistical properties of those fundamental quantities normally used by designers in structural calculations. The concrete strength reduction factor is such a quantity and must therefore be modelled as a random variable. For this purpose its moments were derived in § B.3.2.

$$\bar{c}_1 = 1.053\, c_{1,n} \qquad \text{and} \qquad V_{c_1} = 0.081$$

Clearly the uncertainty of f_{co} lies not only in that of the material strength, but also in the uncertainty imparted by the model. For average quality of construction, a similar c.o.v. of 0.092 for c_1 is reported in Ref. 4-1.

Long-term Cube Strength

The gain in concrete strength beyond 28 days was defined in Eq. 3-3 in order to evaluate its affect on reliability at the ULS of flexure. This should be seen as an attempt to establish whether the advantage of using the higher strength allowed by the design code of practice outweighs the increasing uncertainty which accompanies it. The results of the analysis will indicate whether further investigation is required. With this in mind information from two

sources was combined in § B.3.3 to make a conservative estimate of the mean of the long-term concrete cube strength factor c_2 on the one hand (Ref. 4-14), and an unconservative estimate of its c.o.v. on the other hand (Ref. 4-13).

$$\bar{c}_2 = 1.121\, c_{2,n} \qquad \text{and} \qquad V_{c_2} = 0.102$$

This conservative estimate of the mean with a value 1.30 (see § B.3.3) may be compared with a mean value of 2.13 that was measured in a 22 year old concrete building (Ref. 4-1). A c.o.v. of 0.062 was measured at the same site, but since such information is not available during the design stage the variability of c_2 was instead obtained from a likely range based on professional judgement. The c.o.v. of c_2 is indicative of the inability to accurately estimate $f_{c\infty}$ when f_{cu} is known.

Though not regarded as a basic variable for the purposes of this study, the c.o.v. of the long-term concrete cube strength $f_{c\infty}$ was also derived in § B.3.3 for comparison with that of f_{cu}. For this purpose some correlation between c_2 and f_{cu} was assumed, albeit weak because the strength increase is primarily linked to the manner in which the concrete is cured. As before, the c.o.v. of 0.100 for f_{cu} is compounded by the uncertainty imparted by the model, resulting in a c.o.v. of 0.146 for $f_{c\infty}$.

Modulus of Elasticity

Concrete is approximated as a linear elastic material for deflection calculations at the SLS. The moments of the secant modulus of elasticity of concrete E_c at 28 days are therefore required in the reliability analysis. In § 3.3.1 the characteristic value of E_c was obtained as a function of the characteristic value of f_{cu}. Similarly, the mean value of E_c must be correlated with the mean value of f_{cu}. A mean value of of 37.4 GPa was obtained from Ref. 4-15 (Fig. 7.17), while the c.o.v. is given by Ref. 4-13. This leads to the following moments.

$$\bar{E}_c = 1.1\, E_{c,n} \qquad \text{and} \qquad V_{E_c} = 0.105$$

Since the effect of the gain in concrete strength on reliability at the limit state of deflection is not considered (see § 3.5.1), the moments of the long-term modulus of elasticity are not required.

Creep of Concrete

Creep in concrete structures is a phenomenon that depends on a host of parameters and the scatter of actual data about proposed values may be significant. In view of this scatter it is reasonable to use a simple procedure for design purposes to estimate the creep factor with sufficient precision and using known parameters.

The procedure used in § 3.3.1 permitted a rough estimate of the long-term and 33 day creep factors $\phi_{c\infty}$ and ϕ_{ct} as functions of only a few parameters, such as thickness of the member, ambient relative humidity, and age of the concrete. This particular procedure was developed by ACI Committee 209 (1971) and is one of several methods later evaluated by Rüsch *et al* (Ref. 4-16). Comparison with test values yielded the c.o.v. given below and, since this was an average value for creep at different ages, it is asumed to apply to both $\phi_{c\infty}$ and ϕ_{ct}.

$$\bar{\phi}_{c\infty} = 1.0\ \phi_{c\infty,n} \qquad \text{and} \qquad V_{\phi_{c\infty}} = 0.248$$

The magnitude of this c.o.v. reflects not only physical uncertainty in the data to be used for the prediction method, but also to a great extent modelling uncertainty due to an incomplete understanding of the creep phenomenon. Vrouwenvelder and Siemes (Ref. 4-17) report a similar value of 0.20. In the absence of evidence of systematic error the mean values of the creep factors are taken as the calculated values for the purposes of this study.

4.4.2 Reinforcement

Prestressing steel was the only reinforcement considered for the purposes this study and consisted of high tensile strength 7-wire strand. Moments for the applicable basic variables, in particular those associated with strength and prestress losses, are listed in Table 4-2. Looking at this table, it is evident that the variability of prestressing steel is much less than that of concrete. As for concrete, these random variables are assumed to follow the Normal distribution.

The random behaviour of the ultimate strength of prestressing steel f_{pu} was characterized by Mirza *et al* (Ref. 4-10) and is given below. These values were based on a statistical analysis of testing records from various producers and were adjusted for the rate of loading. The moments are independent of strand size. It is interesting to note that the standard deviation of the yield strength of normal reinforcing steel and prestressing steel are of the same order, while the mean value of the latter is almost four times larger. This explains the very small c.o.v. of f_{pu}.

$$\bar{f}_{pu} = 1.040\ f_{pu,n} \qquad \text{and} \qquad V_{f_{pu}} = 0.025$$

The magnitude of the prestressing force must reflect the prestress losses at the age under consideration. For this purpose, the initial loss factor ζ_i and the long-term loss factor η_∞ were defined in § 3.2 and are used as basic variables in the reliability analysis (see § 5.3.1). For post-transfer losses a c.o.v. of 0.16 is given by Ref. 4-10. However, these losses represent a relatively small fraction of the long-term prestressing force and it can be shown to result in a c.o.v. of only about 0.04 for η_∞. The following more conservative moments are quoted by Ref. 4-18 and are accepted for the purposes of this study.

$$\bar{\eta}_{\infty} = 1.0\ \eta_{\infty,n} \qquad \text{and} \qquad V_{\eta_{\infty}} = 0.08$$

The initial loss factor ζ_i provides for both the instantaneous loss of prestress and the limitation placed on the magnitude of the jacking force. Since the variability of the latter can be controlled through proper calibration of the prestressing jacks, the c.o.v. of ζ_i is taken as half that of η_{∞}.

4.4.3 Dimensions

The uncertainty in the basic dimensions of a cross-section is typically very small. They are controlled by the tolerance limits specified in various building codes, where these limits depend on the type of structure and construction technology that is used. For the purposes of this study, dimensional variability corresponds to good quality construction, as applicable to the precast concrete industry (see § 3.3). Reliability analysis at the SLS of deflection requires moments for the second moment of area of the gross uncracked section I. Using the methods of § 4.2.2 and § 4.2.3, the dimensional variability of this paragraph is combined to quantify the uncertainty of I (see § 5.3.2).

A systematic deviation of actual dimensions from nominal values has been observed. This is explained by the imperfect stiffness of formwork and the subsequent deformation caused by the weight of wet concrete (Ref. 4-19). Furthermore, the standard deviation of dimensional variables tend to be relatively constant over a wide range of nominal values and is therefore independent of member size. In view of the above, the differences between actual and nominal dimensions is best characterized by the mean and standard deviation of the error.

Dimensional variability was investigated by Mirza *et al* (Ref. 4-10) and the relevant quantities are listed in Table 4-2. The c.o.v. decreases for larger sections and for the present study falls within the range 0.005 to 0.050. The span length L_e is set by design considerations and may therefore be treated as a constant. Furthermore, all basic dimensions are assumed to be uncorrelated.

4.5 MODELLING UNCERTAINTY

In most cases of importance to structural design, a clearly defined theoretical model exists which has its origin in the principles of structural mechanics and which has been verified by experiment. When member structural response is derived from material strength and geometrical properties using theoretical models, differences between the derived results and actual *in-situ* response would be expected. In part this is due to the inherent variability in experimental techniques and observations. The greater part of the difference, however, is caused by the use of a simplified theoretical model to represent the physical phenomenon of interest (Ref. 4-4).

Table 4-2: Statistical properties of resistance variables.

X	X_n	$\bar{X}/X_n$	V_X	Distribution	Ref.
Concrete					
f_{cu}	50.0 MPa	1.165	0.100	N	see § B.3.1
f_{co}	33.5 MPa	1.053	0.135	N	4-12 & 4-13
c_1	0.67	1.053	0.081	N	see § B.3.2
c_2	1.16	1.121	0.102	N	4-13 & 4-14
$f_{c\infty}$	58.0 MPa	1.308	0.146	N	see § B.3.3
E_c	34.0 GPa	1.100	0.105	N	4-13 & 4-15
$\phi_{c\infty}$	3.04	1.0	0.248	N	4-16
ϕ_{ct}	1.23	1.0	0.248	N	4-16
Reinforcement					
A_p	700 mm^2	1.012	0.013	N	4-18
f_{pu}	1860 MPa	1.040	0.025	N	4-10
E_p	195 GPa	1.0	0.020	N	4-10
ζ_i	0.706	1.0	0.040	N	4-18
η_∞	0.839	1.0	0.080	N	4-18
η_t	0.919	1.0	0.080	N	4-18
Dimensions [mm]					
b	1500	$(b_n+4.0)/b_n$	$6.4/\bar{b}$	N	4-10
b_w	200	1.0	$4.8/\bar{b}_w$	N	4-10
h	600	$(h_n+3.2)/h_n$	$4.0/\bar{h}$	N	4-10
h_{f1}	50	1.0	$4.8/\bar{h}_{f1}$	N	4-10
h_{f2}	100	1.0	$4.8/\bar{h}_{f2}$	N	4-10
d	528	$(d_n+3.2)/d_n$	$4.4/\bar{d}$	N	4-10
e_1	345	$(e_{1n}+3.2)/e_{1n}$	$4.4/\bar{e}_1$	N	4-10
e_2	110	$(e_{2n}+3.2)/e_{2n}$	$4.4/\bar{e}_2$	N	4-10

Modelling uncertainty therefore arises, but should decrease as improved models become available. This type of uncertainty can conveniently be expressed in terms of the distribution of a modelling variable, which is defined as the ratio between the true and theoretical response. This term is referred to as the modelling error ε and is defined in Eq. 4-52. A mean value of unity indicates that, on average, the theoretical response equals the true response. Frequently the modelling error must be estimated on the basis of professional judgement and experience. However, when experimental data is available it can be estimated from the ratio of test response, representing the true state of nature, to the prediction according to the theoretical model used.

$$\varepsilon = \frac{R_T}{R_M} \tag{4-52}$$

where R_T = true *in-situ* member response
R_M = member response predicted by theoretical model

Modelling error may contain two components: the *systematic error* represented by the mean of ε and the *random error* represented by V_ε (Ref. 4-2). Systematic error arises from factors not accounted for in the theoretical model that tend to consistently bias the model in one direction or the other, while the random error is the variability about the estimated mean value. Eqs. 4-53a and 4-53b indicate how the inherent physical uncertainty of the member response is augmented with modelling uncertainty, analogous to the manner in which statistical uncertainty was treated in § 4.1 (see Eqs. 4-1 and 4-2). A Normal random variable representing the systematic and random errors must thus be included in the reliability analyses at the limit state of flexure (see § 5.2.2) and at the limit state of deflection (see § 5.3.2).

$$\bar{R}_T = \bar{\varepsilon}\, \bar{R}_M \tag{4-53a}$$

$$V_{R_T} = \left(V_\varepsilon^{\,2} + V_{R_M}^{\,2} \right)^{\frac{1}{2}} \tag{4-53b}$$

where $\bar{\varepsilon}$ = systematic error
V_ε = random error

The systematic and random errors can be estimated from experimental data using the unbiased estimators given below (Ref. 4-3), where the ratio of test response to the prediction according to the theoretical model is considered.

$$\bar{\varepsilon} = \frac{1}{n} \sum_{i=1}^{n} \varepsilon_i \tag{4-54a}$$

$$s_{T/M}^2 = \frac{1}{n-1} \sum_{i=1}^{n} (\varepsilon_i - \bar{\varepsilon})^2 \tag{4-54b}$$

where $\bar{\varepsilon}$ = sample mean
$s_{T/M}^2$ = sample variance
n = sample size

The sample variance provides an estimate of the true variance $\sigma_{T/M}^2$, but statistical uncertainty remains. To allow for this uncertainty the sample variance calculated above can be replaced by an upper bound estimate of the true variance. For a Normal distributed random variable the 100 (1 - α) % upper one-sided confidence limit is given by Eq. 4-55 (Ref. 4-20).

$$\sigma_{T/M}^2 = s_{T/M}^2 \left[\frac{n-1}{\chi^2_{1-\alpha;n-1}} \right] \tag{4-55}$$

where $\chi^2_{1-\alpha;n-1}$ = 100 (1 - α) percentage point of the Chi-square distribution with n - 1 degrees of freedom

The c.o.v. obtained directly from a comparison of test response to theoretical response can then be calculated as shown below. However, this variability is assumed to result from three different sources (Ref. 4-13) as indicated by Eq. 4-56.

$$V_{T/M} = \frac{\sigma_{T/M}}{\bar{\varepsilon}}$$

$$V_{T/M} = \sqrt{V_\varepsilon^2 + V_{test}^2 + V_{spec}^2} \tag{4-56}$$

The various factors which contribute to this variability can be delineated as follows.

- V_ε represents the random error of the theoretical model itself.
- V_{test} reflects uncertainties in the measurement of loads, caused by inaccuracies of the gages and errors in readings, and uncertainty in the definition of failure.
- V_{spec} reflects differences between the material strength measured in control specimens and that of the test specimen, as well as variation in actual specimen dimensions from those measured.

If the random error is assumed to be directly determined by the ratio of test response to theoretical response, this disregards errors in the procedures used to determine the test strength, in addition to differences between the material strength and dimensions reported from control specimens and those actually present at the failure section. Accounting for the variability inherent in the test and the specimen leads to a lower random error directly attributed to the theoretical model and Eq. 4-56 must therefore be solved for V_ε.

4.6 SUMMARY

The purpose of this chapter was to gather information on the variability of all the basic random variables which appear in the two limit state equations of interest. These statistical properties were collected from several previous studies and are summarized in Table 4-1 and 4-2, while detailed calculations are presented in Appendix B.

The chapter commenced with a discussion on how the various types of uncertainty should be modelled for inclusion in the reliability analyses. This was followed by a summary of procedures required for pre-processing of certain moments, *viz* moments of simple functions, Taylor-series approximations, the Point Estimate Method and expressions used when the range of values is known.

The Normal distribution was adopted to model the dead load, while the lifetime maximum live load was represented by a Type I Extreme Value distribution of largest values. Whereas the live load at the ULS is based on a 50-year reference period, the variability of this load for deflection calculations was based on the premise that the deflection limit should not be exceeded more than once during any tenancy. Only one load combination will be considered for reliability analysis at each of the two limit states of interest.

The example of many researchers was followed by assuming that the Normal distribution fits all the basic random variables associated with resistance. These variables include the properties of concrete and reinforcement, as well as the dimensions of a member cross-section. Finaly, modelling uncertainty arises when a simplified theoretical model is used to represent physical phenomena of interest. Consequently, a random variable representing systematic and random error should be included in the reliability analyses.

4.7 REFERENCES

4-1 Ellingwood, B., Galambos, T.V., MacGregor, J.G. and Cornell, C.A., *Development of a Probability Based Load Criterion for American National Standard A58*, NBS Special Publication 577, National Bureau of Standards, Washington, 1980.

4-2 Ang, A.H-S. and Tang, W.H., *Probability Concepts in Engineering Planning and Design, Vol. 2: Decision, Risk, and Reliability*, John Wiley and Sons, New York, 1984.

4-3 Benjamin, J.R. and Cornell, C.A., *Probability, Statistics, and Decision for Civil Engineers*, McGraw-Hill, New York, 1970.

4-4 Melchers, R.E., *Structural Reliability: Analysis and Prediction*, Ellis Horwood Series in Civil Engineering, Ellis Horwood Ltd., Chichester, 1987.

4-5 Harr, M.E., *Reliability-Based Design in Civil Engineering*, McGraw-Hill, Johannesburg, 1987.

4-6 SABS 0160:1989 (as amended 1990), *Code of Practice, The General Procedures and Loadings to be Adopted in the Design of Buildings*, SA Bureau of Standards, Pretoria, 1990.

4-7 Shinozuka, M. and Tan, R., *Probabilistic Load Combinations and Crossing Rates*, Proceedings of the Symposium on Probabilistic Methods in Structural Engineering, Engrg Mech Div and Struct Div, ASCE, St.Louis, Missouri, Oct 1981, pp. 229-249.

4-8 Milford, R.V., *Development of Load Factors for inclusion in SABS 0160 (The General Procedures and Loadings to be Adopted in the Design of Buildings)*, Internal Report 85/11, Structural and Geotechnical Engineering Division, National Building Research Institute, CSIR, Pretoria, Oct 1985.

4-9 Galambos, T.V. and Ellingwood, B., *Serviceability Limit States: Deflection*, J Struct Engrg, ASCE, Vol.112, No.1, Jan 1986, pp. 67-84.

4-10 Mirza, S.A., Kikuchi, D.K. and MacGregor, J.G., *Flexural Strength Reduction Factor for Bonded Prestressed Concrete Beams*, ACI J, Vol.77, Jul/Aug 1980, pp. 237-246.

4-11 SABS 0100:1980, *Code of Practice, The Structural Use of Concrete, Part 2: Materials and Execution of Work*, SA Bureau of Standards, Pretoria, 1980.

4-12 Al-Harthy, A.S. and Frangopol, D.M., *Reliability Assessment of Prestressed Concrete Beams*, J Struct Engrg, ASCE, Vol.120, No.1, Jan 1994, pp. 180-199.

4-13 Mirza, S.A. and MacGregor, J.G., *Probabilistic Study of Strength of Reinforced Concrete Members*, Can J Civ Eng, Vol.9, 1982, pp. 431-448.

4-14 Collins, M.P. and Mitchell, D., *Prestressed Concrete Basics*, Canadian Prestressed Concrete Institute, Ottawa, 1987.

4-15 Portland Cement Instiute, *Fulton's Concrete Technology, 6th ed.*, Addis, B.J. (ed.), Midrand, South Africa, 1986.

4-16 Rüsch, H., Jungwirth, D. and Hilsdorf, H.K., *Creep and Shrinkage: Their Effect on the Behaviour of Concrete Structures*, Springer-Verlag, New York, 1983.

4-17 Vrouwenvelder, A.C.W.M. and Siemes, A.J.M., *Probabilistic Calibration Procedure for the Derivation of Partial Safety Factors for the Netherlands Building Codes*, Heron, TNO-Institute for Building Materials and Structures, Vol.32, No.4, 1987, pp. 9-29.

4-18 Naaman, A.E. and Siriaksorn, A., *Reliability of Partially Prestressed Beams at Serviceability Limit States*, PCI J, Vol.27, No.6, Nov/Dec 1982, pp. 66-85.

4-19 Tichy, M. and Vorliçek, M., *Statistical Theory of Concrete Structures*, Irish University Press, Shannon, 1972.

4-20 Bowker, A.H. and Lieberman, G.J., *Engineering Statistics*, Prentice-Hall, Englewood Cliffs, N.J., 1960

CHAPTER 5

RELIABILITY ANALYSIS OF PC MEMBER

The main objective of this study is to estimate the level of reliability implied by the limit states design method as specified by the South African structural codes on which this study is based (i.e. partial safety factors and design criteria). For prestressed concrete design, theoretical models were selected in Chapter 3 to express the structural response of the member at the ULS of flexure and the SLS of deflection in terms of the basic variables. The statistical properties of these basic variables were discussed in Chapter 4 and the stage is therefore set to proceed with the reliability analyses.

Remaining limit states which were not considered for the purposes of this study, but which in practice should be checked that they are not reached, are shear strength and bond stresses at the ULS, and concrete stresses and crack widths at the SLS. Reliability analyses of these and other limit states are reported in Refs. 5-1 through 5-5.

5.1 PRACTICAL FOSM ANALYSIS

The outcome of FOSM reliability analysis is solutions to the most probable failure point, direction cosines, reliability index and probability of failure. These quantities may be used to evaluate the reliability at the limit state of interest. For a practical approach to reliability analysis using the FOSM method, attention should be directed towards the measures outlined below.

In Chapter 2 the reliability index β was defined as the distance from the origin in the reduced variable space to a point on the failure surface at a minimum distance from the origin (see § 2.2). However, the Rackwitz and Fiessler algorithm does not always guarantee global minimum and a breakdown case arises when the trial failure point lies close to a stationary point which is not a minimum (Ref. 5-6). The iteration procedure can only search for local stationary points and cannot distinguish between maxima, minima or saddle points. To ensure that global minimum is obtained in the case of highly non-linear limit state functions, different initial failure points must be assumed. In each case the iteration procedure is repeated until β converges and the relaibility index is then $\beta = \min(\beta_1, \beta_2, \ldots, \beta_n)$ where n denotes the number of initial points considered.

Usually, however, the difficulties associated with obtaining solutions to highly non-linear failure criteria may be avoided by the use of suitable approximation techniques. One method is to replace non-linear terms in the limit state function by substitute random variables and to determine their moments (Ref. 5-6). A disadvantage of this method is that certain basic

variables are consolidated into these substitute random variables and their direction cosines are therefore non-conservative.

Alternatively, a highly non-linear limit state function may be simplified by assuming certain basic variables to be deterministic parameters rather than random variables. Eq. 5-1 may be used as an indication to rate the relative contribution ω_i of a basic variable X_i to the uncertainty in the limit state function (see § 4.2.2). This contribution is proportional to the variance of X_i and to a factor related to the sensitivity of $g(\boldsymbol{X})$ to changes in X_i. Those basic variables taken as deterministic parameters should be taken at their mean avlues.

$$\omega_i = \frac{\left[\frac{\partial g(\boldsymbol{X})}{\partial X_i}\right]_{\mu_x}^2 \sigma_{X_i}^2}{\sum_{i=1}^{n} \left[\frac{\partial g(\boldsymbol{X})}{\partial X_i}\right]_{\mu_x}^2 \sigma_{X_i}^2} \tag{5-1}$$

When the derivatives required by the Rackwitz and Fiessler algorithm are difficult or impossible to determine, a semi-numerical method, based on finite differences, may be employed. This is explained by Eq. 5-2 below (Ref. 5-7).

$$\left[\frac{\partial g}{\partial X_i'}\right]_\star = \frac{dX_i}{dX_i'}\left[\frac{\partial g}{\partial X_i}\right]_\star = \sigma_{X_i}\frac{g(X_i + \Delta X_i)_\star - g(X_i)_\star}{\Delta X_i} \tag{5-2}$$

where $g(X_i + \Delta X_i)_\star = g(X_1^\star, X_2^\star, \ldots\ldots, X_i^\star + \Delta X_i, \ldots\ldots, X_n^\star)$

$g(X_i)_\star = g(X_1^\star, X_2^\star, \ldots\ldots, X_n^\star)$

$\Delta X_i = \frac{X_i^\star}{100}$, say

As discussed in Chapter 2, the linear approximation of the FOSM method is tantamount to replacing a non-linear failure surface with a hyperplane tangent to the failure surface at the most probable failure point (see § 2.2). The accuracy of this approximation depends on the degree of non-linearity of the function $g(\boldsymbol{X})$ and can be assessed in terms of the bounds on the probability of failure p_F as displayed in Eq. 5-3 (Ref. 5-8). The lower bound relates to a failure surface convex towards the origin in the reduced variable space, while the upper bound relates to a failure surface concave towards the origin.

$$1 - \Phi(\beta) < p_F < 1 - \chi_n^2(\beta^2) \tag{5-3}$$

where $\chi_n^2(-)$ = CDF of the chi-square distribution with n degrees of freedom

The Rackwitz and Fiessler algorithm has been programmed by various researchers (see Refs. 5-9 through 5-12). The algorithm is mostly programmed in Fortran code and requires modification to add additional limit state functions. However, for the purposes of this study VAP 1.6 (Ref. 5-13), a Windows-based program, is used for efficient reliability analysis. The main shortcoming of Vap 1.6 is that correlation among basic variables cannot be dealt with.

5.2 RELIABILITY AT ULS OF FLEXURE

The theoretical model required to predict the flexural strength of the prestressed concrete member at the ULS was selected in § 3.4.2. Whereas the variability of the basic variables with regard to physical uncertainty was determined in Chapter 4, moments for modelling uncertainty are derived in the next section.

5.2.1 Modelling Uncertainty

Modelling error ε_M arises from factors not accounted for in the theoretical model for flexural strength and is therefore introduced into Eq. 5-4 (see § 5.2.2). This theoretical model is based on the assumptions listed in § 3.4.1, which include the stress-strain relationships for both the concrete and prestressing steel, the Bernoulli/Navier hypothesis, and the fact that failure of the section is defined in terms of a limiting strain ε_{cu} being reached in the concrete. In accordance with Eqs. 4-53a and 4-53b the random variable ε_M augments the inherent physical uncertainty of the member response with modelling uncertainty.

The modelling error for flexural strength was estimated from experimental data on a limited number of test beams reported by Priestly, Park and Lu (Ref. 5-14). They tested 7 simply supported pretensioned concrete beams with rectangular cross-sections, subject to a zone of constant bending moment. Prestress was transferred at 7 days and the beams were tested at 28 days. All the beam specimens were overreinforced (see § 3.4.4) and failure therefore occurred suddenly. The systematic and random errors were calculated in § B.4.1 from the ratio of test response to the prediction according to the theoretical model. In accordance with Eqs. 4-55 and 4-56, the random error was subsequently modified to also reflect statistical uncertainty and uncertainties arising from the experimental procedures. Statistics on the latter type of uncertainty were obtained from Ref. 5-12 for prestressed beams subject to good quality testing.

$$\bar{\varepsilon}_M = 1.020 \qquad \text{and} \qquad V_{\varepsilon_M} = 0.159$$

The systematic error indicates that, on average, the theoretical model slightly underestimates the true member response. Vrouwenvelder and Siemes (Ref. 5-17) report a value of 0.10 for V_ε while Trautner and Frangopol (Ref. 5-18) quote a c.o.v. of 0.12 for the ultimate concrete

strain ε_{cu}. As the latter quantity forms part of the basic assumptions on which the model for flexural strength is based, the calculated value of V_ε seems acceptable. Note that this value is also applicable to Eq. 5-5b, since the uncertainty regarding the long-term concrete strength $f_{c\infty}$ is already reflected by the c.o.v of the long-term concrete cube strength factor c_2.

5.2.2 Limit State Function

The prestressed concrete member of this study was proportioned as an underreinforced section (see § 3.4.4). This is confirmed by the prestressing steel ratio which is equal to $0.35\rho_b$, where ρ_b is the balanced steel ratio. The balanced steel ratio marks the transition from an underreinforced section to an overreinforced section.

The theoretical model used to calculate flexural strength should correspond to the behaviour regime anticipated from the nominal material properties and dimensions. The selected model therefore applies to the tensile failure mode, where large non-linear elongation of the prestressing steel precedes compression failure of the concrete. Greater variability is associated with beams failing in compression. The limit state of flexure is written as follows.

$$g(X) = \varepsilon_M M_u - M \tag{5-4}$$

The load effect M must be separated into its basic variables, *viz* the applied dead and live load moments. If Eqs. 3-15 and 4-45 are substituted into Eq. 5-4, then the limit state functions based on the 28 days and long-term concrete cube strengths respectively, are as follows.

$$g_{28}(X) = \varepsilon_M f_{pu} A_p \left[d - \frac{f_{pu} A_p}{2 c_1 f_{cu} b} \right] - (M_D + M_L) \tag{5-5a}$$

$$g_{\infty}(X) = \varepsilon_M f_{pu} A_p \left[d - \frac{f_{pu} A_p}{2 c_1 c_2 f_{cu} b} \right] - (M_D + M_L) \tag{5-5b}$$

where M_D = applied dead load moment at midspan
M_L = applied live load moment at midspan
f_{cu} = concrete cube strength at 28 days
c_1 = concrete strength reduction factor
c_2 = long-term concrete cube strength factor
f_{pu} = ultimate strength of prestressing steel
A_p = cross-sectional area of prestressing steel
d = effective depth to prestressing steel
b = width of flange of PC beam section
ε_M = modelling error for flexural strength

Table 5-1: Basic variables for limit state of flexure.

X	X_n	$\bar{X}$	σ_X	Distribution
M_D [kNm]	203.8	214.0	21.4	N
M_L [kNm]	143.0	134.6	33.7	$EX_{I,L}$
f_{cu} [MPa]	50.0	58.23	5.82	N
c_1	0.670	0.706	0.057	N
c_2	1.16	1.30	0.133	N
f_{pu} [MPa]	1860	1934	48.4	N
A_p [mm^2]	700	708	9.21	N
d [mm]	528	531	4.4	N
b [mm]	1500	1504	6.4	N
ε_M	1.00	1.020	0.162	N

Eqs. 5-5a and 5-5b can be classified as non-linear limit state functions with uncorrelated basic variables. Statistical information on all these variables are summarized in Table 5-1. Nominal and mean values of the load effects were calculated in § B.5.1.

5.2.3 Reliability Analysis

The reliability characteristics for a Class 2 prestressed concrete member at the ULS of flexure are summarized in Table 5-2. In general not much correlation exists among the load effect and resistance variables and correlation was therefore ignored for the purposes of this study. Since uncertainty associated with the load effect terms dominates reliability analyses, results are normally arranged such that the nominal load ratio becomes the chief independent parameter. The nominal load ratio for this study can be expressed in the following ways.

	Practical ranges:	*Current study*:
concrete:	$0.5 \leq \frac{L_n}{D_n} \leq 1.5$	$\frac{L_n}{D_n} = \frac{3.39}{4.83} = 0.702$
steel:	$1.0 \leq \frac{L_n}{D_n} \leq 2.0$	for comparison
all:	$\frac{D_n}{D_n + L_n} > 0.5$	$\frac{D_n}{D_n + L_n} = \frac{4.83}{4.83 + 3.39} = 0.588$

Table 5-2: FOSM analysis for ULS of flexure.

$\beta = 3.10$		$p_F = 9.55\times10^{-4}$		
X_i	α_i	x_i^*	$\bar{X}$	$x_i^*/x_{i,n}$
ε_M	-0.910	0.562	1.020	0.562
M_L	0.366	171.6	134.6	1.200
M_D	0.170	225.3	214.0	1.105
f_{pu}	-0.078	1922	1934	1.033
A_p	-0.040	706.8	708	1.010
d	-0.027	530.6	531	1.005
f_{cu}	-0.007	58.11	58.23	1.162
c_1	-0.005	0.705	0.706	1.052
b	-0.0003	1504	1504	1.003

Based on these nominal load ratios and the type of failure, the reliability implied by the South African structural codes on which this study is based can be evaluated in terms of reliability reflected in current design practice. Table 5-3 lists a selection of values for the target reliability index β_T as reported in the literature. From this table it is evident that there is consensus among various code committees that the target reliability index for under-reinforced concrete members in general should lie in the region of 3.0. The value for prestressed concrete in particular is somewhat higher at 3.75 to 3.9.

The calculated reliability index is surprisingly low in view of the fact that the ULS of flexure represents a non-critical limit state in the case of a Class 2 prestressed concrete member (see § 3.2). Reliability analysis at the ULS of flexure was expected to yield a higher reliability index. This condition can be explained with reference to the relatively high uncertainty associated with the modelling error for flexural strength ε_M (c.o.v. 0.159) which results in a lower than expected value for β. A c.o.v. of 0.120, say, for ε_M would have resulted in a β value of 3.81.

Those basic variables which contribute in a significant manner to the uncertainty at the ULS of flexure can be identified from Table 5-2. It is clear that the reliability is dominated by the uncertainty associated with ε_M. This fact supports the notion that a theoretical model with a small random error should be selected. Apart from the dead and live load effects, the contribution of f_{pu}, A_p and d to the overall uncertainty is much less significant. The direction cosines of these variables are one order of magnitude smaller than that associated with ε_M.

Table 5-3: Target reliability for ULS of flexure.

β_T	Comment	Code	Country	Ref.
3.0	ductile, gradual failure modes	SABS 0160:1989	South Africa	5-19
4.0	brittle, sudden failure modes	SABS 0160:1989	South Africa	5-19
3.0	gravity loads	ANSI A58.1:1982	United States	5-19
3.75	prestressed concrete beams	ACI 318-77	United States	5-20
3.9	precast, prestressed concrete	NBS 577	United States	5-12
3.0	gradual failure, 30-year life	CSA S408-1981	Canada	5-21
3.5	sudden failure, 30-year life	CSA S408-1981	Canada	5-21

On the other hand, the uncertainty associated with f_{cu}, c_1 and b have an insignificant effect on the reliabilty. It follows therefore that the gain in concrete strength beyond 28 days would also have little effect on the reliability of a prestressed concrete member at the ULS of flexure. This was confirmed by demonstrating that the reliability index based on the long-term concrete cube strength shows only a marginal increase to 3.12, while the probability of failure drops by 5.1%. Clearly there is little advantage in taking cognisance of increased concrete strength during the design process as far as flexural strength is concerned.

The above observations are further supported by Figure 5-1 where the sensitivity of β with respect to either the mean or c.o.v. of the various basic variables is illustrated. The modelling error for flexural strength ε_M stands out as the curve with the steepest slope in both Figures 5-1a and 5-1b. Accurate knowledge of the c.o.v. of this basic variable therefore plays a significant role in the calculation of reliability. From Figure 5-1b it can be seen that the curves associated with f_{pu}, A_p and d are almost the same. When its slope is compared to that of ε_M it is concluded that the effect of these variables is much less significant. The curves associated with f_{cu}, c_1 and b are also the same, but it is practically horizontal indicating the insignificant effect of these variables on the reliability.

It was noted before that the focus of this study is on the uncertainty of the structural response of a prestressed concrete member, rather than on the uncertainty associated with the loading variables. The dominant role of ε_M can therefore be further emphasized with a FOSM analysis where the loading variables are taken at their mean values. The results of this analysis is given in Table 5-4 and is based on the limit state function in Eq. 5-6 (with loading in Nmm).

$$g_{28}(\boldsymbol{X}) = \varepsilon_M f_{pu} A_p \left[d - \frac{f_{pu} A_p}{2 c_1 f_{cu} b} \right] - 348.6 \times 10^6 \qquad (5\text{-}6)$$

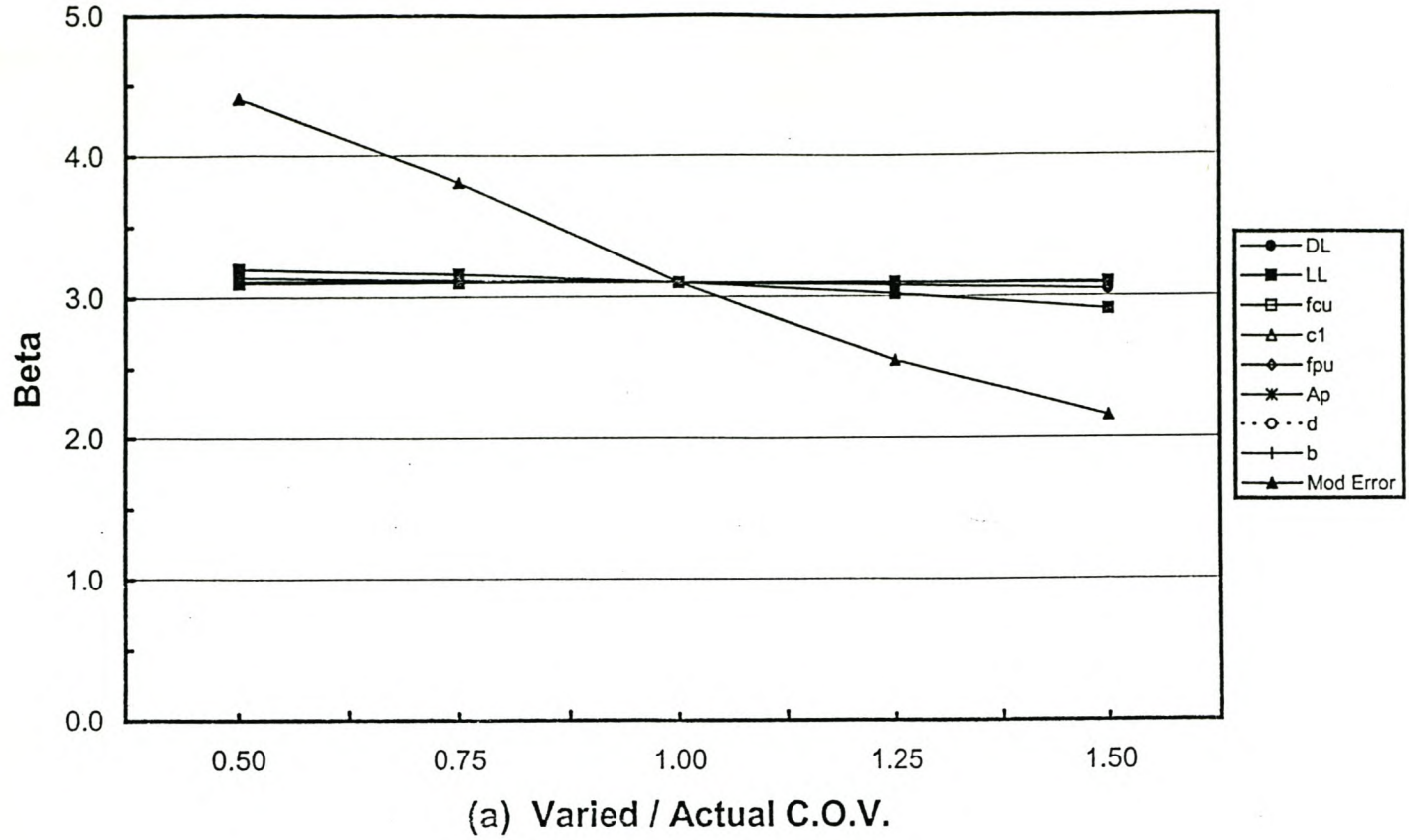

(a) Varied / Actual C.O.V.

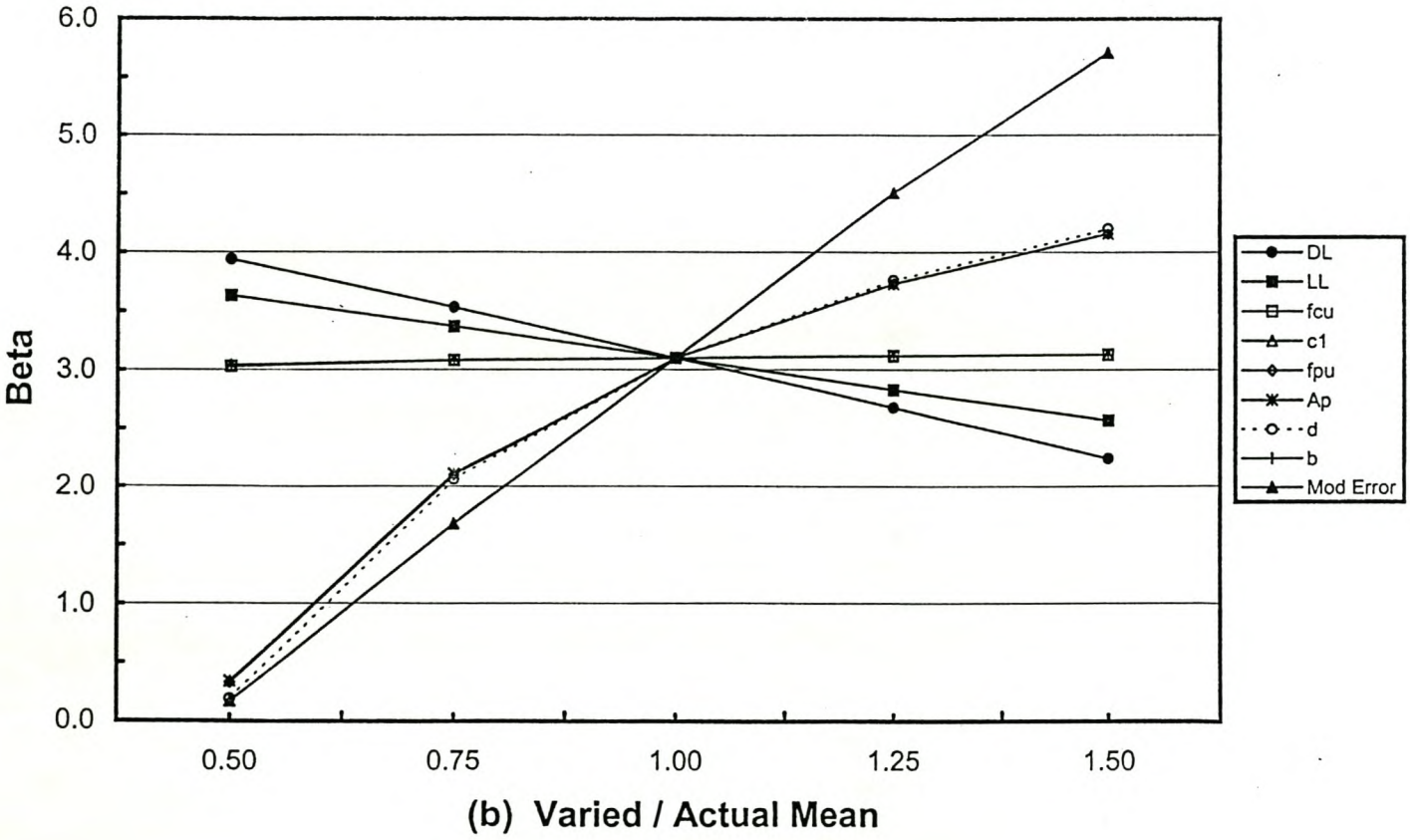

(b) Varied / Actual Mean

Figure 5-1: Sensitivity analysis at ULS of flexure.

Table 5-4: FOSM analysis with deterministic loading variables.

X_i	α_i	x_i^*	$\bar{X}$
ε_M	-0.996	0.494	1.020
f_{pu}	-0.075	1922	1934
A_p	-0.039	706.8	708
d	-0.026	530.6	531
f_{cu}	-0.006	58.11	58.23
c_1	-0.005	0.705	0.706
b	-0.0003	1504	1504

5.3 RELIABILITY AT SLS OF DEFLECTION

The theoretical model required to predict the deflection which affects partitions and finishes at the SLS was derived in § 3.5.1. As noted before, the selection of a Class 2 prestressed concrete member as basis of this study had the advantage that the theoretical model could be based on the assumption of linear elastic behaviour. Attention can therefore be focused on the reliability aspects of this limit state and not on the structural response. Moments for modelling uncertainty at this limit state are derived in the next section.

5.3.1 Modelling Uncertainty

A number of mechanisms contribute to the deflection of a prestressed concrete beam. For a beam uncracked in flexure these mechanisms include the concrete elasticity, the stiffening effect of the bonded prestressing steel on the concrete section, and the effect of creep and relaxation on long-term deflection. In principle all the different mechanisms would contribute to uncertainty in the theoretical model for deflection (Ref. 5-22). In this study modelling uncertainty at the various construction stages are represented by the combination of two kinds of modelling errors: ε_i reflects uncertainty in the instantaneous deflection, while ε_t and ε_∞ reflects uncertainty in the *ratio* of long-term to instantaneous deflection.

$$\varepsilon_{\delta t} = \varepsilon_t \varepsilon_i \tag{5-7a}$$

$$\varepsilon_{\delta \infty} = \varepsilon_\infty \varepsilon_i \tag{5-7b}$$

where $\varepsilon_{\delta t}$ = modelling error for 33 day deflection
$\varepsilon_{\delta \infty}$ = modelling error for long-term deflection
ε_i = modelling error for instantaneous deflection

ε_t = modelling error for ratio of 33 day to instantaneous deflection
ε_∞ = modelling error for ratio of long-term to instantaneous deflection

The effect of all the mechanisms noted above can be accounted for by using the second moment of area of the uncracked *transformed* section in deflection calculations. Furthermore, the material properties used for assessing the modular ratio (see Eq. 5-8 below) should reflect the construction stage under consideration.

$$n = \frac{E_{p\,eff}}{E_{c\,eff}} = (1 - r)(1 + \phi_c)\frac{E_p}{E_c} \tag{5-8}$$

where n = modular ratio
$E_{p\,eff}$ = effective modulus of elasticity of prestressing steel
$E_{c\,eff}$ = effective modulus of elasticity of concrete (see Eq. 3-21)
r = relaxation loss of prestressing steel
ϕ_c = creep factor of concrete

Modelling uncertainty is normally estimated from experimental data. However, for an uncracked prestressed concrete beam it is desirable to choose test beams with ratios of applied moment to cracking moment less than unity. As few of the test beams reported in literature satisfy this requirement, systematic error was estimated in § B.4.2(a) from the ratio of gross to transformed second moment of area (see Eq. 5-9). This approach will provide a lower limit to the systematic error. The presence of the prestressing steel contributes to stiffness, resulting in less deflection and the systematic error will therefore be less than unity.

$$\varepsilon_\delta = \frac{\delta_T}{\delta_M} \equiv \frac{I}{I_{trans}} < 1.0 \tag{5-9}$$

where δ_T = true *in-situ* deflection
δ_M = deflection predicted by theoretical model
I = second moment of area of gross uncracked section
I_{trans} = second moment of area of uncracked transformed section

Experimental work by Washa and Fluck and later reported by Pretorius (Ref. 5-23) was used to estimate an upper limit to the random error in § B.4.2(b). As this data applies to reinforced concrete beams cracked in flexure the calculated random errors were reduced by 25 per cent.

$\bar{\varepsilon}_i = 0.950$ and $V_{\varepsilon_i} = 0.099$
$\bar{\varepsilon}_t = 0.935$ and $V_{\varepsilon_t} = 0.057$
$\bar{\varepsilon}_\infty = 0.867$ and $V_{\varepsilon_\infty} = 0.113$

In order to compare these values with random errors reported elswhere, the random errors applicable to a particular construction stage can be combined in accordance with Eq. 4-19. This is illustrated below for long-term deflection and the value of 0.151 can be compared with a value of 0.170 reported by Retief (Ref. 5-22) for reinforced concrete beams cracked in flexure.

$$V_{\varepsilon_{t\infty}} = \sqrt{V_{\varepsilon_\infty}^2 + V_{\varepsilon_i}^2 + V_{\varepsilon_\infty}^2 V_{\varepsilon_i}^2}$$

$$= 0.151$$

5.3.2 The Second Moment of Area

The deflection of a prestressed concrete member is a function of the second moment of area I of the concrete section (see Figure 3-1) and the probability moments of this basic variable is therefore required for the reliability analysis. Using the methods of § 4.2.2, the dimensional variability characterized in § 4.4.3 was combined to quantify the uncertainty of I. For this purpose all basic dimensional variables were assumed to be uncorrelated.

Taylor-series approximations to the mean and variance were used in § B.5.2 through § B.5.4 in preference to the Point Estimate Method. This enabled correlation among the expressions given in Eqs. 5-10a through 5-10c to be calculated analytically. The effect of correlation on the mean and variance was, however, small. The results are summarised in Table 5-5.

$$A = \sum_i A_i = b\,h_{f_1} + b_w\left(h - h_{f_1}\right) + \frac{1}{2}\left(b - b_w\right)\left(h_{f_2} - h_{f_1}\right) \tag{5-10a}$$

$$y_{bot} = \frac{1}{A}\sum_i A_i\, y_{bot,i} \tag{5-10b}$$

$$= \frac{1}{A}\left\{ b\,h_{f_1}\left[h - \frac{h_{f_1}}{2}\right] + b_w\frac{\left(h - h_{f_1}\right)^2}{2} + \frac{1}{2}\left(b - b_w\right)\left(h_{f_2} - h_{f_1}\right)\left[h - h_{f_1} - \frac{1}{3}\left(h_{f_2} - h_{f_1}\right)\right]\right\}$$

$$I = \sum_i I_i + \sum_i A_i\, y_i^2 \tag{5-10c}$$

$$= \frac{1}{12}\,b\,h_{f_1}^3 + b\,h_{f_1}\left[h - \frac{h_{f_1}}{2} - y_{bot}\right]^2$$

$$+ \frac{1}{12} b_w \left(h - h_{f_1}\right)^3 + b_w \left(h - h_{f_1}\right) \left[y_{bot} - \frac{\left(h - h_{f_1}\right)}{2} \right]^2$$

$$+ \frac{1}{36} \left(b - b_w\right) \left(h_{f_2} - h_{f_1}\right)^3 + \frac{1}{2} \left(b - b_w\right) \left(h_{f_2} - h_{f_1}\right) \left[h - h_{f_1} - \frac{1}{3} \left(h_{f_2} - h_{f_1}\right) - y_{bot} \right]^2$$

where b = width of flange of PC beam section
b_w = width of web of PC beam section
h = overall depth of PC beam section
h_{f1} = min flange depth
h_{f2} = max flange depth

Table 5-5: Moments of the gross uncracked section.

X	$\bar{X}/X_n$	V_X
A	1.004	0.024
y_{bot}	1.005	0.027
I	1.023	0.026

It is evident that the uncertainty in I is small compared to that of the concrete properties. This can be ascribed to various factors. In the first place, the dimensions correspond to good quality construction as is prevalent in the precast concrete industry. Secondly, due to constant standard deviation (see Table 4-2), the effect of variations in the size of a member is less pronounced for deep or large members than for shallow or small cross-sections. Most importantly however, uncracked section behaviour was modelled through the selection of a Class 2 member as basis of this study (see § 3.5.1).

5.3.3 Limit State Function

The serviceability limit state of deflection may be regarded as a problem of capacity versus demand in terms of the general criterion of the limit states design method, as expressed by Eq. 1-5. For a satisfactory design, the deflection δ at the critical section must satisfy the deflection criteria δ_a. The former is obtained from structural analysis and is an uncertain quantity as the loading and structural behaviour are uncertain. Conceptually, the deflection criteria might also be regarded as an uncertain quantity. This would be possible as serviceability criteria are associated with subjective human perceptions and are therefore difficult to specify (see § 3.5.2). The variability is likely to be high, with a c.o.v. in the region of 0.2 to 0.5, even though few data exist to substantiate this claim (Ref. 5-6). A study

of the literature indicates that uncertainty in the deflection limit has, unfortunately, not been quantified. Therefore, in this study, δ_a was taken from the customary deterministic values which are assumed to provide protection against unsightly deflections and against damage to non-structural elements and equipment.

The limit state of deflection is expressed by Eq. 5-11, where δ is the difference between the total long-term deflection δ_∞ and the deflection δ_t which occurs before construction of partitions and application of finishes. The modelling error for deflection ε_δ is expanded using Eqs. 5-7a and 5-7b.

$$\begin{aligned} g(\boldsymbol{X}) &= \delta_a - \varepsilon_\delta \delta \\ &= \delta_a - \varepsilon_\delta (\delta_\infty - \delta_t) \\ &= \delta_a - \varepsilon_\delta (\delta_{p\infty} + \delta_{w\infty} + \delta_{var} - \delta_{pt} - \delta_{wt}) \\ &= \delta_a - (\varepsilon_\infty \varepsilon_i \delta_{p\infty} + \varepsilon_\infty \varepsilon_i \delta_{w\infty} + \varepsilon_i \delta_{var} - \varepsilon_t \varepsilon_i \delta_{pt} - \varepsilon_t \varepsilon_i \delta_{wt}) \end{aligned} \tag{5-11}$$

where ε_i = modelling error for instantaneous deflection
ε_t = modelling error for ratio of 33 day to instantaneous deflection
ε_∞ = modelling error for ratio of long-term to instantaneous deflection

and $\delta_{p\infty}$ = instantaneous elastic plus long-term creep deflection due to prestressing force
$\delta_{w\infty}$ = instantaneous elastic plus long-term creep deflection due to permanent load
δ_{var} = instantaneous elastic deflection due to variable load
δ_{pt} = instantaneous elastic plus 33 day creep deflection due to prestressing force
δ_{wt} = instantaneous elastic plus 33 day creep deflection due to self-weight

As before, the load effects must be seperated into their basic variables (see also Eqs. 3-24 and 4-46).

$$M_{perm} = M_{D_1} + M_{D_2} + \psi_L M_L \tag{5-12a}$$

$$M_{var} = (1 - \psi_L) M_L \tag{5-12b}$$

$$M_{min} \equiv M_{D_1} \tag{5-12c}$$

Similarly, the effective long-term prestressing force was expanded and written in terms of its basic variables.

$$P_\infty = \eta_\infty P_i = -\eta_\infty f_{pi} A_p = -\eta_\infty \zeta_i f_{pu} A_p \tag{5-13}$$

When the various increments of deflection, together with Eqs. 5-12 and 5-13, are substituted into Eq. 5-11, the limit state of deflection reduces to Eq. 5-14 below.

$$g(X) = \delta_a + \varepsilon_\infty \varepsilon_i \frac{\zeta_i f_{pu} A_p}{48 E_c I}(5e_1 + e_2)L_e^2 \left[\eta_\infty + \frac{(1 + \eta_\infty)}{2}\phi_{c\infty} \right] \tag{5-14}$$

$$- \varepsilon_\infty \varepsilon_i \frac{5}{48} \left[\frac{M_{D_1} + M_{D_2} + \psi_L M_L}{E_c I} \right] L_e^2 (1 + \phi_{c\infty})$$

$$- \varepsilon_i \frac{5}{48} \left[\frac{(1 - \psi_L) M_L}{E_c I} \right] L_e^2$$

$$- \varepsilon_t \varepsilon_i \frac{\zeta_i f_{pu} A_p}{48 E_c I}(5e_1 + e_2)L_e^2 \left[\eta_t + \frac{(1 + \eta_t)}{2}\phi_{ct} \right]$$

$$+ \varepsilon_t \varepsilon_i \frac{5}{48} \left[\frac{M_{D_1}}{E_c I} \right] L_e^2 (1 + \phi_{ct})$$

where δ_a = allowable deflection at midspan
ε_i = modelling error for instantaneous deflection
ε_t = modelling error for ratio of 33 day to instantaneous deflection
ε_∞ = modelling error for ratio of long-term to instantaneous deflection
M_{D1} = applied midspan moment due to self-weight
M_{D2} = applied superimposed dead load moment at midspan
M_L = applied live load moment at midspan
ψ_L = sustained live load ratio
E_c = modulus of elasticity of 28 day concrete
$\phi_{c\infty}$ = long-term creep factor
ϕ_{ct} = 33 day creep factor
f_{pu} = ultimate strength of prestressing steel
A_p = cross-sectional area of prestressing steel
ζ_i = initial loss factor
η_∞ = long-term loss factor
η_t = 33 day loss factor
I = second moment of area of gross uncracked section
e_1 = eccentricity at midspan section
e_2 = eccentricity at support sections
L_e = span of PC member

Once again, Eq. 5-14 can be classified as a non-linear limit state function with uncorrelated basic variables. Since the deflection can be expressed as a single analytical function,

Table 5-6: Basic variables for limit state of deflection.

X	X_n	$\bar{X}$	σ_X	Distribution
δ_a [mm]	30.0	—	—	—
ε_i	1.0	0.950	0.094	N
ε_t	1.0	0.935	0.053	N
ε_∞	1.0	0.867	0.098	N
M_{D1} [kNm]	153.0	153.0	16.4	N
M_{D2} [kNm]	50.6	60.7	14.0	N
M_L [kNm]	143.0	93.0	29.8	$EX_{I,L}$
ψ_L	0.3	0.261	0.172	N
E_c [GPa]	34.0	37.4	3.93	N
$\phi_{c\infty}$	3.04	3.04	0.754	N
ϕ_{ct}	1.23	1.23	0.305	N
f_{pu} [MPa]	1860	1934	48.4	N
A_p [mm^2]	700	708	9.21	N
ζ_i	0.706	0.706	0.028	N
η_∞	0.839	0.839	0.067	N
η_t	0.919	0.919	0.074	N
I [10^9 mm^4]	7.323	7.492	0.193	N
e_1 [mm]	345	348	4.4	N
e_2 [mm]	110	113	4.4	N
L_e [m]	15.0	—	—	—

partial derivatives are possible. Statistical information on all the variables are summarized in Table 5-6, while nominal and mean values of the load effects were calculated in § B.5.1.

5.3.4 Reliability Analysis

The limit state function of Eq. 5-14 is highly non-linear and was not suitable for analysis with VAP 1.6. It therefore had to be simplified by assuming certain basic variables to be deterministic parameters rather than random variables (see § 5.1). For this purpose Eq. 5-1

Table 5-7: FOSM analysis for SLS of deflection.

$\beta = 1.67$		$p_F = 4.75\times10^{-2}$	
X_i	α_i	x_i^*	$\bar{X}$
M_L	0.448	111.1	93.0
ϕ_{ct}	0.419	1.443	1.23
η_∞	-0.350	0.800	0.839
η_t	0.321	0.959	0.919
M_{D2}	0.321	68.21	60.7
ψ_L	0.297	0.346	0.261
$\phi_{c\infty}$	-0.285	2.682	3.04
ε_i	0.254	0.990	0.950
ε_t	0.184	0.951	0.935
ε_∞	-0.135	0.845	0.867
M_{D1}	0.095	155.6	153.0

was used in § B.6.1 to rate the relative contribution of the basic variables to the uncertainty in the limit state function and the number of random variables was subsequently reduced from 18 to 11 (see Eq 5-15 below, with applied loading in Nmm). Those variables associated with creep, prestress losses, loading and modelling remained as basic variables. The reliability characteristics for a Class 2 prestressed concrete member at the SLS of deflection are summarized in Table 5-7.

$$
\begin{aligned}
g(\boldsymbol{X}) = 30 &+ 29.97\,\varepsilon_\infty\varepsilon_i\left[\eta_\infty + \frac{(1+\eta_\infty)}{2}\phi_{c\infty}\right] \\
&- 8.36\times10^{-8}\,\varepsilon_\infty\varepsilon_i\left(M_{D_1} + M_{D_2} + \psi_L M_L\right)\left(1 + \phi_{c\infty}\right) \\
&- 8.36\times10^{-8}\,\varepsilon_i\left(1 - \psi_L\right)M_L \\
&- 29.97\,\varepsilon_t\varepsilon_i\left[\eta_t + \frac{(1+\eta_t)}{2}\phi_{ct}\right] \\
&+ 8.36\times10^{-8}\,\varepsilon_t\varepsilon_i M_{D_1}\left(1 + \phi_{ct}\right)
\end{aligned}
\qquad (5\text{-}15)
$$

Table 5-8: Target reliability for SLS of deflection.

β_T	Comment	Code	Country	Ref.
1.8	concrete floor beam	TGB-Algemeen	Netherlands	5-17
1.5	floor beams, occupancy loads	—	United States	5-24

As could be expected from the use of unfactored values in the design, the probability of exceeding the allowable deflection is large. The probability of failure at the SLS of deflection is two orders of magnitude larger than that at the ULS of flexure, but compares well with acceptable practice. See Table 5-8 which lists values for the target reliability index β_T as reflected in current design practice.

As before, a FOSM analysis was also carried out based on the limit state function given below, where the load effects were taken at their mean values. This affords a clearer picture of the relative contribution of the basic variables associated with the structural response to the uncertainty at the SLS of deflection. The results of this analysis is listed in Table 5-9.

$$
\begin{aligned}
g(\boldsymbol{X}) = 30 &+ 29.97\,\varepsilon_\infty \varepsilon_i \left[\eta_\infty + \frac{(1+\eta_\infty)}{2}\phi_{c\infty} \right] \\
&- 8.36\times 10^{-2}\,\varepsilon_\infty \varepsilon_i (213.7 + 93.0\,\psi_L)(1+\phi_{c\infty}) \\
&- 7.775\,\varepsilon_i (1-\psi_L) \\
&- 29.97\,\varepsilon_t \varepsilon_i \left[\eta_t + \frac{(1+\eta_t)}{2}\phi_{ct} \right] \\
&+ 12.79\,\varepsilon_t \varepsilon_i (1+\phi_{ct})
\end{aligned}
\qquad (5\text{-}16)
$$

It is clear that the creep factors ϕ_{ct} and $\phi_{c\infty}$ have a profound effect on the uncertainty, followed by the prestress loss factors η_∞ and η_t. Evidently, accurate specification of these variables would enhance the reliability of the design. However, this requirement should be weighed against the need for simple code provisions that would hold user acceptance (refer to clause 5.8.2 of SABS 0100:1992, Ref. 5-25).

At first glance the effect of the various modelling variables is secondary to that of the creep and prestress loss factors. However, the overall contribution of these variables on the uncertainty at the SLS of deflection of a prestressed concrete member is obtained when the associated direction cosines are combined as shown on the next page. The resulting direction

Table 5-9: FOSM analysis with deterministic loading variables.

X_i	α_i	x_i^*	$\bar{X}$	$x_i^*/x_{i,n}$
ϕ_{ct}	0.518	1.525	1.23	1.240
$\phi_{c\infty}$	-0.415	2.455	3.04	0.808
η_t	0.395	0.974	0.919	1.060
η_∞	-0.393	0.790	0.839	0.942
ε_i	0.296	1.002	0.950	1.002
ψ_L	0.264	0.346	0.261	1.153
ε_t	0.235	0.958	0.935	0.958
ε_∞	-0.191	0.832	0.867	0.832

cosine is comparable to that of the creep factors and indicates that, as in the case of the ULS of flexure, a theoretical model with a small random error should be selected. The contribution of the sustained live load ratio ψ_L is less meaningfull than expected in view of its large c.o.v (0.659).

$$\alpha_{\varepsilon_s} = \sqrt{\alpha_{\varepsilon_i}^2 + \alpha_{\varepsilon_t}^2 + \alpha_{\varepsilon_\infty}^2}$$

$$= 0.423$$

It may be noted that in this analysis the second moment of area I and the modulus of elasticity of the concrete E_c were assumed to be deterministic parameters. Whereas variability in beam stiffness is a major cause of uncertainty in the deflection of cracked concrete members, this is not so in the case of a Class 2 prestressed concrete member. For the same reason the uncertainty associated with the properties of the prestressing steel, f_{pu} and A_p, are negligible.

Figure 5-2 illustrates the results of a sensitivity analysis of β with respect to either the mean or the c.o.v. of the various basic variables. It must be noted that since the variability of the load effects were removed from this analysis, the actual value of β has no real significance. In comparison with the ULS of flexure, the reliability at the SLS of deflection is not dominated by the uncertainty associated with a single basic variable. It is also clear that the reliability is much more sensitive to variations in the mean than to variations in the c.o.v.

Retief (Ref. 5-22) found overall modelling uncertainty, particularly that of the long-term effects, to be the dominant source of uncertainty in predicting the deflection behaviour of a reinforced concrete member. He further noted that, for a fixed beam depth, the expected

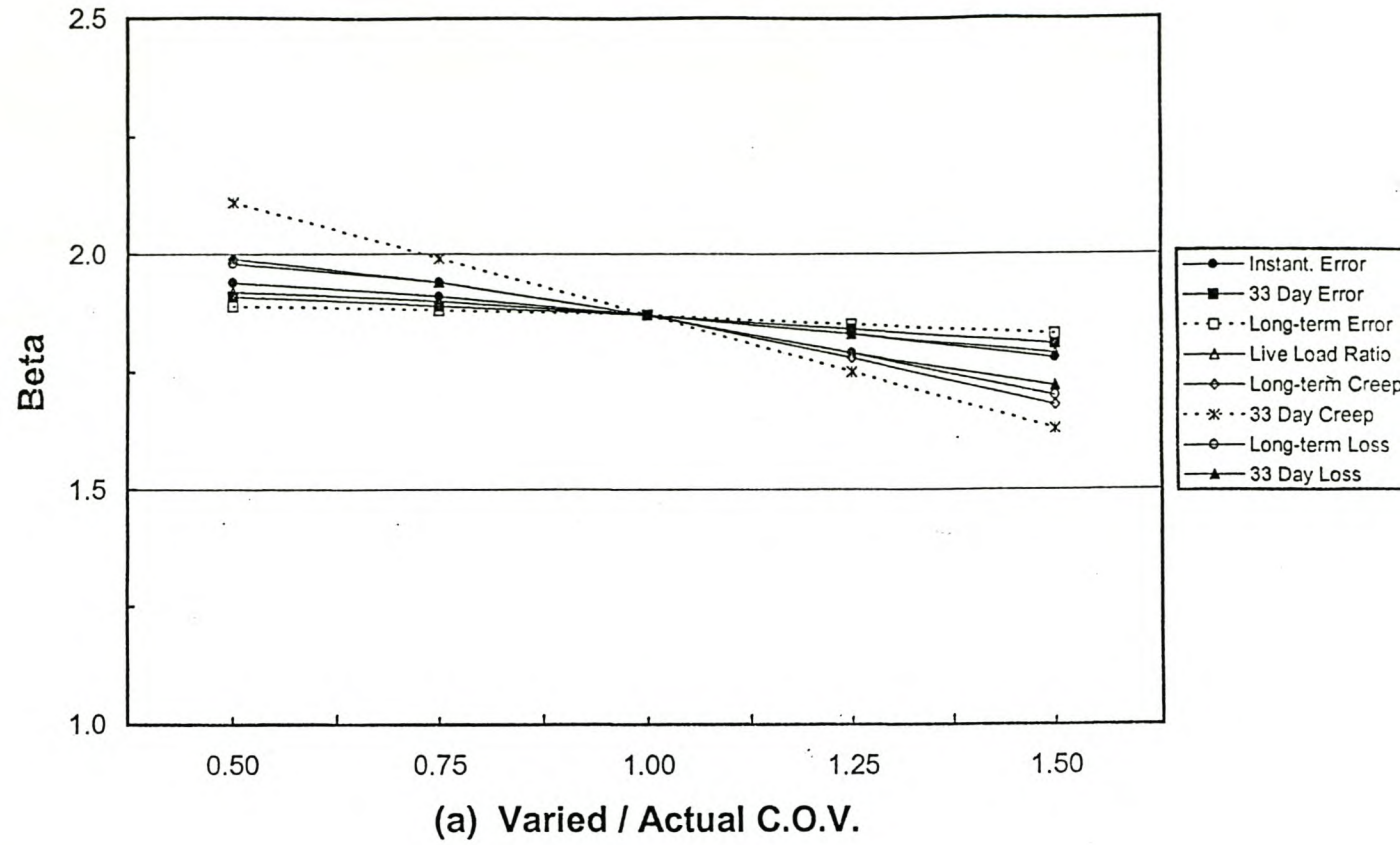

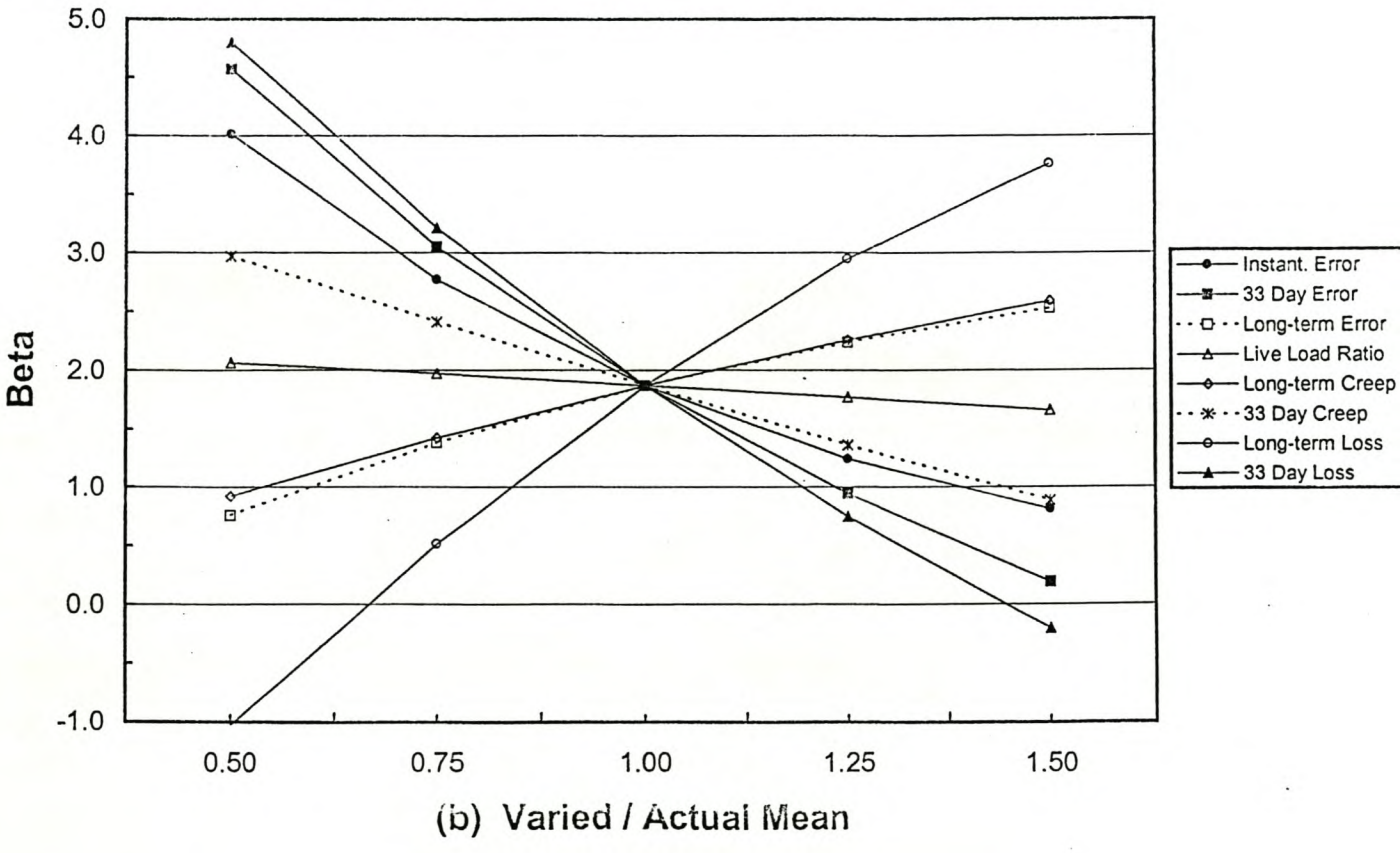

Figure 5-2: Sensitivity analysis at SLS of deflection.

deflection is very much a function of the creep coefficient when using Branson's Method, with an increase in the characteristic deflection from 28 % to almost 50 % above the design limit as $\phi_{c\infty}$ increases from 1.8 to 2.35. The uncertainty in Branson's Method is therefore also dominated by the variability of the creep coefficient. Due to the empirical way in which creep effects are calculated in Branson's Method, its sensitivity to the variability of $\phi_{c\infty}$ is thought to be unrealistic. A more rational model for long-term creep effects such as the effective modulus of elasticity as used by the BS 8110 method would give a more realistic indication of the importance of creep.

5.4 SUMMARY

FOSM reliability analyses were carried out in this chapter at the ULS of flexure and at the SLS of deflection and the reliability indices were found to be 3.10 and 1.67 respectively. Modelling uncertainty were included in both theoretical models with modelling uncertainty at the SLS of deflection found as the combination of three modelling errors related to the various components of deflection.

At the ULS of flexure the reliability is dominated by the uncertainty associated with the modelling error ε_M, whereas the contribution of f_{pu}, A_p and d to the overall uncertainty is much less significant. It was also confirmed that the gain in concrete strength beyond 28 days has little effect on the reliability of a prestressed concrete member at the ULS of flexure.

The limit state function at the SLS of deflection was highly non-linear and was not suitable for analysis with the available software. It therefore had to be simplified by assuming certain basic variables to be deterministic parameters rather than random variables. In contrast with the ULS of flexure, reliability at the SLS of deflection is not dominated by the uncertainty associated with a single basic variable. The creep factors ϕ_{ct} and $\phi_{c\infty}$ and the prestress loss factors η_∞ and η_t all have a significant effect on the uncertainty. It was shown that the overall contribution to uncertainty of the various modelling variables is comparable to that of the creep factors.

5.5 REFERENCES

5-1 Mirza, S.A., *Study of Bond Strength Reliability of Reinforced Concrete Beams*, Proceedings of the 4th International Conference on Civil and Structural Engineering Computing, Civil-Comp 89, Topping, B.H.V. (ed.), London, Sept 1989, pp.203-208.

5-2 Darwin, D., Idun, E.K., Zuo, J. and Tholen, M.L., *Reliability-Based Strength Reduction Factor for Bond*, ACI Struct J, Vol.95, No.4, Jul/Aug 1998, pp. 434-443.

5-3 Li, C.Q. and Melchers, R.E., *Reliability Analysis of Creep and Shrinkage Effects*, J Struct Engrg, ASCE, Vol.118, No.9, Sept 1992, pp. 2323-2337.

5-4 Committee on Fatique and Fracture Reliability of the Committee on Structural Safety and Reliability of the Structural Division, *Fatique Reliability: Development of Criteria for Design*, J Struct Div, Proc ASCE, Vol.108, No.ST1, Jan 1982, pp. 71-88.

5-5 Al-Harthy, A.S. and Frangopol, D.M., *Reliability Assessment of Prestressed Concrete Beams*, J Struct Engrg, ASCE, Vol.120, No.1, Jan 1994, pp. 180-199.

5-6 Melchers, R.E., *Structural Reliability: Analysis and Prediction*, Ellis Horwood Series in Civil Engineering, Ellis Horwood Ltd., Chichester, 1987.

5-7 Retief, J.V., *Semi-numerical Method for Derivatives based on Finite Differences*, Personal Communication, Dept. of Civil Engineering, University of Stellenbosch, South Africa, June 1994.

5-8 Ang, A.H-S. and Tang, W.H., *Probability Concepts in Engineering Planning and Design, Vol. 2: Decision, Risk, and Reliability*, John Wiley and Sons, New York, 1984.

5-9 Der Kiureghian, A. and De Stefano, M., *Efficient Algorithm for Second-Order Reliability Analysis*, J Engrg Mech, ASCE, Vol.117, No.12, Dec 1991, pp. 2904-2923.

5-10 Hsu, F-S. and Wang, K-S., *Algorithm for Evaluation of Second-Moment Reliability Index*, J Chinese Soc Mech Eng, Vol.11, No.2, Apr 1990, pp. 185-191.

5-11 Parkinson, D.B., *Computer Solution for the Reliability Index*, Eng Struct, Vol.2, Jan 1980, pp. 57-62.

5-12 Ellingwood, B., Galambos, T.V., MacGregor, J.G. and Cornell, C.A., *Development of a Probability Based Load Criterion for American National Standard A58*, NBS Special Publication 577, National Bureau of Standards, Washington, 1980.

5-13 Petschacher, M., Simov, G. and Toulev, S., *VaP 1.6 for MS-Windows*, Institute of Struct Engrg, Eidgenössishe Technische Hochschule, Zurich.

5-14 Priestly, M.J.N., Park, R. and Lu, F.P.S., *Moment-Curvature Relationships for Prestressed Concrete in Constant-Moment Zones*, Magazine of Concrete Research, Vol.23, No.75-76, June-Sept. 1971, pp. 69-78.5-5

5-15 SABS 0100:1992, *Code of Practice, The Structural Use of Concrete, Part 1: Design*, SA Bureau of Standards, Pretoria, 1992.

5-16 Marshall, V. and Robberts, J.M., *Prestressed Concrete: Design and Practice*, Concrete Society of Southern Africa, Halfway House, Oct 1995.

5-17 Vrouwenvelder, A.C.W.M. and Siemes, A.J.M., *Probabilistic Calibration Procedure for the Derivation of Partial Safety Factors for the Netherlands Building Codes*, Heron, TNO-Institute for Building Materials and Structures, Vol.32, No.4, 1987, pp. 9-29.

5-18 Trautner, J.J. and Frangopol, D.M., *Safety Sensitivity Functions for Reinforced Concrete Beams*, ACI Struct J, Vol.88, No.5, Sept/Oct 1991, pp. 631-640.

5-19 Milford, R.V., *Risk and Structural Design*, Civ Eng S Afr, Vol.30, No.12, Dec 1988, pp. 569-575.

5-20 Mirza, S.A., Kikuchi, D.K. and MacGregor, J.G., *Flexural Strength Reduction Factor for Bonded Prestressed Concrete Beams*, ACI J, Vol.77, Jul/Aug 1980, pp. 237-246.

5-21 Canadian Standards Association, *Guidelines for the Development of Limit States Design*, CSA Special Publication S408-1981, Ontario, Dec 1981.

5-22 Retief, J.V., *The Reliability of ACI and BS Methods of Deflection Design of Reinforced Concrete Members*, Dept. of Civil Engineering, University of Stellenbosch, South Africa, 1996.

5-23 Pretorius, P.C., *Proposed Calculation Method for Deflections*, Civ Eng S Afr, Vol.27, No.6, June 1985, pp. 303-312.

5-24 Galambos, T.V. and Ellingwood, B., *Serviceability Limit States: Deflection*, J Struct Engrg, ASCE, Vol.112, No.1, Jan 1986, pp. 67-84.

5-25 SABS 0100:1992, *Code of Practice, The Structural Use of Concrete, Part 1: Design*, SA Bureau of Standards, Pretoria, 1992.

CHAPTER 6

CONCLUSIONS AND RECOMMENDATIONS

This chapter deals with conclusions that can be drawn from this study and with recommendations for future work. A single pretensioned concrete T-beam was analysed for the purposes of this study and the intention was therefore to focus on the sensitivity of the reliability of a specific design to uncertainty in the various design parameters. However, the theoretical model used at the ULS of flexure is suitable for any prestressed concrete beam element, while the theoretical model used at the SLS of deflection is limited to Class 2 prestressed concrete members. What remains is to expand the study to cover the practical range of material properties, dimensions and nominal load ratios.

6.1 CONCLUSIONS

The reliability characteristics at the two limit states of interest must be viewed against the background of the following issues.

- The prestressed concrete member which formed the basis of this study was designed following the limit states design method as provided for by the applicable South African structural codes.

- Reliability analyses are usually performed as a function of the nominal live to dead load ratio. The analyses of this study were based on a nominal load ratio of 0.70. As only a subset of all the uncertainties that exist were considered, the reliability analyses yielded notional values of the reliability index.

- The design of a Class 2 prestressed concrete member is governed by the SLS of cracking, which led to a higher than required margin of safety at the (non-critical) ULS of flexure. The prestressed concrete member of this study can be classified as an underreinforced section.

- With reference to the SLS of deflection, the response considered is that of a section uncracked under maximum service loads. Interest only lies in that component of the total deflection which takes place after the construction of partitions and the application of finishes.

- The focus of this study is on the uncertainty associated with the structural response of a prestressed concrete member, rather than on the uncertainty associated with the loading variables.

Based on the results of this study, the reliability characteristics at the ULS of flexure can be summarised as follows.

- The literature indicates that the reliability index for prestressed concrete should lie in the region of 3.75 to 3.90. However, at 3.10 the calculated value is surprisingly low in view of the fact that the ULS of flexure represents a non-critical limit state in the case of a Class 2 prestressed concrete member. This condition can be explained with reference to the relatively high uncertainty associated with the modelling error for flexural strength ε_M (c.o.v. 0.159) which results in a lower than expected value for β. A c.o.v. of 0.120, say, for ε_M would have resulted in a β value of 3.81.

- The reliability is dominated by the uncertainty associated with ε_M. This fact supports the notion that a theoretical model with small systematic and random errors should be selected. Modelling uncertainty should therefore be investigated more thoroughly as it is not conservatively catered for in the code. However, it should also be noted that the study of modelling uncertainty was based on a limited number of test beams and that the results were therfore, to a certain extent, influenced by this small sample. Apart from the dead and live load effects, the contribution of f_{pu}, A_p and d to the overall uncertainty is much less significant. The direction cosines of these variables are one order of magnitude smaller than that associated with ε_M.

- The uncertainty associated with f_{cu}, c_1 and b have an insignificant effect on the reliabilty. The direction cosines of these variables are two or more orders of magnitude smaller than that associated with ε_M. It follows therefore that the gain in concrete strength beyond 28 days would also have little effect on the reliability of a prestressed concrete member. This was confirmed by demonstrating that the reliability index based on the long-term concrete cube strength shows only a marginal increase from 3.10 to 3.12, while the probability of failure drops by 5.1%. There is therefore little advantage in taking cognisance of increased concrete strength during the design process as far as flexural strength is concerned.

Similarly, the reliability characteristics at the SLS of deflection lead to the following conclusions.

- As could be expected from the use of unfactored values in the design, the probability of exceeding the allowable deflection is large. The probability of failure at the SLS of deflection is two orders of magnitude larger than that at the ULS of flexure. At 1.67 the reliability index compares well with acceptable practice.

- In comparison with the ULS of flexure, the reliability at the SLS of deflection is not dominated by the uncertainty associated with a single basic variable. Apart from the dead and live load effects, the creep factors ϕ_{ct} and $\phi_{c\infty}$ have a significant effect on

the uncertainty, followed by the prestress loss factors η_∞ and η_t. The overall contribution of the various modelling variables to the uncertainty at the SLS of deflection is obtained when the associated direction cosines are combined, resulting in a direction cosine comparable to that of the creep factors. The contribution of the sustained live load ratio ψ_L is less meaniningfull than expected in view of its large c.o.v (0.659).

- It was demonstrated that the variability of the second moment of area I and the modulus of elasticity of the concrete E_c can be approximated with deterministic parameters. Whereas variability in beam stiffness is a major cause of uncertainty in the deflection of cracked concrete members, this is not the case for a Class 2 prestressed concrete member. For the same reason the uncertainty associated with the properties of the prestressing steel, f_{pu} and A_p, are negligible.

6.2 RECOMMENDATIONS

This study is concluded with the following recommendations for future work.

- Modelling uncertainty was shown to be a major source of uncertainty at both the ULS of flexure and the SLS of deflection. This implies that the present code provisions should be reviewed to formulate theoretical models with reduced systematic and random errors. This concern can also be adressed with the introduction of a set of partial resistance factors to take account of modelling uncertainty at the different limit states.

- The creep factor ϕ_c and prestress loss factor η were identified as basic variables which have a significant effect on the uncertainty at the SLS of deflection. Evidently, accurate specification of these variables based on more sophisticated models would enhance the reliability of the design. However, this concern should be weighed against the need for simple code provisions that would hold user acceptance. Alternatively, the partial material factor for concrete γ_{mc} may be adjusted to take account of this uncertainty at the SLS of deflection.

- Whereas the live load at the ULS is based on a 50-year reference period, it does not seem reasonable to base serviceability criteria on such a severe requirement. When the variability of this load for deflections calculations is founded on the premise that the deflection limit should not be exceeded more than once during any one tenancy, the mean value ratio is reduced from 0.94 to 0.65. The latter value represents the proportion of the lifetime maximum live load expected to act during one tenancy. This aspect might lead to savings in the design and the effect thereoff should be investigated further.

- SABS 0160:1989 advocates the use of a consistent set of partial material factors, irrespective of the limit state being considered, together with a set of partial resistance factors to take account of the uncertainty associated with different limit states. This approach has not been implemented in SABS 0100-1:1992 in that different partial material factors are specified for various categories of limit states. This inconsistency should be addressed by the selection of a set of partial resistance factors for the various limit states.

- There is a need for a systematic review of the level of reliability achieved through the use of SABS 0100-1:1992 in the design of prestressed concrete members. As a pilot study, based only on the prestressed concrete member of this study, partial resistance factors applicable to the ULS of flexure and the SLS of deflection may be derived. These resistance factors would represent a calibration of SABS 0100-1:1992 as the calculated values of the notional reliability index β_N will be regarded as target values. This would be an attempt to address the inconsistency noted above.

- The reliability basis for the serviceability limit states is not as well developed as that for the ultimate limit states. Research must be directed towards formulating an objective failure criterion for deflection. The uncertainty in the deflection limit must therefore be quantified with a probability distribution to replace the existing subjective failure criterion based on deterministic values.

Finally, it is hoped that the results presented in this study will contribute to the future revision of the current South African structural codes, as well as provide insight into the effect of deterministic assumptions during design on the reliability of prestressed concrete members.

BIBLIOGRAPHY

Abeles, P.W., Bardhan-Roy, B.K. and Turner, F.H., *Prestressed Concrete Designer's Handbook, 2nd ed.*, Viewpoint Publications Series, Cement and Concrete Association, UK, 1979.

Al-Harthy, A.S. and Frangopol, D.M., *Reliability Assessment of Prestressed Concrete Beams*, J Struct Engrg, ASCE, Vol.120, No.1, Jan 1994, pp. 180-199.

Ang, A.H-S. and Cornell, C.A., *Reliability Bases of Structural Safety and Design*, J Struct Div, Proc ASCE, Vol.100, No.ST9, Sept 1974, pp. 1755-1769.

Ang, A.H-S. and Tang, W.H., *Probability Concepts in Engineering Planning and Design, Vol. 2: Decision, Risk, and Reliability*, John Wiley and Sons, New York, 1984.

Benjamin, J.R. and Cornell, C.A., *Probability, Statistics, and Decision for Civil Engineers*, McGraw-Hill, New York, 1970.

Bowker, A.H. and Lieberman, G.J., *Engineering Statistics*, Prentice-Hall, Englewood Cliffs, N.J., 1960

BS 8110:1985, *Structural Use of Concrete, Part 1, Code of Practice for Design and Construction*, British Standards Institution, London, 1985.

Canadian Standards Association, *Guidelines for the Development of Limit States Design*, CSA Special Publication S408-1981, Ontario, Dec 1981.

Chandrasekar, P. and Dayaratnam, P., *Analysis of Probability of Failure of Prestressed Concrete Beams*, Build Sci, Vol.10, 1975, pp. 161-167.

Collins, M.P. and Mitchell, D., *Prestressed Concrete Basics*, Canadian Prestressed Concrete Institute, Ottawa, 1987.

Committee on Fatique and Fracture Reliability of the Committee on Structural Safety and Reliability of the Structural Division, *Fatique Reliability: Development of Criteria for Design*, J Struct Div, Proc ASCE, Vol.108, No.ST1, Jan 1982, pp. 71-88.

Darwin, D., Idun, E.K., Zuo, J. and Tholen, M.L., *Reliability-Based Strength Reduction Factor for Bond*, ACI Struct J, Vol.95, No.4, Jul/Aug 1998, pp. 434-443.

Der Kiureghian, A. and De Stefano, M., *Efficient Algorithm for Second-Order Reliability Analysis*, J Engrg Mech, ASCE, Vol.117, No.12, Dec 1991, pp. 2904-2923.

Ellingwood, B., Galambos, T.V., MacGregor, J.G. and Cornell, C.A., *Development of a Probability Based Load Criterion for American National Standard A58*, NBS Special Publication 577, National Bureau of Standards, Washington, 1980.

Ellingwood, B. and Galambos, T.V., *General Specifications for Structural Design Loads*, Proceedings of the Symposium on Probabilistic Methods in Structural Engineering, Engrg Mech Div and Struct Div, ASCE, St.Louis, Missouri, Oct 1981, pp. 27-42.

Floris, C., *Reliability of a Prestressed Concrete Beam: A Comparison between the Methods of Third and Second Level*, Reliab Engrg and Syst Saf, Vol.23, 1988, pp. 1-22.

Freudenthal, A.M., Garrelt, J.M. and Shinozuka, M., *The Analysis of Structural Safety*, J Struct Div, Proc ASCE, Vol.92, No.ST1, Feb 1966, pp. 267-325.

Galambos, T.V. and Ellingwood, B., *Serviceability Limit States: Deflection*, J Struct Engrg, ASCE, Vol.112, No.1, Jan 1986, pp. 67-84.

Goldstein, A.E., *Changes in SABS 0100: Some Effects on Reinforced Concrete Design*, Concrete Beton, J CSSA, No.62, Feb 1992, pp. 6-10.

Guofan, Z. and Yungui, L., *Reliability Analysis of Reinforced Concrete Structures for Serviceability Limit States*, Proceedings of the 5th International Conference on Structural Safety and Reliability, ICOSSAR, 1989, pp. 2067-2070.

Hamann, R.A. and Bulleit, W.M., *Reliability of Prestressed High-strength Concrete Beams in Flexure*, Proceedings of the 5th Conference on Applications of Probability in Structural and Soil Engineering, Vol.1, Lind, N.C. (ed.), Waterloo, 1987, pp. 141-147.

Harr, M.E., *Reliability-Based Design in Civil Engineering*, McGraw-Hill, Johannesburg, 1987.

Hasofer, A.M. and Lind, N.C., *An Exact and Invariant First-Order Reliability Format*, J Engrg Mech Div, Proc ASCE, Vol.100, No.M1, Feb 1974, pp. 111-121.

Heger, F.J., *Public Safety - Is it Compromised by new LRFD Design Stanards ?*, J Struct Engrg, ASCE, Vol.119, No.4, Apr 1993, pp. 1251-1264.

Hognestad, E., Hanson, N.W. and McHenry, D., *Concrete Stress Distribution in Ultimate Strength Design*, ACI J, Vol.12, 1955. pp. 52-58.

Hsu, F-S. and Wang, K-S., *Algorithm for Evaluation of Second-Moment Reliability Index*, J Chinese Soc Mech Eng, Vol.11, No.2, Apr 1990, pp. 185-191.

Israel, M., Ellingwood, B. and Corotis, R., *Reliability-Based Code Formulations for Reinforced Concrete Buildings*, J Struct Engrg, ASCE, Vol.113, No.10, Oct 1987, pp. 2235-2252.

Kemp, A.R., *Comparisons of International Loading Codes and Options for South Africa*, Proceedings of the S.A. National Conference on Loading, SAICE, Midrand, South Africa, Sept 1998.

Kemp, A.R., *Innovations and Implications of New Limit States Formulation for South African Structural Codes*, Design of Portal Frames Course, Appendix 2, SA Institution of Steel Construction, 1990.

Kemp, A.R., Milford, R.V. and Laurie, J.A.P., *Proposals for a Comprehensive Limit States Formulation for South African Structural Codes*, Civ Eng S Afr, Vol.29, No.9, Sept 1987, pp. 351-360.

Kennedy, D.J.L., *North American Loading for Buildings*, Proceedings of the S.A. National Conference on Loading, SAICE, Midrand, South Africa, Sept 1998.

Kong, F.K. and Evans, R.H., *Reinforced and Prestressed Concrete, 3rd ed.*, Van Nostrand Reinhold, U.K., 1987.

Kong, F.K., Evans, R.H., Cohen, E. and Roll, F., *Handbook of Structural Concrete*, Pitman Books Limited, London, 1983.

Leicester, R.H., *Computation of a Safety Index*, Civ Engrg Trans, Institution of Engineers, Australia, Vol.CE27, No.1, Feb 1985, pp. 55-61.

Li, C.Q. and Melchers, R.E., *Reliability Analysis of Creep and Shrinkage Effects*, J Struct Engrg, ASCE, Vol.118, No.9, Sept 1992, pp. 2323-2337.

MacGregor, J.G., *Load and Resistance Factors for Concrete Design*, Proceedings of the Symposium on Probabilistic Methods in Structural Engineering, Engrg Mech Div and Struct Div, ASCE, St.Louis, Missouri, Oct 1981, pp. 14-26.

Marshall, V. and Robberts, J.M., *Prestressed Concrete: Design and Practice*, Concrete Society of Southern Africa, Halfway House, Oct 1995.

Marshall, V. and Robberts, J.M., *Considerations regarding the Requirements for Minimum Reinforcement in Reinforced Concrete Flexural Members*, Dept. of Civil Egineering, University of Pretoria, South Africa, Dec 1996.

Melchers, R.E., *Reliability Calculation for Structures*, Civ Engrg Trans, Institution of Engineers, Australia, Vol.CE27, No.1, Feb 1985, pp. 124-129.

Melchers, R.E., *Structural Reliability: Analysis and Prediction*, Ellis Horwood Series in Civil Engineering, Ellis Horwood Ltd., Chichester, 1987.

Menzies, J.B. and Gulvanessian, H., *EUROCODE 1 - The Code for Structural Loading*, Proceedings of the S.A. National Conference on Loading, SAICE, Midrand, South Africa, Sept 1998.

Milford, R.V., *Development of Load Factors for inclusion in SABS 0160 (The General Procedures and Loadings to be Adopted in the Design of Buildings)*, Internal Report 85/11, Structural and Geotechnical Engineering Division, National Building Research Institute, CSIR, Pretoria, Oct 1985.

Milford, R.V., *A Guide for Calibrating SABS Material Codes*, Internal Report 86/16, Structural and Geotechnical Engineering Division, National Building Research Institute, CSIR, Pretoria, Oct 1986.

Milford, R.V., *Load Factors for Limit State Codes*, Technical Note, J Struct Engrg, ASCE, Vol.113, No.9, Sept 1987, pp. 2053-2057.

Milford, R.V., *Target Safety and SABS 0160 Load Factors*, Civ Eng S Afr, Vol.30, No.10, Oct 1988, pp. 475-481.

Milford, R.V., *Risk and Structural Design*, Civ Eng S Afr, Vol.30, No.12, Dec 1988, pp. 569-575.

Mirza, S.A., *Study of Bond Strength Reliability of Reinforced Concrete Beams*, Proceedings of the 4th International Conference on Civil and Structural Engineering Computing, Civil-Comp 89, Topping, B.H.V. (ed.), London, Sept 1989, pp. 203-208.

Mirza, S.A., Hatzinikolas, M. and MacGregor, J.G., *Statistical Description of the Strength of Concrete*, J Struct Div, Proc ASCE, Vol.105, No.ST6, 1979, pp. 1021-1037.

Mirza, S.A., Kikuchi, D.K. and MacGregor, J.G., *Flexural Strength Reduction Factor for Bonded Prestressed Concrete Beams*, ACI J, Vol.77, Jul/Aug 1980, pp. 237-246.

Mirza, S.A. and MacGregor, J.G., *Variations in the Dimensions of Reinforced Concrete Members*, J Struct Div, Proc ASCE, Vol.105, No.ST4, 1979, pp. 751-766.

Mirza, S.A. and MacGregor, J.G., *Variability of Mechanical Properties of Reinforcing Bars*, J Struct Div, Proc ASCE, Vol.105, No.ST5, 1979, pp. 921-937.

Mirza, S.A. and MacGregor, J.G., *Statistical Study of Shear Strength of Reinforced Concrete Slenders Beams*, ACI J, Vol.76, No.11, Nov 1979, pp. 1159-1177.

Mirza, S.A. and MacGregor, J.G., *Probabilistic Study of Strength of Reinforced Concrete Members*, Can J Civ Eng, Vol.9, 1982, pp. 431-448.

Naaman, A.E. and Siriaksorn, A., *Reliability of Partially Prestressed Beams at Serviceability Limit States*, PCI J, Vol.27, No.6, Nov/Dec 1982, pp. 66-85.

Nowak, A.S. and Carr, R.I., *Sensitivity Analysis for Structural Errors*, J Struct Engrg, ASCE, Vol.111, No.8, Aug 1985, pp. 1734-1746.

Nowak, A.S. and Lind, N.C., *Practical Code Calibration Procedures*, Can J Civ Eng, Vol.6, 1979, pp. 112-119.

Parkinson, D.B., *Computer Solution for the Reliability Index*, Eng Struct, Vol.2, Jan 1980, pp. 57-62.

Petschacher, M., Simov, G. and Toulev, S., *VaP 1.6 for MS-Windows*, Institute of Struct Engrg, Eidgenössishe Technische Hochschule, Zurich.

Pham, L., *Loads on Buildings and Other Structures - Australian Current Practice and Future Direction*, Proceedings of the S.A. National Conference on Loading, SAICE, Midrand, South Africa, Sept 1998.

Portland Cement Instiute, *Fulton's Concrete Technology, 6th ed.*, Addis, B.J. (ed.), Midrand, South Africa, 1986.

Pretorius, P.C., *Proposed Calculation Method for Deflections*, Civ Eng S Afr, Vol.27, No.6, June 1985, pp. 303-312.

Priestly, M.J.N., Park, R. and Lu, F.P.S., *Moment-Curvature Relationships for Prestressed Concrete in Constant-Moment Zones*, Magazine of Concrete Research, Vol.23, No.75-76, June-Sept. 1971, pp. 69-78.

Rackwitz, R. and Fiessler, B., *Structural Reliability under Combined Random Load Sequences*, Computers and Struct, Vol.9, No.5, November 1978, pp. 489-494.

Ramsey, R.J., Mirza, S.A. and MacGregor, J.G., *Monte Carlo Study of Short-time Deflections of Reinforced Concrete Beams*, ACI J, Vol.76, No.8, Aug 1979, pp. 897-917.

Rao, S.V.K.M. and Dilger, W.H., *Evaluation of Short-term Deflections of Partially Prestressed Concrete Members*, ACI Struct J, Vol.89, No.1, Jan-Feb 1992, pp. 71-78.

Retief, J.V., *Semi-numerical Method for Derivatives based on Finite Differences*, Personal Communication, Dept. of Civil Engineering, University of Stellenbosch, South Africa, June 1994.

Retief, J.V., *The Reliability of ACI and BS Methods of Deflection Design of Reinforced Concrete Members*, Dept. of Civil Engineering, University of Stellenbosch, South Africa, 1996.

Ruiz, S.E. and Soriano, A., *Design Live Loads for Office Buildings in Mexico and The United States*, J Struct Engrg, ASCE, Vol.123, No.6, June 1997, pp. 816-822.

Rüsch, H., Jungwirth, D. and Hilsdorf, H.K., *Creep and Shrinkage: Their Effect on the Behaviour of Concrete Structures*, Springer-Verlag, New York, 1983.

SABS 0100:1992, *Code of Practice, The Structural Use of Concrete, Part 1: Design*, SA Bureau of Standards, Pretoria, 1992.

SABS 0100:1980, *Code of Practice, The Structural Use of Concrete, Part 2: Materials and Execution of Work*, SA Bureau of Standards, Pretoria, 1980.

SABS 0160:1989 (as amended 1990), *Code of Practice, The General Procedures and Loadings to be Adopted in the Design of Buildings*, SA Bureau of Standards, Pretoria, 1990.

Scholz, H., *Appraisal of Deflection and Cracking Models for Partially Prestressed Members*, Civ Eng S Afr, Vol.32, No.1, Jan 1990, pp. 23-33.

Scholz, H. and Pretorius, P.C., *Alternative Creep Deflection Model for Prestressed Sections*, Concrete Beton, Journal of the Concrete Society of Southern Africa, No.67, Feb 1993, pp. 13,16-19.

Shinozuka, M. and Tan, R., *Probabilistic Load Combinations and Crossing Rates*, Proceedings of the Symposium on Probabilistic Methods in Structural Engineering, Engrg Mech Div and Struct Div, ASCE, St.Louis, Missouri, Oct 1981, pp. 229-249.

Standards Association of Australia, *Guidelines for Conversion to Limit State Codes*, Committee BD/6 - Loading of Structures, Canberra, Jan 1985.

Tabsh, S.W., *Reliability Based Parametric Study of Pretensioned AASHTO Bridge Girders*, PCI J, Vol.37, No.5, Sept/Oct 1992, pp. 56-65.

Tabsh, S.W. and Nowak, A.S., *Reliability of Highway Girder Bridges*, J Struct Engrg, ASCE, Vol.117, No.8, Aug 1991, pp. 2372-2388.

Ter Haar, T.R. and Retief, J.V., *A Procedure for Loading Code Calibration*, Dept. of Civil Engineering, University of Stellenbosch, South Africa, 1999.

Thoft-Christensen, P. and Baker, M.J., *Structural Reliability Theory and its Applications*, Springer-Verlag, Berlin, 1982.

Tichy, M. and Vorliçek, M., *Statistical Theory of Concrete Structures*, Irish University Press, Shannon, 1972.

Trautner, J.J. and Frangopol, D.M., *Safety Sensitivity Functions for Reinforced Concrete Beams*, ACI Struct J, Vol.88, No.5, Sept/Oct 1991, pp. 631-640.

Vrouwenvelder, A.C.W.M. and Siemes, A.J.M., *Probabilistic Calibration Procedure for the Derivation of Partial Safety Factors for the Netherlands Building Codes*, Heron, TNO-Institute for Building Materials and Structures, Vol.32, No.4, 1987, pp. 9-29.

Zhao, Y-G. and Ono, T., *System Reliability of Ductile Frame Structures*, J Struct Engrg, ASCE, Vol.124, No.6, June 1998, pp. 678-685.

APPENDIX A

LIMIT STATES DESIGN OF PC MEMBER

A.1.1 DESIGN OBJECTIVE

Make use of the provisions of SABS 0100-1(1992) for flexural design at the serviceability limit state to design a class 2 prestressed concrete T-beam which is simply supported over a span of 15 m in an office environment. Obtain the design loads from SABS 0160(1989) Also make use of the procedures recommended by SABS 0100-1(1992) to check the design flexural strength of the beam at the ultimate limit state and the deflection of the beam at the serviceability limit state.

Use a beam section which is 1500 mm wide and 600 mm deep as shown below.

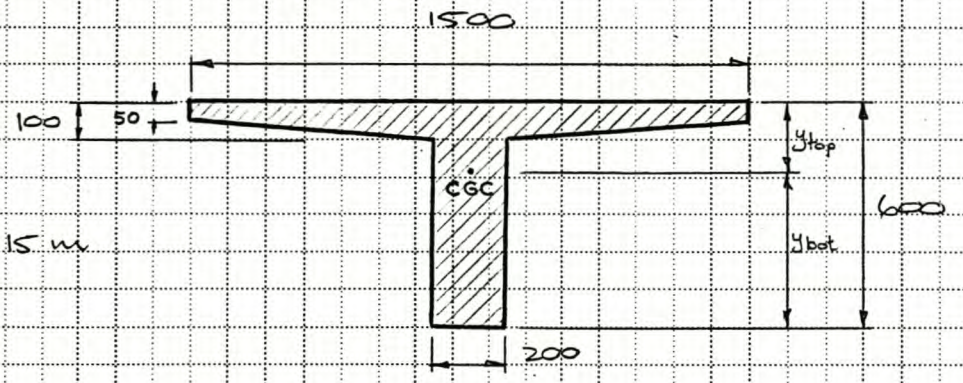

L_e = 15 m

$A = 217{,}5.10^3$ mm^2 $y_{top} = -183$ mm $Z_{top} = -40{,}916.10^6$ mm^3

$I = 7{,}323.10^9$ mm^4 $y_{bot} = 417$ mm $Z_{bot} = 17{,}561.10^6$ mm^3

Indicate all relevant clauses from the design codes of practice in square brackets.

A.1.2 DESIGN LOADS [SABS 0160(1989)]

The beam must be designed to support a uniformly distributed live load as well as a superimposed dead load.

Nominal Dead Loads, D_n

Beams self-weight (specific weight = 25 kN/m³): [5.3.1(a)]

$\therefore D_1 = 25 . 2(7,5 . 10^3/1,5) = 3,63$ kPa

Superimposed dead load (i.e. finishes): [5.3.1(b)]

$\therefore D_2 = 1,20$ kPa

Nominal Live Loads, L_n

Unreduced imposed office floor load: [5.4.1.1(e)]

$L_o = 2,5$ kPa

Floor load reduction factor $= 0,3 + \frac{3,1}{\sqrt{1,5 . 15}} = 0,954$ [5.4.1.3(b)]

$\therefore L_1 = 0,954 . 2,5 = 2,39$ kPa

Partition load: [5.4.1.4(e)]

$L_2 = 1,0$ kPa

Load Combinations at the ULS (take $\gamma_c = 1,0$)

$$w_d = \left(\gamma_{fD} . D_n + \gamma_{fL} . L_n + \sum_{j \neq L} \psi_j \gamma_{fj} Q_{nj}\right) b$$

1) Maximum dead load acting in combination with live load:

$D_n = D_1 + D_2 = 3,63 + 1,20 = 4,83$ kPa

$L_n = L_1 + L_2 = 2,39 + 1,0 = 3,39$ kPa

$\gamma_{f_D} = 1,2$; $\gamma_{f_L} = 1,6$; $Q_{nj} = 0$ [Table 2]

$\therefore w_d = (1,2 \cdot 4,83 + 1,6 \cdot 3,39)1,5 = 16,83\ kN/m$

$M_d = \frac{1}{8} w_d L_e^2 = 473,3\ kNm$ at midspan

2) Maximum dead load acting in isolation:

$D_n = D_1 + D_2 = 3,63 + 1,20 = 4,83\ kPa$

$\gamma_{f_D} = 1,5$; $L_n = 0$; $Q_{nj} = 0$ [Table 2]

$\therefore w_d = (1,5 \cdot 4,83)1,5 = 10,87\ kN/m$

$M_d = \frac{1}{8} w_d L_e^2 = 305,7\ kNm$ at midspan

Load Combinations at the SLS (take $\gamma_c = 1,0$)

$$w_{\substack{min \\ max}} = \left(\gamma_{f_D} D_n + \gamma_{f_L} L_n + \sum_{j \neq L} \psi_j \gamma_{f_j} Q_{nj}\right) b$$

1) At transfer of prestress: Minimum dead load acting in isolation.

$D_n = D_1 = 3,63\ kPa$

$\gamma_{f_D} = 1,0$; $L_n = 0$; $Q_{nj} = 0$ [Table 2]

$\therefore w_{min} = (1,0 \cdot 3,63)1,5 = 5,44\ kN/m$

$M_{min} = \frac{1}{8} w_{min} L_e^2 = 153,0\ kNm$ at midspan

2) Under service loads: Maximum dead load acting in combination with live load

$D_n = D_1 + D_2 = 3,63 + 1,20 = 4,83\ kPa$

$L_n = L_1 + L_2 = 2,39 + 1,0 = 3,39\ kPa$

$\gamma_{f_D} = 1,1$; $\gamma_{f_L} = 1,0$; $Q_{nj} = 0$ [Table 2]

$\therefore w_{max} = (1,1 \cdot 4,83 + 1,0 \cdot 3,39)1,5 = 13,04\ kN/m$

$M_{max} = \frac{1}{8} w_{max} L_e^2 = 366,8\ kNm$ at midspan

3) Under permanent loads: Maximum dead load acting in combination with component of live load considered as being of a sustained nature.

$$w_{perm} = \left(\gamma_{f,D} D_n + \sum_i \psi_i \gamma_{f,i} Q_{ni}\right) b$$

$D_n = D_1 + D_2 = 3,63 + 1,20 = 4,83$ kPa

$Q_{nL} \equiv L_n = L_1 + L_2 = 2,39 + 1,0 = 3,39$ kPa

$\gamma_{f,D} = 1,1$; $\gamma_{f,L} = 1,0$; $\psi_L = 0,3$ [Table 2]

$\therefore w_{perm} = (1,1 \cdot 4,83 + 0,3 \cdot 1,0 \cdot 3,39)1,5 = 9,49$ kN/m

$M_{perm} = \frac{1}{8} w_{perm} L_e^2 = 266,9$ kNm at midspan

4) Under variable load: Component of live load considered as being of an variable nature.

$$w_{var} = \left[(1-\psi_i)\gamma_{f,i} Q_{ni}\right] b$$

$\therefore w_{var} = \left[(1-0,3)1,0 \cdot 3,39\right]1,5 = 3,56$ kN/m

$M_{var} = \frac{1}{8} w_{var} L_e^2 = 100,1$ kNm at midspan

A.1.3 MATERIAL PROPERTIES [SABS 0100-1(1992)]

Concrete

Use normal density concrete for which the characteristic cube strength at 28 days is

$f_{cu} = 50$ MPa

Assume that transfer of prestress will occur at 3 days and that low-pressure steam curing will result in an initial cube strength of

$f_{cu} = 32,5$ MPa

Check minimum required strengths [5.1.5.1]

$f_{cu} > f_{cu,min} = 40\ MPa$ ∴ OK

$f_{ci} > f_{ci,min} = 25\ MPa$ ∴ OK

Modulus of rupture [A.2.4.1.1]

$f_r = 0{,}65\sqrt{f_{cu}} = 4{,}6\ MPa$

Secant modulus of elasticity [Table C.1]

$E_c = 34\ GPa$

$E_{ci} = 28{,}8\ GPa$

Estimate the long-term creep factor ϕ_{∞} (30 years) and the creep factor after 33 days ϕ_{ct}. Assume an ambient relative humidity of 60% (most inland areas)

$$\phi_c(t) = 3{,}5k\left(1{,}58 - \frac{H}{120}\right)t_i^{-0{,}118}\frac{(t-t_i)^{0{,}6}}{10+(t-t_i)^{0{,}6}}$$ [Collins & Mitchell]

where t = age of concrete (days)

t_i = 3 days, age of concrete at loading

k = factor which takes account of volume/surface

H = ambient relative humidity

exposed perimeter $u_1 = 1500 + 2(50 + \sqrt{50^2 + 650^2} + 500) + 200$

$= 4104\ mm$

$$\text{volume/surface} = A/u_1 = \frac{217{,}5\cdot 10^3}{4104} = 53\ mm$$

$k_{\infty} = 0{,}95$ and $k_t = 0{,}85$ [Collins & Mitchell]

∴ $\phi_{\infty} = 3{,}04$ and $\phi_{ct} = 1{,}23$

Prestressing Steel

Use 12,9 mm 7-wire super grade (low relaxation) strand with a nominal steel area of 100 mm² and characteristic ultimate strength of

$f_{pu} = 1860$ MPa

The maximum jacking stress is limited to 75% of the characteristic ultimate strength. [5.8.1.1]

$f_{po} = 0,75\, f_{pu} = 0,75 \cdot 1860 = 1395$ MPa

The modulus of elasticity is

$E_p = 195$ GPa [3.4.2.3]

The short-term design stress-strain relationship for the prestressing steel is approximated with a tri-linear curve [3.4.3.2(c)]

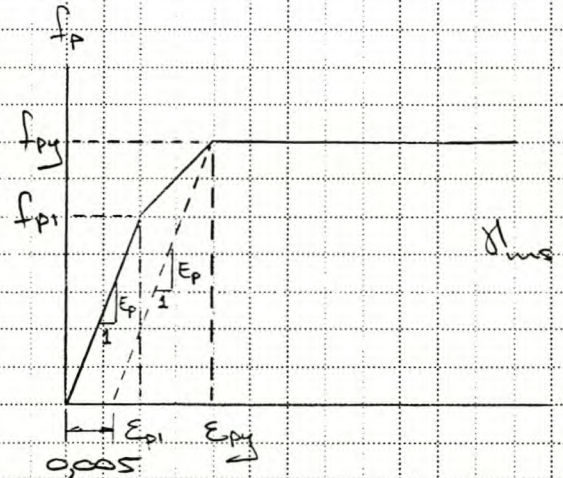

$\gamma_{ms} = 1,15$ [3.5.3.2(a)]

$$f_{py} = f_{pu}/\gamma_{ms} = \frac{1860}{1,15} = 1617 \text{ MPa}$$

$$\varepsilon_{py} = 0,005 + f_{py}/E_p = 0,005 + \frac{1617}{195 \cdot 10^3} = 0,0133$$

$$f_{p1} = 0,8 \cdot f_{pu}/\gamma_{ms} = 1294 \text{ MPa} \quad \text{and} \quad \varepsilon_{p1} = f_{p1}/E_p = 0,0066$$

A.2.1 PERMISIBLE STRESSES [SABS 0100-1(1992)]

The beam is designed as a class 2 prestressed concrete beam for which tensile stresses is allowed, but with no visible cracking (i.e. limited prestress). [3.2.3.3.1.2]

Permissible concrete stresses include a partial safety factor of $\gamma_{mc} = 1,3$ [3.3.4.2]

At transfer of prestress: prestressing force acting at its maximum value P_i, and applied external load acting at its minimum value M_{min}.

Tensile stress limit

$$\sigma_{ti} = 0,45\sqrt{f_{ci}} = 0,45\sqrt{32,5} = 2,57\ MPa \quad [5.3.2.3.2(b)]$$

Compressive stress limit

$$\sigma_{ci} = 0,45\, f_{ci} = 0,45(-32,5) = -14,63\ MPa \quad [5.3.2.3.1]$$

Under service loads: prestressing force acting at its minimum value P_∞, and applied external loading acting at its maximum value M_{max}.

Compressive stress limit

$$\sigma_{c\infty} = 0,33\, f_{cu} = 0,33(-50) = -16,50\ MPa \quad [Table\ 29]$$

Tensile stress limit

$$\sigma_{t\infty} = 0,45\sqrt{f_{cu}} = 0,45\sqrt{50} = 3,18\ MPa \quad [Table\ 30]$$

Note that the magnitude of the stress limitations imposed by the design code of practice makes it possible to assume a linear elastic section for purposes of analysis at the SLS. [5.3.2.1.(b)]

A.2.2 MINIMUM REQUIRED SECTION PROPERTIES

Assume loss-factor $\eta_\infty = 0{,}83$

$$Z_{top,min} = \frac{M_{max} - \eta_\infty M_{min}}{\sigma_{c\infty} - \eta_\infty \sigma_{ti}}$$

$$= \frac{(366{,}8 - 0{,}83 \cdot 153{,}0)\,10^6}{-16{,}50 - 0{,}83(2{,}57)}$$

$$= -12{,}870 \cdot 10^6 \text{ mm}^3 > Z_{top} \quad \therefore \text{OK}$$

$$Z_{bot,min} = \frac{M_{max} - \eta_\infty M_{min}}{\sigma_{t\infty} - \eta_\infty \sigma_{ci}}$$

$$= \frac{(366{,}8 - 0{,}83 \cdot 153{,}0)\,10^6}{3{,}18 - 0{,}83(-14{,}63)}$$

$$= 15{,}650 \cdot 10^6 \text{ mm}^3 < Z_{bot} \quad \therefore \text{OK}$$

A.2.3 THE MAGNEL DIAGRAM (for the midspan section)

Maximum prestressing force P_i: corresponds to value directly after transfer of prestress, includes all instantaneous losses, but excludes all time-dependent losses.

Minimum prestressing force P_∞: corresponds to value after all losses have taken place, i.e. instantaneous and time-dependent losses.

$$\eta_\infty = P_\infty / P_i = 1 - \frac{\% \text{ long-term loss}}{100}$$

(a) $$1/P_i \leq \frac{\left[\frac{Z_{top}}{A} + e\right]}{(\sigma_{ti} Z_{top} - M_{min})}$$

$$= \frac{\left[\frac{-40,016.10^6}{217,5.10^3} + e\right]}{\left[2,57.10^{-3}(-40,016.10^6) - 153.10^3\right]}$$

$$= 719,1.10^{-6} - 3,909.10^{-6}\, e$$

(b) $$1/P_i \leq \frac{\left[\frac{Z_{bot}}{A} + e\right]}{(\sigma_{ci} Z_{bot} - M_{min})}$$

$$= \frac{\left[\frac{17,561.10^6}{217,5.10^3} + e\right]}{\left[-14,63.10^{-3}(17,561.10^6) + 153,0.10^3\right]}$$

$$= -197,0.10^{-6} - 2,440.10^{-6}\, e$$

(c) $\sigma_{co} Z_{top} = -16,50.10^3(-40,016.10^{-3}) = 660,3$ kNm

$\therefore \sigma_{co} Z_{top} > M_{max} = 366,8$ kNm

$$1/P_i \leq \frac{\eta\left[\frac{Z_{top}}{A} + e\right]}{(\sigma_{co} Z_{top} - M_{max})}$$

$$= \frac{0,83\left[\frac{-40,016.10^6}{217,5.10^3} + e\right]}{\left[-16,50.10^{-3}(-40,016.10^6) - 366,8.10^3\right]}$$

$$= -520,4.10^{-6} + 2,828.10^{-6}\, e$$

(d) $\sigma_{t\infty} \cdot z_{bot} = 3,18.10^3 (17,561.10^{-3}) = 55,8$ kNm

$\therefore \sigma_{t\infty} z_{bot} < M_{max} = 366,8$ kNm

$$1/P_i \geq \frac{\eta_\infty \left[\frac{z_{bot}}{A} + e\right]}{(\sigma_{t\infty} z_{bot} - M_{max})}$$

$$= \frac{0,83\left[\frac{17,561.10^6}{217,5.10^3} + e\right]}{\left[3,18.10^{-3}(17,561.10^6) - 366,8.10^3\right]}$$

$$= -215,5.10^{-6} - 2,669.10^{-6} e$$

A.2.4 MAGNITUDE AND ECCENTRICITY OF PRESTRESSING FORCE

Use the Magnel diagram to determine the values of the prestressing force just after transfer P_i and the eccentricity e_1 at the midspan section. It is assumed that the tendons are placed in two evenly spaced layers at a vertical centre to centre spacing of 50 mm, with the centre of the bottom layer 50 mm above the soffit of the beam. This results in a midspan eccentricity of

$e_1 = y_{bot} - 50 - 22 = 345$ mm.

The number of tendons required depends on the maximum permissible jacking force P_o, and on the loss of prestress due to elastic deformation of the concrete.

Loss of prestress due to elastic deformation is assumed to be 6%.

$$\therefore P_i = (1-0,06)P_o = -(1-0,06)\frac{f_{po}}{\gamma_{ms}} . A_p$$

where $\gamma_{ms} = 1,0$ = partial safety factor for steel [3.3.4.2]

$$\therefore A_p \geq -\frac{\gamma_{ms} P_{i,min}}{(1-0,06) f_{po}} = \frac{-1,0(-880.10^3)}{(1-0,06)\,1395} = 671 \text{ mm}^2$$

Use 7 tendons, i.e. $A_p = 7.100 = 700 \text{ mm}^2$

$$\therefore P_i = -(1-0,06)\frac{1395}{1,0}\, 700.10^{-3} = -917,9 \text{ kN}$$

$-962,6 \text{ kN} < P_i < -880,0 \text{ kN}$ $\therefore$ OK

A.2.5 PERMISSIBLE CABLE ZONE

The design of the beam section at the serviceability limit state of flexure was based on the conditions at the critical section (i.e. the midspan section in the case of a symmetrically loaded simply supported beam). Since the bending moment varies along the span, the eccentricity must be varied along the span to ensure that the stress limitations are not exceeded at other sections, if the same prestressing force is to be used over the entire span.

Note: e in [mm] and x in [m].

$$M_{min}(x) = \frac{w_{min}}{2} x (L_e - x) = 2,72 x (15 - x) \quad kNm$$

$$M_{max}(x) = \frac{w_{max}}{2} x (L_e - x) = 6,52 x (15 - x) \quad kNm$$

Bottom cable limits

(a) $$e_a(x) \leq \left[\frac{\sigma_{ti}}{P_i} - \frac{1}{A}\right] Z_{top} - \frac{M_{min}(x)}{P_i}$$

$$= \left[\frac{2,57}{-917,9.10^3} - \frac{1}{217,5.10^3}\right](-40,016.10^6) - \frac{2,72.10^6}{(-917,9.10^3)} x(15-x)$$

$$= 296,0 + 2,963 x(15-x)$$

(b) $$e_b(x) \leq \left[\frac{\sigma_{ci}}{P_i} - \frac{1}{A}\right] Z_{bot} - \frac{M_{min}(x)}{P_i}$$

$$= \left[\frac{-14,63}{-917,9.10^3} - \frac{1}{217,5.10^3}\right](17,561.10^6) - \frac{2,72.10^6}{(-917,9.10^3)} x(15-x)$$

$$= 199,2 + 2,963 x(15-x)$$

Top cable limits

(c) $$e_c(x) \geq \left[\frac{\sigma_{co}}{\eta_\infty P_i} - \frac{1}{A}\right] Z_{top} - \frac{M_{max}(x)}{\eta_\infty P_i}$$

$$= \left[\frac{-16,50}{0,83(-917,9.10^3)} - \frac{1}{217,5.10^3}\right](-40,016.10^6) - \frac{6,52.10^6}{0,83(-917,9.10^3)} x(15-x)$$

$$= -682,7 + 8,558 x(15-x)$$

(d) $$e_d(x) \geq \left[\frac{\sigma_{to}}{\eta_\infty P_i} - \frac{1}{A}\right] Z_{bot} - \frac{M_{max}(x)}{\eta_\infty P_i}$$

$$= \left[\frac{3,18}{0,83(-917,9.10^3)} - \frac{1}{217,5.10^3}\right](17,561.10^6) - \frac{6,52.10^6}{0,83(-917,9.10^3)} x(15-x)$$

$$= -154,0 + 8,558 x(15-x)$$

Cable limits and Selected profile at span/12 points

x [m]	Bottom cable limit $e_b(x)$ [mm]	Top cable limit $e_d(x)$ [mm]	Selected profile $e(x)$ [mm]
0	199	-154	110
1,25	258	-7	182
2,50	292	113	241
3,75	324	207	286
5,00	347	274	319
6,25	361	314	338
7,50	366	327	345

Select a parabolic profile to lie within the cable zone, as shown.

A.2.6 CONSIDERATIONS AFFECTING DESIGN DETAILS [SABS 0100-1(1992)]

Possible tendon layouts at midspan and at the supports are as follows.

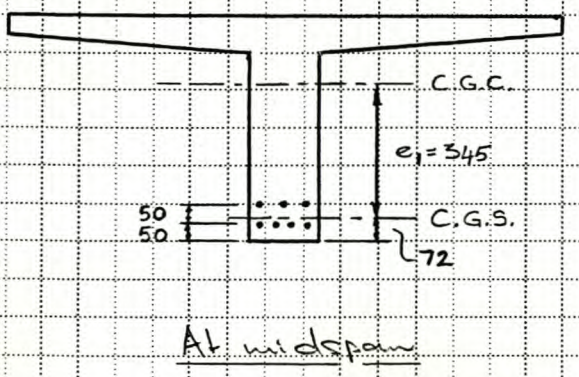

At midspan

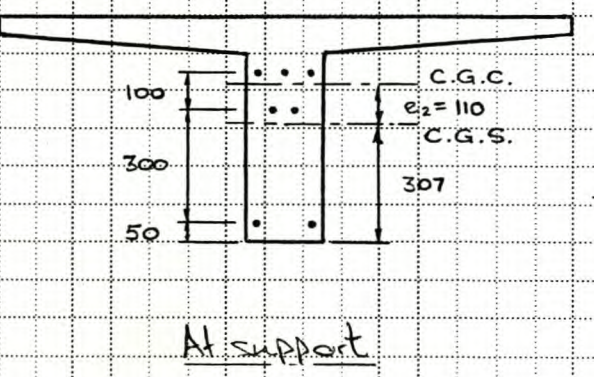

At support

Concrete Cover

The minimum required concrete cover is governed by durability and fire resistance requirements.

For mild conditions of exposure:

Min cover = 20 mm [SABS 0100-2 (1992) Table 5]

For 1,5 h fire resistance (floors):

Min cover = 30 mm [Table 38]

For this member, allowing 10 mm for shear reinforcement

Cover = $50 - 12,9/2 - 10 = 33,5$ mm ∴ OK

Minimum Clear Distances [4.11.2.1.2.2]

Horizontally: $h_{agg} + 5 = 19 + 5 = 24$ mm

Clear spacing = $\frac{1}{3}(200 - 2.25 - 2.10 - 4.12,9) = 26,1$ mm ∴ OK

Vertically: $\frac{2}{3} h_{agg} = \frac{2}{3} 19 = 12,7$ mm

Clear spacing = $50 - 12,9 = 37,1$ mm ∴ OK

Slenderness Limits [4.3.1.6.(a)]

Maximum clear distance between lateral restraints:

$60 b_c = 60.2,5 = 120$ m

where b_c = width of compression flange

Clear distance = 15 m ∴ OK.

Minimum Steel Content [5.9.2.2]

The code uses a deemed-to-satisfy rule, aimed at ensuring that cracking of the concrete would precede ultimate failure: $\frac{100 A_p}{b_w h} = \frac{100.700}{200.600} = 0,58\% > 0,15\%$

∴ OK.

A.2.7 PRESTRESS LOSSES [SABS 0100-1(1992)]

The total loss of prestress can be divided into instantaneous losses, which take place at transfer,
i.e. due to elastic deformation of concrete
and time-dependent losses, which develop with time,
i.e. due to creep of concrete
due to shrinkage of concrete
due to relaxation of prestressing steel

SABS 0100-1(1992) makes use of separate lump sum estimates of the individual loss components, which make provision for the complex interaction which exists among the various components, to estimate the total prestress loss.

$$\Delta f_{pT} = \Delta f_{pE} + \Delta f_{pC} + \Delta f_{pS} + \Delta f_{pR}$$

Elastic Losses (Δf_{pE})

Since the prestressing steel is bonded to the concrete, the changes in steel strain is equal to the concrete strain immediately after transfer. [5.8.2.3.2]

The elastic loss is therefore calculated from

$$\Delta f_{pE} = n_i \frac{(k_E I P_o + A M_{min} e)}{I(A + n_i k_E A_p)}$$

where $k_E = 1 + \frac{A}{I} e^2$ and $n_i = \frac{E_p}{E_{ci}} = \frac{195}{28,8} = 6,771$

Note that this expression assumes that the relaxation

loss which takes place between the time of jacking of the tendons and the time of transfer is negligible. The jacking force is

$$P_o = -\frac{f_{po}}{\gamma_{ms}} A_p = -\frac{1395.700.10^{-3}}{1,0} = -976,5\ kN$$

The prestressing stress f_{pi} and the prestressing force P_i directly after transfer are given by

$$f_{pi} = f_{po} + \Delta f_{pE}$$

$$P_i = -f_{pi} A_p$$

For the section at midspan:

$$k_E = 1 + \frac{217,5.10^3}{7,323.10^9} .345^2 = 4,535 \quad \text{and} \quad M_{mmin} = 153\ kNm$$

$$\Delta f_{pE} = 6,771 \frac{[4,535.7,323.10^9(-976,5.10^3) + 217,5.10^3.153,10^6.345]}{7,323.10^9 (217,5.10^3 + 6,771.4,535.700)}$$

$$= -81,05\ MPa$$

$$f_{pi} = 1395 + (-81,05) = 1314\ MPa$$

$$P_i = -1314.700.10^{-3} = -919,8\ kN$$

Creep Losses (Δf_{pC})

Linear creep theory is used whereby it is assumed that creep strain is linearly related to the elastic strain under constant sustained stress (within the service load range). [5.8.2.5.1]

The creep loss is therefore calculated from

$$\Delta f_{pC} = C_{c\infty} . f_{epermE_p}$$

Calculation of Elastic Losses at span/12 points

x [m]	e [mm]	k_E	M_{min} [kNm]	Δf_{pE} [MPa]	f_{pi} [MPa]	P_i [kN]
0	110	1,359	0	-40,12	1355	-948,4
1,25	182	1,984	468	-80,26	1345	-941,3
2,50	241	2,725	85,0	-60,32	1335	-934,3
3,75	286	3,429	114,8	-68,74	1326	-928,4
5,00	319	4,022	136,0	-75,53	1319	-923,6
6,25	338	4,393	148,8	-79,44	1316	-920,9
7,50	345	4,535	153,0	-81,05	1314	-919,8

where C_{co} = long-term value of the specific creep (i.e. creep strain per unit stress).

f_{cperm} = concrete stress at centroid of prestressing steel, due to prestressing force immediately after transfer, and due to permanent loads.

The values of C_{co} include allowances for the fact that f_{cperm} reduces as the total loss develop (i.e. due to the reduction in prestressing force).

$$f_{cperm} = \frac{P_i}{A} + \frac{P_i e^2}{I} + \frac{M_{perm}}{I}$$

The maximum stress in the section at transfer is

$$f_{cmax} = \frac{P_i}{A} + \frac{P_i e}{Z_{bot}} + \frac{M_{min}}{Z_{bot}}$$

Since M_{perm} causes an relieving effect, w_{perm} is calculated as follows.

$D_n = D_1 + D_2 = 3,63 + 1,20 = 4,83$ kPa

$Q_{nL} \equiv L_n = L_1 + L_2 = 2,39 + 1,0 = 3,39$ kPa

$\gamma_{f_D} = 1,0$; $\gamma_{f_L} = 1,0$; $\psi_L = 0,3$

$\therefore w_{perm} = (1,0 \cdot 4,83 + 0,3 \cdot 1,0 \cdot 3,39)\, 1,5 = 8,76$ kN/m

For the section at midspan:

$M_{perm} = 246,4$ kNm and $M_{max} = 153,0$ kNm

$$f_{cperm} = \frac{-919,8 \cdot 10^3}{217,5 \cdot 10^3} + \frac{-919,8 \cdot 10^3 (345)^2}{7,323 \cdot 10^9} + \frac{246,4 \cdot 10^6 \cdot 345}{7,323 \cdot 10^9}$$

$$= -7,571 \text{ MPa}$$

$$f_{cmax} = \frac{-919,8 \cdot 10^3}{217,5 \cdot 10^3} + \frac{-919,8 \cdot 10^3 \cdot 345}{17,561 \cdot 10^6} + \frac{153,0 \cdot 10^6}{17,561 \cdot 10^6}$$

$$= -13,59 \text{ MPa}$$

$$\frac{f_{cmax}}{f_{ci}} = \frac{-13,59}{-32,5} = 0,418$$

$\therefore \frac{1}{3} < \frac{f_{cmax}}{f_{ci}} < \frac{1}{2}$ and $|f_{ci}| < 40$ MPa

Thus specific creep [5.8.2.5.2 & 5.8.2.5.4]

$$C_{cc} = \left[1 + \frac{(1,25 - 1,0)}{0,5 - 0,333} \cdot (0,418 - 0,333)\right] 48 \cdot 10^{-6} \cdot \frac{40}{|f_{ci}|}$$

$$= 1,127 \cdot 48 \cdot 10^{-6} \cdot \frac{40}{|-32,5|} = 66,58 \cdot 10^{-6} \text{ MPa}^{-1}$$

$$\therefore \Delta f_{pc} = 66,58 \cdot 10^{-6} (-7,571)\, 195 \cdot 10^3$$

$$= -98,30 \text{ MPa}$$

Calculation of Creep Losses at span/12 points

x [m]	e [mm]	P_i [kN]	M_{min} [kNm]	M_{perm} [kNm]	f_{cmax} [MPa]	f_{cperm} [MPa]	$\frac{f_{cmax}}{f_{ci}}$	$C_{t\infty}$ [$\times 10^{-6}$]	Δf_{pc} [MPa]
0	110	-948,4	0	0	-10,30	-5,928	0,317	59,08	-68,29
1,25	182	-941,3	46,8	75,3	-11,42	-6,714	0,351	60,67	-79,43
2,50	241	-934,3	85,0	136,9	-12,28	-7,200	0,378	63,66	-88,54
3,75	286	-928,4	114,8	184,8	-12,85	-7,421	0,398	64,56	-93,42
5,00	319	-923,6	136,0	219,0	-13,28	-7,541	0,409	65,80	-96,76
6,25	338	-920,9	148,8	239,5	-13,49	-7,546	0,415	66,33	-97,60
7,50	345	-919,8	153,0	246,4	-13,59	-7,571	0,418	66,58	-98,30

Shrinkage loss (Δf_{pS})

If it is assumed that the shrinkage strain is uniform over the section, the shrinkage loss is

$$\Delta f_{pS} = \varepsilon_{cs} E_p \qquad [5.8.2.4.2]$$

where ε_{cs} is the ultimate long-term value of the shrinkage strain. This value excludes shrinkage which takes place prior to transfer of prestress. For a relative humidity of the environment of 60%

$$\varepsilon_{cs} = -310.10^{-6} \qquad [\text{Table } 35]$$

Therefore

$$\Delta f_{pS} = -310.10^{-6} . 195.10^{3} = -60,45 \text{ MPa}$$

Relaxation Loss (Δf_{pR})

The prestressing tendons will not be subjected to a constant strain, as is the case during a standard relaxation test, because the member and hence the tendons will shorten as a result of creep and shrinkage of the concrete. This effect is accounted for as follows.

At midspan:

$$|\varepsilon_{cc} + \varepsilon_{cs}| = |C_{c\infty} f_{cparm} + \varepsilon_{cs}|$$

$$= |66,58.10^{-6}(-7,571) + (-810.10^{-6})|$$

$$= 814,1.10^{-6} > 500.10^{-6} \quad [5.8.2.2.2]$$

For low relaxation (super grade) strand and with a jacking stress $f_{po} = 0,75 f_{pu}$, the percentage loss of prestress due to relaxation is

$$\%\text{loss} = \tfrac{1}{2}\left[3 + \frac{8,5-3,0}{80-50}.(75-50)\right] = 3,792 \quad [5.8.2.2.2]$$

$$\therefore \Delta f_{pR} = -\left(\frac{3,792}{100}\right) f_{po} = -52,90 \text{ MPa}$$

Total Loss (Δf_{pT})

The total prestress loss is given by

$$\Delta f_{pT} = \Delta f_{pE} + \Delta f_{pC} + \Delta f_{pS} + \Delta f_{pR}$$

The effective prestressing stress, after all losses have taken place (ie instantaneous and time-dependent) is calculated as follows.

$$f_{pe} = f_{po} + \Delta f_{pT}$$

The loss factor can then be obtained as

$$\eta_\infty = f_{pe} / f_{pi}$$

Summary of Prestress Losses at span/12 points

x [m]	Δf_{pE} [MPa]	Δf_{pc} [MPa]	Δf_{ps} [MPa]	Δf_{pR} [MPa]	Δf_{pT} [MPa]	f_{pi} [MPa]	f_{pe} [MPa]	η_∞
0	-40,12	-68,79	-60,45	-52,90	-221,8	1355	1173	0,8658
1,25	-50,26	-79,43	-60,45	-52,90	-243,0	1345	1152	0,8565
2,50	-60,32	-88,54	-60,45	-52,90	-262,2	1335	1133	0,8485
3,75	-68,74	-93,42	-60,45	-52,90	-275,5	1326	1120	0,8443
5,00	-75,53	-96,76	-60,45	-52,90	-285,6	1319	1109	0,8411
6,25	-79,44	-97,60	-60,45	-52,90	-290,4	1316	1105	0,8394
7,50	-81,05	-98,30	-60,45	-52,90	-292,7	1314	1102	0,8389

A.2.8 Analysis of Stresses

The concrete stresses must be checked to ensure that nowhere along the span will the permissible stresses be exceeded. An uncracked section may be assumed and therefore the following equations may be used.

At transfer of prestress:

$$f_{top,i} = \frac{P_i}{A} + \frac{P_i \cdot e}{Z_{top}} + \frac{M_{min}}{Z_{top}} \leq 2{,}57 \text{ MPa}$$

$$f_{bot,i} = \frac{P_i}{A} + \frac{P_{i.e}}{Z_{bot}} + \frac{M_{min}}{Z_{bot}} \geq -14{,}63 \text{ MPa}$$

Under service loads:

$$f_{top,\infty} = \frac{\eta_\infty P_i}{A} + \frac{\eta_\infty P_i \cdot e}{Z_{top}} + \frac{M_{max}}{Z_{top}} \geq -16{,}50 \text{ MPa}$$

$$f_{bot,\infty} \frac{\eta_\infty P_i}{A} + \frac{\eta_\infty P_i \cdot e}{Z_{bot}} + \frac{M_{max}}{Z_{bot}} \leq 3{,}18 \text{ MPa}$$

Concrete Stresses at Transfer at span/12 points

x [m]	e [mm]	P_i [kN]	M_{min} [kNm]	$f_{top,i}$ [MPa]	$f_{bot,i}$ [MPa]
0	110	-948,4	0	-1,75	-10,30
1,25	188	-941,3	46,8	-1,22	-11,42
2,50	241	-934,3	85,0	-0,79	-12,28
3,75	286	-928,4	114,8	-0,50	-12,85
5,00	319	-923,6	136,0	-0,28	-13,28
6,25	338	-920,9	148,8	-0,17	-13,49
7,50	345	-919,8	153,0	-0,12	-13,59

Concrete Stresses under Service Loads at span/12 points

x [m]	e [mm]	P_i [kN]	η_∞	M_{max} [kNm]	$f_{top,\infty}$ [MPa]	$f_{bot,\infty}$ [MPa]
0	110	-948,4	0,8658	0	-1,52	-8,92
1,25	182	-941,3	0,8565	112,1	-2,84	-5,68
2,50	241	-934,3	0,8485	203,8	-3,96	-2,92
3,75	286	-928,4	0,8443	275,1	-4,88	-0,70
5,00	319	-923,6	0,8411	326,0	-5,53	0,88
6,25	338	-920,9	0,8394	356,6	-5,94	1,87
7,50	345	-919,8	0,8389	366,8	-6,06	2,18

It is therefore clear that the stress limitations imposed by SABS 0100-1 (1992) at the serviceability limit state are satisfied

A.3.1 BASIC ASSUMPTIONS [SABS 0100-1 (1992)]

The beam must be analysed to check that the ultimate moment of resistance M_u exceeds the specified design moment M_d at the critical section. The critical section is located at mid-span in the case of a simply supported symmetrically loaded beam.

The analysis is based on the following basic assumptions: [5.3.3.1]

- Plane sections before bending remain plane after bending.
- The actual stress-strain relationship for the concrete in compression is represented as an equivalent rectangular stress-block. The values of the stress-block factors are,

$$\alpha_1 = \frac{0{,}67}{\gamma_{mc}} \quad \text{and} \quad \beta_1 = 0{,}9$$

and a constant value is assumed for the ultimate strain reached in the extreme compression fibre in bending.

$$\varepsilon_{cu} = -0{,}0035$$

- The tensile strength of the concrete is ignored because it is appropriate to calculate the

ultimate moment of resistance at a section containing a crack, where the influence of the remaining concrete in tension is small.

- The design stress-strain relationship for the prestressing steel is approximated with a tri-linear curve.
- Since the prestressing steel is bonded to the concrete, the change in strain in the steel is taken to be equal to the change in strain in the concrete at the level of the steel.
- The following values are used for the partial material safety factors.

$\gamma_{mc} = 1{,}50$

$\gamma_{ms} = 1{,}15$

A.3.2 ULTIMATE MOMENT OF RESISTANCE

Before M_u can be obtained, the depth to the neutral axis x_c must first be calculated. This can be done in closed-form if an assumption is made about the range within which the strain in the prestressing steel ε_p lies.

The total strain in the prestressing steel at ultimate consists of the following components.

$$\varepsilon_p = \varepsilon_{cp} - \varepsilon_{ce} + \varepsilon_{pe}$$

ε_{pe} is the tensile strain induced in the pre-stressing steel by the effective prestressing stress f_{pe}, which includes all losses.

$$\varepsilon_{pe} = \frac{f_{pe}}{E_p}$$

ε_{ce} is a compressive strain in the concrete at the level of the prestressing steel, induced by the effective prestress acting alone on the elastic uncracked section.

$$\varepsilon_{ce} = \left[\frac{\eta_0 P_i}{A} + \frac{\eta_0 P_i e^2}{I} \right] \frac{1}{E_c}$$

ε_{pe} and ε_{ce} both occur prior to application of the external moment.

ε_{cp} is the change in the strain in the prestressing steel caused by the application of the ultimate moment and is equal to the strain in the concrete at the level of the prestressing steel

$$\varepsilon_{cp} = \left(\frac{d-x}{x} \right) |\varepsilon_{cu}|$$

Once x has been calculated, ε_p must be calculated to check whether the assumption about the range within which ε_p lies is correct.

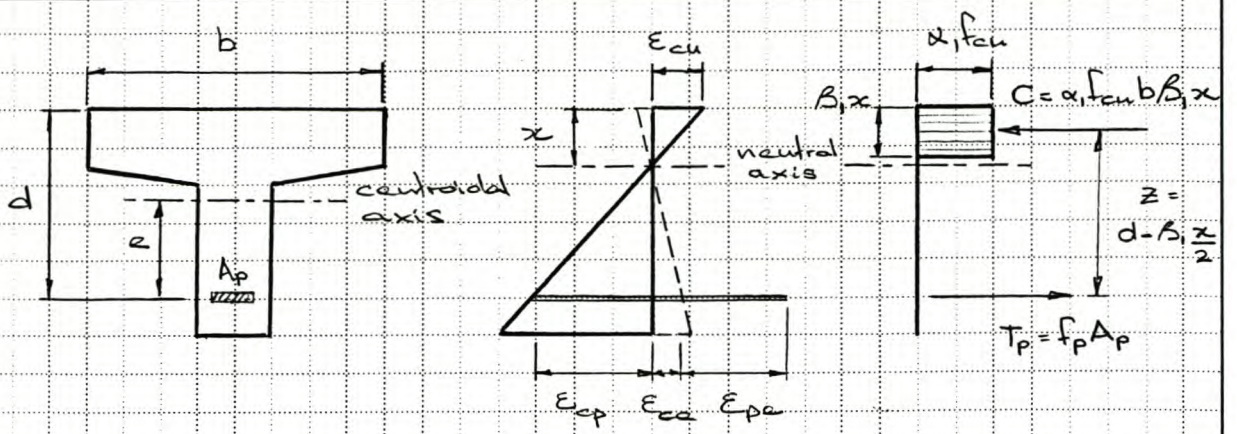

For the section at midspan (i.e. critical section):

$$d = |y_{bp}| + e_1$$
$$= |-183| + 345$$
$$= 528 \text{ mm}$$

Assume $\varepsilon_p > \varepsilon_{py} = 0{,}0133$, and thus

$$f_p = f_{py} = 1617 \text{ MPa}$$

Therefore

$$x = \frac{f_{py} A_p}{\alpha_1 f_{cu} b \beta_1} \qquad \text{where } \alpha_1 = \frac{0{,}67}{1{,}50} = 0{,}45$$
$$= \frac{1617 \cdot 700}{0{,}45 \cdot 50 \cdot 1500 \cdot 0{,}9}$$
$$= 37{,}26 \text{ mm}$$

The entire compression zone therefore falls within the flange. Now check ε_p corresponding to this value of x.

$$\varepsilon_{pe} = \frac{1102}{195 \cdot 10^3} = 0{,}00565$$

$$\varepsilon_{ce} = \left[\frac{0{,}8389\left(-919{,}8.10^{3}\right)}{217{,}5.10^{3}} + \frac{0{,}8389\left(-919{,}8.10^{3}\right)(345)^{2}}{7{,}323.10^{9}}\right]\frac{1}{34.10^{3}}$$

$$= -0{,}00047$$

$$\varepsilon_{cp} = \left(\frac{528 - 37{,}26}{37{,}26}\right)\left|-0{,}0035\right| = 0{,}04610$$

$$\therefore \varepsilon_p = 0{,}04610 + (-0{,}00047) + 0{,}00565$$

$$= 0{,}05222 > \varepsilon_{py}$$

Therefore the steel has yielded and the assumption is correct. The ultimate moment can subsequently be calculated from

$$M_u = \alpha_1 f_{cu} b \beta_1 x \left(d - \beta_1 \frac{x}{2}\right)$$

$$= 0{,}45.50.1500.0{,}9.37{,}26\left(528 - 0{,}9\,\frac{37{,}26}{2}\right)10^{-6}$$

$$= 578{,}6 \text{ kNm}$$

$$M_u > M_d = 473{,}3 \text{ kNm} \quad \therefore \text{OK}$$

A.3.3 Check Failure Mode in Flexure

For a class 2 prestressed concrete member, the design is usually governed by the serviceability limit state of cracking (which is stated by the design code of practice in terms of limiting concrete flexural stresses). Therefore, in this case, the moment of resistance exceeds the specified design moment by a consider-

able margin at the ultimate limit state.

$$\frac{M_u}{M_d} \times 100 = \frac{578,6}{473,3} \cdot 100 = 122,2\ \%$$

For underreinforced (moderately reinforced) sections failure is induced by crushing of the concrete in the compression zone after the section has cracked and the steel has yielded and undergone a large non-linear elongation. This failure mode is ductile because the section can sustain a moment close to the ultimate moment over an wide range of deformations, which is desirable. However, for this type of failure mode to occur the ultimate strain in the concrete (i.e. $\varepsilon_{cu} = -0,0035$) must be reached before the steel fractures ($\varepsilon_{pu} = 0,05$ to $0,065$). For the present case, $\varepsilon_p = 0,05232$ is somewhat high and can only be decreased by increasing the steel content.

Check Cracking Moment (at midspan section):

$$M_{cr} = \frac{f_r}{\gamma_{mc}} \cdot Z_{bot} - \eta P_i \left(\frac{Z_{bot}}{A} + e \right) \qquad \text{where } \gamma_{mc} = 1,0 \ [3.3.4.2]$$

$$= \left[\frac{4,6}{1,0} \cdot 17,561.10^6 - 0,8389 \left(-919,8.10^3 \right) \left(\frac{17,561.10^6}{217,5.10^3} + 345 \right) \right] 10^{-6}$$

$$= 409,3\ \text{kNm} < M_u$$

Therefore cracking of the beam would precede failure (Note, it has been assumed that the cracking load would occur after all prestress losses have taken place.)

$$\frac{M_u}{M_{cr}} \times 100 = \frac{578,6}{409,3} \cdot 100 = 141,4\ \%$$

Note that since the prestressing steel is bonded to the concrete, additional normal reinforcing steel is not required to control cracking.

The deflections must be calculated at the critical section (i.e. at midspan) to check that the allowable deflections are not exceeded at the serviceability limit state. Since the beam is uncracked under the service load, the calculations may be based on the gross concrete section properties. Furthermore, under these conditions it is reasonable to assume that the material properties are linear elastic and therefore the total deflection may be obtained by superposition of the various components due to the prestressing force and the external load. [5.3.6.1]

M_{max} = 3660,8 kNm and M_{cr} = 409,3 kNm at midspan

$\therefore M_{max} < M_{cr}$

The values of the partial material safety factors are as follows: [3.3.4.2]

γ_{mc} = 1,0 } i.e use values of material properties
γ_{ms} = 1,0 } associated with characteristic values

The total deflection should include both the elastic component under the action of the prestressing force and the external load, and the time-dependent creep component which develops under the action of the prestressing force

and the permanent load. [3.3.4.1.3 & 3.3.4.1.4]
Note that the time-dependent shrinkage component will be ignored in these calculations, because it is usually sufficiently small compared to the creep component.

A.4.1 ALLOWABLE DEFLECTIONS [SABS 0100-1(1992)]

The deflection of a prestressed concrete member must be checked at various stages during its life. The following deflection limitations are given in the design code of practice, but should only be considered as a guide to reasonable values for practical design.

	δ_a
Deflection (camber) at transfer of prestress δ_i, to prevent damage to finishes [3.2.3.2.1.3]	$L_e/300$
Long-term deflection under maximum service loads δ_∞, beyond which the deflection will give offence to the occupant [3.2.3.2.1.1]	$L_e/250$
Deflection that affects partitions and finishes δ_d (for brittle partitions) [3.2.3.2.1.2]	$L_e/500$

Deflection of prestressed concrete members at the serviceability limit state is usually controlled by this last requirement. The allowable deflection of $L_e/500$ applies to brittle partitions, in which case the design code of practice also imposes a deflection limitation of 10 mm which is exceeded in the present case, due to the long span.

A.4.2 DEFLECTION AT TRANSFER OF PRESTRESS

Directly after transfer of prestress the prestressing force will be acting at its maximum value, while the applied external load will be acting at its minimum value. The total deflection at transfer of prestress is

$$\delta_i = \delta_{pi} + \delta_{wi}$$

where δ_{pi} = elastic deflection (camber) due to the maximum prestressing force

δ_{wi} = elastic deflection due to the minimum applied external load

For a parabolic cable profile, δ_{pi} is given by

$$\delta_{pi} = \left[\frac{5}{48}\phi_{1i} + \frac{1}{48}\phi_{2i}\right] L_e^2$$

where ϕ_{1i} and ϕ_{2i} are the curvatures at the midspan and support sections, respectively.

$$\phi_{1i} = \frac{P_{1i}\, e_1}{E_{ci} I} = \frac{(-919{,}8 \cdot 10^3)\, 345}{28{,}8 \cdot 10^3 \cdot 7{,}323 \cdot 10^9} = -1{,}5046 \cdot 10^{-6} \text{ rad/mm}$$

$$\phi_{2i} = \frac{P_{2i}\, e_2}{E_{ci} I} = \frac{(-948{,}4 \cdot 10^3)\, 110}{28{,}8 \cdot 10^3 \cdot 7{,}323 \cdot 10^9} = -0{,}4947 \cdot 10^{-6} \text{ rad/mm}$$

$$\therefore \delta_{pi} = \left[\frac{5}{48}\left(-1{,}5046 \cdot 10^{-6}\right) + \frac{1}{48}\left(-0{,}4947 \cdot 10^{-6}\right)\right](15 \cdot 10^3)^2$$

$$= -37{,}58 \text{ mm (camber)}$$

If the prestressing force is assumed to act at a constant value along the span, equal to the value at the midspan section, then

$$\delta_{pi} = \frac{P_i}{48 E_{ci} I}\left(5 e_1 + e_2\right) L_e^2$$

$$= \frac{(-919{,}8 \cdot 10^3)}{48 \cdot 28{,}8 \cdot 10^3 \cdot 7{,}323 \cdot 10^9}\left(5 \cdot 345 + 110\right)\left(15 \cdot 10^3\right)^2$$

$$= -37{,}51 \text{ mm (camber)} \text{ — accept this value.}$$

For a uniformly distributed loading on a simply supported beam, δ_{wi} is

$$\delta_{wi} = \frac{5}{48}\left(\frac{M_{min}}{E_{ci} I}\right) L_e^2$$

$$= \frac{5}{48}\left(\frac{153{,}0 \cdot 10^6}{28{,}8 \cdot 10^3 \cdot 7{,}323 \cdot 10^9}\right)\left(15 \cdot 10^3\right)^2$$

$$= 17{,}00 \text{ mm}$$

$$\therefore \delta_i = -37{,}51 + 17{,}00 = -20{,}51 \text{ mm (camber)}$$

$$\delta_a = \frac{L_e}{300} = \frac{15 \cdot 10^3}{300} = 50 \text{ mm}$$

$|\delta_i| < \delta_a$ $\therefore$ OK

A.4.3 DEFLECTION UNDER LONG-TERM SERVICE LOADS

The prestressing force will be acting at its minimum value, while the applied external load will be acting at its maximum value. The total long-term deflection under service loads consists of the following components:

$$\delta_\infty = \delta_{p\infty} + \delta_{w\infty} + \delta_{var}$$

where $\delta_{p\infty}$ = long-term elastic plus creep deflection (camber), including the long-term change in deflection induced by the loss of prestress, due to the prestressing force.

$\delta_{w\infty}$ = long-term elastic plus creep deflection due to the permanent loads.

δ_{var} = elastic deflection due to the variable load.

For a parabolic cable profile, $\delta_{p\infty}$ is given by

$$\delta_{p\infty} = \left[\frac{5}{48}\Phi_{1\infty} + \frac{1}{48}\Phi_{2\infty}\right] L_e^2$$

where

$$\Phi_{1\infty} = \frac{P_{ii}\, e_i}{E_c I}\left[\eta_{1\infty} + \left(\frac{1+\eta_{1\infty}}{2}\right)\phi_{c\infty}\right]$$

$$= \frac{(-919,8.10^3)\,345}{34.10^3 . 7,823.10^9}\left[0,8389 + \left(\frac{1+0,8389}{2}\right)3,04\right]$$

$$= -4,6316.10^{-6}\ \text{rad/mm}$$

$$\phi_{z\infty} = \frac{P_{zi}\cdot e_z}{E_c I}\left[\eta_{z\infty} + \left(\frac{1+\eta_{z\infty}}{2}\right)\phi_{c\infty}\right]$$

$$= \frac{(-948,4.10^3)\,110}{34.10^3.7,323.10^9}\left[0,8658 + \left(\frac{1+0,8658}{2}\right)3,04\right]$$

$$= -1,5510.10^{-6} \text{ rad/mm}$$

$$\therefore \delta_{p\infty} = \left[\frac{5}{48}\left(-4,6316.10^{-6}\right) + \frac{1}{48}\left(-1,5510.10^{-6}\right)\right]\left(15.10^3\right)^2$$

$$= -115,82 \text{ mm (camber)}$$

If the prestressing force is assumed to act at a constant value along the span, equal to the value at the midspan section, then

$$\delta_{p\infty} = \frac{P_i}{48 E_c I}\left(5e_1 + e_2\right)L_e^2\left[\eta_\infty + \left(\frac{1+\eta_\infty}{2}\right)\phi_{c\infty}\right]$$

$$= \frac{(-919,8.10^3)}{48.34.10^3.7,323.10^9}\left(5.345 + 110\right)\left(15.10^3\right)^2$$

$$\times\left[0,8389 + \left(\frac{1+0,8389}{2}\right)3,04\right]$$

$$= -115,48 \text{ mm (camber)} \quad \text{— accept this value}$$

Since the total long-term deflection will be an upwards camber as shown below, the permanent load induces a relieving effect. Therefore, use $M_{perm} = 246,4$ kNm. For a uniformly distributed loading on a simply supported beam, $\delta_{w\infty}$ is

$$\delta_{w\infty} = \frac{5}{48}\left(\frac{M_{perm}}{E_c I}\right)L_e^2\left(1+\phi_{c\infty}\right) = \frac{5}{48}\left(\frac{246,4\cdot10^6}{34.10^3.7,323.10^9}\right)\left(15.10^3\right)^2\left(1+3,04\right)$$

$$= 93,71 \text{ mm}$$

and δ_{var} is

$$\delta_{var} = \frac{5}{48}\left(\frac{M_{var}}{E_c I}\right) L_e^2$$

$$= \frac{5}{48}\left(\frac{60,1.10^6}{34.10^3 . 7,323.10^9}\right)(15.10^3)^2$$

$$= 9,42 \text{ mm}$$

$\therefore \delta_\infty = -115,48 + 93,71 + 9,42 = -12,35$ mm (camber)

$$\delta_a = \frac{L_e}{250} = \frac{15.10^3}{250} = 60 \text{ mm}$$

$\delta_\infty < \delta_a \therefore$ OK

A.4.4 Deflection affecting Partitions and Finishes

Partitions and finishes will be affected only by that part of the deflection that takes place after their construction or application. Assume that such erection occurs at 1 month after transfer of prestress.

Then $\delta_d = \delta_\infty - \delta_t$

where δ_∞ = total long-term deflection under service loads.

δ_t = deflection before construction of partitions or application of finishes (i.e. at 3 + 30 = 33 days)

and $\delta_t = \delta_{pt} + \delta_{wt}$

where δ_{pt} = the 33 day elastic plus creep deflection (camber), including the change in deflection induced by the loss of prestress at 33 days, due to the prestressing force

δ_{wt} = the 33 day elastic plus creep deflection due to the minimum applied external load.

Find calculate the value of the loss factor η_t at 33 days for the midspan and support sections.

Assume that 50% of the creep, shrinkage and relaxation losses have taken place within the first month after transfer of prestress. [5.8.2.4.4 & 5.8.2.5.5]

$$\Delta f_{pT}' = \Delta f_{pE} + \Delta f_{pc}' + \Delta f_{ps}' + \Delta f_{pR}'$$

$$f_{pt} = f_{po} + \Delta f_{pT}'$$

$$\eta_t = f_{pt} / f_{pi}$$

x [m]	Δf_{pE} [MPa]	$\Delta f_{pc}'$ [MPa]	$\Delta f_{ps}'$ [MPa]	$\Delta f_{pR}'$ [MPa]	$\Delta f_{pT}'$ [MPa]	f_{pi} [MPa]	f_{pt} [MPa]	η_t
0	-40,12	-34,15	-30,23	-26,45	-131,0	1355	1264	0,9328
7,50	-81,05	-49,15	-30,23	-26,45	-186,9	1314	1208	0,9193

For a parabolic cable profile, δ_{pt} is given by

$$\delta_{pt} = \left[\frac{5}{48}\phi_{1t} + \frac{1}{48}\phi_{2t}\right] L_e^2$$

where

$$\phi_{1t} = \frac{P_i e_1}{E_c I}\left[\eta_{1t} + \left(\frac{1+\eta_{1t}}{2}\right)\phi_d\right]$$

$$= \frac{(-919{,}8 \cdot 10^3)\,345}{34 \cdot 10^3 \cdot 7{,}323 \cdot 10^9}\left[0{,}9193 + \left(\frac{1+0{,}9193}{2}\right)1{,}23\right]$$

$$= -2{,}6761\ 10^{-6}\ \text{rad/mm}$$

$$\phi_{2t} = \frac{P_{2i} e_2}{E_c I}\left[\eta_{2t} + \left(\frac{1+\eta_{2t}}{2}\right)\phi_d\right]$$

$$= \frac{(-948{,}4 \cdot 10^3)\,110}{34 \cdot 10^3 \cdot 7{,}323 \cdot 10^9}\left[0{,}9328 + \left(\frac{1+0{,}9328}{2}\right)1{,}23\right]$$

$$= -0{,}8889 \cdot 10^{-6}\ \text{rad/mm}$$

$$\therefore \delta_{pt} = \left[\frac{5}{48}\left(-2{,}6761 \cdot 10^{-6}\right) + \frac{1}{48}\left(-0{,}8889 \cdot 10^{-6}\right)\right]\left(15 \cdot 10^3\right)^2$$

$$= -66{,}89\ \text{mm (camber)}$$

If the prestressing force is assumed to act at a constant value along the span, equal to the value at the midspan section, then

$$\delta_{pt} = \frac{P_i}{48 E_c I}\left(5e_1 + e_2\right) L_e^2\left[\eta_t + \left(\frac{1+\eta_t}{2}\right)\phi_d\right]$$

$$= \frac{(-919{,}8 \cdot 10^3)}{48 \cdot 34 \cdot 10^3 \cdot 7{,}323 \cdot 10^9}\left(5 \cdot 345 + 110\right)\left(15 \cdot 10^3\right)^2 \times \left[0{,}9193 + \left(\frac{1+0{,}9193}{2}\right)1{,}23\right]$$

$$= -66{,}72\ \text{mm (camber)} \quad \text{—— accept this value.}$$

For a uniformly distributed loading on a simply supported beam, δ_{wt} is

$$\delta_{wt} = \frac{5}{48}\left(\frac{M_{min}}{E_c I}\right) L_e^2 (1+\phi_{ct})$$

$$= \frac{5}{48}\left(\frac{153.10^6}{34.10^3 . 7,323.10^9}\right)(15.10^3)^2 (1+1,23)$$

$$= 32,12 \text{ mm}$$

$\therefore \delta_t = -66,72 + 32,12 = -34,60$ mm (camber)

As far as the deflection which affects partitions and finishes is concerned, the permanent load induces a compounding effect. Therefore, recalculate δ_{wo}, using $M_{perm} = 266,9$ kNm

$$\delta_{wo} = \frac{5}{48}\left(\frac{266,9.10^6}{34.10^3 . 7,323.10^9}\right)(15.10^3)^2 (1+3,04)$$

$$= 101,50 \text{ mm}$$

$\therefore \delta_o = -115,48 + 101,50 + 9,42 = +4,56$ mm (camber)

Therefore, the deflection which affects partitions and finishes is

$$\delta_d = -4,56 - (-34,60) = 30,0 \text{ mm}$$

$$\delta_a = \frac{L_e}{500} = \frac{15.10^3}{500} = 30,0 \text{ mm}$$

$\delta_d = \delta_a \therefore$ OK

X

APPENDIX B

DETAILED CALCULATIONS

B.1.1 ULTIMATE MOMENT OF RESISTANCE:

LONG-TERM CONCRETE STRENGTH

$f_{c\infty} = c_2 f_{cu} = 1,16 . 50 = 58$ MPa [Eq. 3-3]

$E_{c\infty} = c_3 E_c = 1,10 . 34 = 37,4$ GPa [Eq. 3-5]

Assume $\varepsilon_p > \varepsilon_{py} = 0,0133$ $\therefore f_p = f_{py} = 1617$ MPa

Therefore $x = \dfrac{f_{py} . A_p}{\alpha_1 . f_{c\infty} . b \beta_1}$ where $\alpha_1 = \dfrac{0,67}{1,50} = 0,45$

$= \dfrac{1617 . 700}{0,45 . 58 . 1500 . 0,9}$ [cf. Eq. 3-14]

$= 32,12$ mm

This entire compression zone falls within flange.

Now check assumption with this value of x

$\varepsilon_{pe} = \dfrac{f_{pe}}{E_p} = \dfrac{1102}{195 . 10^3} = 0,00565$

$\varepsilon_{ce} = \left[\dfrac{\eta_\infty P_i}{A} + \dfrac{\eta_\infty P_i e^2}{I}\right] \dfrac{1}{E_{c\infty}}$

$= \left[\dfrac{0,8389(-919,8 . 10^3)}{217,5 . 10^3} + \dfrac{0,8389(-919,8 . 10^3)(345)^2}{7,523 . 10^9}\right] \dfrac{1}{37,4 . 10^3}$

$= -0,000\,43$

$\varepsilon_{cp} = \left(\dfrac{d-x}{x}\right)|\varepsilon_{cu}| = \left(\dfrac{528 - 32,12}{32,12}\right)|-0,0035| = 0,05403$

$\therefore \varepsilon_p = \varepsilon_{cp} - \varepsilon_{ce} + \varepsilon_{pe} = 0,05403 - (-0,000\,43) + 0,00565$

$= 0,06011 > \varepsilon_{py}$ [Eq. 3-13]

$\therefore M_{up} = f_{py} A_p \left(d - \dfrac{f_{py} A_p}{2 \alpha_1 f_{c\infty} b}\right)$ [Eq. 3-15b]

$= (1860/1,15)\,700 \left\{528 - \dfrac{(1860/1,15)\,700}{2(0,67/1,50)\,58 . 1500}\right\} 10^{-6} = 581,3$ kNm

B.1.2. DEFLECTION : LONG-TERM CONCRETE STRENGTH

Deflection under Long-Term Service Loads

$E_{c\infty} = c_3 E_c = 1{,}10 \cdot 34 = 37{,}4$ GPa

$\delta_{p\infty}' = \delta_{p\infty} \cdot \frac{E_c}{E_{c\infty}} = -115{,}48 \cdot \frac{34}{37{,}4} = -104{,}98$ mm (camber)

$\delta_{w\infty}' = \delta_{w\infty} \cdot \frac{E_c}{E_{c\infty}} = 101{,}50 \cdot \frac{34}{37{,}4} = 92{,}27$ mm

$\delta_{var}' = \delta_{var} \cdot \frac{E_c}{E_{c\infty}} = 9{,}42 \cdot \frac{34}{37{,}4} = 8{,}56$ mm

$\therefore \delta_\infty' = \delta_{p\infty}' + \delta_{w\infty}' + \delta_{var}'$

$= -104{,}98 + 92{,}27 + 8{,}56$

$= -4{,}15$ mm (camber)

Before Construction of Partitions and Application of Finishes

$E_c \approx 34$ GPa at 53 days

$\therefore \delta_t = \delta_{pt} + \delta_{wt}$

$= -66{,}72 + 32{,}12$

$= -34{,}60$ mm

Deflection affecting Partitions and Finishes

$\delta_d' = \delta_\infty' - \delta_t$

$= -4{,}15 - (-34{,}60)$

$= 30{,}45$ mm

$(\approx \delta_d)$

$\delta_a = \frac{L_e}{350} = \frac{15 \cdot 10^3}{350} = 42{,}9$ mm

$\delta_d' < \delta_a \therefore$ OK

B.2.1 DISTRIBUTION OF THE DEAD LOAD EFFECT

$V_D = 0,10$ [Refs. 4-1 & 4-8]

Assume $D \sim LN(\lambda_D ; \zeta_D)$

Calculate: Degree of skewness [Ref. 4-3]

$$\gamma_{D/m_D} = \exp\left[\frac{\zeta_D^2}{2}\right] = \exp\left[\frac{\ln(V_D^2 + 1)}{2}\right]$$

$$= \exp\left[\frac{\ln(0,1^2 + 1)}{2}\right]$$

$$= 1,004988$$

$\gamma_{D/m_D} \simeq 1,0$ $\therefore$ assume $D \sim N(\mu_D ; \sigma_D)$

B.2.2 SELF-WEIGHT AND SUPERIMPOSED DEAD LOAD

$Q_i = C_i B_i A_i$ [Eq. 4-40]

$D = D_1 + D_2$ [Eq. 4-47]

Load Effect due to D_1

$\bar{D}_1 = 1,0\, D_{1,n} \rightarrow$

$V_{C_1} = 0,05 \quad V_{B_1} = 0,05 \quad V_{A_1} = 0,08$ } assumed

$\therefore V_{D_1} = \sqrt{0,05^2 + 0,05^2 + 0,08^2}$ [Eq. 4-42]

$= 0,107 \rightarrow$

Load Effect due to D_2

$\bar{D}_2 = 1,2\, D_{2,n} \rightarrow$

$V_{C_2} = 0,05 \quad V_{B_2} = 0,10 \quad V_{A_2} = 0,20$ } assumed

$\therefore V_{D_2} = \sqrt{0,05^2 + 0,10^2 + 0,20^2}$ [Eq. 4-42]

$= 0,230 \rightarrow$

Load Effect due to D : Linear Combination

$D_n = D_{1,n} + D_{2,n} = 3,63 + 1,20$ [see § A.1.2]

$= 4,83$ kPa

$\bar{D} = \bar{D}_1 + \bar{D}_2 = 1,0 \cdot 3,63 + 1,2 \cdot 1,20$ [Eq. 4-12]

$= 5,07$ kPa

$\therefore \bar{D}/D_n = \frac{5,07}{4,83} = 1,05$ $\therefore$ OK.

Assume $f_{D_1, D_2} = 0$

$\sigma_{D_1} = 0,107 (1,0 \cdot 3,63) = 0,388$ kPa

$\sigma_{D_2} = 0,230 (1,2 \cdot 1,20) = 0,331$ kPa

$\sigma_D = \sqrt{0,388^2 + 0,331^2} = 0,510$ kPa [Eq 4-13]

$\therefore V_D = \frac{0,510}{5,07} = 0,10$ $\therefore$ OK.

Assume: $D_1 \sim N(\bar{D}_1 ; \sigma_{D_1})$

$D_2 \sim N(\bar{D}_2 ; \sigma_{D_2})$

B.2.3 LIFETIME MAXIMUM LIVE LOAD EFFECT

$$L = L_1 + L_2$$

$$L_{1,n} = 2,5\left[0,3 + \frac{3,1}{\sqrt{1,5.15}}\right] = 2,39 \text{ kPa} \qquad \text{[Eq. 4-49]}$$

$$L_{2,n} = 1,0 \text{ kPa}$$

ULS: Calculate $\overline{L}/L_n$

$$\overline{L}_1 = 2,4\left[0,25 + \frac{4,6}{\sqrt{2.1,5.15}}\right] = 2,25 \text{ kPa} \qquad \text{[Ref. 4-1]}$$

$$\therefore \overline{L}_1/L_{1,n} = \frac{2,25}{2,39} = 0,941$$

Assume $\overline{L}_2/L_{2,n} = \overline{L}_1/L_{1,n}$

$$\therefore \overline{L}/L_n = 0,941 \rightarrow$$

$V_L = 0,25$ and $L \sim EX_{I,L}(u_0; \alpha_0)$ [Ref. 4-1]

SLS: Calculate $\overline{L}/L_n$

$$\overline{L}_1/L_{1,n} = 0,65 \qquad \text{[Ref. 4-9]}$$

Assume $\overline{L}_2/L_{2,n} = \overline{L}_1/L_{1,n}$

$$\therefore \overline{L}/L_n = 0,65 \rightarrow$$

$V_L = 0,32$ and $L \sim EX_{I,L}(u_0; \alpha_0)$ [Ref. 4-9]

B.2.4 SUSTAINED LIVE LOAD RATIO

$$\psi_L = L_{sus} / L$$

$\overline{L_{sus}} = 0,575$ kPa
$V_{L_{sus}} = 0,68$
$L_{sus} \sim$ Gamma
[Ref. 4-1]

$\overline{L} = 0,65(2,39 + 1,0) = 2,20$ kPa
$V_L = 0,32$
$L \sim EX_{I,L}(u_0; a_0)$
[see § B.2.3]

Calculate: $\overline{\psi_L} / \psi_{L,n}$

$\overline{\psi_L} \simeq \overline{L_{sus}} / \overline{L} = \frac{0,575}{2,20} = 0,261$ [Eq. 4-25]

$\psi_{L,n} = 0,3$ [SABS 0160 (1989) Table 2]

$\therefore \overline{\psi_L} / \psi_{L,n} = \frac{0,261}{0,3} = 0,870 \rightarrow$

Calculate: V_{ψ_L} (assume $\rho_{L_{sus},L} = 0,3$)

$V_{\psi_L}^2 \simeq V_{L_{sus}}^2 - 2\rho_{L_{sus},L} \cdot V_{L_{sus}} \cdot V_L + V_L^2$ [Eq. 4-26]

$= (0,68)^2 - 2(0,3)(0,68)(0,32) + (0,32)^2$

$\therefore V_{\psi_L} = 0,659 \rightarrow$ (similar results with Taylor-Series, i.e. Eqs. 4-28 & 4-29)

Assume $\psi_L \sim N(\overline{\psi_L}, \sigma_{\psi_L})$

B.3.1 CONCRETE CUBE STRENGTH AT 28 DAYS

$f_{cu,n} = 50$ MPa [§ A.1.3]

$\hat{\sigma}_{f_{cu}} = 5,0$ MPa (good control) [Ref. 4-11]

$f_{cu} \sim N(\overline{f_{cu}}; \sigma_{f_{cu}})$ [eq. Ref. 4-10]

Calculate: $\hat{f}_{cu}$ and $\hat{V}_{f_{cu}}$ (i.e. estimators of moments)

$$P[f_{cu} \leq f_{cu,n}] = \Phi\left[\frac{f_{cu,n} - \hat{f}_{cu}}{\hat{\sigma}_{f_{cu}}}\right] = 0,05 \quad [\text{Eq. } 4\text{-}51]$$

$$\therefore \Phi\left[-\left(\frac{f_{cu,n} - \hat{f}_{cu}}{\hat{\sigma}_{f_{cu}}}\right)\right] = 1 - 0,05 = 0,95$$

$$\therefore \frac{\hat{f}_{cu} - f_{cu,n}}{\hat{\sigma}_{f_{cu}}} = 1,645$$

$$\therefore \hat{f}_{cu} = 1,645 \cdot \hat{\sigma}_{f_{cu}} + f_{cu,n}$$

$$= 1,645 \cdot 5,0 + 50$$

$$= 58,23 \text{ MPa}$$

$$\hat{V}_{f_{cu}} = \hat{\sigma}_{f_{cu}} / \hat{f}_{cu} = 0,086$$

Calculate: $\overline{f_{cu}}$ and $V_{f_{cu}}$ (i.e. true moments)

Assume $\overline{B} = 1,0$ and $V_B = 0,05$

$\overline{f_{cu}} = \overline{B} \cdot \hat{f}_{cu} = 1,0 \cdot 58,23 = 58,23$ MPa [Eq. 4-1]

$$\therefore \overline{f_{cu}} / f_{cu,n} = \frac{58,23}{50,0} = 1,165 \rightarrow$$

$$V_{f_{cu}} = \left(\hat{V}_{f_{cu}}^2 + V_B^2\right)^{1/2} = \left(0,086^2 + 0,05^2\right)^{1/2} \quad [\text{Eq. } 4\text{-}2]$$

$$\approx 0,10 \rightarrow$$

B.3.2 CONCRETE IN SITU FLEXURAL STRENGTH

$$c_1 = f_{co}/f_{cu}$$

$V_{f_{co}} = 0,135$
$f_{co} \sim N(\overline{f_{co}}; \sigma_{f_{co}})$
} (good control) [Ref. 4-13]

$V_{f_{cu}} = 0,10$
$f_{cu} \sim N(\overline{f_{cu}}; \sigma_{f_{cu}})$
} (good control) [see § B.3.1]

Calculate: $\overline{c_1}$ $\left(\text{Assume } \overline{c_1}/c_{1,n} \equiv \overline{f_{co}}/f_{co,n}\right)$

For $f'_{c,n} = 5000$ psi (e.g.): [Ref. 4-12]

$$f_{co,n} = 0,85 f'_{c,n} = 4250 \text{ psi}$$

$$\overline{f_{co}} = 0,675 f'_{c,n} + 1100 = 4475 \text{ psi}$$

$$\therefore \overline{f_{co}}/f_{co,n} = \frac{4475}{4250} = 1,053$$

$\therefore \overline{c_1} = 1,053 . c_{1,n} = 1,053 . 0,67 = 0,706 \rightarrow$

Calculate: V_{c_1} (assume $\rho_{f_{co},f_{cu}} = 0,8$)

$$V_{c_1}^2 \simeq V_{f_{co}}^2 - 2 . \rho_{f_{co},f_{cu}} . V_{f_{co}} . V_{f_{cu}} + V_{f_{cu}}^2 \quad \text{[Eq. 4-26]}$$

$$= (0,135)^2 - 2(0,8)(0,135)(0,10) + (0,10)^2$$

$\therefore V_{c_1} = 0,081 \rightarrow$

Assume $c_1 \sim N(\overline{c_1}; \sigma_{c_1})$

B.3.3 LONG-TERM CONCRETE CUBE STRENGTH

$$\boxed{f_{c\infty} = c_2 f_{cu}}$$

$c_{2,n} = \frac{f_{c\infty,n}}{f_{cu,n}} = \frac{58}{50} = 1,16$ [Ref 3-1, Table 28]

Conservative range c_2 : 1,2 to 1,4 [Ref. 4-14]

Unconservative range c_2 : 1,5 to 2,5 [Ref. 4-13]

$\overline{f_{cu}} = 58,23$ MPa and $V_{f_{cu}} = 0,10$ [see § B.3.1]

Calculate: $\overline{c_2}$ and V_{c_2}

Assume a symmetrical triangular distribution within the range.

$$\overline{c_2} = \tfrac{1}{2}(c_{2u} + c_{2l}) = \tfrac{1}{2}(1,4 + 1,2)$$

$$= 1,30 \rightarrow \text{conservative estimate}$$

$$\therefore \overline{c_2}/c_{2,n} = \frac{1,30}{1,16} = 1,121$$

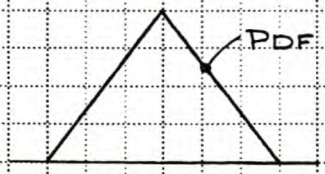

$$V_{c_2} = \frac{1}{\sqrt{6}}\left(\frac{c_{2u} - c_{2l}}{c_{2u} + c_{2l}}\right) = \frac{1}{\sqrt{6}}\left(\frac{2,5 - 1,5}{2,5 + 1,5}\right)$$

$$= 0,102 \rightarrow \text{unconservative estimate}$$

Calculate: $\overline{f_{c\infty}}$ and $V_{f_{c\infty}}$ (assume $f_{c_2,f_{cu}} = 0,2$)

$$\overline{f_{c\infty}} = \overline{c_2}.\overline{f_{cu}} + f_{c_2,f_{cu}}.\sigma_{c_2}.\sigma_{f_{cu}} \quad [\text{Eq. 4-17}]$$

$$= 1,30.58,23 + 0,2(0,102.1,30)(0,1.58,23) = 75,85 \text{ MPa} \rightarrow$$

$$\therefore \overline{f_{c\infty}}/f_{c\infty,n} = \frac{75,85}{58,0} = 1,308$$

$$\sigma^2_{f_{c\infty}} = \left[(\overline{c_2}.\sigma_{f_{cu}})^2 + (\overline{f_{cu}}.\sigma_{c_2})^2 + (\sigma_{c_2}.\sigma_{f_{cu}})^2\right](1 + f^2_{c_2,f_{cu}}) \quad [\text{Eq. 4-18}]$$

$$= \left[(1,30.0,1.58,23)^2 + (58,23.0,102.1,30)^2 + (0,102.1,30.0,1.58,23)^2\right](1+0,2^2)$$

$$\therefore \sigma_{f_{c\infty}} = 11,06 \text{ MPa} \text{ and } V_{f_{c\infty}} = \frac{11,06}{75,85} = 0,146 \rightarrow$$

Assume $f_{c\infty} \sim N(\overline{f_{c\infty}}; \sigma_{f_{c\infty}})$

B.4.1 MODELLING ERROR — FLEXURAL STRENGTH

(a) Data Set

[Ref. 5-14]

	TEST								THEORY		
Beam No	Wires No & ϕ [mm]	A_p [mm²]	f_{pu} [MPa]	f_{pe} [MPa]	d [mm]	f_{cu} [MPa]	$(M_u)_T$ [kNm]	F_p [MPa]	$(M_u)_M$ [kNm]	$(M_u)_T / (M_u)_M$
1	2@7	77,2	1700	831	101,5	52,8	10,50	1543	10,12	1,038
2	4@5	81,1	1740	786	101,5	54,9	11,57	1548	10,65	1,086
3	2@7	77,2	1700	655	142,5	52,3	13,67	1644	15,83	0,864
4	2@7	77,2	1700	656	142,5	44,9	14,73	1578	14,94	0,986
5	4@5	81,1	1625	619	143,5	48,7	17,52	1551	15,67	1,118
6	4@7	154,3	1700	827	101,5	52,4	14,25	1280	14,60	0,976
7	4@5	81,1	1740	940	101,5	54,9	11,61	1579	10,81	1,074

All specimens: $b = 102$ mm, $h = 203$ mm, $E_p = 200$ GPa

(b) Prediction of Strength: Demonstration

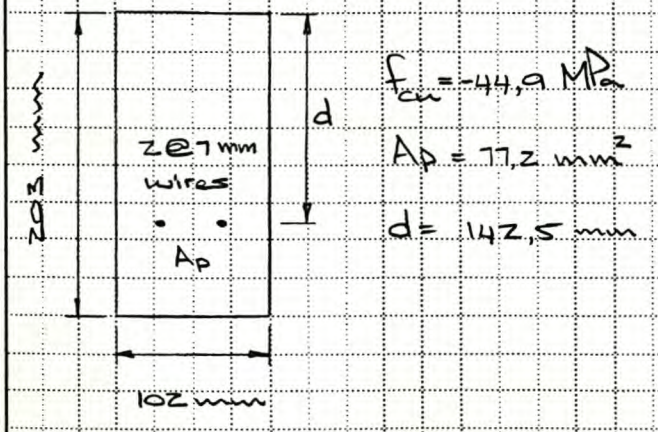

$f_{cu} = 44,9$ MPa

$A_p = 77,2$ mm²

$d = 142,5$ mm

Beam No 4

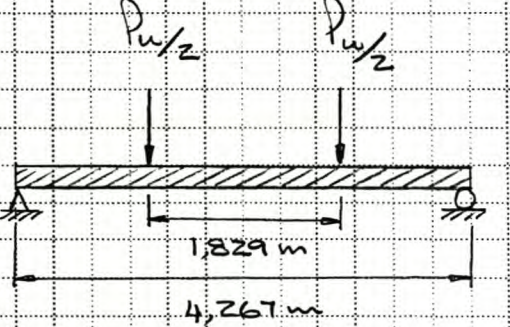

$(M_u)_T = 14,73$ kNm

Test Set-up

Assumed Stress-Strain Relationships [Ref. 5-15]

Concrete: equivalent rectangular stress-block

$$\alpha_1 = \frac{C_1}{\gamma_{mc}} = \frac{0,67}{1,0} = 0,67$$

$$\beta_1 = 0,9$$

$$\varepsilon_{cu} = -0,0035$$

Prestressing Steel:

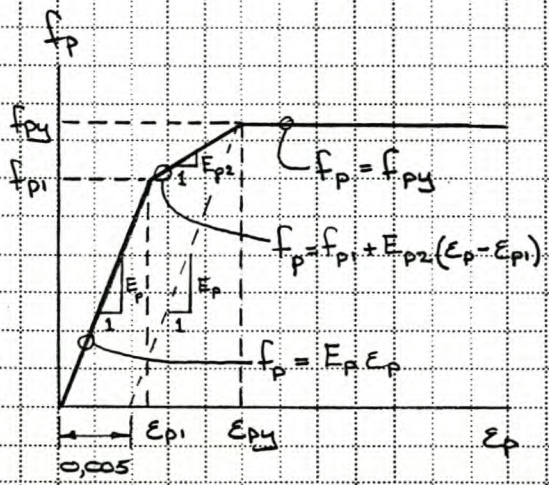

$$f_{py} = \frac{f_{pu}}{\gamma_{ms}} = \frac{1700}{1,0} = 1700 \text{ MPa}$$

$$E_p = 200 \text{ GPa}$$

$$\varepsilon_{py} = 0,005 + \frac{f_{py}}{E_p} = 0,0135$$

$$f_{p1} = 0,8 f_{py} = 1360 \text{ MPa}$$

$$\varepsilon_{p1} = \frac{f_{p1}}{E_p} = 0,0068$$

$$E_{p2} = \frac{f_{py} - f_{p1}}{\varepsilon_{py} - \varepsilon_{p1}} = 50,75 \text{ GPa}$$

$$\Delta\varepsilon_p = \frac{f_{pe}}{E_p} = \frac{656}{200.10^3} = 0,0033$$

Assume $\varepsilon_{p1} < \varepsilon_p < \varepsilon_{py}$, Solve for x

$$f_{pI} = f_{p1} + E_{p2}\left(\Delta\varepsilon_p - |\varepsilon_{cu}| - \varepsilon_{p1}\right) \qquad \text{[see Ref. 5-16]}$$

$$= 1360 + 50,75.10^3\left(0,0033 - |-0,0035| - 0,0068\right)$$

$$= 1005 \text{ MPa}$$

$$\left(\frac{\alpha_1 f_{cu} b \beta_1}{A_p}\right) x^2 + f_{p1} x + E_{p2} |\varepsilon_{cu}| d = 0 \quad \text{[see Ref. 5-16]}$$

$$\therefore \left[\frac{0,67(-44,9)102.0,9}{77,2}\right] x^2 + 1005x + 50,75.10^3 |-0,0035| 142,5 = 0$$

$$\therefore -35,77x^2 + 1005x + 25\,812 = 0$$

$$\therefore x = 44,1 \text{ mm}$$

Check ε_p

$$\varepsilon_p = \varepsilon_{cp} + (\varepsilon_{pe} - \varepsilon_{ce}) \quad \text{[Eq. 3-13]}$$

$$= \left(\frac{d-x}{x}\right)|\varepsilon_{cu}| + \Delta\varepsilon_p$$

$$= \left(\frac{142,5-44,1}{44,1}\right)|-0,0035| + 0,0033$$

$$= 0,011$$

$\varepsilon_{p1} < \varepsilon_p < \varepsilon_{py}$ $\therefore$ Value of x correct

(over-reinforced section — see § 3.4.4)

Calculate f_p at Ultimate

$$f_p = f_{p1} + E_{p2}(\varepsilon_p - \varepsilon_{p1})$$

$$= 1360 + 50,75.10^3(0,011 - 0,0068)$$

$$= 1578 \text{ MPa}$$

Predict Ultimate Moment of Resistance

$$(M_u)_M = f_p A_p \left[d - \beta_1 \frac{x}{2}\right] \quad \text{[cf. Eq. 3-15a]}$$

$$= 1578.77,2\left[142,5 - 0,9.\frac{44,1}{2}\right]10^{-6} = 14,94 \text{ kNm}$$

$$\therefore (M_u)_T / (M_u)_M = \frac{14,73}{14,94} = 0,986 \rightarrow$$

(c) Variability of Modelling Error

Unbiased Estimators

$$\bar{\varepsilon}_M = \frac{1}{n}\sum_{i=1}^{n} \varepsilon_i \quad , n = 7 \qquad \text{[Eq. 4-54a]}$$

$$= 1{,}020$$

where $\varepsilon_i = (M_u)_T / (M_u)_M$

$$s^2_{T/M} = \frac{1}{n-1}\sum_{i=1}^{n} (\varepsilon_i - \bar{\varepsilon}_M)^2 \qquad \text{[Eq. 4-54b]}$$

$$= 7{,}438.10^{-3}$$

95% Upper Bound Estimate

$$\sigma^2_{T/M} = s^2_{T/M}\left[\frac{n-1}{\chi^2_{1-\alpha;n-1}}\right] \quad , \alpha = 0{,}05 \qquad \text{[Eq. 4-55]}$$

$$= 7{,}438.10^{-3}\left[\frac{7-1}{1{,}635}\right]$$

$\therefore \sigma_{T/M} = 0{,}165$ and $V_{T/M} = \dfrac{\sigma_{T/M}}{\bar{\varepsilon}_M} = 0{,}162$

Systematic and Random Error

$\bar{\varepsilon}_M = 1{,}020 \rightarrow$

$$V_\varepsilon = \sqrt{V^2_{T/M} - V^2_{test} - V^2_{spec}} \qquad \text{[Eq. 4-56]}$$

$$= \sqrt{(0{,}162)^2 - (0{,}02)^2 - (0{,}025)^2} \qquad \text{[Ref. 5-12]}$$

$$= 0{,}159 \rightarrow$$

Assume $\varepsilon_M \sim N(\bar{\varepsilon}_M, \sigma_{\varepsilon M})$

B.4.2 MODELLING ERROR — DEFLECTION

(a) Systematic Error

Material Properties [see § A.1.3 & A.2.7]

$E_c = 34{,}0$ GPa $\quad \phi_{ct} = 1{,}23$ $\quad \Gamma_t = 0{,}019$

$E_p = 195{,}0$ GPa $\quad \phi_{c\infty} = 3{,}04$ $\quad \Gamma_\infty = 0{,}038$

Uncracked Transformed Section

$$A_{trans} = A + (n-1)A_p$$

$$y_{bot\,trans} = \frac{1}{A_{trans}}\left[A.y_{bot} + (n-1)A_p(h-d)\right]$$

$$I_{trans} = I + A\left[y_{bot} - y_{bot\,trans}\right]^2 + (n-1)A_p\left[y_{bot\,trans} - (h-d)\right]^2$$

Instantaneous Deflection

$$n_i = \frac{E_p}{E_c} = \frac{195}{34} = 5{,}74$$

$A_{trans\,i} = 228{,}8.10^3$ mm^2

$y_{bot\,trans\,i} = 411{,}8$ mm

$I_{trans\,i} = 7{,}712.10^9$ mm^4

$\therefore$ Assume $\varepsilon_i = \dfrac{I}{I_{trans\,i}} = \dfrac{7{,}323}{7{,}712} = 0{,}950 \rightarrow$ [Eq. 5-9]

Ratio of 33 Day to Instantaneous

$$n_t = \left(\frac{E_p}{E_{c\,eff}}\right)_t = (1-\Gamma_t)(1+\phi_{ct})\frac{E_p}{E_c} = 12{,}55 \quad \text{[Eq 5-8]}$$

$A_{trans\,t} = 225{,}6.10^3$ mm^2

$y_{bot\,trans\,t} = 404{,}6$ mm

$I_{trans\,t} = 8,251.10^9 \text{ mm}^4$

Assume $\varepsilon_{\delta t} \equiv \dfrac{I}{I_{trans\,t}} = \varepsilon_t . \varepsilon_i$ [Eq. 5-9 ; Eq. 5-7a]

$\therefore \varepsilon_t = \dfrac{I_{trans\,i}}{I_{trans\,t}} = \dfrac{7,712}{8,251} = 0,935 \rightarrow$

Ratio of Long-Term to Instantaneous

$n_\infty = \left(\dfrac{E_{p\,eff}}{E_{c\,eff}}\right)_\infty = (1-r_\infty)(1+\phi_{t\infty})\dfrac{E_p}{E_c} = 22,29$ [Eq. 5-8]

$A_{trans\,\infty} = 232,4.10^3 \text{ mm}^2$

$y_{bot\,trans\,\infty} = 394,9 \text{ mm}$

$I_{trans\,\infty} = 8,892.10^9 \text{ mm}^4$

Assume $\varepsilon_{\delta\infty} \equiv \dfrac{I}{I_{trans\,\infty}} = \varepsilon_\infty . \varepsilon_i$ [Eq. 5-9; Eq. 5-7b]

$\therefore \varepsilon_\infty = \dfrac{I_{trans\,i}}{I_{trans\,\infty}} = \dfrac{7,712}{8,892} = 0,867 \rightarrow$

(b) Random Error

Data Base [Ref 5-23]

Beam No	Instantaneous Deflect.			Ratio of Long-Term to Instantaneous		
	$(\delta_i)_T$ [mm]	$(\delta_i)_M$ [mm]	$\frac{(\delta_i)_T}{(\delta_i)_M}$	$\left(\frac{\delta_\infty}{\delta_i}\right)_T$	$\left(\frac{\delta_\infty}{\delta_i}\right)_M$	$\frac{(\delta_\infty/\delta_i)_T}{(\delta_\infty/\delta_i)_M}$
A3|6	17,0	16,0	1,06	2,63	2,87	0,92
B3|6	26,4	26,2	1,01	3,33	3,56	0,94
C3|6	47,8	42,7	1,12	2,95	3,48	0,85
D3|6	17,8	15,2	1,17	2,73	3,50	0,78
E3|6	63,0	50,8	1,24	2,94	3,00	0,98
CS1	3,0	3,0	1,00	2,42	2,50	0,97
CS2	7,9	7,6	1,04	2,19	2,73	0.80
CS3	6,1	5,8	1,05	2,54	3,00	0,85

Instantaneous Deflection

$$s'^2_{T/M} = \frac{1}{n-1}\sum_{i=1}^{n}\left(\varepsilon_i - \overline{\varepsilon_i}\right)^2 \quad \text{where } \varepsilon_i = \frac{(\delta_i)_T}{(\delta_i)_M} \text{ and } n = 8$$

$$= 7{,}027 \cdot 10^{-3} \qquad [\text{Eq } 4\text{-}54\,b]$$

$$\sigma'^2_{T/M} = s'^2_{T/M}\left[\frac{n-1}{\chi^2_{1-\alpha,n-1}}\right] \quad \text{where } \alpha = 0{,}05$$

$$= 7{,}027 \cdot 10^{-3}\left[\frac{8-1}{2{,}167}\right] \qquad [\text{Eq } 4\text{-}55]$$

$\therefore \quad \sigma'_{T/M} = 0,151 \quad$ and $\quad V'_{T/M} = \dfrac{\sigma'_{T/M}}{\bar{\varepsilon}_i} = 0,139$

Assume $V_{T/M} = 0,75\, V'_{T/M} = 0,104$

$\therefore \quad V_{\varepsilon_i} = \sqrt{V_{T/M}^2 - V_{test}^2 - V_{spec}^2}$ [Eq. 4-56]

[Ref 5-9]

$= \sqrt{(0,104)^2 - (0,02)^2 - (0,025)^2}$

$= 0,099 \rightarrow$

Assume $\varepsilon_i \sim N(\bar{\varepsilon}_i, \sigma_{\varepsilon_i})$

Ratio of Long-Term to Instantaneous

$S'^2_{T/M} = \dfrac{1}{n-1} \sum_{i=1}^{n} \left(\varepsilon_i - \bar{\varepsilon}_\infty\right)^2$ where $\varepsilon_i = \dfrac{(\delta_\infty/\delta_i)_T}{(\delta_\infty/\delta_i)_M}$ and $n = 8$

$= 5,884.10^{-3}$ [Eq 4-54b]

$\sigma'^2_{T/M} = S'^2_{T/M} \left[\dfrac{n-1}{\chi^2_{1-\alpha,n-1}}\right]$ where $\alpha = 0,05$

$= 5,884.10^{-3} \left[\dfrac{8-1}{2,167}\right]$ [Eq. 4-55]

$\therefore \quad \sigma'_{T/M} = 0,138 \quad$ and $\quad V'_{T/M} = \dfrac{\sigma'_{T/M}}{\bar{\varepsilon}_\infty} = 0,156$

Assume $V_{T/M} = 0,75\, V'_{T/M} = 0,117$

$$\therefore V_{\varepsilon_\infty} = \sqrt{V_{T/M}^2 - V_{test}^2 - V_{spec}^2} \qquad [Eq.\ 4\text{-}56]$$

$$= \sqrt{(0,117)^2 - (0,02)^2 - (0,025)^2} \qquad [Ref.\ 5\text{-}9]$$

$$= 0,113 \longrightarrow$$

Assume $\varepsilon_\infty \sim N(\bar{\varepsilon}_\infty, \sigma_{\varepsilon\infty})$

Ratio of 33 Day to Instantaneous

Assume $V_{\varepsilon_t} = \frac{1}{2} V_{\varepsilon\infty}$

$$= \frac{1}{2} \cdot 0,113$$

$$= 0,057 \longrightarrow$$

Assume $\varepsilon_t \sim N(\bar{\varepsilon}_t, \sigma_{\varepsilon t})$

B.5.1 NOMINAL AND MEAN VALUES OF LOAD EFFECTS

Applied moment due to self-weight:

$M_{D_1,n} = \frac{1}{8} b D_{1,n} L_e^2$

$= \frac{1}{8}(1,5 \cdot 3,63)(15)^2$

$= 153,0$ kNm

$\therefore \overline{M}_{D_1} = 1,0\, M_{D_1,n}$

$= 1,0 \cdot 153,0$

$= 153,0$ kNm

Applied superimposed dead load moment:

$M_{D_2,n} = \frac{1}{8} b D_{2,n} L_e^2$

$= \frac{1}{8}(1,5 \cdot 1,20)(15)^2$

$= 50,6$ kNm

$\therefore \overline{M}_{D_2} = 1,2\, M_{D_2,n}$

$= 1,2 \cdot 50,6$

$= 60,7$ kNm

Total applied dead load moment:

$M_{D,n} = \frac{1}{8} b D_n L_e^2$

$= \frac{1}{8}(1,5 \cdot 4,83)(15)^2$

$= 203,8$ kNm

$\therefore \overline{M}_D = 1,05\, M_{D,n}$

$= 1,05 \cdot 203,8$

$= 214,0$ kNm

Total applied live load moment:

$M_{L,n} = \frac{1}{8} b L_n L_e^2$

$= \frac{1}{8}(1,5 \cdot 3,39)(15)^2$

$= 143,0$ kNm

ULS: $\overline{M}_L = 0,941\, M_{L,n}$

$= 134,6$ kNm

SLS: $\overline{M}_L = 0,650\, M_{L,n}$

$= 93,0$ kNm

B.5.2 MOMENTS OF GROSS AREA – TAYLOR SERIES APPROX.

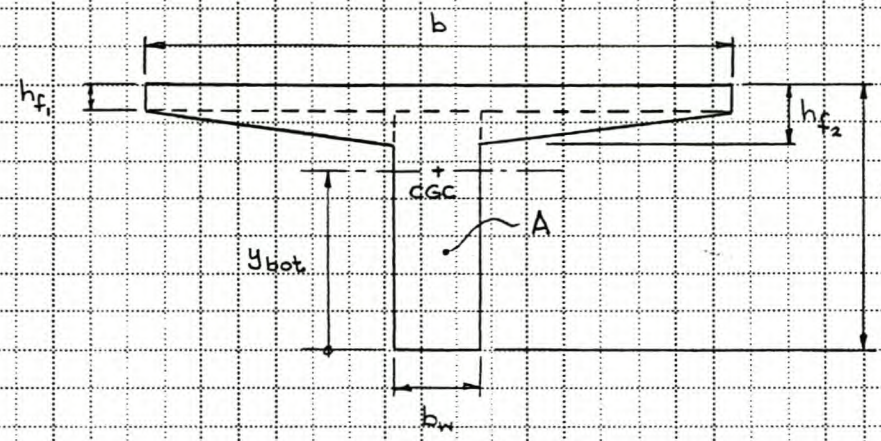

$$A = \sum_{i=1}^{5} A_i = b\,h_{f_1} + b_w(h - h_{f_1}) + \tfrac{1}{2}(b - b_w)(h_{f_2} - h_{f_1}) \qquad [\text{Eq. 5-6a}]$$

X [mm]	X_n	$\overline{X}$	σ_X	V_X	[Table 4-2]
b	1500	1504	6,4	0,004	
b_w	200	200	4,8	0,024	
h	600	603	4,0	0,007	
h_{f_1}	50	50	4,8	0,096	
h_{f_2}	100	100	4,8	0,048	

Assume that no correlation exists among basic dimensional random variables

Calculate: $\overline{A}$ and σ_A

$$\left.\frac{\partial A}{\partial b}\right|_{\overline{X}} = \frac{h_{f_1} + h_{f_2}}{2} = 75{,}0 \qquad \left.\frac{\partial^2 A}{\partial b^2}\right|_{\overline{X}} = 0$$

$$\left.\frac{\partial A}{\partial b_w}\right|_{\overline{X}} = h - \frac{(h_{f_1} + h_{f_2})}{2} = 528 \qquad \left.\frac{\partial^2 A}{\partial b_w^2}\right|_{\overline{X}} = 0$$

$$\left.\frac{\partial A}{\partial h}\right|_{\bar{x}} = b_w = 200 \qquad \left.\frac{\partial^2 A}{\partial h^2}\right|_{\bar{x}} = 0$$

$$\left.\frac{\partial A}{\partial h_{f_1}}\right|_{\bar{x}} = \tfrac{1}{2}(b - b_w) = 652 \qquad \left.\frac{\partial^2 A}{\partial h_{f_1}^2}\right|_{\bar{x}} = 0$$

$$\left.\frac{\partial A}{\partial h_{f_2}}\right|_{\bar{x}} = \tfrac{1}{2}(b - b_w) = 652 \qquad \left.\frac{\partial^2 A}{\partial h_{f_2}^2}\right|_{\bar{x}} = 0$$

$$\bar{A} \approx A(\bar{\mathbf{x}}) + \tfrac{1}{2}\sum_{i=1}^{5}\left[\frac{\partial^2 A(\mathbf{x})}{\partial X_i^2}\right]_{\bar{\mathbf{x}}} \sigma_{x_i}^2 \qquad \text{[Eq 4-28]}$$

$$= 218\,400 + 0$$

$$= 218\,400 \text{ mm}^2 \rightarrow \text{ and } \bar{A}/A_{nom} = 1{,}004$$

$$\sigma_A^2 \approx \sum_{i=1}^{5}\left[\frac{\partial A(\mathbf{x})}{\partial X_i}\right]_{\bar{\mathbf{x}}}^2 \cdot \sigma_{x_i}^2 \qquad \text{[Eq 4-29]}$$

$\therefore \sigma_A = 5185 \text{ mm}^2 \rightarrow$ and $V_A = 0{,}024$

The same results have been obtained with the PEM.

From the PEM also follows that

$$\gamma_1 = \frac{\sum_{i=1}^{32}\left(A_i - \bar{A}\right)^3\left(\frac{1}{2^5}\right)}{\sigma_A^3} = -0{,}003\,931 \qquad \text{[Eq 4-37]}$$

$\therefore$ $f_A(a)$ approx. symetrical — assume $A \sim N(\bar{A}, \sigma_A)$

B.5.3 MOMENTS OF DISTANCE TO CENTROID OF SECTION

$$y_{bot} = \frac{1}{A}\sum_i A_i y_{bot,i} \qquad \text{[Eq.5-6b]}$$

$$= \frac{b h_{f_1}\left(h - \frac{h_{f_1}}{2}\right) + b_w \frac{(h-h_{f_1})^2}{2} + \frac{1}{2}(b-b_w)(h_{f_2}-h_{f_1})(h - \frac{2}{3}h_{f_1} - \frac{1}{3}h_{f_2})}{A}$$

X	X_n	$\bar{X}$	σ_x	V_x	Calculated f
b	1500	1504	6,4	0,004	$f_{b,A} = 0,046$
b_w	200	200	4,8	0,024	$f_{b_w,A} = 0,244$
h	600	603	4,0	0,007	$f_{h,A} = 0,077$
h_{f_1}	50	50	4,8	0,096	$f_{h_{f_1},A} = 0,302$
h_{f_2}	100	100	4,8	0,048	$f_{h_{f_2},A} = 0,302$
A	217500	218400	5185	0,024	

Calculate: Partial derivatives of y_{bot}

$$\left.\frac{\partial y_{bot}}{\partial b}\right|_{\bar{x}} = \frac{1}{A}\left[h_{f_1}\left(h - \frac{h_{f_1}}{2}\right) + \frac{1}{2}\left(h_{f_2}-h_{f_1}\right)\left(h - \frac{2}{3}h_{f_1} - \frac{1}{3}h_{f_2}\right)\right] = 0,194$$

$$\left.\frac{\partial^2 y_{bot}}{\partial b^2}\right|_{\bar{x}} = 0$$

$$\left.\frac{\partial^2 y_{bot}}{\partial b \partial b_w}\right|_{\bar{x}} = 0$$

$$\left.\frac{\partial^2 y_{bot}}{\partial b \partial h}\right|_{\bar{x}} = \frac{1}{A}\left[h_{f_1} + \frac{1}{2}\left(h_{f_2}-h_{f_1}\right)\right] \approx 0$$

$$\left.\frac{\partial^2 y_{bot}}{\partial b \partial h_{f_1}}\right|_{\bar{x}} = \frac{1}{A}\left[h - h_{f_1} - \frac{1}{3}\left(h_{f_2}-h_{f_1}\right) - \frac{1}{2}\left(h - \frac{2}{3}h_{f_1} - \frac{1}{3}h_{f_2}\right)\right] = 0,001$$

$$\left.\frac{\partial^2 y_{bot}}{\partial b \partial h_{f_2}}\right|_{\bar{x}} = \frac{1}{A}\left[\frac{1}{6}\left(h_{f_1}-h_{f_2}\right) + \frac{1}{2}\left(h - \frac{2}{3}h_{f_1} - \frac{1}{3}h_{f_2}\right)\right] = 0,001$$

$$\left.\frac{\partial^2 y_{bot}}{\partial b \partial A}\right|_{\bar{x}} = \frac{1}{A^2}\left[h_{f_1}\left(\frac{h_{f_1}}{2} - h\right) - \frac{1}{2}\left(h_{f_2} - h_{f_1}\right)\left(h - \frac{2}{3}h_{f_1} - \frac{1}{3}h_{f_2}\right)\right] \simeq 0$$

$$\left.\frac{\partial y_{bot}}{\partial b_w}\right|_{\bar{x}} = \frac{1}{A}\left[\frac{1}{2}\left(h - h_{f_1}\right)^2 - \frac{1}{2}\left(h_{f_2} - h_{f_1}\right)\left(h - \frac{2}{3}h_{f_1} - \frac{1}{3}h_{f_2}\right)\right] = 0{,}639$$

$$\left.\frac{\partial^2 y_{bot}}{\partial b_w^2}\right|_{\bar{x}} = 0$$

$$\left.\frac{\partial^2 y_{bot}}{\partial b_w \partial h}\right|_{\bar{x}} = \frac{1}{A}\left[h - h_{f_1} - \frac{1}{2}\left(h_{f_2} - h_{f_1}\right)\right] = 0{,}002$$

$$\left.\frac{\partial^2 y_{bot}}{\partial b_w \partial h_{f_1}}\right|_{\bar{x}} = \frac{1}{A}\left[h_{f_1} - h + \frac{1}{3}\left(h_{f_2} - h_{f_1}\right) + \frac{1}{2}\left(h - \frac{2}{3}h_{f_1} - \frac{1}{3}h_{f_2}\right)\right] = -0{,}001$$

$$\left.\frac{\partial^2 y_{bot}}{\partial b_w \partial h_{f_2}}\right|_{\bar{x}} = \frac{1}{A}\left[\frac{1}{6}\left(h_{f_2} - h_{f_1}\right) - \frac{1}{2}\left(h - \frac{2}{3}h_{f_1} - \frac{1}{3}h_{f_2}\right)\right] = -0{,}001$$

$$\left.\frac{\partial^2 y_{bot}}{\partial b_w \partial A}\right|_{\bar{x}} = \frac{1}{A^2}\left[-\frac{1}{2}\left(h - h_{f_1}\right)^2 + \frac{1}{2}\left(h_{f_2} - h_{f_1}\right)\left(h - \frac{2}{3}h_{f_1} - \frac{1}{3}h_{f_2}\right)\right] \simeq 0$$

$$\left.\frac{\partial y_{bot}}{\partial h}\right|_{\bar{x}} = \frac{1}{A}\left[b h_{f_1} + b_w\left(h - h_{f_1}\right) + \frac{1}{2}\left(b - b_w\right)\left(h_{f_2} - h_{f_1}\right)\right] = 1{,}000$$

$$\left.\frac{\partial^2 y_{bot}}{\partial h^2}\right|_{\bar{x}} = b_w / A = 0{,}001$$

$$\left.\frac{\partial^2 y_{bot}}{\partial h \partial h_{f_1}}\right|_{\bar{x}} = \frac{1}{A}\left[b - b_w - \frac{1}{2}\left(b - b_w\right)\right] = 0{,}003$$

$$\left.\frac{\partial^2 y_{bot}}{\partial h \partial h_{f_2}}\right|_{\bar{x}} = \frac{1}{A}\left[\frac{1}{2}\left(b - b_w\right)\right] = 0{,}003$$

$$\left.\frac{\partial^2 y_{bot}}{\partial h \partial A}\right|_{\bar{x}} = \frac{1}{A^2}\left[-b h_{f_1} - b_w\left(h - h_{f_1}\right) - \frac{1}{2}\left(b - b_w\right)\left(h_{f_2} - h_{f_1}\right)\right] \simeq 0$$

$$\left.\frac{\partial y_{bot}}{\partial h_{f_1}}\right|_{\bar{x}} = \frac{1}{A}\left[bh - b h_{f_1} - b_w\left(h - h_{f_1}\right) - \frac{1}{3}\left(b - b_w\right)\left(h_{f_2} - h_{f_1}\right) - \frac{1}{2}\left(b - b_w\right)\left(h - \frac{2}{3}h_{f_1} - \frac{1}{3}h_{f_2}\right)\right] = 1{,}601$$

$$\left.\frac{\partial^2 y_{bot}}{\partial h_{f_1}^2}\right|_{\bar{x}} = \frac{1}{A}\left[-b + b_w + \tfrac{1}{3}(b-b_w) + \tfrac{1}{3}(b-b_w)\right] = -0{,}002$$

$$\left.\frac{\partial^2 y_{bot}}{\partial h_{f_1}\partial h_{f_2}}\right|_{\bar{x}} = \frac{1}{A}\left[-\tfrac{1}{3}(b-b_w) + \tfrac{1}{6}(b-b_w)\right] = -0{,}001$$

$$\left.\frac{\partial^2 y_{bot}}{\partial h_{f_1}\partial A}\right|_{\bar{x}} = \frac{1}{A^2}\left[-bh + bh_{f_1} + b_w(h-h_{f_1}) + \tfrac{1}{3}(b-b_w)(h_{f_2}-h_{f_1}) + \tfrac{1}{2}(b-b_w)\left(h - \tfrac{2}{3}h_{f_1} - \tfrac{h_{f_2}}{3}\right)\right]$$
$$\simeq 0$$

$$\left.\frac{\partial y_{bot}}{\partial h_{f_2}}\right|_{\bar{x}} = \frac{1}{A}\left[-\tfrac{1}{6}(b-b_w)(h_{f_2}-h_{f_1}) + \tfrac{1}{2}(b-b_w)\left(h - \tfrac{2}{3}h_{f_1} - \tfrac{1}{3}h_{f_2}\right)\right] = 1{,}551$$

$$\left.\frac{\partial^2 y_{bot}}{\partial h_{f_2}^2}\right|_{\bar{x}} = \frac{1}{A}\left[-\tfrac{1}{6}(b-b_w) - \tfrac{1}{6}(b-b_w)\right] = -0{,}002$$

$$\left.\frac{\partial^2 y_{bot}}{\partial h_{f_2}\partial A}\right|_{\bar{x}} = \frac{1}{A^2}\left[\tfrac{1}{6}(b-b_w)(h_{f_2}-h_{f_1}) - \tfrac{1}{2}(b-b_w)\left(h - \tfrac{2}{3}h_{f_1} - \tfrac{1}{3}h_{f_2}\right)\right] \simeq 0$$

$$\left.\frac{\partial y_{bot}}{\partial A}\right|_{\bar{x}} = \frac{1}{A^2}\left[-bh_{f_1}\left(h - \frac{h_{f_1}}{2}\right) - b_w\frac{(h-h_{f_1})^2}{2} - \tfrac{1}{2}(b-b_w)(h_{f_2}-h_{f_1})\left(h - \tfrac{2}{3}h_{f_1} - \tfrac{1}{3}h_{f_2}\right)\right]$$
$$= -0{,}002$$

$$\left.\frac{\partial^2 y_{bot}}{\partial A^2}\right|_{\bar{x}} = \frac{1}{A^3}\left[2bh_{f_1}\left(h - \frac{h_{f_1}}{2}\right) + b_w(h-h_{f_1})^2 + (b-b_w)(h_{f_2}-h_{f_1})\left(h - \tfrac{2}{3}h_{f_1} - \tfrac{1}{3}h_{f_2}\right)\right]$$
$$\simeq 0$$

Calculate: $f_{x_i,A}$ [Eqs. 4-30 & 4-8]

$Cov[b,A] = \frac{1}{2}[75(6{,}4)^2] = 1536 \quad \therefore f_{b,A} = \frac{1536}{6{,}4 \cdot 5185} = 0{,}046$

$Cov[b_w,A] = \frac{1}{2}[528(4{,}8)^2] = 6083 \quad \therefore f_{b_w,A} = \frac{6083}{4{,}8 \cdot 5185} = 0{,}244$

$Cov[h,A] = \frac{1}{2}[200(4{,}0)^2] = 1600 \quad \therefore f_{h,A} = \frac{1600}{4{,}0 \cdot 5185} = 0{,}077$

$Cov[h_{f_1},A] = \frac{1}{2}[652(4{,}8)^2] = 7511 \quad \therefore f_{h_{f_1},A} = \frac{7511}{4{,}8 \cdot 5185} = 0{,}302$

$Cov[h_{f_2},A] = \frac{1}{2}[652(4{,}8)^2] = 7511 \quad \therefore f_{h_{f_2},A} = \frac{7511}{4{,}8 \cdot 5185} = 0{,}302$

Calculate: $\overline{y_{bot}}$ and $\sigma_{y_{bot}}$ [Eqs. 4-28 & 4-29]

$$\overline{y_{bot}} \simeq y_{bot}(\bar{\mathbf{X}}) + \tfrac{1}{2}\sum_{i=1}^{6}\left[\frac{\partial^2 y_{bot}(\mathbf{X})}{\partial X_i^2}\right]_{\bar{\mathbf{X}}}\sigma_{X_i}^2 + \sum_{i=1}^{6}\sum_{j=i+1}^{6}\left[\frac{\partial^2 y_{bot}(\mathbf{X})}{\partial X_i \partial X_j}\right]_{\bar{\mathbf{X}}}\rho_{X_i X_j}\sigma_{X_i}\sigma_{X_j}$$

$$= 419 + \tfrac{1}{2}\left[0(6,4)^2 + 0(4,8)^2 + 0,0001(4,0)^2 - 0,002(4,8)^2 - 0,002(4,8)^2 + 0(5185)^2\right]$$

$$\simeq 419 \text{ mm} \rightarrow \text{and } \overline{y_{bot}} / y_{bot,n} = 1,005$$

$$\sigma_{y_{bot}}^2 \simeq \sum_{i=1}^{6}\left[\frac{\partial y_{bot}(\mathbf{X})}{\partial X_i}\right]_{\bar{\mathbf{X}}}^2 \sigma_{X_i}^2 + 2\sum_{i=1}^{6}\sum_{j=i+1}^{6}\left[\frac{\partial y_{bot}(\mathbf{X})}{\partial X_i}\right]_{\bar{\mathbf{X}}}\left[\frac{\partial y_{bot}(\mathbf{X})}{\partial X_j}\right]_{\bar{\mathbf{X}}}\rho_{X_i X_j}\sigma_{X_i}\sigma_{X_j}$$

$$= \left[(0,194.6,4)^2 + (0,639.4,8)^2 + (1,0.4,0)^2 + (1,601.4,8)^2 + (1,551.4,8)^2 + (-0,002.5185)^2\right]$$

$$+ 2\left[(0,194)(-0,002)(0,046)(6,4)(5185) + (0,639)(-0,002)(0,244)(4,8)(5185) + (1,0)(-0,002)(0,077)(4,0)(5185) + (1,601)(-0,002)(0,302)(4,8)(5185) + (1,551)(-0,002)(0,302)(4,8)(5185)\right]$$

$$= 249,0 - 117,9$$

$$= 131,1$$

$\therefore \sigma_{y_{bot}} = 11,4$ mm $\rightarrow$ and $V_{y_{bot}} = 0,027$

Assume $y_{bot} \sim N(\overline{y_{bot}}, \sigma_{y_{bot}})$

B.5.4 MOMENTS OF THE SECOND MOMENT OF AREA

$$I = \sum_i I_i + \sum_i A_i y_i^2 \qquad \text{[Eq 5-6c]}$$

$$= \tfrac{1}{12} b h_{f_1}^3 + b h_{f_1}\left[h - \frac{h_{f_1}}{2} - y_{bot}\right]^2$$

$$+ \tfrac{1}{12} b_w (h - h_{f_1})^3 + b_w (h - h_{f_1})\left[y_{bot} - \frac{(h - h_{f_1})}{2}\right]^2$$

$$+ \tfrac{1}{36}(b - b_w)(h_{f_2} - h_{f_1})^3 + \tfrac{1}{2}(b - b_w)(h_{f_2} - h_{f_1})\left[h - h_{f_1} - \tfrac{1}{3}(h_{f_2} - h_{f_1}) - y_{bot}\right]^2$$

X	X_n	$\bar{X}$	σ_x	V_x	Calculated f
b	1500	1504	6,4	0,004	$f_{b,y_{bot}} = 0,054$
b_w	200	200	4,8	0,024	$f_{b_w,y_{bot}} = 0,135$
h	600	603	4,0	0,007	$f_{h,y_{bot}} = 0,175$
h_{f_1}	50	50	4,8	0,096	$f_{h_{f_1},y_{bot}} = 0,337$
h_{f_2}	100	100	4,8	0,048	$f_{h_{f_2},y_{bot}} = 0,327$
y_{bot}	417	419	11,4	0,027	

Calculate: Partial derivatives of I

$$\left.\frac{\partial I}{\partial b}\right|_{\bar{x}} = \tfrac{1}{12} h_{f_1}^3 + h_{f_1}\left[h - \frac{h_{f_1}}{2} - y_{bot}\right]^2 + \tfrac{1}{36}(h_{f_2} - h_{f_1})^3$$

$$+ \tfrac{1}{2}(h_{f_2} - h_{f_1})\left[h - h_{f_1} - \tfrac{1}{3}(h_{f_2} - h_{f_1}) - y_{bot}\right]^2 = 1,622 \cdot 10^6$$

$$\left.\frac{\partial^2 I}{\partial b^2}\right|_{\bar{x}} = 0$$

$$\left.\frac{\partial I}{\partial b_w}\right|_{\bar{x}} = \tfrac{1}{12}\left(h-h_{f_1}\right)^3 + \left(h-h_{f_1}\right)\left[y_{bot} - \frac{\left(h-h_{f_1}\right)}{2}\right]^2$$

$$- \tfrac{1}{36}\left(h_{f_2}-h_{f_1}\right)^3 - \tfrac{1}{2}\left(h_{f_2}-h_{f_1}\right)\left[h-h_{f_1}-\tfrac{1}{3}\left(h_{f_2}-h_{f_1}\right)-y_{bot}\right]^2 = 24,974.10^6$$

$$\left.\frac{\partial^2 I}{\partial b_w^2}\right|_{\bar{x}} = 0$$

$$\left.\frac{\partial I}{\partial h}\right|_{\bar{x}} = 2b h_{f_1}\left(h-\frac{h_{f_1}}{2}-y_{bot}\right) + \tfrac{1}{4}b_w\left(h-h_{f_1}\right)^2 - b_w\left(h-h_{f_1}\right)\left[y_{bot}-\frac{\left(h-h_{f_1}\right)}{2}\right]$$

$$+ b_w\left[y_{bot}-\frac{\left(h-h_{f_1}\right)}{2}\right]^2 + \left(b-b_w\right)\left(h_{f_2}-h_{f_1}\right)\left[h-h_{f_1}-\tfrac{1}{3}\left(h_{f_2}-h_{f_1}\right)-y_{bot}\right]$$

$$= 35,155.10^6$$

$$\left.\frac{\partial^2 I}{\partial h^2}\right|_{\bar{x}} = 2b h_{f_1} + \tfrac{1}{2}b_w\left(h-h_{f_1}\right) + \tfrac{1}{2}b_w\left(h-h_{f_1}\right) - b_w\left[y_{bot}-\frac{\left(h-h_{f_1}\right)}{2}\right]$$

$$- b_w\left[y_{bot}-\frac{\left(h-h_{f_1}\right)}{2}\right] + \left(b-b_w\right)\left(h_{f_2}-h_{f_1}\right)$$

$$= 0,269.10^6$$

$$\left.\frac{\partial I}{\partial h_{f_1}}\right|_{\bar{x}} = \tfrac{1}{4}b h_{f_1}^2 - b h_{f_1}\left(h-h_{f_1/2}-y_{bot}\right) + b\left(h-h_{f_1/2}-y_{bot}\right)^2$$

$$- \tfrac{1}{4}b_w\left(h-h_{f_1}\right)^2 + b_w\left(h-h_{f_1}\right)\left[y_{bot}-\frac{\left(h-h_{f_1}\right)}{2}\right]$$

$$- b_w\left[y_{bot}-\frac{\left(h-h_{f_1}\right)}{2}\right]^2 - \tfrac{1}{12}\left(b-b_w\right)\left(h_{f_2}-h_{f_1}\right)^2$$

$$- \tfrac{2}{3}\left(b-b_w\right)\left(h_{f_2}-h_{f_1}\right)\left[h-h_{f_1}-\tfrac{1}{3}\left(h_{f_2}-h_{f_1}\right)-y_{bot}\right]$$

$$- \tfrac{1}{2}\left(b-b_w\right)\left[h-h_{f_1}-\tfrac{1}{3}\left(h_{f_2}-h_{f_1}\right)-y_{bot}\right]^2$$

$$= 9,067.10^6$$

$$\left.\frac{\partial^2 I}{\partial h_{f_1}^2}\right|_{\bar{x}} = \tfrac{1}{2} b h_{f_1} + \tfrac{1}{2} b h_{f_1} - b\left(h - h_{f_1/2} - y_{bot}\right) - b\left(h - h_{f_1/2} - y_{bot}\right)$$

$$+ \tfrac{1}{2} b_w (h - h_{f_1}) + \tfrac{1}{2} b_w (h - h_{f_1}) - b_w\left[y_{bot} - \frac{(h - h_{f_1})}{2}\right]$$

$$- b_w\left[y_{bot} - \frac{(h - h_{f_1})}{2}\right] + \tfrac{1}{6}(b - b_w)(h_{f_2} - h_{f_1})$$

$$+ \tfrac{4}{9}(b - b_w)(h_{f_2} - h_{f_1}) + \tfrac{2}{3}(b - b_w)\left[h - h_{f_1} - \tfrac{1}{3}(h_{f_2} - h_{f_1}) - y_{bot}\right]$$

$$+ \tfrac{2}{3}(b - b_w)\left[h - h_{f_1} - \tfrac{1}{3}(h_{f_2} - h_{f_1}) - y_{bot}\right]$$

$$= -0{,}106 \cdot 10^6$$

$$\left.\frac{\partial I}{\partial h_{f_2}}\right|_{\bar{x}} = \tfrac{1}{12}(b - b_w)(h_{f_2} - h_{f_1})^2 - \tfrac{1}{3}(b - b_w)(h_{f_2} - h_{f_1})\left[h - h_{f_1} - \tfrac{1}{3}(h_{f_2} - h_{f_1}) - y_{bot}\right]$$

$$+ \tfrac{1}{2}(b - b_w)\left[h - h_{f_1} - \tfrac{1}{3}(h_{f_2} - h_{f_1}) - y_{bot}\right]^2$$

$$= 6{,}698 \cdot 10^6$$

$$\left.\frac{\partial^2 I}{\partial h_{f_2}^2}\right|_{\bar{x}} = \tfrac{1}{6}(b - b_w)(h_{f_2} - h_{f_1}) + \tfrac{1}{9}(b - b_w)(h_{f_2} - h_{f_1})$$

$$- \tfrac{2}{3}(b - b_w)\left[h - h_{f_1} - \tfrac{1}{3}(h_{f_2} - h_{f_1}) - y_{bot}\right]$$

$$= -0{,}084 \cdot 10^6$$

$$\left.\frac{\partial I}{\partial y_{bot}}\right|_{\bar{x}} = -2 b h_{f_1}\left(h - h_{f_1/2} - y_{bot}\right) + 2 b_w (h - h_{f_1})\left[y_{bot} - \frac{(h - h_{f_1})}{2}\right]$$

$$- (b - b_w)(h_{f_2} - h_{f_1})\left[h - h_{f_1} - \tfrac{1}{3}(h_{f_2} - h_{f_1}) - y_{bot}\right]$$

$$= -0{,}043 \cdot 10^6$$

$$\left.\frac{\partial^2 I}{\partial y_{bot}^2}\right|_{\bar{x}} = 2bh_{f_1} + 2b_w(h-h_{f_1}) + (b-b_w)(h_{f_2}-h_{f_1}) = 0,437.10^6$$

Calculate: $f_{x_i, y_{bot}}$ [Eqs. 4-30 & 4-8]

$\text{Cov}[b, y_{bot}] = \frac{1}{2}[0,194(6,4)^2] = 3,973 \quad \therefore f_{b,y_{bot}} = \frac{3,973}{6,4 \cdot 11,4} = 0,054$

$\text{Cov}[b_w, y_{bot}] = \frac{1}{2}[0,639(4,8)^2] = 7,361 \quad \therefore f_{b_w,y_{bot}} = \frac{7,361}{4,8 \cdot 11,4} = 0,135$

$\text{Cov}[h, y_{bot}] = \frac{1}{2}[1,000(4,0)^2] = 8,000 \quad \therefore f_{h,y_{bot}} = \frac{8,000}{4,0 \cdot 11,4} = 0,175$

$\text{Cov}[h_{f_1}, y_{bot}] = \frac{1}{2}[1,601(4,8)^2] = 18,444 \quad \therefore f_{h_{f_1},y_{bot}} = \frac{18,444}{4,8 \cdot 11,4} = 0,337$

$\text{Cov}[h_{f_2}, y_{bot}] = \frac{1}{2}[1,551(4,8)^2] = 17,868 \quad \therefore f_{h_{f_2},y_{bot}} = \frac{17,868}{4,8 \cdot 11,4} = 0,327$

Calculate: $\bar{I}$ and σ_I [Eqs. 4-28 & 4-29]

$$\bar{I} \approx I(\bar{\mathbf{x}}) + \frac{1}{2}\sum_{i=1}^{6}\left[\frac{\partial^2 I(\mathbf{x})}{\partial x_i^2}\right]_{\bar{\mathbf{x}}} \sigma_{x_i}^2$$

$$= 7,435.10^9 + \frac{1}{2}\left[0(6,4)^2 + 0(4,8)^2 + 0,269.10^6(4,0)^2 - 0,106.10^6(4,8)^2 - 0,084.10^6(4,8)^2 + 0,437.10^6(11,4)^2\right]$$

$$= 7,435.10^9 + 0,057.10^9$$

$$= 7,492.10^9 \text{ mm}^4 \rightarrow \text{and } \bar{I}/I_n = 1,023$$

$$\sigma_I^2 \approx \sum_{i=1}^{6}\left[\frac{\partial I(\mathbf{x})}{\partial x_i}\right]_{\bar{\mathbf{x}}}^2 \sigma_{x_i}^2 + 2\sum_{i=1}^{6}\sum_{j=i+1}^{6}\left[\frac{\partial I(\mathbf{x})}{\partial x_i}\right]_{\bar{\mathbf{x}}}\left[\frac{\partial I(\mathbf{x})}{\partial x_j}\right] f_{x_i,x_j}\sigma_{x_i}\sigma_{x_j}$$

$$= \left[(1,622.10^6.6,4)^2 + (24,974.10^6.4,8)^2 + (35,155.10^6.4,0)^2 + (9,067.10^6.4,8)^2 + (6,698.10^6.4,8)^2 + (-0,043.10^6.11,4)^2\right.$$

$$+ 2\left[(1{,}622.10^6)(-0{,}043.10^6)(0{,}054)(6{,}4)(11{,}4)\right.$$
$$+ (24{,}974.10^6)(-0{,}043.10^6)(0{,}135)(4{,}8)(11{,}4)$$
$$+ (35{,}155.10^6)(-0{,}043.10^6)(0{,}175)(4{,}0)(11{,}4)$$
$$+ (9{,}067.10^6)(-0{,}043.10^6)(0{,}337)(4{,}8)(11{,}4)$$
$$\left.+ (6{,}698.10^6)(-0{,}043.10^6)(0{,}327)(4{,}8)(11{,}4)\right]$$

$$= 3{,}718.10^{16} - 6{,}523.10^{13}$$

$$= 3{,}711.10^{16}$$

$\therefore \sigma_I = 0{,}193.10^9 \ mm^4 \longrightarrow$ and $V_I = 0{,}026$

Assume $I \sim N(\bar{I}, \sigma_I)$

B.6.1 SELECTION OF DETERMINISTIC PARAMETERS

Use $w_i = \dfrac{\left[\dfrac{\partial g(\mathbf{X})}{\partial X_i}\right]^2_{\mu_x} \sigma_{x_i}^2}{\sum_{i=1}^{n}\left[\dfrac{\partial g(\mathbf{X})}{\partial X_i}\right]^2_{\mu_x} \sigma_{x_i}^2}$ [Eq 5-1]

$\left.\dfrac{\partial g(\mathbf{X})}{\partial \varepsilon_i}\right|_{\mu_x} = -13,2$

$\left.\dfrac{\partial g(\mathbf{X})}{\partial \varepsilon_t}\right|_{\mu_x} = -32,7$

$\left.\dfrac{\partial g(\mathbf{X})}{\partial \varepsilon_\infty}\right|_{\mu_x} = 27,1$

$\left.\dfrac{\partial g(\mathbf{X})}{\partial M_{D1}}\right|_{\mu_x} = -1,13.10^{-7}$

$\left.\dfrac{\partial g(\mathbf{X})}{\partial M_{D2}}\right|_{\mu_x} = -2,78.10^{-7}$

$\left.\dfrac{\partial g(\mathbf{X})}{\partial M_L}\right|_{\mu_x} = -13,1.10^{-8}$

$\left.\dfrac{\partial g(\mathbf{X})}{\partial \psi_L}\right|_{\mu_x} = -18,5$

$\left.\dfrac{\partial g(\mathbf{X})}{\partial E_c}\right|_{\mu_x} = 3,35.10^{-4}$

$\left.\dfrac{\partial g(\mathbf{X})}{\partial \Phi_{c\infty}}\right|_{\mu_x} = 6,30$

$\left.\dfrac{\partial g(\mathbf{X})}{\partial \Phi_{ci}}\right|_{\mu_x} = -14,2$

$\left.\dfrac{\partial g(\mathbf{X})}{\partial \varepsilon_{fpu}}\right|_{\mu_x} = 0,0175$

$\left.\dfrac{\partial g(\mathbf{X})}{\partial A_p}\right|_{\mu_x} = 0,0478$

$\left.\dfrac{\partial g(\mathbf{X})}{\partial \xi_{si}}\right|_{\mu_x} = 47,9$

$\left.\dfrac{\partial g(\mathbf{X})}{\partial \eta_{s\infty}}\right|_{\mu_x} = 62,2$

$\left.\dfrac{\partial g(\mathbf{X})}{\partial \eta_{Lt}}\right|_{\mu_x} = -43,0$

$\left.\dfrac{\partial g(\mathbf{X})}{\partial d_1}\right|_{\mu_x} = 0,0912$

$\left.\dfrac{\partial g(\mathbf{X})}{\partial d_2}\right|_{\mu_x} = 0,0182$

$\left.\dfrac{\partial g(\mathbf{X})}{\partial I}\right|_{\mu_x} = 1,68.10^{-9}$

$$\sum_{i=1}^{18} \left[\frac{\partial g(\mathbf{X})}{\partial X_i}\right]^2_{\mu_X} \sigma_{X_i}^2 = 129,1$$

Uncertainty contributions to $g(\mathbf{X})$ in decreasing order:

$$w_{\phi_{co}} = \frac{(6,30)^2(0,754)^2}{129,1} = 0,17478$$

$$w_{\phi_{ct}} = \frac{(-14,2)^2(0,305)^2}{129,1} = 0,14529$$

$$w_{\eta_{co}} = \frac{(62,2)^2(0,067)^2}{129,1} = 0,13453$$

$$w_{M_L} = \frac{(-13,1.10^{-8})^2(29,8.10^6)^2}{129,1} = 0,11805$$

$$w_{M_{DZ}} = \frac{(-2,78.10^{-7})^2(14.10^6)^2}{129,1} = 0,11733$$

$$w_{\psi_L} = \frac{(-18,5)^2(0,172)^2}{129,1} = 0,07843$$

$$w_{\eta_t} = \frac{(-43,0)^2(0,074)^2}{129,1} = 0,07843$$

$$w_{\varepsilon_{co}} = \frac{(27,1)^2(0,098)^2}{129,1} = 0,05463$$

$$w_{M_{DI}} = \frac{(-1,13.10^{-7})^2(16,4.10^6)^2}{129,1} = 0,02660$$

$$w_{\varepsilon_t} = \frac{(-32,7)^2(0,053)^2}{129,1} = 0,02327$$

$$* \quad w_{\zeta_i} = \frac{(47,9)^2(0,028)^2}{129,1} = 0,01393$$

$$* \quad w_{E_c} = \frac{(3,35.10^{-4})^2(3,93.10^3)^2}{129,1} = 0,01343$$

$$w_{\varepsilon_i} = \frac{(-13,2)^2(0,094)^2}{129,1} = 0,01193$$

* $w_{fpH} = \frac{(0,0175)^2 (48,4)^2}{129,1} = 0,00556$

* $w_{Ap} = \frac{(0,0478)^2 (9,21)^2}{129,1} = 0,00150$

* $w_{el} = \frac{(0,0912)^2 (4,4)^2}{129,1} = 0,00125$

* $w_I = \frac{(1,68.10^{-9})^2 (0,193.10^9)^2}{129,1} = 0,00081$

* $w_{ez} = \frac{(0,0182)^2 (4,4)^2}{129,1} = 0,00005$

* Corresponding parameters assumed to be deterministic